STRINGQFT

String-Theoretic Construction
of Quantum Field Theory

VOLUME XVIII

Worldsheet Constructions of Quantum Field Theory

Xingyang Yu

StringQFT v1.0 / Source build candidate

Drafted with AI assistance under the supervision of the author.
Manuscript free to read. All rights reserved.

Contents

How to read this volume **iv**

XVIII.1 Why topological string field theory truncates to QFT **1**
XVIII.1.1 What is actually being truncated? . . . 1
XVIII.1.2 The propagator remembers nonharmonic fields . . . 2
XVIII.1.3 Where a disappearing strip keeps its weight . . . 5
XVIII.1.4 From the cubic vertex to a field action . . . 8
XVIII.1.5 Why retaining cohomology is a further operation . . . 10
XVIII.1.6 Exit dictionary and limits . . . 11
Following an internal line . . . 13

XVIII.2 Open A-model on T^*M: Chern–Simons theory **16**
XVIII.2.1 How a boundary vertex becomes a gauge interaction . . . 16
XVIII.2.2 Flatness, finite gauge changes and the center . . . 18
XVIII.2.3 The empty disk is not an empty perturbation series . . . 20
XVIII.2.4 Three coupling symbols with different jobs . . . 21
XVIII.2.5 Compute a partition function by gluing . . . 23
XVIII.2.6 Why the quantum answer remembers framing . . . 25
From a local vertex to a compact observable . . . 27

XVIII.3 Wilson loops, knots and open strings **30**
XVIII.3.1 A brane that remembers a knot . . . 30
XVIII.3.2 Intersection strings and the winding operator . . . 32
XVIII.3.3 The exact unknot and its representations . . . 33
XVIII.3.4 Framing and the center factor . . . 35
XVIII.3.5 Linked and knotted observables . . . 36
XVIII.3.6 The observable at fixed t_H . . . 38
Keeping the normalization through a knot calculation . . . 41

XVIII.4 Chern–Simons theory and the resolved conifold **45**
XVIII.4.1 The cycle that changes . . . 45
XVIII.4.2 What the ribbon surface determines . . . 47
XVIII.4.3 The absolute sphere vacuum . . . 48
XVIII.4.4 Two routes to every positive degree . . . 50
XVIII.4.5 Genus coefficients and the normalization left over . . . 52
XVIII.4.6 What the worldsheet mechanism explains . . . 56
XVIII.4.7 The domains of the comparison . . . 59

Reading the conifold comparison coefficient by coefficient 61
Exercises 61
Sources and scope 63

XVIII.5 Open B-model and holomorphic Chern–Simons theory 65
XVIII.5.1 Boundary symmetry selects a holomorphic bundle 66
XVIII.5.2 Ordered disks become a target action 67
XVIII.5.3 Curvature and gauge symmetry 69
XVIII.5.4 A BRST state can be obstructed 71
XVIII.5.5 The cubic coupling detects the obstruction 73
XVIII.5.6 Why complexes help describe boundary states 74
Working through the obstruction before solving for a field 76

XVIII.6 Closed B-model and Kodaira–Spencer theory 80
XVIII.6.1 A closed-string state changes holomorphicity 80
XVIII.6.2 Residual states and the constrained propagator 82
XVIII.6.3 The cubic action and its allowed variations 84
XVIII.6.4 A nonzero cubic on an unobstructed torus family 87
XVIII.6.5 Long tubes, sewing and the one-loop determinant 89
XVIII.6.6 Nodal boundaries and the holomorphic anomaly 92
Choosing the variable that is allowed to vary 95
Exercises 96
Sources and scope 96

XVIII.7 Dijkgraaf–Vafa: matrix models and glueball superpotentials 98
XVIII.7.1 From wrapped curves to a protected coupling 98
XVIII.7.2 Why the open theory becomes a matrix 100
XVIII.7.3 Cuts, Ward identities and glueballs 102
XVIII.7.4 Why four dimensions select planar graphs 104
XVIII.7.5 Gaussian periods, thresholds and gauge input 106
XVIII.7.6 A quartic interaction by two routes 108
XVIII.7.7 What the dictionary determines 110
Repeating the quartic calculation at fixed filling 112
Exercises 113
Sources and scope 114

XVIII.8 Minimal strings, Kontsevich and JT gravity 117
XVIII.8.1 What the boundary remembers 117
XVIII.8.2 Building a minimal worldsheet 118
XVIII.8.3 Why matrix size must scale with criticality 120
XVIII.8.4 What the Kontsevich integral proves 122
XVIII.8.5 From JT geometry to a density 124
XVIII.8.6 Cutting surfaces and knowing what is averaged 126
XVIII.8.7 Exit dictionary 128
Which limit controls a thermal boundary? 128
XVIII.8.8 Written exercises 129

XVIII.9 $N = 2$ strings and self-dual fields **132**
XVIII.9.1 What the worldsheet constraints remove . . . 132
XVIII.9.2 One state with a nonzero cubic interaction . . . 134
XVIII.9.3 Why generic four-point scattering vanishes . . . 135
XVIII.9.4 Reconstructing a self-dual connection . . . 138
XVIII.9.5 Reconstructing self-dual geometry . . . 140
XVIII.9.6 What the dictionary establishes . . . 141
Checking a zero without erasing the interaction . . . 143
Exercises . . . 143
Sources and scope . . . 144

XVIII.10 Twistor lines and gluon amplitudes **146**
XVIII.10.1 Why a line can know an amplitude . . . 146
XVIII.10.2 Spacetime points become twistor lines . . . 147
XVIII.10.3 The chiral content of the open B-model . . . 149
XVIII.10.4 A current cycle and eight odd moduli . . . 150
XVIII.10.5 An independent Yang–Mills recursion . . . 152
XVIII.10.6 What the answer says in singular limits . . . 155
XVIII.10.7 Double traces reveal the extra sector . . . 156
Extracting a component before comparing amplitudes . . . 157
Written exercises . . . 158
Sources and scope . . . 159

XVIII.11 4d Chern–Simons, twisted M-theory and integrability **161**
XVIII.11.1 A position that becomes a spectral parameter . . . 161
XVIII.11.2 Partial flatness and the role of the boundary . . . 162
XVIII.11.3 The spectral curve selects possible families . . . 164
XVIII.11.4 A nonholomorphic propagator produces a holomorphic crossing 166
XVIII.11.5 Color invariance gives the classical Yang–Baxter equation . . 168
XVIII.11.6 An exact fundamental matrix and the framing qualification . 170
XVIII.11.7 A distinct five-dimensional noncommutative theory . . . 172
XVIII.11.8 What the twisted M-theory origin supplies . . . 173
What an exact permutation matrix tests . . . 176

XVIII.12 Two-dimensional Yang–Mills and the Gross–Taylor expansion **178**
XVIII.12.1 Electric flux and sewing . . . 179
XVIII.12.2 A Young diagram separates area from branching . . . 180
XVIII.12.3 From electric representations to sheet permutations . . . 182
XVIII.12.4 Connected surfaces at degree two . . . 184
XVIII.12.5 Fixed twist points and the information in an inverse . . . 186
XVIII.12.6 Opposite orientations interact in $SU(N)$ . . . 187
XVIII.12.7 The density cap and the direction of the dictionary . . . 189
Following connectedness through the reverse dictionary . . . 190
Written exercises . . . 191
Sources and scope . . . 191

How to read this volume

A worldsheet construction can determine a field action, a protected coupling, a scattering recipe or a family of surface amplitudes. These outputs answer different questions. This volume follows the operation that turns string states and their interactions into the specified target quantity. Each route begins by choosing the worldsheet theory, its boundary conditions or insertions, and the part of the target theory that those data control.

The opening route concerns topological open strings. Chapter XVIII.1 explains how removing oscillator excitations leaves a field complex rather than only a finite list of states. Its projected inverse is the operator carried by an internal strip. XVIII.2 applies the disk product and pairing to Chern–Simons theory, then supplies the compact quantum data needed for gluing and framing. XVIII.3 adds knot branes and representation-valued observables. XVIII.4 compares the sphere free energy with a closed-string curve expansion, retaining the continuation and normalization that make the coefficient equality precise. A first reading of these four chapters should follow one object through all four stages: field, propagator, observable and connected free energy.

The next route changes from the A-model to the B-model. XVIII.5 constructs the relative holomorphic Chern–Simons action and exhibits a first-order state that cannot be extended to a global holomorphic deformation. XVIII.6 instead changes complex structure and explains why a nonzero cubic need not obstruct a closed-string deformation. The contrast is calculable. The open example has a constant obstruction outside the image of the differential; the closed example separates background parameters from allowed exact-field variations. XVIII.7 uses further reduction, geometric and chiral inputs to relate matrix planar data to specified four-dimensional holomorphic couplings. The key question throughout this route is which variable is varied and what is held fixed.

The final route contains several distinct uses of worldsheet methods. XVIII.8 follows minimal-string boundaries, intersection numbers and JT thermal observables. Its matrix ensembles organize surfaces with a different physical interpretation from the glueball matrix model. XVIII.9 uses a constrained worldsheet spectrum to reconstruct interacting self-dual fields and a generic four-point cancellation. XVIII.10 derives a relative twistor-line amplitude recipe and compares a family of rational functions with ordinary Yang–Mills recursion. XVIII.11 turns the position of a line in a holomorphic direction into a spectral parameter and derives a bounded integrability dictionary. XVIII.12 starts with independently defined two-dimensional Yang–Mills theory and reorganizes its

fixed-degree expansion into covering surfaces. This last chapter deliberately reverses the principal direction of the volume.

These routes use overlapping mathematics without identifying all their physical theories. A matrix size can count auxiliary index loops without being a spacetime gauge rank. A spectral curve needs a branch, differential and observable before its periods acquire a physical interpretation. A cubic functional needs its domain of variation before its stationary equation can be read off. The worked calculations make these distinctions locally, so that their formulas can be reused with their conditions intact.

Readers following the gauge-action route can begin with XVIII.1–XVIII.7 and then turn to the line operators in XVIII.11. Readers interested in amplitudes should retain the field/cohomology distinction from XVIII.1, read the open B-model construction in XVIII.5, and then follow XVIII.9–XVIII.10. For random surfaces, XVIII.8 and XVIII.12 offer complementary directions; the connected free-energy calculations in XVIII.3–XVIII.4 supply useful preparation. These are reading routes, rather than equivalences between their endpoints.

Each chapter includes a calculation guide before its exercises. The guide returns to an existing example and identifies the order of operations needed to reproduce it. The exercises provide further practice. For benchmark submissions, see `benchmark/PROTOCOL.md`. Chapter-end Sources and scope distinguish mathematical calculations from sourced worldsheet, geometric and physical premises. Those distinctions remain part of the result even when the algebra can be repeated exactly.

Chapter XVIII.1

Why topological string field theory truncates to QFT

A string field has infinitely many oscillator components. A gauge field on a three-manifold has only three local components, but each component is an arbitrary function of position. How can the first description reduce to the second? The distinction between oscillator excitations and spatial dependence is the starting point. Removing excited string oscillators can leave an entire field theory on a brane.

We study open topological A-model strings ending on the zero section of T^*M. Here M is a closed oriented Riemannian three-manifold. A flat unitary bundle E supplies Chan–Paton coefficients. The twist and the boundary form complex were introduced in Chapters V.1 and V.6. We recall their physical identification, then derive the propagator that makes the reduction useful for interactions. The reader should be able to distinguish a field from its cohomology class, compute a Fourier-mode contraction, and explain why a worldsheet strip can contribute even when its integrand tends to zero at every fixed length.

The construction has a special domain. It uses the open A-model on an exact cotangent target, together with its topological Ward identities and sewing prescription. The cubic algebra of string field theory provides a bridge to the field action. The bridge does not require a treatment of physical superstring field theory. Chapter 2 will develop the Chern–Simons normalization and its observables; here the task is to understand how the field variables, vertices and propagator survive the worldsheet limit.

XVIII.1.1 What is actually being truncated?

In the large-t topological limit, the low-lying string wavefunctions depend on bosonic zero modes $q \in M$ and fermionic zero modes χ. Excited oscillators are in their vacuum. The fermionic variables anticommute, so their expansion terminates, while the coefficient functions retain arbitrary q dependence. With the source-local identification $\chi = -dq$,

this gives the form complex

$$\mathcal{H}_{\text{form}} = \Omega^\bullet(M, \operatorname{End} E), \qquad Q = d, \qquad d^2 = 0. \tag{XVIII.1.1}$$

Here and below d is the covariant exterior differential of the flat reference connection. Flatness is what makes it a differential. The equality $Q = d$ uses the stated identification of fermionic zero modes; nilpotence alone would not identify the string BRST operator with an exterior derivative.

There are only four possible form degrees on M, from zero to three. There are still infinitely many functions in each degree. On the flat torus with coordinates of period 2π and trivial E, a one-form can be written as

$$A(q) = \sum_{n \in \mathbb{Z}^3} \sum_{j=1}^{3} A_{j,n} e^{in\cdot q}\, dq^j, \qquad A_{j,n} \in \operatorname{Mat}_N(\mathbb{C}). \tag{XVIII.1.2}$$

The absence of oscillator creation operators in this expression has not removed any of the Fourier labels n. Smoothness constrains the decay of the coefficients as $|n|$ grows. It does not restrict the sum to $n = 0$.

BRST cohomology asks a different question. It identifies closed states modulo exact states. For the scalar trivial-bundle torus, its dimensions are

$$\dim H^p(T^3, \mathbb{C}) = \binom{3}{p}, \qquad p = 0, 1, 2, 3. \tag{XVIII.1.3}$$

For trivial rank-N Chan–Paton coefficients, these dimensions become $N^2\binom{3}{p}$. This multiplicity uses the constant matrix basis of $\operatorname{End} E$. An arbitrary flat bundle need not have the same cohomology. Even in the trivial case, H^1 describes linearized physical classes rather than all one-forms entering the field action.

Figure XVIII.1.1 separates the two reductions. The first arrow removes string oscillator excitations using the A-model dynamics. The second passes from forms to harmonic representatives using a metric and Hodge theory. Interactions make this second operation more than a restriction of variables: nonharmonic fields can be internal lines even when external states are harmonic. We therefore need an inverse kinetic operator on the complement of the harmonic space.

For a fixed target Laplace eigenvalue λ, the low-lying worldsheet energy scales as $1/t$. This statement does not cover arbitrarily large λ uniformly. Thus the limit is a statement about the sourced low-lying sector, with target modes held fixed during the comparison. Treating t as a spacetime momentum cutoff would obscure precisely the spatial field dependence that remains in (XVIII.1.2).

XVIII.1.2 The propagator remembers nonharmonic fields

A propagator must invert the kinetic operator where that inverse exists. On our compact positive Hodge complex, the obstruction is the harmonic subspace. Let d^* be the adjoint

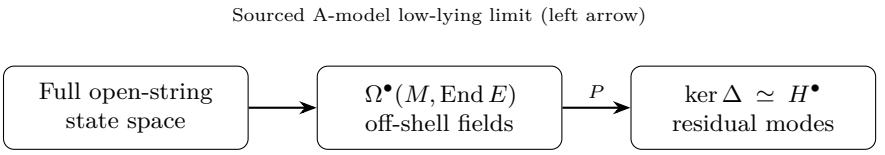


Figure XVIII.1.1: Two distinct reductions for the cotangent open A-model. The left arrow is the sourced oscillator reduction. The right arrow projects the resulting differential complex onto harmonic representatives. Constructing residual interactions also requires the homotopy on the complementary modes.

of d with respect to the positive L^2 inner product, and define

$$\Delta = dd^* + d^*d, \qquad (u, \Delta u) = \|du\|^2 + \|d^*u\|^2. \tag{XVIII.1.4}$$

The inner product includes the Riemannian metric and the Hermitian metric on $\operatorname{End} E$. Unitarity of the flat connection is part of this setup. Both terms on the right are nonnegative. Hence a harmonic form is simultaneously closed and coclosed,

$$\ker \Delta = \ker d \cap \ker d^*. \tag{XVIII.1.5}$$

Conversely, a closed and coclosed form is annihilated by Δ directly from its definition. Positivity therefore gives both directions of the identification.

Compact elliptic Hodge theory supplies the orthogonal projector P onto this kernel and a canonical Green operator G. Normalize the latter to vanish on the kernel,

$$G\Delta = \Delta G = 1 - P, \qquad GP = PG = 0. \tag{XVIII.1.6}$$

Writing $G = \Delta^{-1}$ without its domain would lose this normalization. An inverse eigenvalue $1/\lambda$ is meaningful for $\lambda > 0$; it is not assigned to a harmonic mode. The existence of P and G is the mathematical input. We can now derive the relation needed for propagation.

On smooth forms, d and d^* commute with Δ and with its Green operator. Define a degree-minus-one operator $h = d^*G$. Then

$$dh + hd = (dd^* + d^*d)G = 1 - P. \tag{XVIII.1.7}$$

The same commutation and $(d^*)^2 = 0$ give

$$h^2 = (d^*)^2 G^2 = 0, \qquad hP = Ph = 0. \tag{XVIII.1.8}$$

The projector is not a small correction. It says which variables remain as residual fields rather than receiving a propagator. Applying (XVIII.1.7) to a closed form makes the cohomological content explicit,

$$du = 0 \quad \Longrightarrow \quad u = Pu + dhu. \tag{XVIII.1.9}$$

Thus u and Pu differ by an exact form. This establishes why harmonic representatives compute cohomology. It also displays the operator h that is needed before internal nonharmonic fields can be removed from interactions.

For a general smooth form, the decomposition instead retains both differential terms,

$$u = Pu + dd^*Gu + d^*dGu. \tag{XVIII.1.10}$$

The second and third summands are respectively exact and coexact. Figure XVIII.1.2 represents this splitting. Although it is convenient to use a metric to construct the splitting, no metric independence of a quantum amplitude follows from this algebra alone. The physical sewing prescription will tell us why this particular homotopy is the internal-edge operator.

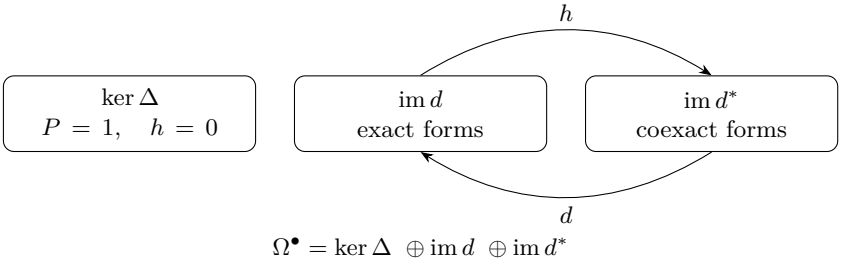


Figure XVIII.1.2: The orthogonal Hodge splitting on closed compact M with a flat unitary coefficient bundle. On exact forms $dh = 1$, while on coexact forms $hd = 1$; the arrows change form degree. Harmonic forms are residual variables, with no inverse Laplace eigenvalue assigned to them.

We can see every sign and the harmonic exception explicitly on the flat torus. Write ϵ_j for left wedge by dq^j, and ι_j for contraction with its Euclidean dual vector. Their exterior-algebra relations are

$$\{\epsilon_i, \epsilon_j\} = 0, \qquad \{\iota_i, \iota_j\} = 0, \qquad \{\epsilon_i, \iota_j\} = \delta_{ij}. \tag{XVIII.1.11}$$

For example, contraction of $dq^i \wedge \alpha$ gives $\delta_{ij}\alpha - dq^i \wedge \iota_j\alpha$. Adding $dq^i \wedge \iota_j\alpha$ leaves $\delta_{ij}\alpha$, which proves the mixed relation on any form. Put $\epsilon_n = \sum_j n_j\epsilon_j$ and $\iota_n = \sum_j n_j\iota_j$. Multiplying the mixed relation by n_in_j gives

$$\epsilon_n\iota_n + \iota_n\epsilon_n = |n|^2\, 1. \tag{XVIII.1.12}$$

This relation holds on the entire exterior algebra, not only on scalar states.

Differentiating $e^{in\cdot q}$ fixes the Fourier sign. We include a positive auxiliary differential scale s to keep that sign and its reciprocal in view; the physical torus differential has $s = 1$. It is not a new radius or a change of the worldsheet dictionary. On a mode n the operators are

$$d_n = is\epsilon_n, \qquad d_n^* = -is\iota_n, \qquad \Delta_n = s^2|n|^2\, 1. \tag{XVIII.1.13}$$

The adjoint has the opposite sign because complex conjugation sends i to $-i$. For $n \neq 0$, the Green operator and homotopy are therefore

$$G_n = \frac{1}{s^2|n|^2}\,1, \qquad h_n = -\frac{i\iota_n}{s|n|^2}, \qquad P_n = 0. \tag{XVIII.1.14}$$

Substitution reduces $d_n h_n + h_n d_n = 1$ to (XVIII.1.12). At $n = 0$ every derivative vanishes, so the correct separate branch is

$$d_0 = d_0^* = h_0 = G_0 = 0, \qquad P_0 = 1. \tag{XVIII.1.15}$$

A mode with one zero component is not on this branch. For instance, $(0, 2, 3)$ has $|n|^2 = 13$ and uses (XVIII.1.14).

Take $n = (1, 2, -2)$ for a worked calculation. The contraction of dq^1 is one and the squared norm is nine. Hence

$$h_n(dq^1) = -\frac{i}{9s}, \qquad d_n(1) = is(dq^1 + 2dq^2 - 2dq^3), \qquad h_n d_n(1) = 1. \tag{XVIII.1.16}$$

The last identity illustrates acyclicity on scalars. To see acyclicity in all degrees, choose a covector basis whose first member is parallel to n. Wedge by n pairs each form lacking that covector with the corresponding form containing it. In three dimensions the degree-wise ranks are

$$\big(\operatorname{rank} d_n|_{\Omega^0}, \operatorname{rank} d_n|_{\Omega^1}, \operatorname{rank} d_n|_{\Omega^2}\big) = (1, 2, 1), \qquad n \neq 0. \tag{XVIII.1.17}$$

These ranks refer to one scalar exterior factor. The matrix factor multiplies them by N^2 for trivial rank-N E. At zero momentum all differentials vanish and the dimensions are $(1, 3, 3, 1)$ per matrix component, reproducing (XVIII.1.3).

Finally, this mode argument extends to smooth fields. For fixed $s > 0$, the norm of h_n decays as $|n|^{-1}$. Multiplication by this factor preserves rapid Fourier decay. We may therefore apply the contraction mode by mode to a smooth form and obtain another smooth form. The calculation is not restricted to a finite Fourier sum. On a noncompact M, a manifold with boundary, or a nonunitary or nonflat reference bundle, the spectral and domain assumptions must be reconsidered before using the same inverse.

XVIII.1.3 Where a disappearing strip keeps its weight

The Hodge homotopy has a worldsheet origin. Sewing open strings introduces a strip of length ℓ. Its evolution suppresses positive worldsheet energies, and integration over the strip modulus includes an antighost insertion b. To understand what this operation does, first keep the upper length cutoff R finite. Suppose $Q^2 = b^2 = 0$ and

$$L = Qb + bQ, \qquad H_R = \int_0^R d\ell\, b\, e^{-\ell L}. \tag{XVIII.1.18}$$

We assume L is nonnegative self-adjoint, Q and b commute with its spectral resolution on a common invariant domain, and both annihilate its kernel. These hypotheses hold for the compact Hodge realization used here. They are not being inferred for an arbitrary string state space.

On the positive spectral subspace, integrate the exponential before taking any limit. With P the kernel projector,

$$H_R = bL^{-1}(1 - e^{-RL})(1 - P). \tag{XVIII.1.19}$$

There is no kernel term because $bP = 0$. Anticommuting Q through the integral gives a useful boundary expression,

$$QH_R + H_R Q = \int_0^R d\ell\, Le^{-\ell L} = 1 - e^{-RL}. \tag{XVIII.1.20}$$

The last expression is also zero on the kernel. On its complement, a spectral gap lets R tend to infinity. The result obeys

$$H = bL^{-1}(1 - P), \qquad QH + HQ = 1 - P. \tag{XVIII.1.21}$$

The total derivative in strip length has left a boundary contribution. This is the elementary reason that a topological variation need not remove a degeneration region of moduli space.

Now insert the low-lying A-model dictionary. In the source normalization, for fixed target eigenvalues at large t,

$$Q = d, \qquad L_0 \simeq a(t)\Delta, \qquad b_0 \simeq a(t)d^*, \qquad a(t) = \frac{\pi}{2t}. \tag{XVIII.1.22}$$

The parameter t controls the sigma-model deformation. It is distinct from the strip length. The asymptotic signs indicate statements about the low-lying sector of the source theory. For the next calculation we use the limiting form model in which $L = a\Delta$ and $b = ad^*$ hold exactly. Cancelling the two factors of a after integrating gives

$$bL^{-1}(1 - P) = ad^*(a\Delta)^{-1}(1 - P) = d^*G = h. \tag{XVIII.1.23}$$

This cancellation explains how a finite field propagator survives. Its physical identification with the gauge-fixed Chern–Simons propagator additionally uses the source's strip insertion and sewing measure.

There is a tempting wrong order of operations. For a positive target eigenvalue λ, the scalar weight multiplying d^* is

$$K_t(\ell; \lambda) = \frac{\pi}{2t} \exp\left(-\frac{\pi\lambda\ell}{2t}\right). \tag{XVIII.1.24}$$

At each fixed ℓ, this tends to zero as t tends to infinity. The integration interval, however, is unbounded. Its exact accumulated weight is

$$I_t(R; \lambda) = \int_0^R K_t(\ell; \lambda) d\ell = \frac{1 - e^{-\pi\lambda R/(2t)}}{\lambda}. \tag{XVIII.1.25}$$

At fixed finite R, this also tends to zero. If we instead remove the length cutoff at fixed t, the integral is $1/\lambda$. Thus the iterated limits disagree,

$$\lim_{t\to\infty}\lim_{R\to\infty} I_t(R;\lambda) = \frac{1}{\lambda}, \qquad \lim_{R\to\infty}\lim_{t\to\infty} I_t(R;\lambda) = 0. \tag{XVIII.1.26}$$

There is no integrable bound, uniform in t, that would justify the attempted exchange on the half-line. Each kernel has the same area while spreading over larger strip lengths.

The location of that area can be calculated rather than guessed. Change variables to $u = a(t)\ell$. Then

$$\int_0^\infty K_t(\ell;\lambda)d\ell = \int_0^\infty e^{-\lambda u}du = \frac{1}{\lambda}. \tag{XVIII.1.27}$$

Lengths of order t correspond to finite u. In particular a moving window $R = ct$, with $c > 0$, captures the fraction

$$\frac{I_t(ct;\lambda)}{I_t(\infty;\lambda)} = 1 - e^{-\pi\lambda c/2}. \tag{XVIII.1.28}$$

This fraction is independent of t. Figure XVIII.1.3 shows the effect at $\lambda = 1$: height decreases, the distribution broadens, and the accumulated weight still approaches one. The long strip retains the field-theory internal line.

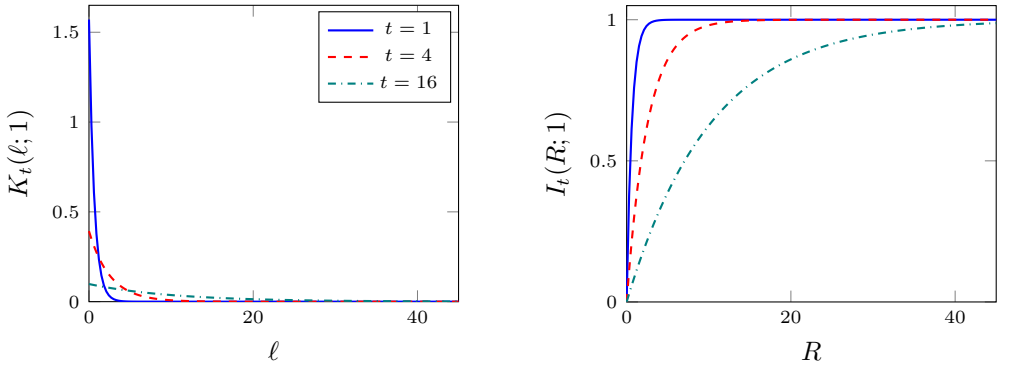


Figure XVIII.1.3: Exact limiting-form kernels (left) and their accumulated integrals (right), generated from (XVIII.1.24)–(XVIII.1.25) at $\lambda = 1$. Blue solid, red dashed and teal dash-dotted curves have $t = 1, 4, 16$, respectively. Each kernel has total area one over the half-line, although the weight moves beyond any fixed finite length window as t grows. The panels show a finite window of that half-line.

The kernel branch remains essential throughout this argument. For a harmonic state the scalar formula $1/\lambda$ must not be used. In the Hodge model, $d^*P = 0$, so the actual strip insertion annihilates that state. Harmonic variables remain outside the internal inverse. The scalar limit also says nothing by itself about oscillator corrections, loop regularization or contact terms. Those issues require the physical measure and sewing analysis. What has been derived is the precise long-strip mechanism in the limiting form sector.

XVIII.1.4 From the cubic vertex to a field action

Propagation alone does not construct an interacting theory. We also need the open-string vertices. The relevant string-field template is a cyclic differential graded algebra: a degree-one field A, a degree-one differential Q, an associative product, and a cyclic integral of total degree minus three. In the A-model limit their physical identification is

$$Q \longmapsto d, \qquad A \cdot B \longmapsto A \wedge B, \qquad \int \longmapsto \int_M \mathrm{Tr}\,. \tag{XVIII.1.29}$$

The product on the right includes ordered matrix multiplication. For homogeneous matrix-valued forms, cyclicity includes the exterior sign,

$$\int_M \mathrm{Tr}(\alpha \wedge \beta) = (-1)^{|\alpha||\beta|} \int_M \mathrm{Tr}(\beta \wedge \alpha), \qquad |\alpha| + |\beta| = 3. \tag{XVIII.1.30}$$

One cannot reorder Chan–Paton matrices independently of the form factors. Figure XVIII.1.4 indicates the cyclic boundary order underlying the cubic interaction.

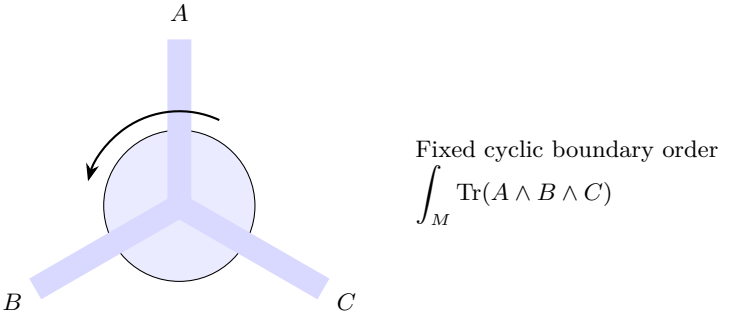


Figure XVIII.1.4: Schematic cubic open-string vertex with three sewn strips. The indicated cyclic order labels the ordered form and Chan–Paton factors in the disk vertex. For degree-one forms, cycling a factor past the other two has positive exterior sign. The diagram specifies an ordering; it does not parametrize disk moduli.

Using the quadratic and cubic disk identifications gives the classical form action. We now take A to be the ordinary degree-one connection fluctuation about the flat reference, and suppress wedge symbols between forms,

$$S[A] = \kappa \int_M \mathrm{Tr}\left(\frac{1}{2} A\, dA + \frac{1}{3} A^3\right), \qquad \kappa = \frac{k}{2\pi}. \tag{XVIII.1.31}$$

The parameter k here is bare. The action is the Chern–Simons expression $k \int \mathrm{Tr}(A\, dA + 2A^3/3)/(4\pi)$ in the convention recalled from Chapter V.6. Its quantum shift, reality and framing dictionary are tasks for Chapter 2. No extra factor of i is supplied by the complex graded algebra alone.

We can derive its variation without assuming the equation of motion. Since M has no boundary, Stokes' theorem and $|A| = 1$ give

$$\int_M \mathrm{Tr}(A\, d\delta A) = \int_M \mathrm{Tr}(dA\, \delta A) = \int_M \mathrm{Tr}(\delta A\, dA). \tag{XVIII.1.32}$$

The sign in the first equality follows from $d(A\delta A) = dA\delta A - A\, d\delta A$. Moving a degree-two form past a degree-one form gives positive sign in the second equality. The two quadratic variations therefore coincide,

$$\delta\left[\frac{1}{2}\int_M \mathrm{Tr}(A\, dA)\right] = \int_M \mathrm{Tr}(\delta A\, dA). \tag{XVIII.1.33}$$

For the cubic term, cyclically moving a degree-one factor past two degree-one factors also gives positive sign. Its three terms are equal,

$$\delta\left[\frac{1}{3}\int_M \mathrm{Tr}(A^3)\right] = \int_M \mathrm{Tr}(\delta A\, A^2). \tag{XVIII.1.34}$$

Combining them identifies the curvature and the literal stationary equation,

$$\delta S = \kappa \int_M \mathrm{Tr}(\delta A\, F), \qquad F = dA + A^2, \qquad \kappa F = 0. \tag{XVIII.1.35}$$

For $\kappa \neq 0$ and nondegenerate trace pairing, arbitrary variations impose $F = 0$. At $\kappa = 0$ the action vanishes and imposes no equation. The latter case cannot be used as a perturbative expansion with the same kinetic inverse.

Infinitesimal gauge invariance follows from the same graded algebra. For a degree-zero parameter ε, use

$$\delta_\varepsilon A = d\varepsilon + A\varepsilon - \varepsilon A. \tag{XVIII.1.36}$$

Expanding the derivative of F gives $dF = dA\, A - A\, dA$. The commutator with A cancels these two terms,

$$dF + AF - FA = 0. \tag{XVIII.1.37}$$

Integration by parts and cyclicity then yield

$$\delta_\varepsilon S = -\kappa \int_M \mathrm{Tr}\big[\varepsilon(dF + AF - FA)\big] = 0. \tag{XVIII.1.38}$$

This proves classical infinitesimal invariance. It does not determine a large-gauge phase or a quantum measure. Those require additional global and quantum information.

Why is the cotangent example special enough to use these vertices without smooth nonconstant disk corrections? Write the symplectic form as $\omega = d\theta$, where θ is the canonical one-form. On the zero section, θ restricts to zero. For a smooth compact unpunctured pseudoholomorphic disk u with boundary on that section, Stokes' theorem gives

$$\mathrm{Area}(u) = \int_D u^*\omega = \int_{\partial D} u^*\theta = 0. \tag{XVIII.1.39}$$

For a compatible almost complex structure, the area is a positive multiple of the Dirichlet energy. A zero-energy map has vanishing derivative, so u is constant. Exactness and the boundary restriction have done the work. Noncompactness of the ambient target alone would not imply this conclusion.

A degeneration into constant pieces joined by long strips is not a smooth nonconstant disk of the type excluded by (XVIII.1.39). Such configurations can still produce propagators and interactions. The topological Ward argument for t independence and the measure at these degenerations are physical inputs of the A-model construction. Together with the source's sewing analysis they support the special perturbative open-sector reduction. The disk area calculation supplies one ingredient; it does not prove quantum decoupling of the closed sector or a nonperturbative string/field-theory equivalence.

XVIII.1.5 Why retaining cohomology is a further operation

We have retained an off-shell field complex and an interacting action. Suppose the next goal is a theory only of residual harmonic variables. It is insufficient to set every complementary variable to zero. Solving for those variables, or integrating them out, can create interactions among the variables that remain. A small algebraic example isolates the issue without the complications of gauge fixing.

Let x be retained and y eliminated in the action

$$S(x,y) = \frac{m}{2}y^2 + gyx^2, \qquad m \neq 0. \tag{XVIII.1.40}$$

Stationarity with respect to y gives

$$\frac{\partial S}{\partial y} = my + gx^2 = 0, \qquad y_*(x) = -\frac{g}{m}x^2. \tag{XVIII.1.41}$$

Substitute both terms of the action, keeping their relative sign,

$$S(x,y_*) = \frac{g^2x^4}{2m} - \frac{g^2x^4}{m} = -\frac{g^2x^4}{2m}. \tag{XVIII.1.42}$$

Setting $y = 0$ at the beginning would instead give zero. The induced quartic is an exchange effect: two cubic couplings communicate through the eliminated variable with inverse coefficient $1/m$.

Completing the square makes the same calculation transparent,

$$S(x,y) = \frac{m}{2}\left(y + \frac{g}{m}x^2\right)^2 - \frac{g^2x^4}{2m}. \tag{XVIII.1.43}$$

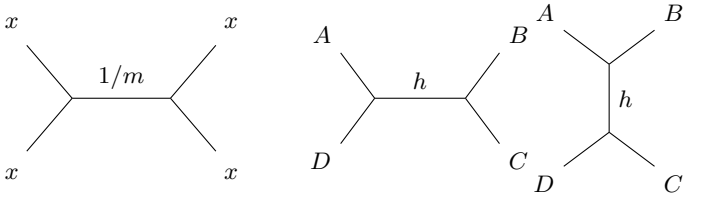
For real $m > 0$ and fixed real x, the real Gaussian integral is convergent and gives

$$\int_{\mathbb{R}} dy\, e^{-S(x,y)} = \sqrt{\frac{2\pi}{m}}\, e^{g^2x^4/(2m)}. \tag{XVIII.1.44}$$

Its x-dependent effective action is exactly (XVIII.1.42); the determinant is independent of x. The negative quartic is not a stable potential for an unrestricted subsequent real x integral. This is a local elimination example, not a string model or a proposed BRST doublet.

The limiting cases explain the domain of the elimination. At $g = 0$, the two variables decouple and the quartic vanishes. At fixed g, x and $m \to \infty$, it also vanishes. At $m \to 0$, the inverse coefficient is singular. The equation for y then ceases to determine y in terms of x. A variable with zero kinetic coefficient belongs among residual variables, exactly as a harmonic mode did in the Hodge discussion.

In the actual form complex, h is the operator on internal edges when nonharmonic variables are eliminated. The source's cyclic disk four-point construction has two channels for a fixed cyclic order. Each channel contains intermediate propagation, even though its external physical states can be represented by cohomology classes. Figure XVIII.1.5 puts this worldsheet structure beside the auxiliary exchange. The comparison explains why an internal inverse matters. It does not identify the amplitudes of the two systems or fix the signs of general higher products.



Auxiliary exchange
$S_{\text{eff}} = -g^2x^4/(2m)$

Two disk channels
cyclic order A, B, C, D

Figure XVIII.1.5: Left: eliminating an auxiliary variable connects two cubic couplings through $1/m$ and induces a quartic. Right: both disk diagrams have clockwise external order A, B, C, D. The horizontal internal edge separates (D, A) from (B, C); the vertical edge separates (A, B) from (C, D). Each contains the form propagator h. Both pictures retain intermediate variables, but the auxiliary polynomial is not a model for the disk amplitude or its signs.

The distinction can now be stated operationally. Cohomology classifies linearized external states. The action supplies interaction vertices on the full form complex. A residual effective theory additionally requires internal propagation and elimination. Knowing the dimensions $(1, 3, 3, 1)$ does not supply those interactions. Chapter V.6 introduces their higher-operation language; the cubic action and long-strip calculation here show why that language is needed.

XVIII.1.6 Exit dictionary and limits

The construction begins with a physical boundary condition: open A-model strings end on the exact zero section of T^*M. Its low-lying oscillator vacuum is a wavefunction on

M, so its coefficients are fields. The source identifies its differential with d, its quadratic and cubic vertices with the cyclic form expressions, and its integrated strip with the nonharmonic propagator. We summarize the operations in the following dictionary,

$$\begin{aligned} \text{low-lying string states} &\longleftrightarrow \Omega^\bullet(M, \operatorname{End} E), \\ \text{BRST differential} &\longleftrightarrow d, \\ \text{ordered disk vertex} &\longleftrightarrow \int_M \operatorname{Tr}(A^3), \\ \text{integrated internal strip} &\longleftrightarrow d^* G, \\ \text{linearized physical states} &\longleftrightarrow H^\bullet(M, \operatorname{End} E). \end{aligned} \tag{XVIII.1.45}$$

The first four lines construct ingredients of a field theory. The last line is a statement about physical classes. The distinction prevents a finite cohomology calculation from replacing the interacting field problem.

Each ingredient also identifies a useful boundary of the example. For a general Lagrangian brane, the disk area need not vanish and disk corrections can change the interaction algebra. For noncompact M or a boundary, the Green operator requires its own domain and boundary conditions. With a curved reference connection, nilpotence of the covariant differential requires a separate check; the flat-complex hypothesis used here no longer applies. Closed-string dynamics requires separate analysis even when the smooth compact disk argument holds.

Chapter 2 starts from the resulting open Chern–Simons action and develops its coupling and framing data. The holomorphic Chern–Simons and BCOV constructions in Chapters 5–6 require their own worldsheet dictionaries; replacing the letter d in this chapter would not derive them. The reverse Gross–Taylor expansion in Chapter 12 answers a different question, beginning with a field theory and organizing it as a string expansion. Here the direction has remained from worldsheet states and sewing to the field theory on the brane.

Following an internal line

To use the reduction in a calculation, begin with the field space rather than with a count of physical states. The external field in (XVIII.1.2) has arbitrary smooth Fourier coefficients. At a cubic vertex these fields are multiplied before any harmonic projection. An intermediate component produced by that multiplication can therefore lie outside cohomology. It is precisely on that component that the Green operator acts. Projecting every field to cohomology at the outset would remove the internal line that is meant to transmit the interaction.

The Fourier example provides a way to follow this operation without suppressing the differential. For the stated nonzero momentum, first wedge with the momentum covector, then contract with its dual. Reversing these two operations gives the other term in (XVIII.1.12). Neither term alone is an inverse on every form degree. Their sum is the scalar squared norm, which cancels the denominator of the Green operator. The factors is and $-i/s$ then cancel as well. At zero momentum this sequence is replaced by the separate projector branch. There is no limiting assignment of an infinite propagator to the residual field.

The strip calculation adds the physical ingredient to this algebra. Its length is integrated over a noncompact interval. When the topological metric parameter changes, the interval of lengths contributing appreciably can move to arbitrarily large values. Inspecting a fixed strip length consequently misses part of the integral. This is why a vanishing fixed-length integrand can still give the finite internal-edge homotopy. The relevant order is to perform the strip integral with the harmonic projection specified, then take the stated low-mode limit.

Chapter XVIII.2 uses the resulting product, differential and pairing to fix the relative gauge-action coefficients. The quantum level, compact gauge sector and framing data enter there as additional input. Keeping this order separates the worldsheet explanation of the field action from the quantum information needed to calculate its observables.

Exercises

1. On the trivial rank-N bundle over the period-2π torus, compare the oscillator vacuum, $\Omega^1(T^3, \operatorname{End} E)$ and $H^1(T^3, \operatorname{End} E)$. Explain which space retains arbitrary Fourier coefficients and which has dimension $3N^2$. Does every one-form define a physical BRST class?

2. Use ϵ_n and ι_n with the positive auxiliary scale s. For $n = (1, 2, -2)$ derive d_n, d_n^*, G_n, h_n and evaluate $h_n(dq^1)$ and $h_n d_n(1)$. Derive the ranks in degrees zero, one and two. Give the separate $n = 0$ answer and explain the factor N^2 for trivial Chan–Paton coefficients. Check that $n = (0, 2, 3)$ uses the nonzero-mode branch.

3. For $\lambda > 0$, integrate $K_t(\ell; \lambda)$ up to R. Compute both iterated limits in R and t, with their order written explicitly. Then set $R = ct$ and determine the fraction of the full integral captured by this window. Explain why pointwise convergence does not determine the half-line integral.

4. Vary the cyclic form action on closed M, displaying the integration-by-parts and cubic cyclicity signs. State the literal field equation at arbitrary κ and explain what changes at $\kappa = 0$. Separately, prove constancy of a smooth compact unpunctured pseudoholomorphic disk on the exact zero section. Which boundary and positivity hypotheses are needed? Why does ambient noncompactness not suffice?

5. Eliminate y from (XVIII.1.40) by stationarity and by completing the square. For real $m > 0$, evaluate the fixed-x Gaussian integral. Explain the limits $g = 0$, $m \to \infty$ and $m \to 0$, and why the resulting quartic is not a stable standalone real potential.

6. Assess the statement: "BRST cohomology is finite, therefore every topological string is exactly a finite theory." Identify the confusions about fields and classes, the special role of exact disks, and the measure, boundary and quantum assumptions that an actual reduction needs.

Sources and scope

The cotangent open A-model construction is perturbative. The limiting form-sector identification uses the topological twist and the bare Chern–Simons normalization stated above. The physical construction depends on the worldsheet assumptions described below.

§1. The worldsheet identification of low-lying states with $\mathrm{End}(E)$-valued forms uses Witten (1995), arXiv v2 pp. 21–22, (3.19)–(3.22) [WS-T]. V.1 and V.6 provide the twist and boundary prerequisites. The torus comparison illustrates the distinction between cohomology and off-shell fields.

§2. [MATH] Positivity identifies the harmonic kernel. [MATH] The normalized Green operator gives the homotopy and side conditions. Hodge existence is imported from Demailly (2002), Part I, Theorem 3.15 and proof, Corollary 3.16 (printed pp. 15–16; PDF pp. 27–28), and §4.C, Theorems 4.16–4.17 (printed pp. 19–20; PDF pp. 31–32). Apply the flat Hermitian bundle statement to $\mathrm{End}(E)$; the source's harmonic projector is our P. [MATH] Exterior-algebra relations and the Fourier signs are derived locally. [MATH] Smooth torus acyclicity and the scalar/per-component ranks, with the trivial-bundle N^2 qualifier, follow from the mode contraction and rapid decay. The source propagator anchor is Witten pp. 34–35, (4.10)–(4.14).

§3. [MATH] The truncated spectral integral and its boundary identity hold under the stated domain assumptions. [MATH] The scalar integral and noncommuting limits are derived explicitly. [WS-T] The physical identification with the gauge-fixed CS propagator uses Witten pp. 34–35, (4.10)–(4.14), together with (3.21)–(3.22). The scalar calculation does not prove the worldsheet measure or convergence of the full moduli integral.

§4. [MATH] Variation, Bianchi identity and infinitesimal invariance are local graded calculations; flatness requires nonzero κ. [WS-T] Quadratic/cubic vertex identification uses Witten pp. 24–30, (4.1)–(4.2), (4.7)–(4.9). [MATH] Exactness, the zero-section boundary condition and positivity prove constancy of the stated compact disks; Witten pp. 26–30, (4.3)–(4.4). [WS-T] The perturbative reduction retains the source's Ward, anomaly, measure and sewing hypotheses, pp. 30–38. The explicit closed-sector caution on p. 36 remains outside the disk conclusion.

§5–6. [MATH] Auxiliary elimination is a local algebraic example with $m \neq 0$ and a real Gaussian interpretation only at $m > 0$. [WS-T] The two cyclic disk channels are sourced structurally to Witten pp. 36–38, (4.15)–(4.19). No new four-point amplitude or general signed transfer formula is computed.

The physical Ward identities and Hodge existence remain inputs. The perturbative sewing retains degeneration contributions even at zero disk area, and the strip inverse leaves harmonic modes external.

References

Demailly, J.-P. (2002). "L^2 Hodge Theory and Vanishing Theorems". In: *Introduction to Hodge Theory*. Vol. 8. SMF/AMS Texts and Monographs. Part I, Theorem 3.15 and proof, Corollary 3.16, Section 4.C, Theorems 4.16–4.17; printed pages 15–16 and 19–20. American Mathematical Society and Societe Mathematique de France.

Witten, E. (1995). "Chern-Simons Gauge Theory As A String Theory". In: *Prog. Math.* 133. Version 2; source page anchors refer to the 60-page arXiv PDF, pp. 637–678. arXiv: `hep-th/9207094`.

Chapter XVIII.2

Open A-model on T^*M: Chern–Simons theory

A Chern–Simons gauge field is a one-form on a three-manifold. In the open A-model on T^*M, the same one-form is a ghost-number-one boundary string field. This identification is more than a match of state spaces. The cyclic order of three boundary insertions produces the nonabelian cubic interaction, while the two-string pairing supplies the kinetic term. Together they assemble the Chern–Simons action.

We take M to be a closed oriented three-manifold and put N zero-section branes on it, with a flat unitary reference bundle E and $B = 0$. Chapter 1 identified the reduced open-string field complex with $\Omega^\bullet(M, \operatorname{End} E)$ and its integrated strip with the propagator on nonharmonic forms. Here we use those ingredients to construct the gauge action. We then ask which further quantum information is needed to compute a partition function. The answer will involve a shifted coupling and a choice of two-framing. Neither follows by varying the classical action.

The compact calculation in this chapter concerns $SU(2)$ Chern–Simons theory at positive integer level. It is an additional quantum field-theory input, connected to the worldsheet construction by the action and coupling dictionary. The local $U(N)$ brane action by itself does not determine its global quantum completion. Chapters 3 and 4 will develop Wilson loops and large-N relations; the present chapter supplies the gauge and framing conventions they need.

XVIII.2.1 How a boundary vertex becomes a gauge interaction

The low-lying ghost-one string field is $\Psi = \chi^a A_a(q)$. The zero modes χ^a behave as anticommuting basis one-forms, so $A = A_a\, dq^a$ is an $\operatorname{End} E$-valued one-form. The boundary product combines exterior multiplication with ordered matrix multiplication.

For three possibly different fields, the disk correlator has the form

$$\int d^3q\, d^3\chi\ \mathrm{Tr}[(\chi^a A_a)(\chi^b B_b)(\chi^c C_c)] = \int_M \mathrm{Tr}(A\wedge B\wedge C), \qquad \int d^3\chi\, \chi^1\chi^2\chi^3 = 1. \tag{XVIII.2.1}$$

The right-hand side retains the boundary order. Exchanging two insertions changes both an exterior sign and the matrix order. The sourced worldsheet identification and cyclic action are needed to turn this formal zero-mode integral into a string interaction.

One small matrix calculation shows why order matters. Put $H = \mathrm{diag}(1,-1)$ and let E_{12}, E_{21} be the elementary 2×2 matrices. On a unit-period coordinate chart with orientation $dx\wedge dy\wedge dz$, choose three polarized insertions

$$A_1 = aH\,dx, \qquad A_2 = bE_{12}\,dy, \qquad A_3 = cE_{21}\,dz. \tag{XVIII.2.2}$$

Since $\mathrm{Tr}(HE_{12}E_{21}) = 1$, their single ordered vertex is abc. If instead $A = A_1 + A_2 + A_3$ is one field, expansion of $\mathrm{Tr}(A^3)$ includes all six permutations. Exterior signs and matrix commutators combine to give

$$\mathrm{Tr}(A^3) = 3\,\mathrm{Tr}\big(A_x[A_y, A_z]\big)\,dx\wedge dy\wedge dz = 6abc\,dx\wedge dy\wedge dz. \tag{XVIII.2.3}$$

Replacing the matrices by commuting numbers would set this cubic to zero. The factor six also explains why one polarized disk vertex must not be identified with the full cubic polynomial.

It is useful to account for the six terms rather than absorb them into the notation A^3. The three cyclic words $HE_{12}E_{21}$, $E_{12}E_{21}H$ and $E_{21}HE_{12}$ have trace $+1$ and preserve the orientation of $dx\wedge dy\wedge dz$. The other three words have trace -1 and reverse that orientation. Thus every term contributes $+abc$ to the oriented volume form. A cyclic disk vertex chooses one boundary order; the polynomial $\mathrm{Tr}(A^3)$ substitutes the same sum $A_1 + A_2 + A_3$ into all three slots. This distinction is also why the noncommutative Chan–Paton product is a structural part of the gauge interaction.

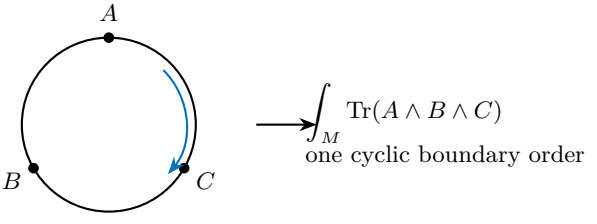


Figure XVIII.2.1: Three boundary insertions retain a cyclic order. Their matrix-valued wedge product is one polarized vertex; substituting one summed field in every slot produces the six terms in $\mathrm{Tr}(A^3)$.

The cyclic open-string field action supplies a quadratic coefficient $1/2$ and a cubic

coefficient $1/3$. With $Q = d_E$, its reduced functional is

$$\begin{aligned} I[A] &= \int_M \operatorname{Tr}\left(\frac{1}{2}A \wedge d_E A + \frac{1}{3}A^3\right), \\ S_k[A] &= \frac{k}{2\pi} I[A] = \frac{k}{4\pi}\int_M \operatorname{Tr}\left(A \wedge d_E A + \frac{2}{3}A^3\right). \end{aligned} \tag{XVIII.2.4}$$

Thus the coefficient of I is $\kappa = k/(2\pi)$, where k is the bare level. The matrix example has $dA = 0$ and $I[A] = 2abc$. It tests the cubic normalization but cannot measure the kinetic coefficient; the latter comes from the sourced two-string pairing. For a nonzero flat reference connection, d_E acts on fluctuations and the full action also retains the reference value and global bundle information.

The two terms in I have different jobs. The pairing $\int_M \operatorname{Tr}(A \wedge d_E A)$ connects two off-shell one-forms and supplies the inverse kinetic operator after gauge fixing. The ordered product $\int_M \operatorname{Tr}(A^3)$ joins three such fields. Degree counting selects both: $A \wedge d_E A$ and A^3 are three-forms and can be integrated over M. The one-form field itself is not replaced by its cohomology class before these operations are formed. In particular, the nonharmonic field modes whose propagator was derived in Chapter 1 can appear between the cubic vertices. This is the concrete sense in which the worldsheet product constructs a field theory rather than just a finite vector space of states.

We use the formal matrix connection A, fundamental trace and $F = dA + A^2$. The polynomial witness uses complex matrices and therefore does not choose a compact integration contour. For a comparison written with a Hermitian connection A_H and $A = -iA_H$, the trace polynomial becomes $-\operatorname{Tr}(A_H dA_H - 2iA_H^3/3)$. Its overall minus must travel with the corresponding level and orientation convention. The positive-level quantum formulas below use one fixed sourced convention; they are not deduced from a Hermiticity label in another presentation.

XVIII.2.2 Flatness, finite gauge changes and the center

What equation does the action impose? For $\mathrm{CS}_3(A) = \operatorname{Tr}(A\,dA + 2A^3/3)$, the graded product rule and cyclic trace give

$$\delta\,\mathrm{CS}_3(A) = 2\operatorname{Tr}(\delta A \wedge F) - d\operatorname{Tr}(A \wedge \delta A), \qquad F = dA + A^2. \tag{XVIII.2.5}$$

To see the origin of the total derivative, vary the two pieces separately. Integration by parts is encoded in

$$\delta\operatorname{Tr}(A \wedge dA) = \operatorname{Tr}(\delta A \wedge dA + A \wedge d\delta A) = 2\operatorname{Tr}(\delta A \wedge dA) - d\operatorname{Tr}(A \wedge \delta A). \tag{XVIII.2.6}$$

For the cubic piece, cyclically moving a degree-one variation past two degree-one factors gives no sign, so $\delta\operatorname{Tr}(A^3) = 3\operatorname{Tr}(\delta A \wedge A^2)$. These two calculations produce (XVIII.2.5), including its boundary term. The same graded multiplication gives $d_A F = dF + A \wedge$

$F - F \wedge A = 0$ from $F = dA + A^2$; this is the Bianchi identity used in the infinitesimal gauge argument. On closed M the total derivative integrates to zero. Therefore

$$\delta S_k = \frac{k}{2\pi} \int_M \operatorname{Tr}(\delta A \wedge F), \qquad k \neq 0 \quad \Longrightarrow \quad F = 0 \tag{XVIII.2.7}$$

for a nondegenerate trace pairing and unrestricted local variations. A manifold with boundary needs a boundary condition or boundary action. Infinitesimally, $\delta_\epsilon A = d_A \epsilon$, and $d_A F = 0$ turns the variation into a total derivative. This local argument does not impose level quantization.

The constant field from (XVIII.2.2) illustrates the force of A^2. On the unit-period three-torus its curvature components are

$$F_{xy} = 2abE_{12}, \qquad F_{yz} = bcH, \qquad F_{zx} = 2acE_{21}. \tag{XVIII.2.8}$$

Although every derivative vanishes, the field is flat within this ansatz only if $ab = bc = ca = 0$. The action is $S_k = kabc/\pi$, and differentiation of $I = 2abc$ gives $(2bc, 2ac, 2ab)$. Contracting δA with the three components of F in (XVIII.2.7) produces the same coefficients. This is an off-shell algebraic example, not a classification of flat $SU(2)$ connections.

For example, changing only a gives $\delta A = \delta a\, H dx$. Only the $dy \wedge dz$ curvature component contributes to the integral, and $\operatorname{Tr}(H \cdot bcH) = 2bc$. Hence $\delta I = 2bc\, \delta a$, exactly the derivative of $2abc$. The b and c variations work by the same oriented wedge pairing with F_{zx} and F_{xy}. This calculation separates two statements that are easy to conflate: the field is constant in position, but its connection matrices fail to commute.

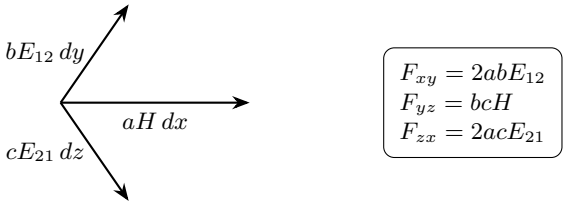


Figure XVIII.2.2: Three constant matrix coefficients on the unit torus. Coordinate derivatives vanish, but commutators give the curvature components on the right. The arrows label directions rather than gauge parallel transport.

A finite gauge transformation carries information that an infinitesimal one misses. Set $A^g = g^{-1}Ag + g^{-1}dg$ and $\theta = g^{-1}dg$. The Maurer–Cartan equation $d\theta = -\theta^2$ yields

$$\mathrm{CS}_3(A^g) - \mathrm{CS}_3(A) = -d \operatorname{Tr}(dg\, g^{-1} \wedge A) - \frac{1}{3} \operatorname{Tr}(\theta^3). \tag{XVIII.2.9}$$

In particular, a pure gauge has $\mathrm{CS}_3(\theta) = -\operatorname{Tr}(\theta^3)/3$. For maps into $SU(N)$, $N \geq 2$, define the winding orientation by

$$w(g) = -\frac{1}{24\pi^2} \int_M \operatorname{Tr}(\theta^3) \in \mathbb{Z}, \qquad S_k[A^g] - S_k[A] = 2\pi k\, w(g). \tag{XVIII.2.10}$$

The integrality is a topological input for the stated group and trace normalization. It makes e^{iS_k} invariant for integer k. Neither the local variation nor the differential-form manipulation alone proves this integrality or settles other global gauge groups.

There is a useful local $U(N)$ decomposition. Write $A = B + aI_N$ with $\operatorname{Tr} B = 0$. In the cubic term, $\operatorname{Tr}(B \wedge B)$ is the trace of a commutator and vanishes; also $a \wedge a = 0$. Consequently,

$$\mathrm{CS}_3(B + aI_N) = \mathrm{CS}_3(B) + Na \wedge da. \tag{XVIII.2.11}$$

The quadratic cross terms vanish because $\operatorname{Tr} B = 0$ and $d \operatorname{Tr} B = 0$. The remaining central quadratic piece is $\operatorname{Tr}(I_N^2)a \wedge da = Na \wedge da$. In the cubic expansion the only possible term linear in a is proportional to $a \wedge \operatorname{Tr}(B \wedge B)$, which is zero. This direct expansion fixes the coefficient for the charge-one central field without treating the quotient group as a product of independent quantum theories. The charge-one central generator is I_N, so its local coefficient is Nk. Normalizing that generator to $I_N/\sqrt{N}$ while still calling its charge one would change the question. Globally $U(N) = (SU(N) \times U(1))/\mathbb{Z}_N$; the quotient and line and spin choices prevent (XVIII.2.11) from being a factorization of complete partition functions. The $SU(2)$ example below is a separately specified simple-group theory.

XVIII.2.3 The empty disk is not an empty perturbation series

The vanishing of smooth disk instantons is a sharp property of the zero section. On T^*M let $\theta_{\mathrm{can}} = p_a\, dq^a$ and $\omega = d\theta_{\mathrm{can}}$. Because θ_{can} restricts to zero on M, a smooth compact unpunctured J-holomorphic disk u with boundary on M obeys

$$\int_D u^*\omega = \int_{\partial D} u^*\theta_{\mathrm{can}} = 0. \tag{XVIII.2.12}$$

For compatible J, positivity of holomorphic area makes such a disk constant. Exactness and the boundary restriction, rather than noncompactness of T^*M, do the work. The statement concerns this class of smooth disks.

The perturbation series also probes the boundaries of worldsheet moduli space. Two disk vertices can be joined by a long strip. Chapter 1 showed that the integrated strip becomes $d_E^* G$ on the complement of residual modes, even though a fixed-length kernel has a vanishing large-deformation limit. The worldsheet Ward identity, measure and sewing prescription used in that conclusion are imported from the selected open A-model construction. Thus (XVIII.2.12) does not erase the sewn graphs. It also does not establish a full nonperturbative equivalence between the open string and quantum Chern–Simons theory.

One positive Laplace eigenvalue λ displays the mechanism without repeating the Hodge construction. In the low-lying form model of Chapter 1, write $L = a\Delta$ and $b = ad_E^*$, with $a > 0$ tending to zero in the large-deformation limit. The strip-length integral has the scalar factor

$$a \int_0^R e^{-a\lambda\ell}\, d\ell = \frac{1 - e^{-a\lambda R}}{\lambda} \quad \longrightarrow_{R\to\infty} \quad \frac{1}{\lambda}. \tag{XVIII.2.13}$$

At each fixed R, sending a to zero instead gives zero. The two limits select different parts of moduli space. The long strip contributes an inverse eigenvalue when its full length range is included; a harmonic mode with $\lambda = 0$ remains a residual field and receives no inverse. This elementary spectral comparison explains how a degeneration survives the smooth-disk argument, while the physical measure and sewing remain sourced premises.

The topology of a sewn diagram can be read directly from its ribbon graph. Suppose a connected vacuum graph has V cubic vertices, E_{g} propagator edges, b index faces and ribbon genus g. A vertex from I/u carries u^{-1}, a propagator carries u, and each closed index face carries N. Thickening the graph gives a surface retracting to it, hence

$$V - E_{\mathrm{g}} = 2 - 2g - b, \qquad u^{E_{\mathrm{g}} - V} N^b = u^{2g-2+b} N^b. \tag{XVIII.2.14}$$

This counts powers only; no graph integral or symmetry factor has been evaluated. The subscript on E_{g} distinguishes the number of graph edges from the Chan–Paton bundle E.

For the theta graph, $V = 2$ and $E_{\mathrm{g}} = 3$. Its cyclic orders can give either three faces on a sphere or one face on a torus. The corresponding powers are uN^3 and uN. Their equal u power is fixed by the same abstract counts $E_{\mathrm{g}} - V = 1$; their different N powers remember the cyclic order at the vertices. This is the first reason ribbon structure matters for the large-N discussion in Chapter 3. At the classical action match $u = u_0 = 2\pi/k$. The quantum expansion parameter introduced next is different.

The face count can be reconstructed from half-edges rather than guessed from a drawing. Number the six darts $0, \ldots, 5$ and pair opposite ends of edges by $\alpha = (03)(14)(25)$. A vertex permutation σ records the cyclic order of the three incident darts at each vertex. Follow an index face by applying α and then σ, so its cycles are those of $\sigma\alpha$. The two choices in Figure XVIII.2.3 give

$$\begin{aligned} \sigma_0 &= (012)(354): \quad \sigma_0\alpha = (05)(13)(24), \\ \sigma_1 &= (012)(345): \quad \sigma_1\alpha = (042315). \end{aligned} \tag{XVIII.2.15}$$

The first has three boundary cycles and the second has one. Capping those boundaries changes the genus through $2 - 2g = V - E_{\mathrm{g}} + b$. This procedure is the precise index-loop meaning of the powers N^3 and N.

XVIII.2.4 Three coupling symbols with different jobs

The coefficient in (XVIII.2.4) gives a bare expansion variable when $k \neq 0$,

$$S_k = \frac{I}{u_0}, \qquad u_0 = \frac{2\pi}{k}. \tag{XVIII.2.16}$$

Matching a disk vertex fixes this number. A regulator and its phase enter a quantum path integral; they are not contained in that classical comparison. For compact positive-level $SU(N)$ theory, the sourced quantum result uses $K_{\mathrm{eff}} = k + h^\vee$ with $h^\vee = N$. In

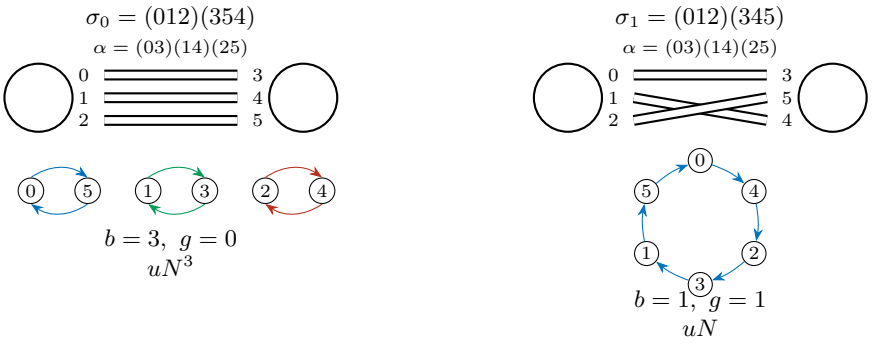


Figure XVIII.2.3: The same theta graph has two ribbon cyclic orders. The upper double lines are its three bands, with darts numbered at the vertex discs. Below, arrows follow the boundary permutation $\sigma\alpha$: three separate two-dart walks on the left and one six-dart walk on the right. The crossing on the right is a planar projection of the genus-one ribbon embedding.

that convention $c_2(\mathrm{adj}) = 2N$, so $h^\vee = c_2(\mathrm{adj})/2$. We therefore keep three symbols distinct:

$$u_0 = \frac{2\pi}{k}, \qquad u = \frac{2\pi}{k + h^\vee}, \qquad x = iu, \qquad q = e^x. \tag{XVIII.2.17}$$

The real u and imaginary x follow the sourced topological-string parameter translation. Neither is the physical type-II string coupling or the sigma-model deformation parameter of Chapter 1. The quantum shift does not instruct us to replace k by $k + h^\vee$ in the bare action.

The distinction can be expressed as a ratio,

$$\frac{u}{u_0} = \frac{k}{k + h^\vee}. \tag{XVIII.2.18}$$

At large k this tends to one, which explains why the tree-level coefficient is a useful first approximation. At finite k it is different from one even before a particular observable is computed. The shift encodes a quantum choice in the compact gauge theory, including the regulator and phase convention, while u_0 records the disk action coefficient. Figure XVIII.2.4 keeps those operations on separate paths. The imaginary variable x is the exponent used in $q = e^x$; dropping its factor of i would replace a unit-modulus root of unity at positive integral k by a real exponential.

The difference is visible at large positive k,

$$u = \frac{2\pi}{k}\left(1 - \frac{h^\vee}{k} + \frac{(h^\vee)^2}{k^2} + O(k^{-3})\right). \tag{XVIII.2.19}$$

For $SU(2)$ at $k = 1$, $u_0 = 2\pi$ but $u = 2\pi/3$ and $x = 2\pi i/3$. This low-level value is a useful convention check, though the large-k series is not accurate there. The local

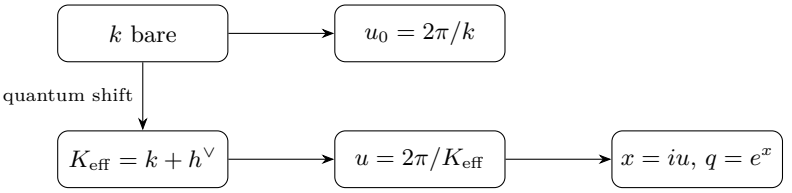


Figure XVIII.2.4: The bare action coefficient fixes u_0. The positive-level quantum shift defines a separate effective parameter and its imaginary continuation.

charge-one $U(1)$ term in (XVIII.2.11) has no nonabelian adjoint shift deduced from this formula. A complete $U(N)$ quantum package needs global information beyond the local split. At $k = 0$ the bare inverse-coupling expansion is unavailable, and the positive-level quantum formulas do not cover negative k without an orientation and phase translation.

In particular, the $k = 1$ example has $q = e^{2\pi i/3}$. Substituting k instead of $k + 2$ would give $q = e^{2\pi i} = 1$ and would also alter the modular denominator in the next section. This is a concrete way to catch a bare/effective coupling mix-up. It does not mean the $SU(2)$ modular Hilbert space was obtained from the local $U(2)$ center decomposition.

XVIII.2.5 Compute a partition function by gluing

We now import the compact $SU(2)_k$ quantum Chern–Simons construction, with k a positive integer. A solid torus prepares a state in the Hilbert space of its boundary torus. Basis states are labelled $n = 0, \ldots, k$, corresponding to spins $n/2$, and the empty core prepares $|0\rangle$. Gluing two solid tori by the identity gives $S^2 \times S^1$ and pairs normalized vacuum states to 1. Gluing by the modular transformation S, which exchanges meridian and longitude, gives S^3. Therefore

$$Z(S^2 \times S^1) = \langle 0|0\rangle = 1, \qquad Z(S^3; f_0) = \langle 0|S|0\rangle = S_{00}. \tag{XVIII.2.20}$$

The reference two-framing f_0 will be fixed in the next section. This construction of the compact Hilbert space and gluing map is additional quantum field-theory input; it is not a computation of the full $U(2)$ brane partition function.

The two gluings differ by a geometric operation on the boundary torus. A meridian bounds a disk inside each solid torus; a longitude runs along its core. Under the identity identification, the two meridians are matched in the product decomposition. Under S, a meridian on one side is identified with a longitude on the other. This is why the same pair of vacuum states can produce two different closed three-manifolds. The amplitude is a matrix element of the gluing map, not simply the product of two scalar solid-torus amplitudes.

Set $r = k + 2$. The sourced modular matrix is the finite sine transform

$$S_{mn} = \sqrt{\frac{2}{r}} \sin \frac{\pi(m+1)(n+1)}{r}, \qquad 0 \le m, n \le k. \tag{XVIII.2.21}$$

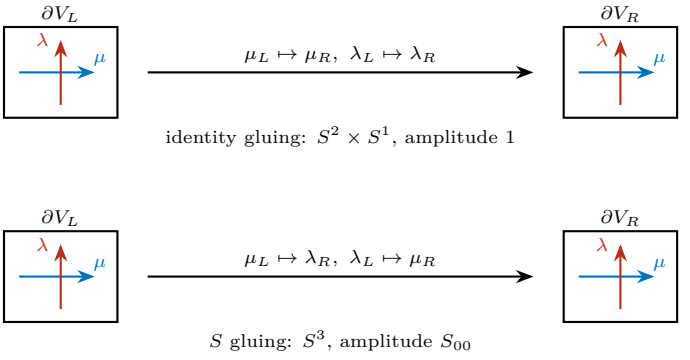


Figure XVIII.2.5: Each rectangle is a cut-open boundary torus of a solid torus V_L or V_R, with meridian μ and longitude λ marked by colored arrows. The meridian bounds a disk inside its solid torus. The upper map preserves the two cycle types; the lower exchanges them. Cycle orientations are suppressed in this schematic, while the compact quantum construction fixes the corresponding modular S matrix.

Its normalization can be checked without assuming the answer. For $1 \le a, b < r$, use $2 \sin A \sin B = \cos(A-B) - \cos(A+B)$ and define $C_\ell = \sum_{j=1}^{r-1} \cos(\pi \ell j / r)$. Then $C_0 = r - 1$. If ℓ is odd, pairing j with $r - j$ gives $C_\ell = 0$. If ℓ is nonzero and even with $|\ell| < 2r$, a nontrivial rth-root sum including $j = 0$ vanishes, so $C_\ell = -1$. Hence

$$\sum_{j=1}^{r-1} \sin \frac{\pi a j}{r} \sin \frac{\pi b j}{r} = \frac{C_{a-b} - C_{a+b}}{2} = \frac{r}{2} \delta_{ab}, \qquad S^{\mathsf{T}} S = 1. \tag{XVIII.2.22}$$

The finite sum proves the orthogonality for every integer $r \ge 3$; a few numerical levels would not suffice.

At the smallest allowed level, $k = 1$ and $r = 3$, the matrix is

$$S = \frac{1}{\sqrt{2}} \begin{pmatrix} 1 & 1 \\ 1 & -1 \end{pmatrix}, \qquad S^{\mathsf{T}} S = 1, \qquad S_{00} = \frac{1}{\sqrt{2}}. \tag{XVIII.2.23}$$

This two-state calculation makes the gluing interpretation tangible. The identity pairing uses the norm of $|0\rangle$, while S takes the overlap between the vacuum and its meridian-longitude transform. At higher level the same distinction remains, with the finite sine transform replacing this 2×2 matrix.

The vacuum element gives the promised partition function,

$$Z(S^3; f_0) = \sqrt{\frac{2}{r}} \sin \frac{\pi}{r}, \qquad r = k + 2. \tag{XVIII.2.24}$$

At $k = 1, 2, 4$ the values are respectively $1/\sqrt{2}$, $1/2$ and $1/(2\sqrt{3})$. Expanding the sine at large r yields

$$Z(S^3; f_0) = \pi \sqrt{2}\, r^{-3/2} \left(1 - \frac{\pi^2}{6 r^2} + \frac{\pi^4}{120 r^4} + O(r^{-6}) \right). \tag{XVIII.2.25}$$

Using k in place of r already gives the wrong $k = 1$ value. Although S^3 has only the trivial flat connection up to gauge equivalence, that connection has a three-dimensional adjoint H^0 stabilizer. It is not an acyclic isolated saddle. The gluing formula supplies the normalization; deleting zero modes from a naive determinant is no derivation of (XVIII.2.24).

The stabilizer can be seen without evaluating a determinant. For the trivial flat connection, the covariant differential on adjoint-valued zero-forms is the ordinary differential. Constant $\mathfrak{su}(2)$-valued functions are therefore closed, and there is no degree-minus-one space from which they could be exact. Thus $H^0(S^3; \operatorname{ad} A_{\mathrm{triv}}) \simeq \mathfrak{su}(2)$ has dimension three. A single gauge-equivalence class of flat connections says nothing about the absence of these automorphisms. In a stationary-phase calculation they must be treated as gauge stabilizer modes, not discarded as if the saddle were acyclic.

XVIII.2.6 Why the quantum answer remembers framing

The classical action uses orientation but no metric. Its quantum partition function has a framing anomaly. The relevant choice here is a two-framing of the natural Spin(6) bundle $TM \oplus TM$, with the diagonal $SO(3)$ lift. The canonical reference f_0 is fixed through a bounding four-manifold by $\operatorname{Sign}(W) = p_1(2TW, f_0)/6$. Differences of two-framings form an integer torsor; the relative $p_1/2$ fixes its unit. This is a three-manifold choice, distinct from the normal-vector framing of an individual Wilson loop.

We first calculate the coefficient entering the anomaly, conditional on the supplied affine $SU(2)_k$ current algebra and Sugawara state. With $t^a = \sigma^a/2$, $\epsilon_{012} = +1$ and vacuum annihilated by J^a_m for $m \geq 0$, these inputs read

$$[J^a_m, J^b_n] = i\epsilon_{abc} J^c_{m+n} + \frac{k}{2} m \delta_{ab} \delta_{m+n,0}, \qquad L_{-2}|0\rangle = \frac{\sum_a J^a_{-1} J^a_{-1}|0\rangle}{k+2}. \tag{XVIII.2.26}$$

Commute the two positive modes through the two negative modes in the vacuum norm. The central contractions and the two structure-constant contractions combine as

$$J^a_1 \sum_b J^b_{-1} J^b_{-1}|0\rangle = (k+2) J^a_{-1}|0\rangle. \tag{XVIII.2.27}$$

The two central commutators each contribute $kJ^a_{-1}/2$. For the remaining term, commute J^c_0 through J^b_{-1} and use $\sum_{b,c} \epsilon_{abc}\epsilon_{cbd} = -2\delta_{ad}$; the two factors of i then contribute $+2J^a_{-1}$. A final contraction with $\langle 0|J^a_1$ gives $k/2$ for each of the three colors. Therefore

$$\sum_{a,b} \langle 0| J^a_1 J^a_1 J^b_{-1} J^b_{-1}|0\rangle = \frac{3k(k+2)}{2}. \tag{XVIII.2.28}$$

Since $\langle 0|L_2 L_{-2}|0\rangle = c/2$, division by $(k+2)^2$ gives

$$c = \frac{3k}{k+2}. \tag{XVIII.2.29}$$

This verifies a consequence of the stated quantum realization; the classical disk calculation did not construct that realization. The four-current norm alone is even in the structure-constant sign. The Pauli orientation in (XVIII.2.26) also fixes $\langle J_1^0 J_0^1 J_{-1}^2 \rangle = ik/2$, while the central term gives $\langle J_m^a J_{-m}^a \rangle = km/2$ for $m > 0$. Its linear dependence on m is required by the current Jacobi identity.

Indeed, write the central part of a same-color commutator as $f(m)\delta_{m+n,0}$. Antisymmetry requires $f(-m) = -f(m)$. The Jacobi identity for three different colors and modes $m, n, -m-n$ leaves a central combination proportional to

$$f(m+n) + f(-m) + f(-n) = 0. \tag{XVIII.2.30}$$

The stated $f(m) = km/2$ satisfies this for arbitrary integer modes. Low-mode inner products alone would not determine the entire central function; the Jacobi relation supplies a general algebraic constraint. Neither calculation, by itself, proves that the affine representation is physically realized by the brane construction.

The sourced two-framing generator needs a sign translation. Its integer n_{FG} rises by one under a right Dehn twist T, and its phase is $\exp(-2\pi i n_{\mathrm{FG}} c/24)$. The relative characteristic-class construction fixes this as one generator, rather than an unknown multiple. Define this chapter's coordinate $s = -n_{\mathrm{FG}}$. Then the imported framing law reads

$$Z(M; f+s) = \exp\left(\frac{2\pi i s c}{24}\right) Z(M; f), \qquad c = \frac{3k}{k+2}. \tag{XVIII.2.31}$$

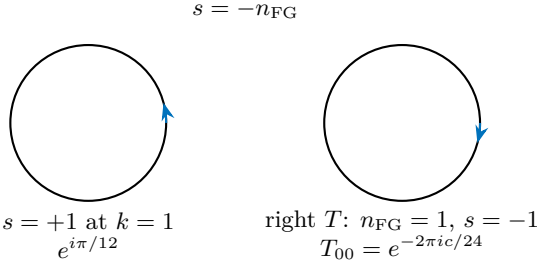


Figure XVIII.2.6: The two-framing coordinate reverses the Freed–Gompf generator. The right T twist has the inverse phase of positive s. Angles are schematic except for the $k = 1$ label.

In this notation a positive right twist has $s = -1$. The modular matrix has $T_{nn} = \exp[2\pi i(h_n - c/24)]$, where $h_n = n(n+2)/(4r)$. Therefore right multiplication by T on the vacuum gluing amplitude multiplies it by $T_{00} = \exp(-2\pi i c/24)$, precisely the $s = -1$ phase. We use this right-twist comparison with the stated source orientation; it does not require a rule for every possible left twist.

The order of operations matters in this comparison. Starting with $\langle 0|S|0\rangle$, right multiplication gives $\langle 0|ST|0\rangle = T_{00} S_{00}$ because T acts first on the right vacuum state. The phase is therefore determined by $h_0 = 0$. A left multiplication would act on the bra and requires its own gluing and orientation convention; we do not infer its sign

by moving T through S. Figure XVIII.2.6 displays the right-twist sign relative to the book's positive s coordinate.

At $k = 1$, $c = 1$, and a positive unit of s multiplies the partition function by $e^{i\pi/12}$. At $k = 3$, $c = 9/5$, so a shift by $s = 24$ multiplies it by $e^{18\pi i/5}$, which is not one. In the large-k limit c approaches $3 = \dim SU(2)$, but replacing it by 3 at finite k changes the phase. Quantum framing dependence is compatible with classical metric independence. The distinct framing of Wilson loops enters the observables of Chapter 3.

From a local vertex to a compact observable

A useful way to repeat this chapter's construction is to keep three operations on separate lines of the calculation. First multiply the matrix-valued forms. The exterior signs retain the ordering of the disk insertions, while the ordinary matrix trace retains the Chan–Paton information. The constant-field example tests this cubic product particularly well because its derivative term vanishes. For the same reason it cannot determine the coefficient of the kinetic term. That coefficient must come from the pairing used in the action.

Next vary the action before imposing flatness. The curvature is the result of that variation, rather than a condition used to simplify it in advance. A field that is flat only to first order need not be a stationary point of the nonlinear functional. This matters for perturbation theory, whose internal fields are off shell. It also explains why replacing the action by its value on flat connections would discard the mechanism that produces the propagator and vertices.

Finally choose the compact quantum problem. In the $SU(2)$ gluing example, the empty solid torus specifies a vector, and a boundary identification specifies an operator between such vectors. The orthogonality calculation normalizes that operator. To reproduce S_{00}, use the vacuum labels at both ends of the finite sine transform; to reproduce the identity gluing, use the inner product instead. These are different operations even though the same two empty solid tori are involved. The reference two-framing must also be carried through the comparison.

This sequence prepares the Wilson-loop calculation in XVIII.3. Placing a representation on a solid-torus core changes the state that is paired by the gluing map. It does not change the classical cubic disk coefficient. The bare level, shifted quantum denominator and framing phase therefore retain the different jobs assigned to them here.

Exercises

1. Compute the ordered vertex for $aH\,dx$, $bE_{12}\,dy$, $cE_{21}\,dz$, then expand $\operatorname{Tr}(A^3)$ for their sum. Use the supplied cyclic coefficients to recover $\kappa = k/(2\pi)$. Explain why this constant example does not determine the quadratic normalization.

2. For the constant torus connection in (XVIII.2.2), calculate all three independent curvature components and vary $I = 2abc$. Compare your gradients with (XVIII.2.7).

3. Derive the charge-one central term for $A = B + aI_N$. Separately take closed oriented M, fundamental trace, $g : M \to SU(N)$ with $N \geq 2$, and $A = \theta = g^{-1}dg$. Use $d\theta = -\theta^2$ and the stated integrality of $w(g)$ to compute the finite gauge shift. Name the global information absent from the local central split.

4. A theta graph has darts $0, \ldots, 5$, edge involution $(03)(14)(25)$, and either vertex permutation $(012)(354)$ or $(012)(345)$. Count face cycles, find g, b, and give the powers of u, N. Explain why the smooth-disk area argument does not remove the sewn diagrams.

5. Expand u through order k^{-3}, find x and q, and explain why replacing k by $k + N$ in the bare action would change the disk coefficient.

6. Prove (XVIII.2.22) for general integer $r \geq 3$. Evaluate (XVIII.2.24) at $k = 1, 2, 4$ and its large-r expansion. Explain why the unique flat connection on S^3 is not acyclic.

7. Starting from (XVIII.2.26), evaluate the four-current norm and c. Compare a positive s shift with right multiplication by T, converting explicitly from n_{FG}. Test whether $s = 24$ has trivial phase at $k = 3$.

Sources and scope

The perturbative open-sector construction uses the form sector and integrated strip of Chapter 1. The bare level, shifted coupling and two-framing conventions are specified above. The compact quantum $SU(2)$ calculation uses the separate field-theory input cited below and leaves the full $U(N)$ quantum theory open.

§1. [WS-T] Ghost-one forms and ordered disk vertices use Witten (1995), arXiv v2 pp. 28–30, (4.6)–(4.9), together with the form-sector identification of Chapter 1. [MATH] Coefficient matching follows from the stated cyclic action and the bare trace normalization. The polarized vertex and six-term polynomial are computed here.

§2. [MATH] Graded variation, transgression, constant matrix curvature and the local charge-one center are derived here. Normalized $SU(N)$ winding integrality and the compact phase convention use Witten (1989); general global $U(N)$ completion is not supplied.

§3. [MATH] Exactness, zero-section boundary condition and compatible positivity prove the compact smooth-disk statement. [WS-T] The sewn open-sector conclusion uses the measure and degeneration prescription of Witten (1995), pp. 30–38, and the integrated strip of Chapter 1. [MATH] The ribbon power follows from Euler characteristic and the stated vertex and propagator weights.

§4–5. [MATH] u_0, u, x are a conditional parameter translation; the positive-level shift is an imported quantum result from Witten (1989), pp. 359–360, (2.16)–(2.17), and the open-string notation follows Mariño (2005), (2.10), (2.14), (3.11), (5.14). [MATH] $SU(2)_k$ torus states and S gluing use Witten (1989), pp. 389–390, (4.37)–(4.39). [MATH] Sine orthogonality and the asymptotic series are derived here. The nonacyclic trivial-connection warning is in Witten (1989), p. 362.

§6. [MATH] The current-mode norm implies c conditional on the affine and Sugawara inputs. [ANOM] The imported quantum framing coefficient follows Witten (1989), (2.25), with the canonical origin from Atiyah (1990), §2 and Proposition 1, and the generator unit and sign from Freed and Gompf (1991), (1.3)–(1.5), before Theorem 2.3 and Appendix B. [MATH] The right-T and $k = 3$ phase comparisons follow algebraically. A knot's normal framing is a separate observable choice.

The worldsheet measure and the quantum current representation are inputs. The global $U(N)$ theory requires additional data beyond the perturbative identification and compact $SU(2)$ example.

References

Atiyah, M. (1990). "On Framings of 3-Manifolds". In: *Topology* 29, pp. 1–7. DOI: 10.1016/0040-9383(90)90021-B.

Freed, D. S. and R. E. Gompf (1991). "Computer Calculation of Witten's 3-Manifold Invariant". In: *Commun. Math. Phys.* 141, pp. 79–117.

Mariño, M. (2005). "Chern-Simons Theory and Topological Strings". In: *Rev. Mod. Phys.* 77, pp. 675–720. DOI: 10.1103/RevModPhys.77.675. arXiv: hep-th/0406005.

Witten, E. (1989). "Quantum Field Theory and the Jones Polynomial". In: *Commun. Math. Phys.* 121, pp. 351–399. DOI: 10.1007/BF01217730.

Witten, E. (1995). "Chern-Simons Gauge Theory as a String Theory". In: *Prog. Math.* 133, pp. 637–678. arXiv: hep-th/9207094.

Chapter XVIII.3

Wilson loops, knots and open strings

A gauge field can detect a closed curve through its holonomy. Taking a trace of that holonomy in a representation gives a Wilson loop; changing the embedding of the curve can change its expectation value. How can an open string remember that embedding? The answer is to add a second brane whose position in the cotangent bundle is determined by the knot. Strings stretching between this brane and the zero section then insert a generating function of Wilson loops into the gauge theory.

The simplest example, the unknot, already shows how representations and winding numbers enter the same answer. A Hopf link and a trefoil show what additional information is lost if one only studies the unknot. Finally, the large-N expansion reorganizes the result by powers characteristic of surfaces with a boundary. This chapter develops these statements within the quantum Chern–Simons and mixed-string inputs stated below; the identification of a new target geometry is a further question for Chapter 4.

XVIII.3.1 A brane that remembers a knot

Let K be a smooth embedded oriented circle in an oriented three-manifold M. The conormal of K consists of covectors that annihilate its tangent:

$$L_K = N^*K = \{(q,p) \in T^*M : q \in K, \quad p(v) = 0 \text{ for every } v \in T_qK\}. \tag{XVIII.3.1}$$

At each point of K this gives a two-dimensional fiber, so L_K has dimension three. Its intersection with the zero section is exactly K. The fiber directions matter: they record how the circle sits in M, while the common locus is where strings with one end on each brane can live.

Let $\theta = p_i\, dq^i$ be the tautological one-form. A tangent vector to L_K projects to a tangent vector to K; its pairing with p therefore vanishes. Thus $\theta|_{L_K} = 0$, and the pullback of $d\theta$ vanishes as well. Since L_K has half the dimension of T^*M, it is an exact

Lagrangian. This argument does not assert that it is special Lagrangian for an arbitrary metric and phase.

More explicitly, let $\pi : T^*M \to M$ be the projection and $\iota : L_K \hookrightarrow T^*M$ the inclusion. For $X \in T_{(q,p)}L_K$, the base component lies in T_qK, so the definition of the tautological form gives

$$(\iota^*\theta)(X) = p(d\pi\, X) = 0, \qquad \iota^*(d\theta) = d(\iota^*\theta) = 0. \tag{XVIII.3.2}$$

The dimension count uses one base direction and two independent annihilating covectors:

$$\dim L_K = 1 + (3-1) = 3 = \tfrac{1}{2}\dim T^*M. \tag{XVIII.3.3}$$

The vanishing one-form supplies a global primitive, namely zero. At a point of the circle the fiber is a plane of covectors normal to the tangent, not a single preferred normal vector. Moving around the circle carries this plane along the embedding. This is the geometric data used when the mixed open strings are introduced in the next section.

For a concrete local picture, take a circle of radius R in $\mathbb{R}^3$, with angular coordinate s and coordinates (r, s, z) nearby. The conormal is $r = R$, $z = 0$, $p_s = 0$, with p_r, p_z free. The zero covector in every fiber traces the circle itself. If instead one shifts the fiber by $p_s = c$, the restricted one-form is $c\,ds$: it is closed, but for nonzero c has nonzero integral around the circle and is not exact. A variable shift $p_s = a(p_r, p_z, s)$ gives $d\theta| = da \wedge ds$, which generally does not vanish. A displacement of the fibers is therefore not automatically another exact Lagrangian.

For s of period 2π, the distinction between closed and exact appears in the period

$$\oint_K c\, ds = 2\pi c. \tag{XVIII.3.4}$$

The constant shift remains Lagrangian but is not exact when $c \neq 0$. In contrast, the choice $a = p_r$ gives

$$\theta| = p_r\, ds, \qquad d\theta| = dp_r \wedge ds \neq 0, \tag{XVIII.3.5}$$

so this shifted three-manifold is not even Lagrangian. These examples separate the local condition on the symplectic form from the global period condition on a primitive.

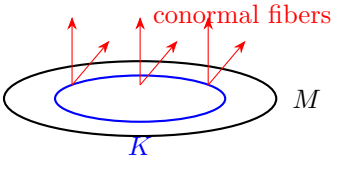


Figure XVIII.3.1: The zero section and the conormal meet along K. The arrows indicate fiber directions schematically, not a projection of the full six-dimensional geometry.

XVIII.3.2 Intersection strings and the winding operator

Put N zero-section branes on M and auxiliary branes on L_K. The construction of Ooguri and Vafa supplies a bifundamental scalar in the mixed open-string sector localized on K. Integrating this Gaussian field with the prescribed normalization gives a determinant. The mixed spectrum, measure, zero modes and determinant phase are physical inputs; the finite algebra below describes the consequence of that input.

Write U for the holonomy on K and $B = V_{\mathrm{OV}}^{-1}$ for the inverse auxiliary holonomy. Introduce a formal marker v for degree. For finite eigenvalue alphabets u_i and b_α, define

$$Z(U,B;v) = \prod_{i,\alpha}(1 - v u_i b_\alpha)^{-1} = \exp\left[\sum_{n\geq 1} \frac{v^n}{n} \operatorname{Tr} U^n \operatorname{Tr} B^n\right]. \tag{XVIII.3.6}$$

The second equality is a formal power-series identity. The factor $1/n$ is the coefficient in $-\log(1-y)$: a single winding-n trace appears in the logarithm, while the exponential combines disconnected contributions. In the physical determinant, square-root lifts and the normalization must also be chosen. For example, the inverse of the symmetric sine determinant carries the prefactor $(\det U)^{M/2}(\det V)^{-N/2}$ for the chosen lifts. Merely writing both determinants as one does not choose every square-root branch.

The first two degrees expose the distinction between winding and representation. With $p_n(U) = \operatorname{Tr} U^n$ and similarly for B,

$$Z = 1 + v p_1(U) p_1(B) \tag{XVIII.3.7}$$

$$+ \frac{v^2}{2}\big[p_1(U)^2 p_1(B)^2 + p_2(U) p_2(B)\big] + O(v^3). \tag{XVIII.3.8}$$

The two terms at degree two are required together. Using $s_{(2)} = (p_1^2 + p_2)/2$ and $s_{(1,1)} = (p_1^2 - p_2)/2$, they equal $v^2[s_{(2)}(U)s_{(2)}(B) + s_{(1,1)}(U)s_{(1,1)}(B)]$. At all formal degrees the Cauchy identity gives

$$Z(U,B;v) = \sum_R v^{|R|} s_R(U) s_R(B). \tag{XVIII.3.9}$$

Thus the same operator can be read as winding traces or as Wilson loops in Young-diagram representations. Equation (XVIII.3.9) is an identity of finite alphabets, before any quantum expectation value is taken.

The determinant in the source arises before the formal marker is introduced. To see its normalization, let the auxiliary matrix have size M and write its eigenvalues as v_α. With chosen square-root lifts, each eigenvalue of the mixed operator is

$$u_i^{-1/2} v_\alpha^{1/2} - u_i^{1/2} v_\alpha^{-1/2} = u_i^{-1/2} v_\alpha^{1/2}(1 - u_i v_\alpha^{-1}). \tag{XVIII.3.10}$$

Multiplication over all i, α yields

$$(\det C)^{-1} = (\det U)^{M/2}(\det V)^{-N/2} \prod_{i,\alpha}(1 - u_i v_\alpha^{-1})^{-1}. \tag{XVIII.3.11}$$

The inverse auxiliary holonomy is therefore a consequence of this displayed factorization, not a change of notation one can make without also changing the determinant. The formal series in v counts the number of boxes after the physical normalization has been fixed. In particular it should not be mistaken for a physical mass regulator.

One can see the Cauchy identity directly from finite matrices. For two alphabets of equal length r, put $\Delta(u) = \prod_{i<j}(u_j - u_i)$ and similarly for b. The finite Cauchy determinant is

$$\det_{i,j} \frac{1}{1 - v u_i b_j} = \frac{v^{r(r-1)/2} \Delta(u) \Delta(b)}{\prod_{i,j}(1 - v u_i b_j)}. \tag{XVIII.3.12}$$

For $r = 2$, the determinant has numerator $v(u_2 - u_1)(b_2 - b_1)$: it vanishes at $v = 0$, as the left side must. Expanding each entry as a geometric series and applying Cauchy–Binet selects strictly increasing powers. Subtracting the staircase $(0, 1, \ldots, r-1)$ turns those powers into a partition and removes the same factor $v^{r(r-1)/2}$. The two resulting alternants divided by their Vandermondes are the two Schur characters. Padding the shorter alphabet with zeros extends the result to unequal finite sizes. At any fixed degree only finitely many partitions contribute.

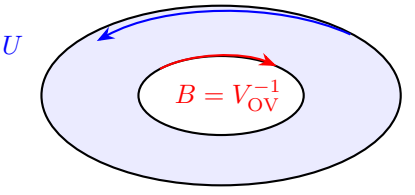


Figure XVIII.3.2: The two oriented annulus boundaries couple to the two holonomies. The inverse auxiliary holonomy and the orientation must be kept together. The weight $1/n$ occurs in the connected logarithm.

XVIII.3.3 The exact unknot and its representations

Now specialize to S^3 and a zero-framed unknot. We use compact $SU(N)_k$ quantum Chern–Simons theory, with $N \geq 2$ and positive integer k, as an additional input. Set

$$x = \frac{2\pi i}{k + N}, \quad q = e^x, \quad z = e^{x/2}, \quad t_H = Nx, \quad a = e^{t_H/2}. \tag{XVIII.3.13}$$

The logarithm lifts are part of the convention. In formal continuations these symbols are used independently where stated. The symbol t_H is a coupling parameter here; no geometric Kähler parameter has yet been identified with it.

A solid torus with a Wilson line along its core prepares a state labelled by R. Gluing two solid tori by the modular S transformation produces S^3; normalizing by the empty S^3 amplitude gives

$$d_R = W_R(\bigcirc) = \frac{S_{0R}}{S_{00}}. \tag{XVIII.3.14}$$

This is a quantum dimension. Its ordinary dimension appears only in the appropriate classical limit. For polynomial representations one may evaluate the Schur character on the centered alphabet

$$U_0 = \mathrm{diag}(z^{N-1}, z^{N-3}, \dots, z^{1-N}), \qquad d_R = s_R(U_0). \tag{XVIII.3.15}$$

For example, define $[m] = (z^m - z^{-m})/(z - z^{-1})$. Then

$$d_{(1)} = [N], \qquad d_{(2)} = \frac{[N][N+1]}{[2]}, \qquad d_{(1,1)} = \frac{[N][N-1]}{[2]}. \tag{XVIII.3.16}$$

As $z \to 1$ at fixed N these become N, $N(N+1)/2$ and $N(N-1)/2$. In the finite compact theory the representations must be integrable. The formulas in degree at most d have sufficient level $k \geq d$ for the polynomial labels used here, with their Young-diagram lifts retained.

The finite geometric sum is especially useful:

$$\mathrm{Tr}\, U_0^n = \sum_{j=1}^{N} z^{n(N+1-2j)} = \frac{\sinh(nt_H/2)}{\sinh(nx/2)}. \tag{XVIII.3.17}$$

At a removable zero of the ratio the finite sum defines its value. Combining this with the Cauchy identity gives the formal connected generator

$$F_{\mathrm{conn}} = \log\langle Z\rangle_{\bigcirc} = \sum_{n\geq 1} \frac{v^n\, \mathrm{Tr}\, B^n}{n} \frac{\sinh(nt_H/2)}{\sinh(nx/2)}. \tag{XVIII.3.18}$$

Our sign is $F_{\mathrm{conn}} = -F_{\mathrm{OV}}$. The full series is a formal, degreewise continuation, not an infinite set of independent integrable states at one fixed level. At any chosen degree one can use the stated level bound to compare the character calculation with the compact theory.

The character specialization follows from an explicit ratio of alternants. If $R_i = 0$ after the last row of R, then

$$s_R(U_0) = \prod_{1\leq i<j\leq N} \frac{z^{R_i - R_j + j - i} - z^{-(R_i - R_j + j - i)}}{z^{j-i} - z^{-(j-i)}}. \tag{XVIII.3.19}$$

The centering of U_0 cancels the overall powers in the ratio. For the two-box cases an efficient derivation uses the identities

$$s_{(2)} = \frac{p_1^2 + p_2}{2}, \qquad s_{(1,1)} = \frac{p_1^2 - p_2}{2}, \qquad p_n(U_0) = [N]_{z^n}, \tag{XVIII.3.20}$$

where $[N]_{z^n} = (z^{nN} - z^{-nN})/(z^n - z^{-n})$. Substitution and factoring the numerator give the two answers in (XVIII.3.16). This also shows the difference between symmetrizing two fundamental indices and simply squaring the fundamental quantum dimension.

The finite geometric sum can be derived without dividing by a quantity that might vanish at a root of unity. Starting with its N terms,

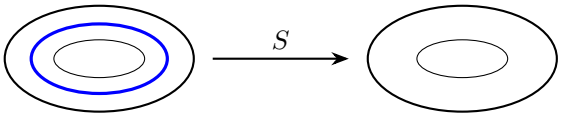
$$\sum_{j=1}^{N} z^{n(N+1-2j)} = z^{n(N-1)} \frac{1 - z^{-2nN}}{1 - z^{-2n}}. \tag{XVIII.3.21}$$

This ratio simplifies to (XVIII.3.17) when its denominator is nonzero; the original finite sum gives the continuation at removable zeros. For $N = 3$, for example, the three weights are $z^{2n}, 1, z^{-2n}$. This check also makes clear that U_0 has exactly N eigenvalues, including the central 1 only when N is odd.

Why does the same specialization evaluate the full generating function? For each fixed representation the compact gluing input supplies $\langle \operatorname{Tr}_R U \rangle = s_R(U_0)$. Inserting it into the Schur expansion gives

$$\langle Z \rangle_{\bigcirc} = \sum_R v^{|R|} s_R(U_0) s_R(B) = \prod_{i,\alpha} (1 - v(U_0)_i b_\alpha)^{-1}, \tag{XVIII.3.22}$$

with the equality read degree by degree in the specified level range. It is a property of this one-unknot functional. It is not a rule that allows one to replace holonomies of linked components by independent copies of U_0.



core state R vacuum state 0

$$W_R(\bigcirc) = S_{0R}/S_{00}$$

Figure XVIII.3.3: The two solid-torus states are glued by S. The empty gluing amplitude S_{00} supplies the vacuum normalization.

XVIII.3.4 Framing and the center factor

A knot has an additional geometric datum: a nonzero normal vector field determines a nearby push-off. The linking of the knot with that push-off is its integer self-linking f. A unit change of f changes the Wilson value by a representation-dependent phase. This knot framing is distinct from the manifold two-framing discussed in Chapter 2.

For a Young diagram R, let $\ell = |R|$ and $\varkappa_R = \sum_i R_i(R_i - 2i + 1)$. The supplied quantum twist gives

$$W^{(f)}_{SU,R} = \exp\left[\frac{xf}{2}\left(N\ell + \varkappa_R - \frac{\ell^2}{N}\right)\right] W^{(0)}_{SU,R}. \tag{XVIII.3.23}$$

The expression in parentheses is twice the quadratic Casimir in the convention with fundamental trace normalization $1/2$. For the $SU(2)$ fundamental, $\ell = 1$ and $\varkappa = 0$, so the factor is $q^{3f/4}$.

A useful source convention adds a relative Abelian phase on S^3. For a link with chosen Young lifts, define

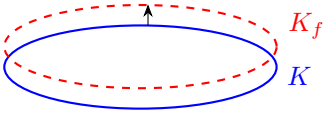
$$W_{\mathrm{MV}}(L) = \exp\left[\frac{x}{2N}\left(\sum_i \ell_i^2 f_i + 2\sum_{i<j} \ell_i \ell_j \operatorname{lk}_{ij}\right)\right] W_{SU}(L). \tag{XVIII.3.24}$$

For the same $SU(2)$ fundamental knot this changes the framing factor to q^f. The ratio $q^{f/4}$ is observable in the chosen normalization. Equation (XVIII.3.24) defines a relative S^3 prescription with fixed Young lifts; it does not by itself construct a global $U(N)$ theory or derive the Abelian denominator from the bare center coupling of Chapter 2. The pairwise linking term will be essential in the next example.

To see how the extra phase changes a knot, use (XVIII.3.24) for one component. Multiplying the $SU(N)$ twist by $\exp(xf\ell^2/2N)$ cancels the last term in (XVIII.3.23):

$$\frac{W^{(f)}_{\mathrm{MV,R}}}{W^{(0)}_{\mathrm{MV,R}}} = \exp\left[\frac{xf}{2}(N\ell + \varkappa_R)\right]. \tag{XVIII.3.25}$$

For two boxes $\varkappa_{(2)} = 2$ while $\varkappa_{(1,1)} = -2$. Their twists differ even though both diagrams have $\ell = 2$. The phase therefore remembers the representation, not merely the number of strands. The later flat-coordinate redefinition in the source is a separate operation and can introduce an additional sign; it should not be inserted into this raw framing rule.



$f = \mathrm{lk}(K, K_f)$

Figure XVIII.3.4: A normal field defines the push-off. Adding one twist to that field changes its self-linking by one. This knot framing is distinct from the two-framing of the ambient three-manifold.

XVIII.3.5 Linked and knotted observables

The unknot specialization cannot be applied separately to each component of every link. For a Hopf link, modular gluing couples the two labels. At $SU(2)$ level $k = 3$, both fundamental labels are self-conjugate and

$$W_{SU}(\mathrm{Hopf}) = \frac{S_{11}}{S_{00}} = \frac{\sin(4\pi/5)}{\sin(\pi/5)} = 1, \qquad W_{SU}(\bigcirc)^2 = \frac{3+\sqrt{5}}{2}. \tag{XVIII.3.26}$$

The second number is the value for two unlinked unknots. Linking has changed the answer, despite each component being an unknot.

For a knot calculation, fix the crossing convention rather than a handedness name: take the inverse of Witten's braid operator B_W, namely $R_{SU} = B_W^{-1}$, with symmetric and antisymmetric eigenvalues $q^{-1/(2N)}z$ and $-q^{-1/(2N)}z^{-1}$. Set

$$D = \frac{a-a^{-1}}{z-z^{-1}}, \quad D_S = D\frac{az-a^{-1}z^{-1}}{(z-z^{-1})(z+z^{-1})}, \quad D_A = D\frac{az^{-1}-a^{-1}z}{(z-z^{-1})(z+z^{-1})}. \tag{XVIII.3.27}$$

These are the fundamental and two-channel quantum dimensions. For the closure of the two-strand braid σ^m, define $T_m = z^m D_S + (-z^{-1})^m D_A$. If m is odd the closure is a knot; removing its blackboard framing gives

$$W_{SU}^{(0)}(\widehat{\sigma^m}) = a^{-m} T_m. \tag{XVIII.3.28}$$

At $m = 1$ this is D, the unknot. At $m = 3$ it gives the declared trefoil K_σ and the reduced value

$$P_\sigma = \frac{W_{SU}^{(0)}(K_\sigma)}{D} = a^{-2}(z^2 + z^{-2}) - a^{-4}. \tag{XVIII.3.29}$$

The mirror is obtained by $(z, a) \mapsto (z^{-1}, a^{-1})$; this mirror is the trefoil convention used in the example of Labastida and Mariño. For $N = 2$, $a = z^2$ and $P_\sigma = q^{-1} + q^{-3} - q^{-4}$. The two-channel compact derivation requires integrable channels; in particular $SU(2)$ requires $k \geq 2$.

There is a useful recurrence behind the same result. If $H_m = a^{-m} T_m$, its two eigenvalues are z/a and $-z^{-1}/a$, so

$$H_m = \frac{z - z^{-1}}{a} H_{m-1} + \frac{1}{a^2} H_{m-2}, \qquad H_0 = D^2, \quad H_1 = D. \tag{XVIII.3.30}$$

Applying it twice recovers (XVIII.3.29). For even m, however, the closure has two components and linking number $m/2$. With zero self-framing on each component, $W_{SU} = q^{-m/(2N)} T_m$, $W_{\mathrm{MV}} = T_m$, and $H_m = a^{-m} T_m$. Hence $W_{\mathrm{MV}} = a^{2\,\mathrm{lk}} H_m$. These are different normalizations of the link observable, and the phase must be included when comparing a skein calculation to compact gluing.

The two-channel derivation also makes the framing correction explicit. The fundamental twist is $\theta_F = q^{(N-1/N)/2}$. In the braid trace, each crossing contributes the common factor $q^{-1/(2N)}$, and removing the blackboard framing of an odd m closure contributes θ_F^{-m}. Together they simplify as

$$\theta_F^{-m} q^{-m/(2N)} = q^{-mN/2} = a^{-m}. \tag{XVIII.3.31}$$

For $m = 3$, substitute the two dimensions and combine terms over the common denominator:

$$\frac{T_3}{D} = \frac{z^3(az - a^{-1}z^{-1}) - z^{-3}(az^{-1} - a^{-1}z)}{(z - z^{-1})(z + z^{-1})} = a(z^2 + z^{-2}) - a^{-1}. \tag{XVIII.3.32}$$

Multiplication by a^{-3} gives the polynomial in (XVIII.3.29). A direct smoothing calculation gives a different check of the same declared diagram. In the $SU(2)$ specialization set $z = A^2$, and let a vertical smoothing carry weight A, a horizontal one weight A^{-1}, and a closed loop $d = -A^2 - A^{-2}$. The eight states have loop counts

state	VVV	VVH	VHV	HVV	VHH	HVH	HHV	HHH
loops	2	1	1	1	2	2	2	3

(XVIII.3.33)

A state with h horizontal smoothings contributes $A^{3-2h}d^{\#\text{loops}-1}$. Summing these eight contributions and removing writhe $+3$ gives

$$(-A^3)^{-3}(-A^5 - A^{-3} + A^{-7}) = A^{-4} + A^{-12} - A^{-16}. \tag{XVIII.3.34}$$

This agrees with the $SU(2)$ specialization of the channel calculation. Reversing all crossings replaces A by A^{-1} and reverses the writhe.

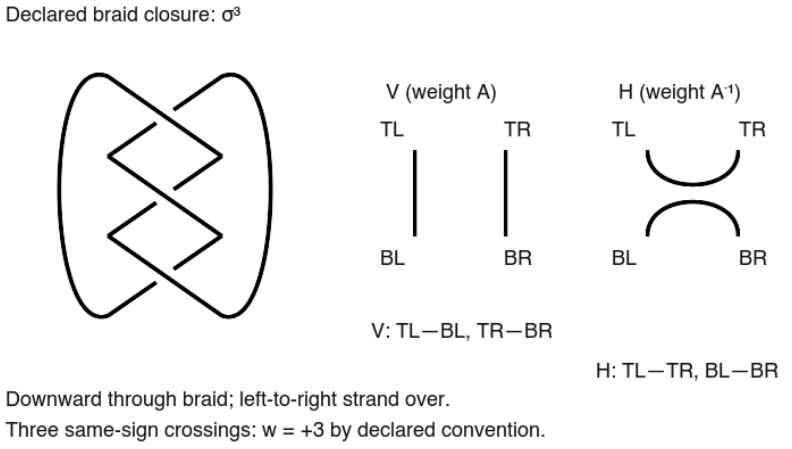


Figure XVIII.3.5: The declared two-strand trefoil closure and its two smoothings. The downward left-to-right strand crosses over; reversing each crossing gives the mirror, with $A \mapsto A^{-1}$ and writhe -3. The crossing in the channel calculation is $R_{SU} = B_W^{-1}$.

For comparison, the closures $\widehat{\sigma^0}$ and $\widehat{\sigma^2}$ are respectively the two-component unlink and Hopf link. The latter's two crossings carry linking number one. Equation (XVIII.3.24) then supplies the factor $q^{1/N}$ between its relative MV and SU values for two fundamental components, while the conversion to H_2 also includes the non-Abelian framing normalization. Writing these three observables separately prevents an apparent discrepancy between gluing and the recurrence.

XVIII.3.6 The observable at fixed t_H

The winding expression (XVIII.3.18) has two instructive limits. At fixed t_H and formal $x \to 0$, the coefficient of $v^n \operatorname{Tr} B^n$ is

$$(e^{nt_H/2} - e^{-nt_H/2})\left(\frac{1}{n^2 x} - \frac{x}{24} + \frac{7n^2x^3}{5760} + O(x^5)\right). \tag{XVIII.3.35}$$

The powers $x^{-1}, x, x^3, \ldots$ have the pattern associated with one boundary and increasing genus. This is an organization of the conditional quantum answer; the expansion alone does not compute separate worldsheet integrals or a particle spectrum.

By contrast, keeping N fixed forces $t_H = Nx$ to zero with x. The fundamental unknot becomes

$$[N] = N + \frac{N(N^2-1)}{24}x^2 + O(x^4). \tag{XVIII.3.36}$$

For $x = iu$ the quadratic correction changes sign, as in the expansion of the sine ratio. Confusing the two paths would turn a finite classical dimension into a spurious $1/x$ divergence.

The trefoil also illustrates what finite algebra can and cannot establish. With $\delta = z - z^{-1}$, (XVIII.3.29) implies

$$\delta W_{SU}^{(0)}(K_\sigma) = (2a^{-1} - 3a^{-3} + a^{-5}) + \delta^2(a^{-1} - a^{-3}). \tag{XVIII.3.37}$$

The displayed numerator has integer Laurent coefficients. This finite observation is not, on its own, a construction of a BPS spectrum or a proof of a geometric transition. The concrete question carried forward is which additional geometry and physical dictionary reproduce the Wilson generating function, including its framing and normalization.

The distinction between the two limits can be read directly from the denominator:

$$\frac{1}{2\sinh(y/2)} = \frac{1}{y} - \frac{y}{24} + \frac{7y^3}{5760} + O(y^5), \qquad y = nx. \tag{XVIII.3.38}$$

At fixed t_H the numerator in (XVIII.3.17) stays finite as $x \to 0$, producing the leading $1/x$. At fixed N it instead vanishes linearly with x, canceling that pole. The cancellation takes place before the power series is organized. The formal path $N = t_H/x$ is an asymptotic continuation; it is not a claim that every point of the path corresponds to an integer-rank compact theory.

The integer numerator follows just as directly. Since $D = (a - a^{-1})/\delta$ and $z^2 + z^{-2} = \delta^2 + 2$,

$$\delta W_{SU}^{(0)}(K_\sigma) = (a - a^{-1})\left[a^{-2}(\delta^2 + 2) - a^{-4}\right] \tag{XVIII.3.39}$$

$$= (a^{-1} - a^{-3})\delta^2 + 2a^{-1} - 3a^{-3} + a^{-5}. \tag{XVIII.3.40}$$

This calculation tells us exactly which finite coefficients have been found. A count of states would require a separate physical identification of the coefficients, its grading, and the appropriate sign and normalization conventions.

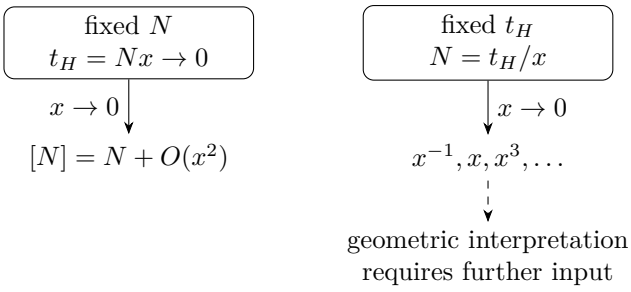


Figure XVIII.3.6: Two parameter paths organize the same formal expression differently. The dashed arrow records a question for the next chapter, not an identification established by the series.

Keeping the normalization through a knot calculation

The two-box example is a compact exercise in how the string observable retains representation information. Start with the power sums of the chosen holonomy. Squaring the first power sum counts the ordered tensor product, while the second power sum follows a single cycle through both tensor slots. Adding or subtracting these expressions and dividing by two selects the symmetric or antisymmetric character. The alternant formula supplies the same answer directly. This comparison concerns a specified finite degree, with the stated level bound when it is interpreted in the compact quantum theory.

For the two-strand knot, the next operation is propagation in these two channels. Raise each crossing eigenvalue to the braid power, multiply by the corresponding quantum dimension, and sum. Only then apply the declared framing correction and divide by the unknot when forming the reduced polynomial. The order makes it possible to locate a normalization error. A wrong channel dimension already changes the unknot specialization; a wrong braid eigenvalue changes the dependence on the braid power; a wrong framing factor changes the overall monomial. These changes have distinct physical meanings.

An even closure needs one further distinction. The two strands can close into different components, so their mutual linking contributes to the relative center prescription. A self-framing assigned to one component cannot absorb that mutual phase without changing the convention. The compact $SU(2)$ Hopf comparison and the continued MV expression consequently have to be translated before their values are compared.

The large-rank limit is another operation on this already normalized observable. Holding N fixed or holding t_H fixed follows different paths through the same formula. Neither path by itself makes t_H a geometric Kähler period. Chapter XVIII.4 supplies the separate conifold comparison, including the continuation and normalization data that such a geometric reading requires.

Exercises

1. Prove that the conormal of an embedded circle is exact Lagrangian. For the circle example, compare the shifts $p_s = c$ and $p_s = a(p_r, p_z, s)$.

2. Expand the determinant in (XVIII.3.6) to order v^2. Rewrite the result using the symmetric and antisymmetric Schur characters, and explain the origin of $1/n$ in its logarithm.

3. Derive the determinant prefactor in the chosen square-root lifts. Explain why determinant-one holonomies do not by themselves fix every lift or the zero-mode prescription.

4. Derive the three values in (XVIII.3.16) and their fixed-N classical limits. State the level restriction used for the two-box examples.

5. Compute the $SU(2)$ fundamental knot-framing factor and its ratio to the relative MV factor. Explain why neither is a manifold two-framing change.

6. Compute the level-three Hopf and unlink values. Derive (XVIII.3.29) from the two channels, then find its mirror and explain the linking correction for an even braid closure.

7. Derive (XVIII.3.35) through x^3 and the fixed-N expansion through x^2. Derive the trefoil integer numerator and explain what further input a geometric or BPS interpretation needs.

Sources and scope

The following section-keyed statements distinguish mathematical consequences from physical inputs. Page and equation locators use Ooguri and Vafa 2000, arXiv:hep-th/9912123v3; Mariño and Vafa 2001, arXiv:hep-th/0108064v1; Labastida and Mariño 2000, arXiv:hep-th/0004196v3; and Labastida, Mariño, and Vafa 2000, arXiv:hep-th/0010102v1. The Witten locators refer to the cited journal edition.

- §1: Conormal exactness and the intersection with the zero section are **MATH**; see Ooguri and Vafa 2000, pp. 6–7, eq. (3.1).
- §2: The mixed Gaussian scalar is a sourced **WS-T** input; its measure, zero modes and phase are not derived by finite algebra Ooguri and Vafa 2000, pp. 6–8, eqs. (3.1)–(3.7). The determinant and Cauchy expansion are **MATH** conditional on the stated normalization and lifts.
- §3: Unknot gluing and Weyl specialization are **MATH** within the supplied compact Chern–Simons/WZW construction Witten 1989, p. 391, eqs. (4.42)–(4.46); Ooguri and Vafa 2000, pp. 8–9, eqs. (3.7)–(3.14); Mariño and Vafa 2001, pp. 17–18, eqs. (5.1)–(5.4). The degreewise generator has the finite-level qualifications stated in the text.
- §4: Knot twists and the fixed-lift relative S^3 phase are **MATH** consequences of the sourced quantum prescriptions Mariño and Vafa 2001, pp. 8–10, eqs. (3.9)–(3.19); Labastida, Mariño, and Vafa 2000, pp. 23–25, eqs. (4.27)–(4.40). The relative phase does not supply a global $U(N)$ theory.
- §5: The Hopf comparison, declared trefoil and mirror, and link-normalization translations are **MATH** conditional on the quantum gluing and skein inputs Witten 1989, pp. 381–382 and 392, eqs. (4.18)–(4.23) and (4.47); Labastida and Mariño 2000, pp. 19–20, eqs. (4.3)–(4.7); Labastida, Mariño, and Vafa 2000, pp. 23–25, eqs. (4.27)–(4.40).
- §6: The two asymptotic paths and finite integer numerator are **MATH** consequences of the displayed formulas; compare Ooguri and Vafa 2000, p. 9, eqs. (3.8)–(3.14), and Labastida and Mariño 2000, pp. 19–20. This does not establish a BPS spectrum, an all-knot theorem, or a geometric transfer.

References

Labastida, J. M. F. and M. Mariño (2000). "Polynomial Invariants for Torus Knots and Topological Strings". In: arXiv: `hep-th/0004196`.

Labastida, J. M. F., M. Mariño, and C. Vafa (2000). "Knots, Links and Branes at Large N". In: arXiv: `hep-th/0010102`.

Mariño, M. and C. Vafa (2001). "Framed Knots at Large N". In: arXiv: `hep-th/0108064`.

Ooguri, H. and C. Vafa (2000). “Knot Invariants and Topological Strings”. In: *Nucl. Phys. B* 577, pp. 419–438. arXiv: hep-th/9912123.
Witten, E. (1989). “Quantum Field Theory and the Jones Polynomial”. In: *Commun. Math. Phys.* 121, pp. 351–399. DOI: 10.1007/BF01217730.

Chapter XVIII.4

Chern–Simons theory and the resolved conifold

Open strings on the zero section of T^*S^3 give a protected perturbative Chern–Simons sector. Their matrix indices draw surfaces with holes. A closed string expansion would have to replace those holes by a new geometric parameter. The conifold transition suggests where that parameter can live: a three-sphere disappears at a singular point, and a two-sphere appears in a different smooth geometry. The question is which observable actually follows this change.

We compare the connected positive-curve-degree rational coefficients obtained from a declared lift of the exact sphere vacuum with those of the absolute local theory on $\mathcal{O}(-1) \oplus \mathcal{O}(-1) \to \mathbb{P}^1$. The sphere modular theorem and the absolute local-curve theorem are separately supplied inputs. We will derive the coefficient equality at every positive degree, keeping the normalization outside that comparison visible. This is the controlled content of the large-N comparison developed here.

The reader needs the open construction of Chapters 1–2, the conifold geometry of Volume IV, Chapter 5, and the absolute local-curve theory of Volume V, Chapter 7. Chapter 3 explains why relative Wilson observables alone cannot determine the vacuum normalization. We take $F = \log Z$ throughout. A logarithm selects connected contributions, whereas Z also contains products of disconnected worldsheets.

XVIII.4.1 The cycle that changes

The conifold is the rank-at-most-one locus of a complex 2×2 matrix. A linear change of its four entries puts its equation in quadric form. Its singular and deformed versions can be written

$$\det M = 0, \qquad \sum_{a=1}^{4} z_a^2 = 0, \qquad X_\epsilon = \left\{ \sum_{a=1}^{4} z_a^2 = \epsilon \right\}. \tag{XVIII.4.1}$$

At $\epsilon \neq 0$, the gradient $2(z_1, \ldots, z_4)$ cannot vanish on X_ϵ. On the phase-rotated slice $\epsilon > 0$, the real locus is a three-sphere of radius $\sqrt{\epsilon}$. It contracts as $\epsilon \to 0$.

Recall the cotangent description to see which brane this sphere supports. Write $z = a + ib$ with $a, b \in \mathbb{R}^4$. Then

$$|a|^2 - |b|^2 = \epsilon, \qquad a \cdot b = 0, \qquad q = \frac{a}{\sqrt{\epsilon + |b|^2}}, \quad q \cdot b = 0. \tag{XVIII.4.2}$$

Thus (q, b) is a point of T^*S^3 after using the round metric to identify tangent and cotangent vectors. Conversely $a = \sqrt{\epsilon + |b|^2}\, q$ reconstructs z. The real sphere is $b = 0$, exactly the zero section on which the open A-model branes sit. This is a topological description of the smooth quadric, not a claim that arbitrary metrics agree.

The small resolution changes the operation. Choose an image line $[s : t] \in \mathbb{P}^1$ and require both columns of M to lie in it:

$$\widetilde{X} = \{(M, [s : t]) : \operatorname{im} M \subset \mathbb{C}(s, t)\}, \qquad M = \begin{pmatrix} su & sv \\ tu & tv \end{pmatrix}. \tag{XVIII.4.3}$$

For $M \neq 0$ of rank one, its image determines the line uniquely. At $M = 0$, every line is allowed, giving the exceptional $\mathbb{P}^1$. In the chart $s \neq 0$, put $s = 1$ and $t = w$. In the chart $t \neq 0$, the fiber coordinates become $(u', v') = (wu, wv)$. These are the two tautological line-bundle transitions. Hence the total space is the local curve $\mathcal{O}(-1) \oplus \mathcal{O}(-1)$. The other incidence choice uses a row line and gives the other small resolution.

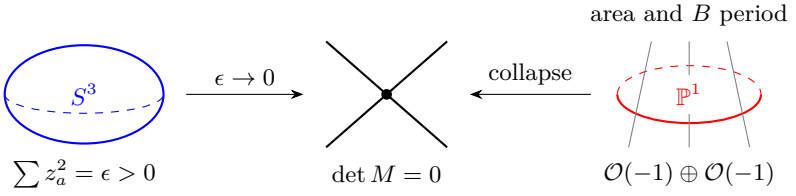


Figure XVIII.4.1: Three distinct local geometries. The deformed quadric contains the real zero-section S^3; the singular quadric has a node; the chosen incidence resolution contains an exceptional $\mathbb{P}^1$. The arrows pass through a singular geometry. The deformation ϵ and the area/B period are different parameters. No smooth interpolation or quantum equivalence is represented by these arrows.

To compare curve degrees, use the same dimensionless coordinate as the closed A-model. Let t_β denote the complexified period of the exceptional curve. The comparison chooses

$$x = \frac{2\pi i}{K} = i\lambda, \quad K = k + N, \quad T = Nx, \quad q_{\text{decay}} = e^{-x}, \quad Q = e^{-T} = e^{2\pi i t_\beta}. \tag{XVIII.4.4}$$

Thus $T = -2\pi i t_\beta$ modulo $2\pi i\mathbb{Z}$. This specifies the translation in the calculation; ribbon counting will not derive a physical period identification. The parameter q_{decay} is the inverse of the quantum variable used for knots in Chapter 3.

A positive-degree connected free energy has the form

$$F_{>0}(Q,x)=\sum_{d\geq 1}Q^d a_d(x), \qquad Z_{\mathrm{red}}=\exp F_{>0}=1+Qa_1+Q^2\left(a_2+\tfrac{1}{2}a_1^2\right)+\cdots. \tag{XVIII.4.5}$$

The coefficient of Q^2 in Z_{red} includes two disconnected degree-one components. The coefficient in $F_{>0}$ does not. Removing connected degree-zero components is part of the absolute local-curve definition used below; it does not remove contracted irreducible components attached to a positive-degree map.

XVIII.4.2 What the ribbon surface determines

A double-line diagram translates powers of rank into holes of an oriented surface. It tells us how an open amplitude can be organized as a closed genus expansion. It does not determine the closed target or its absolute partition function.

In the specified action normalization, a propagator contributes x, a cubic vertex contributes x^{-1}, and a closed index face contributes N. If a connected ribbon graph has V vertices, E edges and h faces, its coupling and rank factor is

$$x^{E-V}N^h. \tag{XVIII.4.6}$$

Thicken the graph to an oriented surface with h boundary components. Its deformation retract is the graph, so its Euler characteristic is

$$V-E=2-2g-h. \tag{XVIII.4.7}$$

Eliminating $E-V$ and then inserting $T=Nx$ gives

$$x^{E-V}N^h=x^{2g-2+h}N^h=x^{2g-2}T^h. \tag{XVIII.4.8}$$

The factor x^{2g-2} is the closed genus weight. Summing the holes at fixed g would produce a function of T. This motivates holding T fixed while N grows and x decreases. It differs from the fixed-N weak-coupling expansion of a knot invariant.

The cyclic order at a vertex matters as much as the underlying graph. Label the six half-edges of a theta graph by $1,2,3$ on the first vertex and $4,5,6$ on the second. Pair the edges by

$$\alpha=(1\,4)(2\,5)(3\,6), \quad \sigma_0=(1\,2\,3)(4\,6\,5), \quad \sigma_1=(1\,2\,3)(4\,5\,6). \tag{XVIII.4.9}$$

Following an edge and then the next half-edge around its endpoint traces a face. With permutations composed right to left, these face permutations are

$$\sigma_0\alpha=(1\,6)(2\,4)(3\,5), \qquad \sigma_1\alpha=(1\,5\,3\,4\,2\,6). \tag{XVIII.4.10}$$

Thus the two cyclic orders give three faces and one face, respectively. The abstract graph still has $V=2$ and $E=3$ in both cases. Equation (XVIII.4.7) now determines

$$(h,g)=(3,0): \quad xN^3=x^{-2}T^3, \qquad (h,g)=(1,1): \quad xN=T. \tag{XVIII.4.11}$$



Figure XVIII.4.2: The same theta graph with two rotation systems. The edge pairing is $\alpha = (14)(25)(36)$. The displayed cycles of $\sigma\alpha$ explicitly trace every face. Opposite orders at the two vertices give three faces and genus zero; the same orders give one face and genus one. The plane drawing alone does not specify the second ribbon surface.

Changing a cyclic order has changed the genus, with no change in the number of vertices or propagators. The genus here belongs to the ribbon worldsheet, not to the target threefold.

The open A-model construction supplies the protected perturbative action subject to its Ward, measure and sewing premises. A compact quantum theory contains more information, including the shifted level, integrable representations, sphere gluing, and a two-framing convention. The counting in this section fixes none of those. We therefore turn to a specified modular vacuum before extracting a closed coefficient.

XVIII.4.3 The absolute sphere vacuum

The relative normalization of Wilson loops cancels the vacuum amplitude. Here the vacuum itself is the starting object, so the global theory and its prefactor have to be chosen first. Take $N \geq 2$ and positive integral bare level k. For the compact $SU(N)_k$ theory, the supplied modular theorem and sphere-gluing prescription give $Z(S^3) = S_{00}$. In long-root-length-squared-two conventions,

$$S_{00}^{SU} = \frac{i^p}{\sqrt{N} K^{(N-1)/2}} \sum_{w \in W} \epsilon(w) e^{-2\pi i(\rho, w\rho)/K}, \qquad p = \frac{N(N-1)}{2}. \tag{XVIII.4.12}$$

Here W is the type-A Weyl group, $\epsilon(w)$ its sign, and ρ half the sum of positive roots. The phase in this formula belongs to the chosen positive sphere reference. It cannot be discarded before evaluating the Weyl sum.

A root is $e_i - e_j$ with $i < j$. Since $(\rho, e_i - e_j) = j - i$, each height m occurs once for every pair $(i, i+m)$, hence $N - m$ times. The Weyl denominator makes the phase cancellation explicit:

$$\sum_{w \in W} \epsilon(w) e^{-2\pi i(\rho, w\rho)/K} = \prod_{\alpha > 0} \left(e^{-\pi i(\alpha,\rho)/K} - e^{\pi i(\alpha,\rho)/K} \right) \tag{XVIII.4.13}$$

$$= (-i)^p \prod_{\alpha > 0} 2 \sin \frac{\pi(\alpha, \rho)}{K} = (-i)^p P_N. \tag{XVIII.4.14}$$

The prefactor satisfies $i^p(-i)^p = 1$. At rank two the sum is $-2i\sin(\pi/K)$, and multiplication by i makes it positive. Grouping roots by height now gives

$$P_N = \prod_{m=1}^{N-1} \Big[2\sin\frac{\pi m}{K}\Big]^{N-m}, \qquad Z_{SU} = \frac{P_N}{\sqrt{N}K^{(N-1)/2}}. \tag{XVIII.4.15}$$

The prefactor also has a geometric lattice origin. If D_r is the determinant of the rank-r type-A Cartan matrix, expansion of its tridiagonal determinant yields

$$D_r = 2D_{r-1} - D_{r-2}, \quad D_0 = 1,\ D_1 = 2, \qquad D_r = r+1. \tag{XVIII.4.16}$$

At $r = N-1$, the weight-to-root covolume ratio is $1/N$. The square root in the modular formula is therefore $1/\sqrt{N}$. Root counting and this determinant explain the finite algebra. The modular representation and gluing theorem remain the input that makes it a quantum sphere amplitude.

There is a second specified sphere object. For odd k, use the quotient with its supplied charge-selection and orbit data,

$$\frac{SU(N)_k \times U(1)_{NK}}{\mathbb{Z}_N}. \tag{XVIII.4.17}$$

We denote it by NS to keep that global choice explicit. Its abelian vacuum supplies $1/\sqrt{NK}$, and the quotient orbit supplies N. Consequently

$$\frac{S_{00}^{NS}}{S_{00}^{SU}} = \frac{N}{\sqrt{NK}} = \sqrt{\frac{N}{K}}, \qquad Z_{NS} = \frac{P_N}{K^{N/2}}. \tag{XVIII.4.18}$$

This is not an automatic meaning of the symbol $U(N)$ in a local action. Splitting a local connection as $A = A_{su} + aI_N$ gives bare center coefficient Nk. Equation (XVIII.4.17) instead specifies the global quantum center NK. Passing between them would require regularization and global or spin data that the local action does not supply.

For the concrete example $N = 2, k = 3$, the only positive root has height one. Keeping the Cartan prefactor and then the quotient factor gives

$$Z_{SU} = \sqrt{\frac{2}{5}}\sin\frac{\pi}{5}, \qquad Z_{NS} = \frac{2}{5}\sin\frac{\pi}{5}, \qquad \frac{Z_{NS}}{Z_{SU}} = \sqrt{\frac{2}{5}}. \tag{XVIII.4.19}$$

Replacing $K = 5$ by the bare $k = 3$ would change both the sine and the prefactor. Omitting the quotient factor changes the absolute answer even though it will leave the positive-degree kernel unchanged.

In free energies the difference survives as a genus-one logarithm. Continuing the positive ratio on the chosen logarithm lift gives

$$F_{SU} - F_{NS} = -\tfrac{1}{2}\operatorname{Log}\frac{N}{K} = -\tfrac{1}{2}\operatorname{Log}\frac{T}{2\pi i}. \tag{XVIII.4.20}$$

We will retain this term after extracting the positive-degree part. An equality of those coefficients is compatible with unequal sphere normalizations.

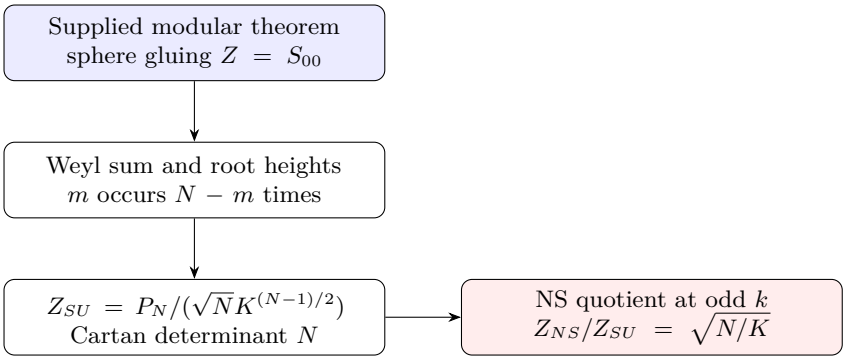


Figure XVIII.4.3: The absolute sphere calculation begins with supplied compact modular and gluing data. Weyl root heights and the Cartan determinant explain the finite SU expression. The NS quotient is a separately specified odd-k model, not a consequence of the local center term Nk.

XVIII.4.4 Two routes to every positive degree

The sphere product is finite in rank. The closed curve expansion is infinite in degree. The bridge is an endpoint term in an elementary finite sum, followed by a declared formal lift. We first derive the split in a convergent domain, so that no interchange of divergent root-of-unity sums enters the argument.

Continue clockwise from $x = 2\pi i/K$ to positive real x, using $\operatorname{Log} i = i\pi/2$. Temporarily write $q = q_{\mathrm{decay}}$ for readability. For integer N and $|q| < 1$,

$$2\sinh\frac{mx}{2} = e^{mx/2}(1-q^m), \qquad \log P_N^{\sinh} = \frac{xN(N^2-1)}{12} + \sum_{m=1}^{N-1}(N-m)\log(1-q^m). \tag{XVIII.4.21}$$

The polynomial follows from $\sum_{m=1}^{N-1} m(N-m) = N(N^2-1)/6$. The continued positive sine reference has an additional i^{-p}; it is not part of $P_N^{\sinh}$.

To expand the logarithm, evaluate $S_N(z) = \sum_{m=1}^{N-1}(N-m)z^m$. Multiplication by $1-z$ telescopes once, and a second multiplication isolates both endpoints:

$$(1-z)S_N(z) = (N-1)z - \sum_{m=2}^{N} z^m, \tag{XVIII.4.22}$$

$$(1-z)^2 S_N(z) = (N-1)z - Nz^2 + z^{N+1}. \tag{XVIII.4.23}$$

Thus for $z \neq 1$,

$$S_N(z) = N\frac{z}{1-z} - \frac{z}{(1-z)^2} + \frac{z^{N+1}}{(1-z)^2}. \tag{XVIII.4.24}$$

At $N = 3$ the result is $2z + z^2$. At $N = 1$ the sum vanishes: the endpoint cancels the two bulk terms exactly. This latter limit shows why dropping the endpoint is not an approximation to the finite identity.

Insert $\log(1-q^m) = -\sum_{d\geq 1} q^{md}/d$ and apply (XVIII.4.24) at $z = q^d$. The result separates three contributions:

$$\log P_N^{\sinh} = \frac{xN(N^2-1)}{12} + N\log\prod_{m\geq 1}(1-q^m) + \log M(q) - \sum_{d\geq 1}\frac{q^{Nd}q^d}{d(1-q^d)^2}, \quad \text{(XVIII.4.25)}$$

where $M(q) = \prod_{m\geq 1}(1-q^m)^{-m}$ is the MacMahon function. For example its logarithm is $\sum_{d\geq 1} q^d/[d(1-q^d)^2]$, the second bulk term after the signs from the logarithmic expansion are included.

Only now set $q^N = Q = e^{-T}$ in the endpoint and declare Q independent of generic q. This defines the formal lift used in this chapter:

$$F_{>0}^{CS}(Q,x) = -\sum_{d\geq 1}\frac{Q^d q^d}{d(1-q^d)^2}, \qquad a_d(x) = -\frac{q^d}{d(1-q^d)^2}. \quad \text{(XVIII.4.26)}$$

It follows from an integer-N analytic identity, but the independent-Q interpretation is additional structure. The finite values $Q = q^N$ alone do not uniquely determine an interpolation with two independent variables. Nor have the polynomial and logarithmic functions of T become analytic constants at $Q = 0$.

The second route starts from the absolute local-curve theory recalled in Volume V, Chapter 7. The base is $\mathbb{P}^1$, the two normal line bundles have degrees $(-1,-1)$, and the fiber torus acts anti-diagonally. Every connected component has positive degree. Negative degree of the pulled-back normal bundles forces sections to vanish on positive-degree components; this zero propagates along attached contracted components. Thus this particular local geometry has the required proper map loci. This does not license an absolute theory for an arbitrary noncompact target.

The supplied absolute balanced local-curve theorem gives its disconnected fixed-degree coefficient as a sum over partitions. In the present continued variable its hook form is

$$Z'_d = \sum_{\mu\vdash d}(-1)^d\prod_{\square\in\mu}\frac{q^{h_\square}}{(1-q^{h_\square})^2}, \qquad Z_{BP} = 1 + \sum_{d\geq 1} Q^d Z'_d. \quad \text{(XVIII.4.27)}$$

Here $h_\square$ is the hook length of a box, counting the box itself and the boxes to its right and below. Vacuum one has been added separately. Disconnected arithmetic genus can be negative, since the genus weight multiplies over components. Equation (XVIII.4.27) is an imported absolute theorem, not a relative invariant with its required markings deleted.

For completeness, the symmetric-function conversion explains why these hook coefficients give exactly (XVIII.4.26). Put $n(\mu) = \sum_i (i-1)\mu_i$ and $y = (q^{1/2}, q^{3/2}, \ldots)$. The supplied principal hook specialization reads

$$s_\mu(y) = \frac{q^{|\mu|/2 + n(\mu)}}{\prod_{\square\in\mu}(1-q^{h_\square})}. \quad \text{(XVIII.4.28)}$$

Summing arms and legs of every box gives

$$\sum_{\square\in\mu} h_\square = |\mu| + n(\mu) + n(\mu^t), \qquad s_\mu(y)s_{\mu^t}(y) = \prod_{\square\in\mu}\frac{q^{h_\square}}{(1-q^{h_\square})^2}. \quad \text{(XVIII.4.29)}$$

Dual Cauchy with the degree marker $-Q$ therefore converts the partition sum into an infinite product:

$$Z_{BP} = \sum_{\mu} (-Q)^{|\mu|} s_{\mu}(y) s_{\mu^t}(y) = \prod_{i,j \geq 1} (1 - Qq^{i+j-1}) = \prod_{m \geq 1} (1 - Qq^m)^m. \quad \text{(XVIII.4.30)}$$

For each m, there are m pairs of positive integers with $i + j - 1 = m$. Taking the logarithm, first in $|q| < 1$ and then as rational coefficients at generic q, gives

$$[Q^d] \log Z_{BP} = -\frac{1}{d} \sum_{m \geq 1} m q^{md} = -\frac{q^d}{d(1-q^d)^2} = a_d(x). \quad \text{(XVIII.4.31)}$$

This is the all-degree derivation. Finite partition examples test the translation; they do not replace the absolute theorem or dual Cauchy.

At degree two both partitions have hooks $2, 1$. Consequently

$$Z_2' = \frac{2q^3}{(1-q)^2(1-q^2)^2}, \quad a_1 = -\frac{q}{(1-q)^2}, \quad a_2 = -\frac{q^2}{2(1-q^2)^2}. \quad \text{(XVIII.4.32)}$$

Indeed

$$\frac{a_1^2}{2} + a_2 = \frac{q^2[(1+q)^2 - (1-q)^2]}{2(1-q)^2(1-q^2)^2} = \frac{2q^3}{(1-q)^2(1-q^2)^2}. \quad \text{(XVIII.4.33)}$$

Keeping one partition would halve this answer. Keeping only a_2 would confuse connected and disconnected maps.

Finally $q = e^{-i\lambda}$ converts the same rational function to the sine frame:

$$\frac{q^d}{(1-q^d)^2} = \frac{1}{4\sinh^2(dx/2)}, \qquad a_d(i\lambda) = \frac{1}{d[2\sin(d\lambda/2)]^2}. \quad \text{(XVIII.4.34)}$$

The continuation changes the sign of the squared denominator. Changing the free-energy sign independently would change the result again. The equality holds coefficientwise away from the poles of the individual rational function.

XVIII.4.5 Genus coefficients and the normalization left over

The rational kernel determines all positive degrees before the genus expansion is taken. Expanding it at small λ reveals the multiple-cover weights and also identifies the information this operation leaves out.

For $y = d\lambda$, the Taylor expansion of the sine gives

$$[2\sin(y/2)]^2 = y^2 \left(1 - \frac{y^2}{12} + \frac{y^4}{360} - \frac{y^6}{20160} + \cdots\right). \quad \text{(XVIII.4.35)}$$

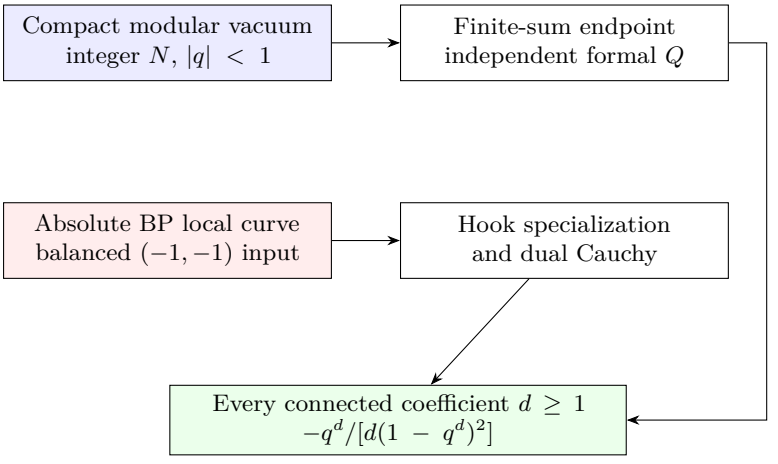


Figure XVIII.4.4: Two supplied starting objects lead to the same rational coefficient. The upper path is the continued compact sphere product and its endpoint lift. The lower path is the absolute balanced local-curve theorem and hook/dual-Cauchy algebra. This equality of connected positive-degree coefficients does not compare the full partition functions or supply an independent physical proof of all the imported theorems.

Inverting this series determines the coefficients successively. If the inverse factor is $1 + b_1y^2 + b_2y^4 + b_3y^6 + \cdots$, cancellation of the y^2, y^4, y^6 terms gives

$$b_1 = \frac{1}{12}, \qquad b_2 = \frac{b_1}{12} - \frac{1}{360} = \frac{1}{240}, \qquad b_3 = \frac{b_2}{12} - \frac{b_1}{360} + \frac{1}{20160} = \frac{1}{6048}. \tag{XVIII.4.36}$$

Thus the contribution of cover degree d is

$$a_d(i\lambda) = \frac{1}{d^3\lambda^2} + \frac{1}{12d} + \frac{d\lambda^2}{240} + \frac{d^3\lambda^4}{6048} + O(\lambda^6). \tag{XVIII.4.37}$$

To sum the covers, recall the polylogarithm

$$\mathrm{Li}_s(Q) = \sum_{d\geq 1} \frac{Q^d}{d^s}, \qquad |Q| < 1, \tag{XVIII.4.38}$$

with continuation only in the specified domains. Summing over degrees at fixed Q gives the first four genera:

$$F_{>0}(Q, i\lambda) = \frac{\mathrm{Li}_3(Q)}{\lambda^2} - \frac{1}{12}\log(1-Q) + \frac{\lambda^2}{240}\frac{Q}{(1-Q)^2} \tag{XVIII.4.39}$$

$$+ \frac{\lambda^4}{6048}\frac{Q(1+4Q+Q^2)}{(1-Q)^4} + O(\lambda^6). \tag{XVIII.4.40}$$

At $d = 2$, the four weights are $1/8$, $1/24$, $1/120$ and $1/756$. The genus-zero weight decreases as d^{-3}, whereas the higher-genus weights grow with degree. This is why a fixed-degree expansion and a sum at a physical root of unity require different care.

To recover the whole continued sphere reference, restore the terms retained in (XVIII.4.25) and the absolute prefactor. On the branch fixed above,

$$Z_{NS}^{\mathrm{cont}} = \Big(\frac{x}{2\pi i}\Big)^{N/2} i^{-p} P_N^{\sinh}. \tag{XVIII.4.41}$$

The Dedekind eta transformation, used here as a supplied modular identity, is conveniently expressed for its product as

$$L(x) := \log \prod_{m\geq 1} (1 - e^{-mx}) = -\frac{\pi^2}{6x} + \tfrac{1}{2}\log\frac{2\pi}{x} + \frac{x}{24} + L(4\pi^2/x). \tag{XVIII.4.42}$$

It applies first at positive real x. The logarithms in $NL(x)$ cancel the real logarithm of the prefactor, while their imaginary parts remain. With $T = Nx$, the full identity is

$$F_{NS}^{\mathrm{cont}} = F_{>0} + \log M(e^{-x}) + \frac{T^3/12 - \pi^2 T/6 - i\pi T^2/4}{x^2} - \frac{T}{24} + \frac{T}{x} L(4\pi^2/x). \tag{XVIII.4.43}$$

For example $xN(N^2-1)/12 + Nx/24 = T^3/(12x^2) - T/24$. The phase follows from

$$-\frac{i\pi N}{4} - \frac{i\pi N(N-1)}{4} = -\frac{i\pi N^2}{4}. \tag{XVIII.4.44}$$

These two short calculations fix terms that would be lost if a sinh product were equated directly with a positive sine product.

Contribution	Continued free-energy term
Positive curve degree	$F_{>0} = -\sum_{d\geq 1} Q^d q^d/[d(1-q^d)^2]$
Polynomial	$(T^3/12 - \pi^2 T/6)/x^2$
Analytic phase	$-i\pi T^2/(4x^2)$
MacMahon	$\log M(e^{-x})$
Genus-one linear	$-T/24$
SU instead of NS	$-\frac{1}{2}\,\mathrm{Log}[T/(2\pi i)]$
Dual eta	$(T/x)L(4\pi^2/x)$
Two-framing shift	$2\pi i s c/24$, for integral s

Figure XVIII.4.5: Contributions to the continued sphere free energy in (XVIII.4.43). Only the first row belongs to the declared positive-Q lift. The SU logarithm and the two-framing shift are separate additions for the corresponding choices. Polynomial and logarithmic functions of T have not become analytic Q-adic constants. MacMahon is a specified local normalization, not an unrestricted degree-zero integral.

At fixed positive T, the last term is exponentially small as $x \to 0^+$. It is an exact term in this finite-product continuation and is absent from every algebraic order of its genus asymptotics. It must not be identified with a pure-C worldsheet contribution or promoted to a nonperturbative completion at physical level.

The MacMahon asymptotic series has its own derivation. First expand the rational kernel,

$$(1-e^{-dx})^{-2}e^{-dx}=\sum_{m\geq 1} me^{-dmx}. \tag{XVIII.4.45}$$

Taking the Mellin transform term by term in a right half-plane and applying Mellin inversion gives

$$\log M(e^{-x})=\frac{1}{2\pi i}\int_{c-i\infty}^{c+i\infty}\Gamma(s)\zeta(s+1)\zeta(s-1)x^{-s}\,ds, \qquad c>2. \tag{XVIII.4.46}$$

The pole at $s=2$ contributes $\zeta(3)x^{-2}$. At $s=0$, the product of the two simple poles of $\Gamma(s)$ and $\zeta(s+1)$ combines with $\zeta(-1)=-1/12$. Multiplication by x^{-s} gives $\log x/12+\zeta'(-1)$. The residues at negative even integers then yield

$$\log M(e^{-x})\sim \frac{\zeta(3)}{x^2}+\frac{\log x}{12}+\zeta'(-1) \tag{XVIII.4.47}$$

$$+\sum_{g\geq 2}\frac{B_{2g}B_{2g-2}}{2g(2g-2)(2g-2)!}x^{2g-2}. \tag{XVIII.4.48}$$

Here B_{2g} are Bernoulli numbers with $B_2=1/6$, $B_4=-1/30$. The first two higher terms are $-x^2/2880$ and $-x^4/725760$. Contour displacement and remainder estimates belong to the positive-real asymptotic statement. This is not a convergent power series defining the physical finite-level answer.

A further normalization appears when changing the book two-framing by an integer s:

$$\frac{Z^{(s)}}{Z^{(0)}}=e^{2\pi i s c/24}, \qquad c_{SU}=\frac{k(N^2-1)}{K}, \qquad c_{NS}=c_{SU}+1. \tag{XVIII.4.49}$$

Knot framing and sphere two-framing are different operations. Nor is a Gaussian continuation phase automatically the latter. At $N=2,k=3$, $c_{NS}=14/5$. Equating a lifted phase $\exp(i\pi N^2/4)$ to the framing exponent as real numbers gives $s=30/7$. Equating the exponentials instead requires

$$\frac{sc_{NS}}{24}-\frac{N^2}{8}\in\mathbb{Z}. \tag{XVIII.4.50}$$

The integer $s=30$ satisfies this condition, with difference 3. It is a single arithmetic witness, not a global framing prescription. At $N=3,k=5$, $c_{NS}=6$, and the condition becomes $s/4-9/8\in\mathbb{Z}$, or $2s-9\in 8\mathbb{Z}$, which has no integer solution. A universal framing claim cannot follow from the first witness.

Absolute phases also expose literal source discrepancies. They are useful here because they show why we anchored the sphere amplitude to its explicit modular normalization. In the Gaussian and group-volume formulas of the worldsheet source, taking $\operatorname{Log} i=i\pi/2$ gives

$$Z_{\mathrm{Gauss}}=e^{i\pi N^2/4}Z_{\mathrm{np}}^{\mathrm{ref}}, \qquad Z_{\mathrm{np}}^{\mathrm{ref}}=\left(\frac{2\pi}{K}\right)^{N^2/2}\frac{G_2(N+1)}{(2\pi)^{N/2}}, \tag{XVIII.4.51}$$

where $G_2(N+1) = \prod_{j=1}^{N-1} j!$. Its printed subsequent formula instead has $e^{i\pi N^2/8}$. The ratio is $e^{-i\pi N^2/8}$, equal to $-i$ at $N = 2$. This is not a logarithm ambiguity by $2\pi i$.

A second discrepancy is a later reciprocal-level identification $K = 1/\lambda_s$, while the same source's earlier section uses $\lambda_2 = i/K$, $t_2 = iN/K$. With $b = 1/K$ the log consistent with the preceding Gaussian expansion is

$$\mathrm{Log}(2\pi i N b) = \mathrm{Log}\, T. \tag{XVIII.4.52}$$

Substituting that earlier t_2 literally into the later printed $\mathrm{Log}(2\pi i t)$ instead gives $\mathrm{Log}(iT)$ and an additional $i\pi/2$ on this lift. The corresponding free-energy difference is $i\pi N^2/4$. Higher-genus ratio powers are unchanged; low-genus phases are not.

Finally, another source's minus-exponent Weyl sum and positive sinh product differ by $(-1)^p$. Already at rank two,

$$e^{-x/2} - e^{x/2} = -2\sinh(x/2). \tag{XVIII.4.53}$$

These are three failed literal equalities, not three choices silently absorbed into a positive reference. Their exact anchors are given in the chapter-end sources. A separate printed Binet-type expression contains $\tan(t/z)$ and has an interior pole at $z = 1, t = \pi/2$. We do not use that improper integral as a Gamma representation. No published erratum or intended correction is asserted. The finite factorial product and Mellin route suffice for the asymptotics used here.

XVIII.4.6 What the worldsheet mechanism explains

The coefficient calculation has used two independently specified mathematical objects. The worldsheet description addresses a different question: how can regions of a closed worldsheet create boundaries carrying an open sector? Its central picture cuts the twisted conifold model into H and C regions. Both are regions of the Higgs-branch theory. The separately infrared-decoupled Coulomb theory is not the C region in this construction.

Keep the source coordinates distinct before performing a contour calculation. The Chern–Simons discussion of that source uses the earlier pair

$$t_2 = \frac{iN}{K}, \quad \lambda_2 = \frac{i}{K}, \quad T = 2\pi t_2, \quad x = 2\pi\lambda_2. \tag{XVIII.4.54}$$

Its GLSM section instead has the FI/theta coefficient and effective twisted superpotential

$$u_{\mathrm{GLSM}} = \frac{\theta}{2\pi} + ir, \qquad W = u_{\mathrm{GLSM}}\Sigma. \tag{XVIII.4.55}$$

Here r is the source FI parameter, θ the theta angle and Σ the twisted chiral field. Denote the genus coupling of this discussion by η_{GLSM}. At $r = 0$ its u_{GLSM} is real for real θ. The earlier t_2 is imaginary for physical positive N, K. Their zero-area real slices cannot be equated by a positive real factor 2π. We therefore compute in each coordinate separately.

Choose a cutoff in $|\sigma|$, where σ is the scalar of Σ. The source integrates the large-$|\sigma|$ C region and describes its interfaces with H regions by boundary amplitudes. A C surface of genus g with $h \geq 1$ H boundaries has a count of real moduli/supercurrent insertions

$$n_{g,h} = 6g + 3h - 6. \tag{XVIII.4.56}$$

For $n_{g,h} > 0$, the source's correlator and measure argument makes the differentiated amplitude single-valued in the relevant boundary parameter. Its monodromy contour then gives zero. This is a protected-worldsheet argument conditional on the stated Ward, measure and factorization premises. Merely counting the insertions would not prove single-valuedness or fix the integration cycle.

The disk and annulus are exceptions to that count. For an annulus the source takes two boundary contours. Schematically its contribution has the form

$$\oint d\sigma_0 \oint d\sigma_0' \, \partial_{\sigma_0} \partial_{\sigma_0'} F_{0,2}(\sigma_0, \sigma_0'). \tag{XVIII.4.57}$$

The differentiated integrand is single-valued in the other boundary variable under the source prescription; taking that contour annihilates the result. This is the separate annulus argument. The disk instead survives and produces one factor for each newly created H boundary.

The measure carries physical information from the C region. In the source model, the charged chiral fields are massive there. Integrating them out induces a dilaton, whose contribution changes the field-space measure from $d\sigma$ to $d\sigma/\sigma^2$. We use this source result as an input; the linear superpotential alone would not determine it. With the explicitly normalized contour, its disk consequence is

$$D(u_{\mathrm{GLSM}}) = \frac{1}{2\pi i} \oint_{|\sigma|=\varepsilon} \frac{d\sigma}{\sigma^2} e^{u_{\mathrm{GLSM}}\sigma}, \tag{XVIII.4.58}$$

$$e^{u\sigma} = 1 + u\sigma + \tfrac{1}{2}u^2\sigma^2 + \cdots, \qquad D(u_{\mathrm{GLSM}}) = u_{\mathrm{GLSM}}. \tag{XVIII.4.59}$$

An ordinary unnormalized contour gives $2\pi i u_{\mathrm{GLSM}}$. If the factor σ^{-2} is dropped, the integrand is holomorphic and the answer is zero. Thus the induced measure is essential to the claimed disk weight. The residue computes its consequence; it does not derive that physical measure from the superpotential.

A field rescaling also changes it. If $\sigma' = b\sigma$, then

$$\frac{d\sigma}{\sigma^2} = b\,\frac{d\sigma'}{\sigma'^2}, \qquad e^{u\sigma} = e^{(u/b)\sigma'}. \tag{XVIII.4.60}$$

The residue remains $b(u/b) = u$ when both changes are included. A coordinate rotation with the Jacobian suppressed is a different contour calculation.

Under its topological deformation and boundary Dirichlet limit, the source identifies H-domain boundary amplitudes with its specific A-brane sector. Sewing h surviving disks onto it supplies u_{GLSM}^h in that source normalization. This explains the form of an open expansion after C regions create boundaries. It does not classify all A-branes, and it does not prove a measure-preserving field map from (XVIII.4.55) to (XVIII.4.4).

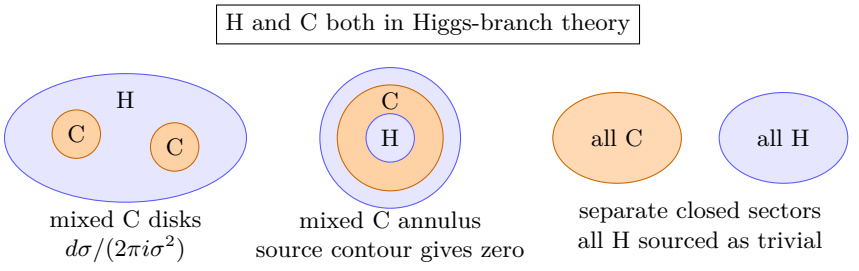


Figure XVIII.4.6: H/C decomposition inside the Higgs-branch theory. Orange C disks can end on the blue H region and carry the sourced normalized measure $d\sigma/(2\pi i\sigma^2)$. The orange annulus has H on both sides of its boundaries. Stable mixed C components and the annulus have distinct sourced vanishing arguments. All-C and the separately sourced trivial all-H sector have no such mixed boundary. The excluded infrared Coulomb theory is a different object. Boundary pictures do not establish a coordinate dictionary or sewing normalization.

The all-H closed surface is separately called trivial in the source. A surface that is all C has no H boundary and is not eliminated by the mixed-boundary argument.

The all-C amplitude uses a further source input. The source takes the inverse of Σ as a local field coordinate, with

$$d(\sigma^{-1}) = -\frac{d\sigma}{\sigma^2}. \tag{XVIII.4.61}$$

Thus the induced measure becomes an ordinary differential up to orientation, while the superpotential becomes inverse-linear in the new coordinate. The source relates this Landau–Ginzburg model to a topologically twisted $SL(2,\mathbb{R})/U(1)$ coset at level three and supplies its genus amplitude. We import that relation and amplitude, including their physical measure assumptions; a coordinate change by itself does not derive them. These are steps within the sourced C description, not a field map to the Chern–Simons variables. For $g \geq 2$, they supply the all-C term in its own variables,

$$\eta_{\mathrm{GLSM}}^{2g-2}\frac{B_{2g}}{2g(2g-2)u_{\mathrm{GLSM}}^{2g-2}}. \tag{XVIII.4.62}$$

The closed kernel independently has conifold singularities in T. In the continued x frame its first functions are

$$F_0^{>0}(T) = -\operatorname{Li}_3(e^{-T}), \quad F_1^{>0}(T) = -\tfrac{1}{12}\log(1-e^{-T}), \quad F_2^{>0}(T) = -\frac{1}{240}\frac{e^{-T}}{(1-e^{-T})^2}. \tag{XVIII.4.63}$$

For example $F_0''(T) = \log(1-e^{-T}) = \log T + O(T)$; integrating twice gives the singular piece $T^2\log T/2$, up to polynomial terms. The genus-one singularity is $-\log T/12$ up

to regular/additive terms, and

$$F_2^{>0}(T) = -\frac{1}{240T^2} + O(1), \qquad F_g^{>0}(T) \sim \frac{B_{2g}}{2g(2g-2)T^{2g-2}} \quad (g \geq 2). \quad \text{(XVIII.4.64)}$$

For the general pole, the genus-g cover coefficient in the continued frame is $B_{2g}d^{2g-3}/[2g(2g-2)!]$. Its sum behaves as $\Gamma(2g-2)T^{-(2g-2)}$, giving the stated factor. This comparison concerns the leading singularity, not the regular pieces of the functions.

If, and only as a conditional algebraic substitution, both

$$T = au_{\mathrm{GLSM}} \quad \text{and} \quad x = a\eta_{\mathrm{GLSM}}, \qquad a \neq 0, \quad \text{(XVIII.4.65)}$$

are imposed, the coupled leading poles obey

$$x^{2g-2}\frac{B_{2g}}{2g(2g-2)T^{2g-2}} = \eta_{\mathrm{GLSM}}^{2g-2}\frac{B_{2g}}{2g(2g-2)u_{\mathrm{GLSM}}^{2g-2}}. \quad \text{(XVIII.4.66)}$$

At genus two, rotating only T by i flips the sign of the pole; rotating x by the same factor compensates it. Dropping the all-C term would remove this source-side pole contribution, conditional on both relations in (XVIII.4.65). The physical field, coupling, branch, measure and sewing dictionary establishing those relations has not been supplied. The low-genus logarithms require their own contact and branch translation as well. This explicit gap limits the worldsheet interpretation while leaving the independent rational CS/BP calculation intact.

XVIII.4.7 The domains of the comparison

There are five different operations in the preceding calculation. First comes the exact compact finite product at integral level. Second comes an analytic continuation of that product at integer rank. Third comes the declared endpoint lift to independent formal Q. Fourth comes a fixed-T genus asymptotic expansion. A full nonperturbative completion would be a fifth object; the first four do not construct it.

At physical level, every sine in (XVIII.4.15) is nonzero because

$$1 \leq m \leq N-1 < K = N+k. \quad \text{(XVIII.4.67)}$$

Yet an isolated cover with $d = K$ in (XVIII.4.34) has $\sin(d\lambda/2) = \sin\pi = 0$. For $N = 2, k = 3$, the finite product contains only $2\sin(\pi/5)$, while the degree-five closed coefficient has a pole. The original split was established for $|q| < 1$, and its individual terms cannot be specialized independently to this root of unity to define the compact sphere value.

The result we can use is precise. Under the compact modular input, the declared endpoint lift, the absolute balanced local-curve theorem and hook/dual-Cauchy identities, both routes give (XVIII.4.31) for every positive degree as a rational function of generic q. The local elementary-cluster result in Volume V, Chapter 8 provides its own specified curve interpretation. It is not a second independent physical derivation if it shares the same mathematical inputs.

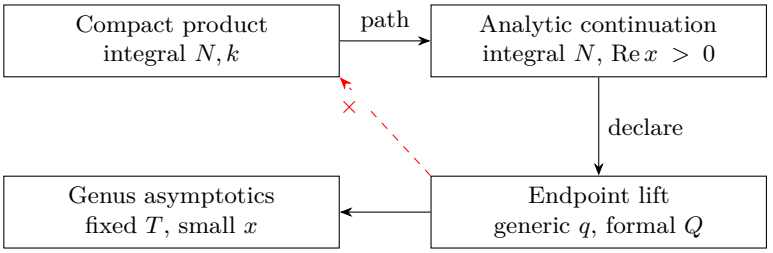


Figure XVIII.4.7: Domains and order of operations. A chosen analytic path continues the integer-rank finite product. Endpoint extraction then defines an independent-Q formal series, and a further fixed-T expansion gives genus asymptotics. The crossed arrow forbids termwise specialization of isolated covers at a physical root of unity. A full nonperturbative completion needs additional information and is outside these arrows.

The calculation leaves the full finite-N closed/open equality, connected degree zero, global quantum package, physical worldsheet dictionary and nonperturbative completion open. The exact continued reference (XVIII.4.43) records terms that the reduced comparison does not see. Retaining them is what makes the scope of the positive-degree agreement useful: we can calculate the common observable without confusing it with the stronger equivalence it motivates.

Reading the conifold comparison coefficient by coefficient

The positive-degree comparison is most useful when read as a reproducible coefficient calculation. Fix the continuation and the logarithm lift first. Choose a degree and a genus, expand the continued kernel in the stated variable, and collect the cover contribution. The second route begins with the balanced local-curve input and uses its own specified normalization. Equality is asserted for the coefficients after these translations. Moving a sign or an overall factor between the two routes without recording the translation would alter the equality being tested.

The logarithm is essential in this operation. The sphere partition function contains disconnected contributions, whereas the free energy organizes connected surfaces. The positive-degree part then removes a different kind of information, namely terms independent of the curve degree. It is therefore possible to determine every coefficient in that part and still leave an absolute normalization undecided. No disagreement follows merely because one route retains an additional polynomial or degree-zero term. One must first ask whether that term is among the quantities compared.

The conifold singularity gives a second reading of the same distinction. At genus zero the displayed second derivative has a logarithmic singularity. Integrating it recovers the singular term but also leaves integration polynomials. At higher genus the leading pole identifies the most singular part of the cover sum. Regular terms require further information. This is why a leading-singularity agreement carries less information than equality of the full positive-degree function, and why neither replaces the separate absolute-vacuum normalization.

The B-model chapters now change the construction rather than merely renaming this answer. Their starting objects are a Dolbeault complex and a holomorphic volume form. The same interest in connected amplitudes and relative normalization remains useful, but the variables and physical premises have to be supplied anew. In XVIII.7 these distinctions return when matrix periods are compared with glueball couplings.

Exercises

1. Using the edge pairing and both rotation systems of Figure XVIII.4.2, trace every face, determine h and g, and compute $x^{E-V}N^h$ both at fixed N and in terms of fixed $T = Nx$. Explain why the same abstract graph can describe two genera.

2. For the positive sphere reference of $SU(2)$ at $k = 3$, evaluate Z_{SU}, Z_{NS}/Z_{SU}, c_{SU}, c_{NS} and each $s = 1$ two-framing phase. Explain which inputs would be missing if only the local bare center coefficient were given.

3. Prove (XVIII.4.24) for positive integer N and $z \neq 1$. Specialize to $N = 3$, then insert $z = q^d$. Identify the term giving positive powers of Q and explain why Q is independently formal only after a lift has been specified.

4. Use the hook formula (XVIII.4.27) for both partitions of two. Derive the Q^2

coefficient and compare it with exponentiating the connected CS result. Explain the different roles of dual Cauchy and a finite degree-two check.

5. Expand the degree-two sine coefficient through λ^4, including the λ^{-2} term. Which terms in Figure XVIII.4.5 are detected by this positive-degree operation? Explain why an SU/NS normalization discrepancy can survive the equality of all those coefficients.

6. Compute the normalized and ordinary disk contours in (XVIII.4.58)–(XVIII.4.59), and repeat after omitting σ^{-2}. Determine the genus-two all-C pole in the independent u_{GLSM} coordinate before its genus coupling is included. Compare the coupled leading poles under *both* $T = au_{\mathrm{GLSM}}$ and $x = a\eta_{\mathrm{GLSM}}$. Explain the effects of omitting the pure all-C closed sector while retaining mixed C disks, and identify which annulus, measure and H-boundary statements require source premises rather than residue algebra.

7. At $N = 2, k = 3$, compare the regularity of the finite product with the isolated $d = K$ cover. Compute the real lifted value of s for the Gaussian phase, and find an integer giving the same exponential in the NS model. Test whether such an integer exists at $N = 3, k = 5$. Classify the finite-product, independent-Q and genus statements by domain, and explain why neither the pole nor a framing witness proves full partition-function equality.

Sources and scope

The open-sector construction is perturbative. The vacuum comparison uses the positive-degree formal observable with the fundamental trace and curve-coordinate conventions specified above.

§1. The incidence resolution and exceptional fiber [MATH] and the smooth quadric and cotangent topology [MATH] are discussed in Volume IV, Chapter 5. See KW98 p.7 after (16), MSY06 pp.65–66 and KS00 pp.14,19. The protected perturbative zero-section construction [WS-T] uses Chapters 1–2 and Witten (1992), pp.21–22 (3.20)–(3.22), pp.28–35. Ward, measure, gauge-fixing and sewing premises remain inputs; the quantum modular completion is separately supplied. The geometry recall leaves the metric and smooth-transition interpretation as separate questions.

§2. The rank power follows from the Euler characteristic and the vertex and propagator weights of Gopakumar and Vafa (1999), pp.4–5 (2.1)–(2.2) [MATH]. The theta face traces are explicit examples, not a target-geometry identification. No full quantum completion follows from ribbon topology.

§3. The root-height multiplicities and Cartan determinant follow from the root system [MATH]. The sphere amplitude uses the compact modular gluing theorem of Mariño (2004a), p.6 (2.23),(2.27),(2.29) [MATH]. The specified odd-k quotient uses Naculich and Schnitzer (2007), pp.3–5 (2.1)–(2.6),(2.15) [MATH]. Their ratio gives the SU/NS logarithm on the chosen branch [MATH]. Bare Nk and global NK are distinct; even-level/spin variants are excluded.

§4. The finite-sum endpoint identity [MATH] precedes a convergent integer-rank split and the declared lift [MATH]. Volume V, Chapter 7 uses the absolute balanced local-curve theorem [MATH], Bryan and Pandharipande (2008), pp.7–9 definitions/Assumption 1 and pp.33–34 Corollary 7.3, and the hook/dual-Cauchy conversion under the cited identities [MATH]. For the rational coefficient equality in all positive degrees and the sine translation [MATH], see Gopakumar and Vafa (1999), pp.10–12 (3.7),(3.10),(3.13). Absolute BP, rather than deletion of relative markings, supplies the closed object. Imported theorem proofs are not re-proved here.

§5. [MATH] Genus-zero through genus-three cover weights. [MATH] Full continued NS reference under the eta identity and specified branch. [MATH] MacMahon asymptotics under Mellin-contour hypotheses. [MATH] Literal Gaussian phase conflict, Ooguri and Vafa (2002), pp.11–12 (2.1),(2.7),(2.8). [MATH] Reciprocal-level/section-2 coupling conflict, pp.8,13 before (2.11) and (2.12). [MATH] Minus-exponent Weyl/product sign conflict, Mariño (2004b), p.50 (4.3),(4.5). These discrepancies arise when the printed expressions are compared in the same conventions. The separate printed tan caution is Ooguri and Vafa (2002), p.12 (2.9); it is not used as a proof or a fourth replacement comparison. No published erratum is asserted. [MATH] $N = 2, k = 3, s = 30$ exponentiated phase witness, not a universal framing prescription. The source uses $F_{GV} = -\log Z$, opposite our sign; its coupling continuation must be translated at the same time.

§6. [WS-T] Stable mixed C vanishing under supplied Ward, single-valuedness, measure and factorization arguments, Ooguri and Vafa (2002), pp.25–26. [WS-T] Separate mixed-annulus contour argument, p.26 (4.11). [MATH] Normalized disk residue conditional on the supplied measure and superpotential, pp.27–28 (4.12)–(4.13). [WS-T] Source-specific H-boundary deformation/Dirichlet identification, pp.31–32; all-H separately trivial at p.32 footnote 5. [WS-T] All-C higher-genus formula in its independent GLSM coordinate, pp.29–30 (4.16)–(4.19), including the sourced twisted-theory/LG-coset and measure inputs. [MATH] Conditional common-scaling pole algebra only under *both* $T = au_{\mathrm{GLSM}}$ and $x = a\eta_{\mathrm{GLSM}}$. [MATH] Independent continued-T low-genus singularities modulo stated polynomial/additive terms. Source physical field/coupling/branch/measure/sewing identification is unestablished. The separate infrared Coulomb theory is excluded.

§7. The finite product can be regular even when an isolated cover term has a root-of-unity pole [MATH]. Termwise specialization can therefore fail. A finite-N, degree-zero, global or nonperturbative equivalence would require further input.

Finite comparisons include ranks 2–4, degrees through four and genera through three, with supplementary rank-five and degree-five/genus-six checks. The cited theorems and worldsheet premises have their own hypotheses.

References

Bryan, J. and R. Pandharipande (2008). "The Local Gromov–Witten Theory of Curves". In: *J. Amer. Math. Soc.* 21, pp. 101–136. arXiv: `math/0411037`.

Gopakumar, R. and C. Vafa (1999). "On the Gauge Theory/Geometry Correspondence". In: *Adv. Theor. Math. Phys.* 3, pp. 1415–1443. arXiv: `hep-th/9811131`.

Mariño, M. (2004a). "Chern–Simons Theory and Topological Strings". In: arXiv: `hep-th/0406005`.

Mariño, M. (2004b). "Les Houches Lectures on Matrix Models and Topological Strings". In: arXiv: `hep-th/0410165`.

Naculich, S. G. and H. J. Schnitzer (2007). "Level-rank Duality of the U(N) WZW Model, Chern–Simons Theory, and 2d qYM Theory". In: arXiv: `hep-th/0703089`.

Ooguri, H. and C. Vafa (2002). "Worldsheet Derivation of a Large N Duality". In: *Nucl. Phys. B* 641, pp. 3–34. arXiv: `hep-th/0205297`.

Witten, E. (1992). "Chern–Simons Gauge Theory as a String Theory". In: arXiv: `hep-th/9207094`.

Chapter XVIII.5

Open B-model and holomorphic Chern–Simons theory

An open string has two ways to reveal the geometry of its boundary condition. Its states describe infinitesimal changes of that boundary. Its disk interactions decide which changes can coexist. In the B-model these become a particularly concrete pair of objects: a Dolbeault complex and a holomorphic gauge action. The first counts possible infinitesimal deformations of a bundle. The second imposes their nonlinear compatibility.

We will construct this action and follow one deformation far enough to see the difference. On a compact complex three-torus, two individually allowed matrix modes have a nonzero commutator. Their sum is a BRST state, but its square is a nontrivial cohomology class. It cannot be continued to a solution even at second order. A cubic disk coupling measures precisely this obstruction. This gives a reason to retain interactions after identifying the state space.

The reader needs complex forms, matrix gauge transformations, and the B twist recalled in Volume V, Chapter 1. Volume V, Chapter 6 supplies the open-string and bundle interpretation; Chapter 1 of this volume explains the passage from string products to a target action. We recall the necessary signs here. Throughout, X is a smooth compact Kähler complex threefold without boundary, with a chosen nowhere-vanishing holomorphic three-form Ω. The bundle E is holomorphic and has finite rank. A local or noncompact use of the action requires compact support or specified falloff. We work in the classical perturbative open topological sector. The BRST-compatible boundary interaction, measure, sewing and large-metric reduction are the physical ingredients of the construction.

XVIII.5.1 Boundary symmetry selects a holomorphic bundle

What target geometry can a space-filling B boundary carry? Recall why the twist is useful. We use the ordinary zero-center geometric B sector, with $Z = \widetilde{Z} = 0$ for the worldsheet central charges. The scalar B charge obeys $Q_B^2 = Z$, so this restriction is required before taking BRST cohomology. A scalar fermionic charge Q survives on the worldsheet, so its cohomology can describe states without choosing a spatial polarization. The B fermions include a scalar $\eta^{\bar\imath}$, a scalar θ_i, and a worldsheet one-form ρ^i. For a free space-filling boundary, the full boundary conditions are

$$\partial_n \Phi = 0, \qquad \theta_i|_{\partial\Sigma} = 0, \qquad \iota^*_{\partial\Sigma}(*\rho^i) = 0. \tag{XVIII.5.1}$$

Here n is the outward normal, $*$ is the worldsheet Hodge operator, and $\iota_{\partial\Sigma}$ is the boundary inclusion. The last condition removes the normal component of ρ, rather than its tangential component. It is part of the free boundary, alongside the Neumann condition on the map Φ.

A boundary also transports a Chan–Paton vector in E. Ordinary connection holonomy alone has the wrong BRST variation: it would constrain both the $(0,2)$ and $(1,1)$ curvature components. The B boundary instead uses an improved holonomy with a curvature-dependent fermion coupling. The improvement cancels the unwanted mixed-curvature variation. Its surviving background requirement is

$$F_E^{0,2} = 0, \qquad D = \bar\partial_E, \qquad D^2 = 0. \tag{XVIII.5.2}$$

This is holomorphic integrability. A holomorphic bundle can have nonzero $(1,1)$ curvature; it need not be a flat connection. The improvement and the boundary conditions in (XVIII.5.1) are supplied by the worldsheet construction. The algebra below uses them, rather than deriving them from target gauge invariance.

The surviving scalar fermions give an efficient representation of boundary states. In a holomorphic coordinate patch and holomorphic bundle frame, choose the source-local normalization

$$Qz^i = 0, \qquad [Q, \bar z^{\bar\imath}] = -\eta^{\bar\imath}, \qquad Q\eta^{\bar\imath} = 0, \qquad \eta^{\bar\imath} \longleftrightarrow -d\bar z^{\bar\imath}. \tag{XVIII.5.3}$$

Thus, for a matrix-valued scalar f, the two minus signs give

$$Qf = -\eta^{\bar\imath}\partial_{\bar\imath} f \longleftrightarrow d\bar z^{\bar\imath}\partial_{\bar\imath} f = \bar\partial f. \tag{XVIII.5.4}$$

The same map acts on coefficients with fermions. For example, a degree-one state $u_{\bar\jmath}\eta^{\bar\jmath}$ represents $-u_{\bar\jmath} d\bar z^{\bar\jmath}$. Its variation is

$$Q(u_{\bar\jmath}\eta^{\bar\jmath}) = -(\partial_{\bar\imath} u_{\bar\jmath})\eta^{\bar\imath}\eta^{\bar\jmath} \longleftrightarrow -\tfrac{1}{2}(\partial_{\bar\imath} u_{\bar\jmath} - \partial_{\bar\jmath} u_{\bar\imath}) d\bar z^{\bar\imath} d\bar z^{\bar\jmath}. \tag{XVIII.5.5}$$

This is exactly the Dolbeault derivative of the represented one-form. The factor $1/2$ in the unrestricted double sum disappears if the expansion is over ordered pairs $i < j$.

Covariantizing this local calculation gives the off-shell complex and its states:

$$\mathcal{B} = \Omega^{0,*}(X, \operatorname{End} E), \qquad Q = D, \qquad \mathcal{H}^q = H^{0,q}(X, \operatorname{End} E), \quad 0 \le q \le 3. \tag{XVIII.5.6}$$

In addition to the zero-center worldsheet premise, nilpotence in this bundle realization uses the integrable reference background. Scalar spin alone supplies neither condition. The degree q is the topological form degree used in this chapter; it is not a universal identification with every reparametrization ghost convention.

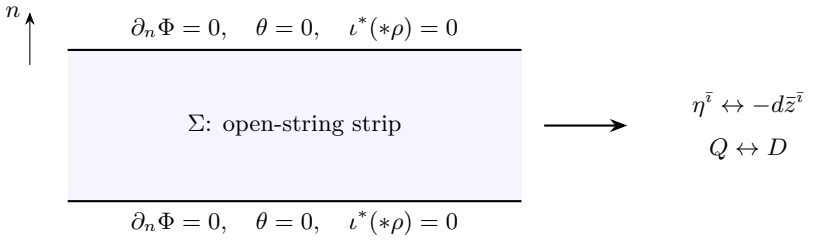


Figure XVIII.5.1: A strip with free space-filling B boundaries. The map is Neumann, θ vanishes, and the boundary pullback of $*\rho$ vanishes on both edges. The surviving scalar η labels antiholomorphic form directions. The arrow represents the low-mode identification of the boundary complex, with the improved holonomy and BRST-compatible measure understood.

A state and a field have different jobs here. The classical deformation field is an arbitrary $a \in \mathcal{B}^1$ before imposing equations. Only at first order about the background does its equation reduce to $Da = 0$, and only after quotienting by $D\epsilon$ does it define a class in $\mathcal{H}^1$. Replacing the whole field space by this cohomology at the outset would remove the fields needed to enforce nonlinear compatibility. The next section constructs that compatibility from ordered disks.

XVIII.5.2 Ordered disks become a target action

A disk records an order of boundary insertions. That order survives the low-mode reduction as matrix composition, while the fermions become exterior forms. For homogeneous elements of $\mathcal{B}$, define

$$uv = u \wedge v \quad \text{with matrix composition}, \qquad D(uv) = (Du)v + (-1)^{|u|}u(Dv). \tag{XVIII.5.7}$$

The notation uv always includes both operations. Anticommuting the forms does not commute the matrices.

A disk pairing must also absorb the target zero modes. On a complex threefold the chosen holomorphic form supplies the trace functional

$$\tau(u) = \int_X \Omega \wedge \operatorname{Tr} u, \qquad \langle u, v \rangle = \tau(uv), \qquad \tau(u) = 0 \quad \text{if } |u| \neq 3. \tag{XVIII.5.8}$$

We place Ω first. The trace is the ordinary fundamental matrix trace. For compact X without boundary, or the specified support condition, holomorphicity of Ω and Stokes' theorem give $\tau(Du) = 0$. Matrix trace cyclicity together with the exterior sign gives

$$\tau(uv) = (-1)^{|u||v|}\tau(vu), \qquad \langle Du, v\rangle = -(-1)^{|u|}\langle u, Dv\rangle. \tag{XVIII.5.9}$$

On cohomology this becomes the Serre pairing under the compact smooth hypotheses. Off shell it is already the pairing needed for the action.

For a concrete disk calculation, let $e_j = d\bar{z}^j$ and choose

$$P = \begin{pmatrix} 0 & 1 \\ 0 & 0 \end{pmatrix}, \quad R = \begin{pmatrix} 0 & 0 \\ 1 & 0 \end{pmatrix}, \quad T = \begin{pmatrix} 1 & 0 \\ 0 & 0 \end{pmatrix}, \qquad (u, v, w) = (Pe_1, Re_2, Te_3). \tag{XVIII.5.10}$$

The matrix products and the exterior permutations are separate steps:

$$\begin{gathered} \operatorname{Tr}(PRT) = 1, \quad \operatorname{Tr}(RTP) = 1, \quad \operatorname{Tr}(RPT) = 0; \\ e_2e_3e_1 = e_1e_2e_3, \quad e_2e_1e_3 = -e_1e_2e_3. \end{gathered} \tag{XVIII.5.11}$$

Consequently the coefficients of $e_1e_2e_3$ in the three full insertion products are

$$\operatorname{Tr}(uvw) : 1, \qquad \operatorname{Tr}(vwu) : 1, \qquad \operatorname{Tr}(vuw) : 0. \tag{XVIII.5.12}$$

A cyclic move of one degree-one insertion past two others has sign $+1$. A transposition is a different operation and changes the disk amplitude. The matrix T was chosen to make this difference visible.

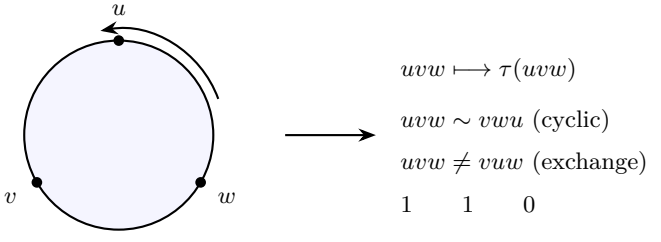


Figure XVIII.5.2: An oriented disk with cyclically ordered insertions u, v, w. Moving the starting point preserves the cyclic word. Exchanging two adjacent insertions changes the word. For the displayed matrix/form example, the ordered and cyclic coefficients are one, whereas the exchanged coefficient is zero. The arrow sends the boundary word to $\tau(uvw)$, not to a symmetrized trace.

The cubic open-string functional recalled in Chapter 1 combines its differential, product and pairing. Substituting (XVIII.5.6)–(XVIII.5.8) gives

$$S[a] = \kappa_B\left(\tfrac{1}{2}\langle a, Da\rangle + \tfrac{1}{3}\langle a, a^2\rangle\right) = \kappa_B \int_X \Omega \wedge \operatorname{Tr}\left(\tfrac{1}{2}aDa + \tfrac{1}{3}a^3\right). \tag{XVIII.5.13}$$

This is holomorphic Chern–Simons theory relative to the chosen integrable reference bundle. The deformation a is a global $\operatorname{End} E$-valued form even when E has no global

frame. The construction fixes the relative coefficients 1/2 and 1/3; its overall constant κ_B remains symbolic and nonzero. Rescaling Ω changes that normalization unless the coupling is translated accordingly.

The passage to (XVIII.5.13) uses the B-model large-metric low-mode reduction and disk sewing. It does not assert that all excited states have ceased to exist at finite metric parameter. The resemblance to the A-model Chern–Simons construction is useful, but the B boundary conditions and B reduction supply the physical identification here. The next step is to see why its equation precisely reconstructs an allowed holomorphic background.

XVIII.5.3 Curvature and gauge symmetry

Which nonlinear condition replaces first-order closure? Define the deformed Dolbeault operator on sections by $\nabla = D + a$. Its square is

$$\nabla^2 s = (D+a)^2 s = (Da + a^2)s = Fs, \qquad F = Da + a^2. \tag{XVIII.5.14}$$

Thus $F = 0$ means that the deformed bundle is still holomorphic. An off-shell field can have $F \neq 0$ and must remain available when varying the action.

To derive the equation, first keep the exact derivative in the kinetic variation. With δa of degree one,

$$\delta \operatorname{Tr}(aDa/2) = \tfrac{1}{2}\operatorname{Tr}(\delta a\, Da + aD\delta a), \qquad D\operatorname{Tr}(a\delta a) = \operatorname{Tr}(Da\,\delta a - aD\delta a). \tag{XVIII.5.15}$$

Since degrees two and one commute under the cyclic trace, the two kinetic contributions combine. Cyclicity of three degree-one factors similarly identifies all three cubic variations. Therefore

$$\delta L = \operatorname{Tr}\big(\delta a(Da + a^2)\big) - \tfrac{1}{2}D\operatorname{Tr}(a\delta a), \qquad \delta S = \kappa_B \tau(\delta a F). \tag{XVIII.5.16}$$

The second equality uses the stated integration conditions. The local matrix trace pairing is nondegenerate, Ω is nowhere zero, and the off-shell variations are arbitrary. With $\kappa_B \neq 0$ the Euler equation is consequently

$$F = Da + a^2 = 0. \tag{XVIII.5.17}$$

The action is holomorphic; it is not a positive real energy functional. Integrability alone therefore says nothing about a stability or D-term condition.

A useful off-shell example keeps the commutator visible. In a local trivialization put $D = \bar\partial$, $e_j = d\bar z^j$, and use the matrices P, R of the disk example:

$$a = Ae_1 + Be_2, \qquad A = \bar z^2 P, \quad B = \bar z^1 R, \qquad F = \big(R - P + \bar z^1 \bar z^2 [P,R]\big)e_1 e_2. \tag{XVIII.5.18}$$

The derivative part is $\partial_{\bar 1} B - \partial_{\bar 2} A = R - P$, and the product part is $[A, B]$. This nonsymmetric local polynomial background is curved. It illustrates the operator identities without imposing the answer $F = 0$ in advance; its coordinate coefficients are not a proposed global torus field.

Gauge covariance is most efficiently derived on sections. Choose the frame convention $s \mapsto g^{-1}s$, with g a smooth complex invertible bundle automorphism. Requiring $\nabla^g = g^{-1}\nabla g$ gives

$$a^g = g^{-1}ag + g^{-1}Dg, \qquad (\nabla^g)^2 = g^{-1}\nabla^2 g, \qquad F^g = g^{-1}Fg. \tag{XVIII.5.19}$$

For $g = 1 + \epsilon + O(\epsilon^2)$ this becomes $\delta_\epsilon a = D\epsilon + [a, \epsilon]$. The adjoint differential on a homogeneous form is

$$D_a u = Du + au - (-1)^{|u|}ua, \qquad D_a^2 u = (Da + a^2)u - u(Da + a^2) = Fu - uF. \tag{XVIII.5.20}$$

In expanding the square, terms containing Du cancel between the two applications of D_a; the remaining derivative terms are $Da\,u - uDa$, and the two quadratic terms are $a^2u - ua^2$. This also explains why the adjoint complex is a differential only on an integrable background, apart from special central-curvature cases.

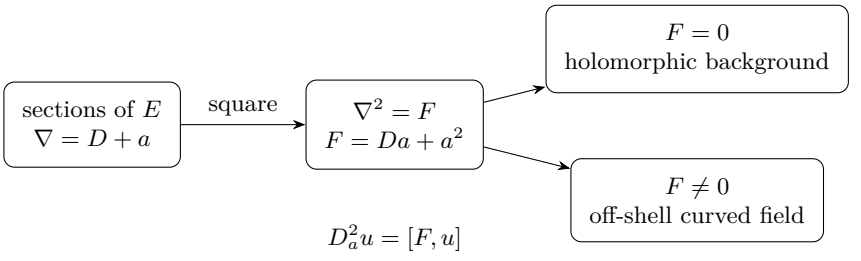


Figure XVIII.5.3: The operator $D + a$ acts on sections; its square is multiplication by F. On the branch $F = 0$ it defines a holomorphic bundle. Off shell, its adjoint square is $[F, \cdot]$. Noncentral curvature obstructs an adjoint cochain complex; central curvature can leave that adjoint square zero while the operator on sections still has nonzero square F. The curved polynomial example in the text tests the general distinction.

The Bianchi identity follows from the same signs, without equations of motion:

$$DF = (Da)a - aDa, \qquad D_a F = DF + aF - Fa = 0. \tag{XVIII.5.21}$$

Apply (XVIII.5.16) to $\delta_\epsilon a = D_a\epsilon$. Because ϵ has degree zero and D_a is a graded derivation,

$$\delta_\epsilon S = \kappa_B \tau((D_a\epsilon)F) = \kappa_B \tau\big(D_a(\epsilon F) - \epsilon D_a F\big) = 0. \tag{XVIII.5.22}$$

The trace of the adjoint commutator vanishes, and the remaining D term integrates to zero. This establishes infinitesimal invariance of the relative action. It does not quantize κ_B or establish invariance under arbitrary disconnected gauge transformations. We now use the nonlinear equation itself to distinguish states from actual deformations.

XVIII.5.4 A BRST state can be obstructed

A first-order state solves only the linear part of (XVIII.5.17). To see what happens next in a fully global example, take

$$X = \left(\mathbb{C}/(2\pi\mathbb{Z} + 2\pi i\mathbb{Z})\right)^3, \quad E = \mathcal{O}_X^2, \quad z^j = x^j + iy^j, \quad e_j = d\bar{z}^j. \tag{XVIII.5.23}$$

Here x^j, y^j are real periodic coordinates. This torus has trivial canonical bundle; the example does not require holonomy exactly $SU(3)$. The trivial bundle makes $D = \bar{\partial}$ act componentwise on matrices.

We first compute the entire smooth Dolbeault cohomology, so that the subsequent global obstruction does not rest on a finite selection of modes. A Fourier coefficient has character

$$\begin{aligned} \chi_{m,n} &= \exp\left(i\sum_j (m_j x^j + n_j y^j)\right), \qquad \partial_{\bar{z}^j} = \tfrac{1}{2}(\partial_{x^j} + i\partial_{y^j}), \\ D\chi_{m,n} &= \chi_{m,n}\sum_j \lambda_j e_j, \qquad \lambda_j = \tfrac{1}{2}(im_j - n_j). \end{aligned} \tag{XVIII.5.24}$$

The factor $1/2$ and the minus sign on n_j follow directly by differentiation. On this mode, D is exterior multiplication by $\lambda = \sum_j \lambda_j e_j$. For $(m,n) \neq 0$, define contraction by

$$h_{m,n} = \frac{\sum_j \bar{\lambda}_j \iota_j}{\sum_j |\lambda_j|^2}, \qquad \iota_j e_k + e_k \iota_j = \delta_{jk}, \qquad \sum_j |\lambda_j|^2 = \tfrac{1}{4}\sum_j (m_j^2 + n_j^2) > 0. \tag{XVIII.5.25}$$

The contraction identity immediately gives, with the scalar denominator retained,

$$Dh_{m,n} + h_{m,n}D = \frac{\sum_{j,k} \lambda_j \bar{\lambda}_k (e_j\iota_k + \iota_k e_j)}{\sum_j |\lambda_j|^2} = 1. \tag{XVIII.5.26}$$

Every closed nonzero mode is therefore exact. This is also an argument for smooth forms: their Fourier coefficients decay faster than any power of frequency, and the coefficients of $h_{m,n}$ have size $O(|(m,n)|^{-1})$. Applying h preserves that decay. We set $h = 0$ on the zero mode instead of dividing by zero.

Let Π_0 project a smooth periodic form to its constant Fourier coefficient. The global result is

$$\begin{aligned} Dh + hD &= 1 - \Pi_0, \\ H^{0,q}(X, \operatorname{End}\mathcal{O}_X^2) &\simeq \operatorname{Mat}_2(\mathbb{C}) \otimes \Lambda^q\langle e_1, e_2, e_3\rangle, \quad \dim H^{0,q} = 4\binom{3}{q}. \end{aligned} \tag{XVIII.5.27}$$

In degrees zero through three the dimensions are $(4, 12, 12, 4)$. This count uses the smooth all-mode contraction and the trivial rank-two bundle. It would not be the answer for an arbitrary holomorphic bundle.

Choose $P = E_{12}$, $R = E_{21}$ and now introduce the traceless matrix $H = [P, R] = \mathrm{diag}(1, -1)$. Consider the closed degree-one field

$$a_1 = Pe_1 + Re_2, \qquad Da_1 = 0, \qquad a_1^2 = (PR - RP)e_1e_2 = He_1e_2. \tag{XVIII.5.28}$$

A formal deformation $a(t) = ta_1 + t^2a_2 + \cdots$ must satisfy

$$F(a(t)) = tDa_1 + t^2(Da_2 + a_1^2) + O(t^3) = 0. \tag{XVIII.5.29}$$

The second-order equation is $Da_2 = -He_1e_2$. But for every smooth periodic a_2,

$$\Pi_0(Da_2) = 0, \qquad \Pi_0(He_1e_2) = He_1e_2 \neq 0. \tag{XVIII.5.30}$$

The first equality is the vanishing of the average of a derivative on each periodic coordinate. It rules out a solution globally. The prescribed first-order BRST class is obstructed.

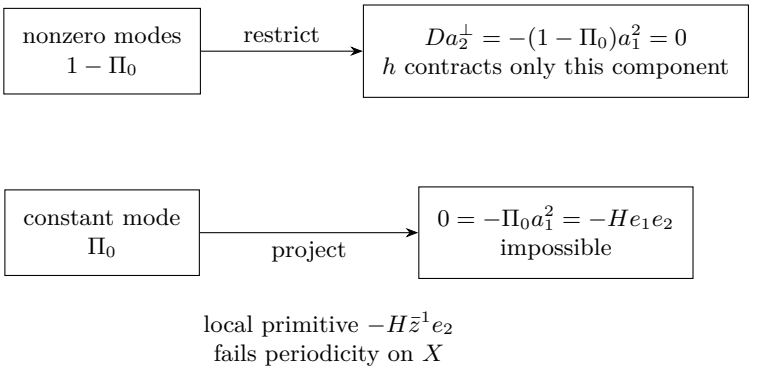


Figure XVIII.5.4: The smooth Fourier complex separates the second-order equation into two components. Write $a_2^\perp = (1 - \Pi_0)a_2$. Contraction by h handles only the nonzero-mode part $(1 - \Pi_0)$; in this example its right-hand side is zero. The constant projection instead requires $0 = -He_1e_2$, which is impossible. A coordinate-patch primitive uses $\bar{z}^1$ and fails periodicity, so it cannot solve that global condition.

Two possible misunderstandings are worth resolving by calculation. First, a change of representative cannot cure this obstruction. For degree-zero ϵ, use $Da_1 = 0$ and $D^2 = 0$ to find

$$(a_1 + D\epsilon)^2 - a_1^2 = D\big(\epsilon a_1 - a_1\epsilon + \epsilon D\epsilon\big). \tag{XVIII.5.31}$$

Thus the obstruction class is unchanged. Second, local exactness does not imply global exactness:

$$e_1e_2 = D(\bar{z}^1e_2) \quad \text{on a coordinate patch}, \qquad \bar{z}^1 \mapsto \bar{z}^1 + 2\pi \quad \text{around the real first cycle.} \tag{XVIII.5.32}$$

The local candidate $a_2 = -H\bar{z}^1e_2$ is not periodic. Conversely, if P and R are replaced by commuting constant diagonal matrices, their commutator vanishes and ta_1 itself solves the full equation. It is the ordered nonabelian product, together with the global domain, that obstructs the original state.

XVIII.5.5 The cubic coupling detects the obstruction

Can a disk amplitude see the failure found in the preceding section? Pair the obstruction with a third constant state $b = He_3$. Because $\operatorname{Tr} H^2 = 2$ and moving e_3 past two forms has sign $+1$,

$$\langle b, a_1^2 \rangle = \int_X \Omega \wedge \operatorname{Tr}(H^2) e_3 e_1 e_2 = 2V, \qquad V = \int_X \Omega \wedge e_1 e_2 e_3. \tag{XVIII.5.33}$$

This pairing is nonzero, so it detects a nonzero cohomology class, rather than just a nonzero chosen representative. An exact obstruction would pair to zero with the closed b by integration by parts.

Fix $\Omega = dz^1 dz^2 dz^3$ and the real complex orientation $dx^1 dy^1 dx^2 dy^2 dx^3 dy^3$. The sign of V matters for comparing amplitudes. Three swaps interleave the holomorphic and antiholomorphic differentials:

$$\Omega e_1 e_2 e_3 = -\prod_{j=1}^{3} (dz^j \wedge d\bar{z}^j), \qquad dz^j \wedge d\bar{z}^j = -2i\, dx^j \wedge dy^j. \tag{XVIII.5.34}$$

Each real coordinate has period 2π, so

$$V = -(-2i)^3 (2\pi)^6 = -8i(2\pi)^6. \tag{XVIII.5.35}$$

It is a complex integral with this specified ordering, not the positive Riemannian volume.

Now let x, y, z denote complex amplitudes, distinct from the real coordinates x^j, y^j, and restrict the field to

$$a = xPe_1 + yRe_2 + zHe_3. \tag{XVIII.5.36}$$

All coefficients are constant, so the kinetic term vanishes in this subsector. The six exterior permutations of the cubic combine into a commutator trace:

$$\begin{aligned} \frac{\operatorname{Tr}(a^3)}{e_1 e_2 e_3} &= xyz\ \operatorname{Tr}(PRH - PHR - RPH \\ &\qquad + RHP + HPR - HRP) \\ &= 3xyz\ \operatorname{Tr}\big(H[P,R]\big) = 6xyz. \end{aligned} \tag{XVIII.5.37}$$

The action and its derivative are consequently

$$\frac{S}{\kappa_B V} = 2xyz, \qquad \frac{1}{\kappa_B V}\frac{\partial S}{\partial z} = 2xy. \tag{XVIII.5.38}$$

At $z = 0$, $a^2 = xyHe_1e_2$, and (XVIII.5.16) gives the same answer by pairing with $\partial a/\partial z = He_3$. Thus the nonlinear incompatibility of the two first-order modes is the derivative of a cubic coupling to a dual mode.

The third matrix is H, not the matrix T in the disk-order example. Their tasks differ: T distinguishes insertion exchange from cyclicity, whereas H pairs with the

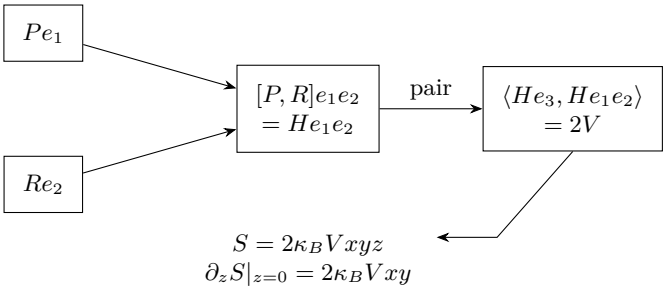


Figure XVIII.5.5: The two modes Pe_1 and Re_2 produce the obstruction He_1e_2. Pairing it with He_3 gives $2V$. The same ordered three-mode interaction gives $S = 2\kappa_B V xyz$, whose derivative in the third amplitude recovers that pairing. The diagram depicts a coupling among off-shell hCS modes, with no stability or matrix-integral prescription attached.

commutator obstruction. Substituting H into the earlier exchange test can accidentally make matrix and exterior signs cancel; it would obscure that lesson.

The commuting limit checks the mechanism. For $a = \sum_j A_j e_j$ with constant pairwise commuting coefficients,

$$Da = 0, \qquad a^2 = \sum_{i<j} [A_i, A_j] e_i e_j = 0, \qquad a^3 = 0. \tag{XVIII.5.39}$$

A constant field on a rank-one bundle is a special case. This does not make the kinetic term vanish for arbitrary nonconstant abelian fields. The finite set of constant matrices above is a subsector of the classical hCS action. Calling it the Dijkgraaf–Vafa matrix integral would additionally require a geometry, reduction, integration prescription and physical F-term dictionary. Those are the subject of Chapter 7; the present calculation supplies a local interaction and its global obstruction test.

XVIII.5.6 Why complexes help describe boundary states

The same boundary construction has more than one type of bundle endpoint. If the source endpoint carries E and the target carries F, a state is a bundle map with a form attached. Its off-shell space and on-shell classes are

$$\mathcal{B}(E,F) = \Omega^{0,*}(X, \mathrm{Hom}(E,F)), \qquad H^q\mathcal{B}(E,F) = H^{0,q}(X, E^* \otimes F). \tag{XVIII.5.40}$$

Here $\mathrm{Hom}(E,F)$ means maps $E \to F$. If these maps are arranged into blocks, the book's matrix block X_{ij} instead denotes a map $E_j \to E_i$. The order of composition follows the actual maps, not the names of mathematical arrows chosen elsewhere.

For locally free holomorphic E, the Dolbeault resolution computes the mathematical

Ext groups:

$$\begin{aligned} 0 \longrightarrow \mathcal{O}(E^* \otimes F) &\longrightarrow \Omega^{0,0}(E^* \otimes F) \\ &\xrightarrow{D} \Omega^{0,1}(E^* \otimes F) \xrightarrow{D} \cdots , \\ \mathrm{Ext}^q(E,F) &\simeq H^{0,q}(X, E^* \otimes F). \end{aligned} \tag{XVIII.5.41}$$

The resolution is exact locally and uses fine sheaves, so global cohomology is computed by its smooth forms. Local freeness makes $\mathrm{Hom}(E,-)$ exact. These hypotheses explain why this simple formula cannot be transferred unchanged to arbitrary sheaves with smaller-dimensional support. The mathematical resolution theorem is an imported result; the physical identification with open states uses the bundle boundary construction.

Composition has a physical role. If u maps E to F and v maps F to G, joining the boundary intervals gives vu, and

$$D(vu) = (Dv)u + (-1)^{|v|} vDu. \tag{XVIII.5.42}$$

It follows that composition descends to cohomology: changing a closed factor by an exact factor changes the product by an exact term. Bundles, Hom complexes, and this composition form the small differential-graded description needed here. More general category statements require additional objects and identifications.

Why do complexes enter at all? A resolution may replace one description by several bundle terms with a differential. To see the redundancy concretely, consider the ordinary cochain complex

$$C^0 = \mathbb{C} \xrightarrow{d^0=1} C^1 = \mathbb{C}, \qquad C^k = 0 \ (k \neq 0, 1). \tag{XVIII.5.43}$$

Its degree-minus-one map $h : C^1 \to C^0$ is also the identity, and $h = 0$ on all other degrees. Hence

$$(dh + hd)|_{C^0} = hd = 1, \qquad (dh + hd)|_{C^1} = dh = 1. \tag{XVIII.5.44}$$

Every closed vector is exact. Adding this contractible pair to a complex adds no cohomology. This is the simplest model of why redundant terms in resolutions should not create new states.

For two ordinary cochain complexes, a homogeneous degree-k map has differential

$$\delta f = d_F f - (-1)^k f d_E. \tag{XVIII.5.45}$$

Applying δ again gives

$$\begin{aligned} \delta^2 f &= d_F^2 f - (-1)^k d_F f d_E - (-1)^{k+1} d_F f d_E + (-1)^{2k+1} f d_E^2 \\ &= d_F^2 f - f d_E^2 = 0. \end{aligned} \tag{XVIII.5.46}$$

The cancellation of the middle terms is why the sign depends on the degree of the map. This calculation concerns ordinary cochain complexes; it does not set a general graded-superconnection sign system for hCS.

The category language preserves maps and their composition, not just dimensions of state spaces. It does not determine which branes are physically stable, nor establish an

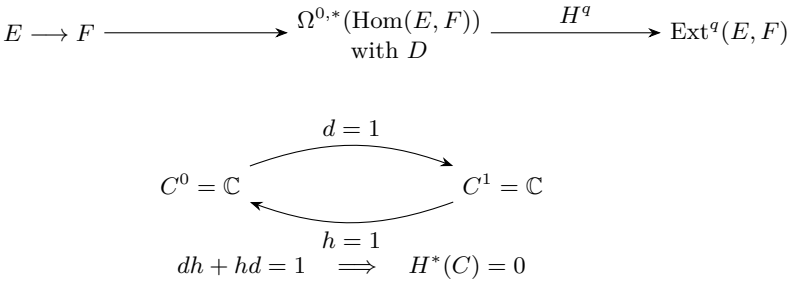


Figure XVIII.5.6: Bundle maps acquire a Dolbeault differential, and taking its cohomology gives Ext for locally free bundles. Below, an identity two-term cochain complex is contracted by h in the reverse direction: $dh + hd = 1$. Removing that summand preserves cohomology. The arrows describe these precise mathematical operations; no arrow assigns physical stability to a complex.

equivalence with all possible B boundary conditions. There is also a reason to remember the off-shell complex: eliminating fields outside cohomology can induce higher effective products. A cubic off-shell action therefore does not force every effective superpotential to be cubic.

The chapter has connected boundary symmetry, a state complex, ordered products, and a nonlinear target equation. The torus example makes their different roles measurable: the state survives D, its square survives cohomology, and a third state detects it through the cubic. Chapter 6 changes the closed target complex structure instead of the open bundle differential. Chapter 7 will need further geometric and physical information to turn a reduction into a four-dimensional F-term calculation.

Working through the obstruction before solving for a field

The torus example teaches a practical order for nonlinear deformation problems. Begin with the prescribed first-order field and calculate its quadratic source. The product in (XVIII.5.28) combines two separate antisymmetries. The exterior forms exchange with a minus sign, while the matrices need not commute. Together they produce the matrix commutator, which is constant in this example. The first-order equation only tests the Dolbeault derivative, so it does not see that commutator. The second-order equation does.

Before choosing a primitive, take the constant Fourier projection of the second-order equation. A derivative of a smooth periodic coefficient has zero average. The source instead has the nonzero constant coefficient shown in (XVIII.5.30). This is already a contradiction. No choice of nonzero Fourier modes in the unknown field can cancel a constant source, because the Dolbeault operator preserves each Fourier label. Searching for a more elaborate inverse operator cannot change this conclusion.

The contraction (XVIII.5.26) explains exactly where inversion would have worked.

For a nonzero mode, wedge and contraction sum to the positive norm of the Dolbeault symbol. Dividing by that norm makes every closed nonzero-mode source exact. At zero mode both the differential and its symbol vanish. The projector term in (XVIII.5.27) retains this exception. Dropping it would incorrectly turn the local patch primitive into a global periodic field. The distinction is geometric rather than a matter of choosing a convenient gauge.

There is also a way to observe the obstruction through the action without solving for the second-order field. Keep the three constant amplitudes in (XVIII.5.36). The kinetic term vanishes because their derivatives vanish. Expanding the cubic gives six ordered words, each carrying the exterior permutation sign. Cyclicity groups these words into the commutator expression already displayed. Differentiating with respect to the third amplitude then detects the product of the first two. This is the same nonzero source seen by the projected curvature equation. The action and the integrability test are two descriptions of one obstruction, rather than two unrelated numerical tests.

This example also identifies the role of the field being varied. The constant amplitudes are coordinates on a chosen off-shell subsector. Restricting to an integrable locus before varying would set the obstructing combination to zero by assumption. The Euler equation would then no longer teach us which first-order state fails to extend. Retaining off-shell variables is what lets the open-string action distinguish a linear BRST class from an actual nearby holomorphic bundle.

The next chapter offers a deliberately different comparison. Closed complex-structure deformations on its compact Kähler domain have a constrained exact-field equation and an imported unobstructedness result. A nonzero cubic there can coexist with an unobstructed family. The calculation here does not supply a general rule that every nonzero cubic must obstruct every deformation problem.

Exercises

These exercises use smooth forms on a compact Kähler complex threefold X without boundary, with a chosen nowhere-zero holomorphic three-form Ω. Let E be a holomorphic bundle, $D = \bar\partial_E$ its integrable reference differential on $\operatorname{End} E$, and $a \in \Omega^{0,1}(X, \operatorname{End} E)$. Products combine wedge multiplication with matrix composition. Set $\tau(u) = \int_X \Omega \wedge \operatorname{Tr} u$, with Ω first, and take $\kappa_B \neq 0$. For homogeneous forms, $D(uv) = Du\, v + (-1)^{|u|} u\, Dv$ and $\tau(uv) = (-1)^{|u||v|}\tau(vu)$. Each answer must include its reasoning and domain of validity.

1. **Boundary complex.** In a local holomorphic frame use $[Q, \bar z^j] = -\eta^j$, $Q\eta^j = 0$, $Qz^j = 0$. Compute Qf and $Q(u_j\eta^j)$ with odd η^j and even coefficients. Translate them with $\eta^j = -d\bar z^j$ into the Dolbeault complex. For a nontrivial bundle explain how the differential changes and which background condition makes its square zero. Does the form degree equal every possible worldsheet ghost grading?

2. **Disk order.** Let $e_j = d\bar z^j$, $P = E_{12}$, $R = E_{21}$ and $T = \operatorname{diag}(1, 0)$. For $u = Pe_1$, $v = Re_2$, $w = Te_3$, compute the coefficients of $e_1e_2e_3$ in $\operatorname{Tr}(uvw)$, $\operatorname{Tr}(vwu)$ and $\operatorname{Tr}(vuw)$. Account separately for matrix and exterior signs. Explain cyclicity and why it does not permit arbitrary exchange of disk insertions.

3. **Action variation.** Starting with $L = \mathrm{Tr}(aDa/2 + a^3/3)$, derive its variation including the exact derivative before integration. Obtain the Euler equation of $S = \kappa_B \int_X \Omega \wedge L$. Replace $1/3$ by a scalar c and determine c for which that equation is $Da + a^2 = 0$. State the support or boundary condition and the role of $\kappa_B \neq 0$.

4. **Gauge and curvature.** Define $F = Da + a^2$ and $D_a u = Du + au - (-1)^{|u|}ua$. Derive $D_a^2 u$ for homogeneous u and $D_a F$. With sections transforming as $s \mapsto g^{-1}s$, derive a^g and F^g for smooth complex invertible g. Use these identities to establish infinitesimal action invariance. Identify the terms invalidated by $D^2 \neq 0$, and explain whether this calculation quantizes κ_B.

5. **Global obstruction.** Take $X = (\mathbb{C}/(2\pi\mathbb{Z} + 2\pi i\mathbb{Z}))^3$, $E = \mathcal{O}_X^2$, $D = \bar{\partial}$, $z^j = x^j + iy^j$, and $a_1 = E_{12}e_1 + E_{21}e_2$. Expand $F(a(t)) = 0$ for $a(t) = ta_1 + t^2 a_2 + \cdots$. Compute the second-order obstruction and prove that no smooth periodic a_2 cancels it, using zero Fourier projection or integration. Compare with a primitive on a coordinate patch and explain its failure globally. Check invariance of the obstruction class when a_1 changes by $D\epsilon$. Then repeat the constant-matrix argument for pairwise commuting diagonal coefficients.

6. **Cubic diagnostic.** On the same torus let $H = \mathrm{diag}(1, -1)$, $\Omega = dz^1 dz^2 dz^3$, with real orientation $dx^1 dy^1 dx^2 dy^2 dx^3 dy^3$. For $a = xPe_1 + yRe_2 + zHe_3$, where x, y, z now denote complex amplitudes, compute $V = \int_X \Omega e_1 e_2 e_3$ and $S/(\kappa_B V)$. Compare the derivative with respect to z to the pairing of He_3 with the obstruction in Exercise 5. Check the commuting and constant rank-one-bundle (abelian) limits. Explain what additional physical information would be needed to call this a stable brane vacuum or the Dijkgraaf–Vafa matrix integral.

7. **Contractible pairs.** For the cochain complex $C^0 = \mathbb{C}$, $C^1 = \mathbb{C}$, $d^0 = \mathrm{id}$ and other groups zero, construct a degree-minus-one h and show $dh + hd = \mathrm{id}$. For two ordinary cochain complexes $(E^\bullet, d_E)$ and $(F^\bullet, d_F)$ and a degree-k map f, derive $\delta^2 f$ from $\delta f = d_F f - (-1)^k f d_E$. Explain what removal of a contractible summand preserves and why this alone supplies no physical stability criterion or general graded hCS sign convention.

Sources and scope

§XVIII.5.1. The full free B boundary and improved holonomy require $F_E^{0,2} = 0$ without an additional $F_E^{1,1} = 0$ condition [WS-T]; Witten (1995), physical PDF pp. 15–16, 19, (3.5), (3.12)–(3.14), and Diaconescu (2001), physical p. 5, (2.8)–(2.9). The classical large-metric low-mode complex and its states are the Dolbeault complex and cohomology [WS-T]; Witten, physical pp. 22–23, (3.23)–(3.24). This uses BRST-compatible boundary and measure assumptions, not a finite-metric Hilbert-space theorem. Recall V.1 and V.6.

§XVIII.5.2. The ordered product and degree-three Ω trace are the classical disk algebra under the stated sewing and measure assumptions [WS-T]; Witten, physical p. 24, (4.1), and B reduction in §4.5, physical pp. 48–49, (4.52); Diaconescu, physical p. 6, (2.11). Witten's (4.8) is an A-model illustration, not the B-model source. Substitution gives the relative action with coefficients $1/2, 1/3$

and undetermined nonzero κ_B [WS-T]; same anchors and Witten (4.2), (4.51). No integer level or absolute four-dimensional coupling is determined.

§XVIII.5.3. Variation including $-D\,\mathrm{Tr}(a\delta a)/2$ and the Euler equation follow from graded cyclicity with the stated boundary/support and nonzero-coupling hypotheses [MATH]. Curvature covariance and $D_a^2 = \mathrm{ad}_F$ follow from operator conjugation and graded expansion [MATH]. Bianchi and infinitesimal action invariance follow without equations of motion [MATH]. These are the displayed derivations; the finite gauge convention is the inverse of Witten's action on sections. No large-gauge quantization or quantum completion follows.

§XVIII.5.4. The nonzero-mode contraction preserves smooth periodic Fourier series [MATH]; the analytic proof is (XVIII.5.26) and its decay argument. The trivial rank-two torus dimensions are $4\binom{3}{q}$ [MATH]; (XVIII.5.27), not an arbitrary-bundle formula. The prescribed first-order class has nonexact second-order obstruction He_1e_2 [MATH]; constant projection and representative calculation (XVIII.5.30)–(XVIII.5.31). A first-order state can have an obstruction to extending it as a global deformation.

§XVIII.5.5. The dual pairing is $2V$, $V = -8i(2\pi)^6$, and the normalized three-mode action is $2xyz$ [MATH]; (XVIII.5.33)–(XVIII.5.38). Commuting constant matrices have vanishing curvature and cubic [MATH]; (XVIII.5.39). The modes are off shell, not stable vacua or the DV integral. The disk witness T and obstruction witness H have different purposes.

§XVIII.5.6. Locally free Ext is computed by the Dolbeault resolution under the stated smooth complex and bundle hypotheses [MATH]; imported resolution theorem, with Katz and Sharpe (2003), physical pp. 4–5, and (XVIII.5.41) explaining its use. Ungraded bundle Hom complexes describe the controlled open topological states [WS-T]; Diaconescu, physical pp. 6–7, (2.14)–(2.16); physical pp. 14–16 restrict the broader categorical conclusions. The ordinary Hom differential squares to zero and the identity pair is contractible [MATH]; (XVIII.5.44)–(XVIII.5.46). Effective products and physical stability require further arguments.

The ordinary B twist and the relative holomorphic Chern–Simons action use the form order, fundamental trace and undetermined coupling specified above. The worldsheet boundary and sewing hypotheses are physical inputs. Stable-brane classification, quantum equivalence and normalization of a four-dimensional superpotential require further input.

References

Diaconescu, D.-E. (2001). "Enhanced d-brane categories from string field theory". In: *JHEP* 06, p. 016. DOI: 10.1088/1126-6708/2001/06/016. arXiv: hep-th/0104200.

Katz, S. H. and E. Sharpe (2003). "D-branes, open string vertex operators, and Ext groups". In: *Adv. Theor. Math. Phys.* 6. Source edition hep-th/0208104v4; chapter locators use 1-based physical PDF pages, pp. 979–1030. DOI: 10.4310/ATMP.2002.v6.n6.a1. arXiv: hep-th/0208104.

Witten, E. (1995). "Chern-Simons gauge theory as a string theory". In: *Prog. Math.* 133, pp. 637–678. arXiv: hep-th/9207094.

Chapter XVIII.6

Closed B-model and Kodaira–Spencer theory

A closed B-string can change the complex structure of its target. This statement has a direct field-theory meaning. A marginal state specifies a first-order change in the antiholomorphic derivative; consistency of the changed derivative then supplies a nonlinear equation for a target-space field. The field takes values in the holomorphic tangent bundle, so its interaction involves the commutator of vector fields. The matrix commutator of the open B-model is replaced by a geometric operation.

We shall construct the relative classical Kodaira–Spencer functional on a smooth compact Kähler Calabi–Yau threefold X, with a chosen nowhere-zero holomorphic volume form Ω. Its dynamical field is an exact deformation relative to a fixed harmonic background. This separation is the central physical point. On a small family of complex tori, the field equation vanishes identically while the background response is a nonzero cubic. The cubic therefore measures an interaction without obstructing the moduli.

The reader needs the B-twist and its Dolbeault state space from V.1, the residual-state projector from XVIII.1, and the Hodge-frame conventions of V.5. We recall each ingredient when it enters. Compact Kähler Hodge theory and the $\partial\bar\partial$ lemma are mathematical inputs. The worldsheet measure, sewing and regulated loop comparison are additional physical inputs; we distinguish them from the classical calculation. The chapter ends by explaining the one-loop determinant and the nodal origin of the holomorphic anomaly.

XVIII.6.1 A closed-string state changes holomorphicity

The geometric B-model state space consists of Dolbeault polyvectors. A polyvector has an antiholomorphic form slot and a holomorphic vector slot,

$$\mathrm{PV}^{p,q}(X) = \Omega^{0,q}(X, \wedge^p T^{1,0}X), \qquad H_Q \simeq \bigoplus_{p,q} H^{0,q}(X, \wedge^p T^{1,0}X). \tag{XVIII.6.1}$$

Here the identification with physical topological states uses the ordinary zero-center B-twist and its quantum R-symmetry conditions. In particular a marginal complex-structure state lies in $H^{0,1}(X, T^{1,0}X)$. A representative is a Beltrami differential. In a holomorphic volume chart we write

$$\Omega = dz^1 \wedge dz^2 \wedge dz^3, \qquad e_a = d\bar{z}^a, \quad v_i = \partial_i, \quad \mu = \mu_a{}^i e_a \otimes v_i. \tag{XVIII.6.2}$$

The local question is operational: which functions should count as holomorphic after switching on μ? Replace the old antiholomorphic tangent space by its graph under μ. Its basis and its action on functions are

$$E_a = \partial_{\bar{a}} + \mu_a{}^i \partial_i, \qquad D_\mu f = \bar{\partial} f + \mu_a{}^i e_a \partial_i f. \tag{XVIII.6.3}$$

A new holomorphic function is annihilated by all E_a. Figure XVIII.6.1 shows this graph in a complexified tangent space. It is a picture of tangent subspaces, rather than a worldsheet embedded in X.

Commuting two graph derivatives gives the obstruction to a common local holomorphic coordinate system. The terms containing two derivatives of f cancel because those derivatives are symmetric while $e_a \wedge e_b$ is antisymmetric. Thus

$$D_\mu^2 f = \sum_{a<b} \left(\partial_{\bar{a}} \mu_b{}^i - \partial_{\bar{b}} \mu_a{}^i + \mu_a{}^j \partial_j \mu_b{}^i - \mu_b{}^j \partial_j \mu_a{}^i \right) e_a \wedge e_b \, \partial_i f. \tag{XVIII.6.4}$$

We define the bracket by these ordinary vector commutators and form wedges. For two degree-one fields its components are

$$[\mu, \nu]_{ab}{}^i = \mu_a{}^j \partial_j \nu_b{}^i - \mu_b{}^j \partial_j \nu_a{}^i + \nu_a{}^j \partial_j \mu_b{}^i - \nu_b{}^j \partial_j \mu_a{}^i. \tag{XVIII.6.5}$$

Consequently the integrability condition is the Maurer–Cartan equation,

$$F_\mu \equiv \bar{\partial}\mu + \frac{1}{2}[\mu, \mu] = 0. \tag{XVIII.6.6}$$

Integrability must be accompanied by transversality to the conjugate graph. That condition ensures that the two graphs split the complexified real tangent space. A sufficiently small smooth Beltrami differential satisfies it; the formal equation alone does not impose it.

The simplest example already distinguishes integrability from transversality. On a complex torus with $z = x + iy$ and real periods 2π, take a constant u. Then

$$E = \partial_{\bar{z}} + u\partial_z, \qquad \zeta = z - u\bar{z}, \qquad E\zeta = 0. \tag{XVIII.6.7}$$

If $u = s + it$, the real transformation and its determinant are

$$\begin{pmatrix} \Re\zeta \\ \Im\zeta \end{pmatrix} = \begin{pmatrix} 1-s & -t \\ -t & 1+s \end{pmatrix} \begin{pmatrix} x \\ y \end{pmatrix}, \qquad \det = 1 - |u|^2. \tag{XVIII.6.8}$$

For $|u| < 1$ this gives an actual nearby complex torus. The differential $d\zeta = dz - u\, d\bar{z}$ is periodic, while ζ changes by a lattice vector under a period of x or y. A coordinate on the covering space need not be a single-valued function on the quotient.

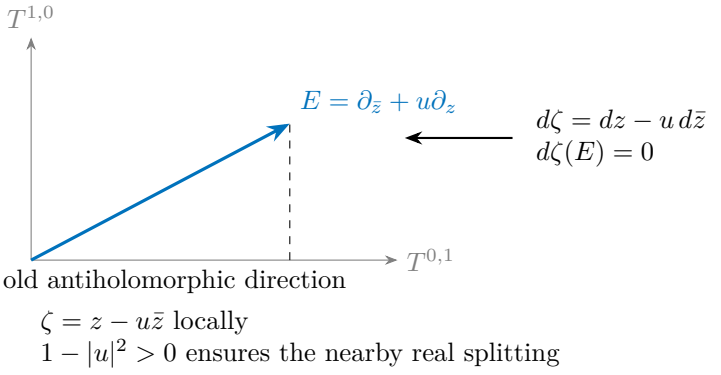


Figure XVIII.6.1: A schematic graph in the complexified target tangent space. The blue direction spans the deformed antiholomorphic subspace. Its annihilator is $d\zeta$. The axes label the two old complex subspaces; their plotted angle has no metric meaning. Transversality to the conjugate graph is an additional condition on the real complex structure.

Linearizing (XVIII.6.6) at the origin and allowing infinitesimal coordinate changes gives

$$\bar{\partial}\mu_1 = 0, \qquad \mu_1 \sim \mu_1 + \bar{\partial}\epsilon, \qquad [\mu_1] \in H^{0,1}(X, T^{1,0}X). \tag{XVIII.6.9}$$

At finite μ, the infinitesimal transformation $\delta\mu = \bar{\partial}\epsilon + [\mu, \epsilon]$ gives $\delta F_\mu = [F_\mu, \epsilon]$ by the derivation property and Jacobi identity. This is covariance of the integrability equation. The action we construct below uses a smaller field domain, and its allowed parameters must preserve that domain. Keeping these two statements separate will prevent us from varying the wrong fields.

XVIII.6.2 Residual states and the constrained propagator

A propagator solves a differential equation after removing its zero modes. The closed B-model adds a volume-form constraint to this familiar statement. Contract the holomorphic vector slot with Ω using the explicit map

$$J(e_I \otimes v_{j_1} \wedge \cdots \wedge v_{j_p}) = \left(\iota_{j_p} \cdots \iota_{j_1}\Omega\right) \wedge e_I, \qquad J\colon \mathrm{PV}^{p,q} \longrightarrow \Omega^{3-p,q}. \tag{XVIII.6.10}$$

Holomorphic differential forms occur first. All resulting form products use ordinary total-degree exterior signs. For example

$$J(v_1) = dz^2 \wedge dz^3, \quad J(v_2) = -dz^1 \wedge dz^3, \quad J(v_3) = dz^1 \wedge dz^2. \tag{XVIII.6.11}$$

The product of two polyvectors wedges their antiholomorphic and vector slots separately, without an additional shifted sign. These conventions fix the sign of the interaction

rather than leaving it implicit in a prime symbol. The geometric antighost constraint is volume preservation,

$$\partial J\mu = 0 \quad \Longleftrightarrow \quad \sum_i \partial_i \mu_a{}^i = 0. \tag{XVIII.6.12}$$

The worldsheet identification of BRST with $\bar\partial$ and of the additional constraint with ∂ on contracted forms is a physical input from the B-model. The Hodge consequences can then be calculated directly.

Choose a compatible Ricci-flat Kähler metric and define the positive Laplacian and its Green operator by

$$L_\partial = \partial\partial^\dagger + \partial^\dagger\partial, \qquad G_\partial L_\partial = L_\partial G_\partial = 1 - P, \qquad h_\partial = \partial^\dagger G_\partial. \tag{XVIII.6.13}$$

Here P projects to harmonic forms and G_∂ vanishes on that space. Commutation with ∂ gives

$$\partial h_\partial + h_\partial \partial = 1 - P, \qquad h_\partial P = 0. \tag{XVIII.6.14}$$

On the constrained space $\ker\partial$, Hodge theory has the particularly useful splitting

$$\ker\partial = \mathcal{H}_\partial \oplus \operatorname{im}\partial, \qquad \mu = x + a, \quad Jx \in \mathcal{H}^{2,1}_\partial, \quad a' = Ja \in \operatorname{im}\partial. \tag{XVIII.6.15}$$

The full form space also has an $\operatorname{im}\partial^\dagger$ summand. It is absent in this equation because we have already restricted to $\ker\partial$. Figure XVIII.6.2 keeps that domain visible. We hold x fixed and propagate only a. These nonharmonic target-space modes are eigenmodes of a geometric Laplacian, not massive string oscillators.

The inverse and its failure on zero modes can be seen without a spectral approximation. On the flat torus write a Fourier wave as

$$w_{m,n} = e^{i(m\cdot x + n\cdot y)}, \quad \partial_j = \tfrac{1}{2}(\partial_{x_j} - i\partial_{y_j}), \quad \partial_{\bar\jmath} = \tfrac{1}{2}(\partial_{x_j} + i\partial_{y_j}). \tag{XVIII.6.16}$$

Both integer vectors matter. Direct differentiation gives

$$\partial w_{m,n} = w_{m,n}\alpha, \quad \bar\partial w_{m,n} = w_{m,n}\beta, \qquad \alpha_j = \frac{im_j + n_j}{2}, \quad \beta_j = \frac{im_j - n_j}{2}. \tag{XVIII.6.17}$$

With an orthonormal exterior basis, set $h_\alpha = \iota_{\bar\alpha}/|\alpha|^2$ for a nonzero mode. The contraction rule for a one-form α is

$$\iota_{\bar\alpha}(\alpha\wedge\eta) = |\alpha|^2\eta - \alpha\wedge\iota_{\bar\alpha}\eta, \qquad (\alpha\wedge)h_\alpha + h_\alpha(\alpha\wedge) = 1. \tag{XVIII.6.18}$$

For instance $m = (1,0,0)$ and $n = (1,0,0)$ give $\alpha_1 = (1+i)/2$, $\beta_1 = (-1+i)/2$, and $|\alpha|^2 = 1/2$. The two symbols have the same norm but different coefficients, so replacing one by the other before differentiation loses information.

Define the homotopy to vanish at $(m,n) = 0$. The preceding exterior identity then holds on every nonzero integer mode and yields

$$\{\partial, h\} = 1 - P_0 \tag{XVIII.6.19}$$

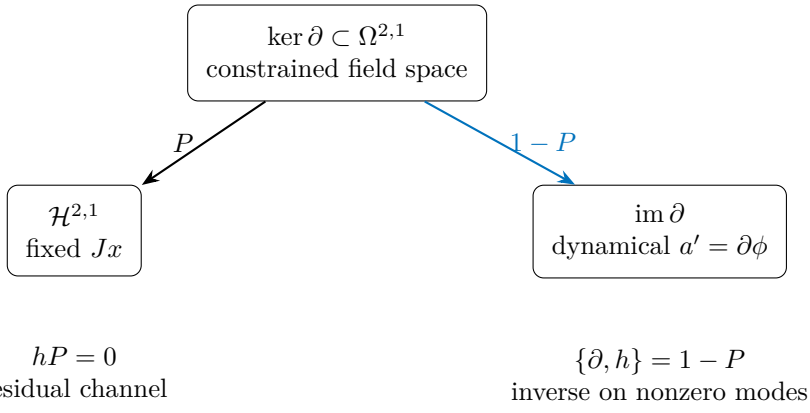


Figure XVIII.6.2: Hodge splitting after imposing the closed-B volume constraint. Harmonic forms label external backgrounds. Exact forms carry the dynamical field. This is the decomposition of $\ker \partial$; the full form space also contains $\operatorname{im} \partial^\dagger$. The projector prevents inversion of residual states.

on all smooth periodic forms. Smooth Fourier coefficients decrease faster than any power; the multiplier h is of order $|m, n|^{-1}$, so the resulting series remains smooth. This is an all-mode argument. At zero mode, averaging any periodic derivative gives zero,

$$\langle \partial_j f \rangle = 0, \qquad \partial\eta = c \neq 0 \text{ constant} \quad \Longrightarrow \quad 0 = c, \tag{XVIII.6.20}$$

which rules out a global inverse on constants. The harmonic background cannot be fed into the propagator.

Our normalization is $L_{\bar\partial} = \{\bar\partial, \bar\partial^\dagger\} = L_\partial$ on Kähler forms. A source convention $\Delta = 2L_{\bar\partial}$ gives an anticommutator of ∂ with $\partial^\dagger/\Delta$ equal to $(1 - P)/2$. It cannot simultaneously give $1 - P$ under that literal normalization. We use (XVIII.6.14) with its explicitly defined L throughout.

XVIII.6.3 The cubic action and its allowed variations

We now seek a functional whose Euler equation is integrability. The volume-preserving constraint makes the bracket a ∂ derivative. This is why a cubic pairing can produce the nonlinear term of (XVIII.6.6). Let $B = J(\mu\mu)$. In a volume chart, differentiating its coefficients produces two kinds of terms: divergences of each vector and crossed derivatives between the two vectors. The divergences vanish when $\partial J\mu = 0$. The crossed terms give

$$J[\mu, \nu] = -\partial J(\mu\nu), \qquad \partial J\mu = \partial J\nu = 0. \tag{XVIII.6.21}$$

For example the coefficient of $dz^k \wedge e_a \wedge e_b$ in B, with $a < b$, is $2\epsilon_{ijk}\mu_a{}^i\mu_b{}^j$. Applying ∂ to this expression and contracting the two epsilon tensors reproduces the bracket above

with a minus sign. We can display the general calculation before testing its sign. Define $\operatorname{div} V$ by $\mathcal{L}_V\Omega = (\operatorname{div} V)\Omega$, where V is a holomorphic-type vector field with smooth coefficients and $\mathcal{L}_V = \partial\iota_V + \iota_V\partial$ in this calculation. Cartan's contraction commutator gives

$$\partial(\iota_W\iota_V\Omega) = \mathcal{L}_W\iota_V\Omega - \iota_W\partial\iota_V\Omega \tag{XVIII.6.22}$$

$$= -\iota_{[V,W]}\Omega + (\operatorname{div} W)\iota_V\Omega - (\operatorname{div} V)\iota_W\Omega. \tag{XVIII.6.23}$$

Set $V = \mu_a$ and $W = \nu_b$, multiply by $e_a \wedge e_b$, and antisymmetrize in a, b. The last two terms vanish separately when the fields preserve Ω; the first is exactly the negative vector bracket in (XVIII.6.21). The same calculation with $W = \epsilon$ will give the mixed identity below. Thus the constraint removes explicit divergence terms rather than changing the definition of the bracket. A small nonzero example now fixes the contraction sign concretely.

Take a local polynomial field, which is not periodic on the torus,

$$\mu = z^3 e_1 \otimes v_2 + z^2 e_2 \otimes v_3. \tag{XVIII.6.24}$$

Its divergence vanishes, and direct vector differentiation gives

$$\frac{1}{2}[\mu,\mu] = (z^3 v_3 - z^2 v_2)e_1 \wedge e_2, \qquad B = 2z^2 z^3 dz^1 \wedge e_1 \wedge e_2. \tag{XVIII.6.25}$$

Consequently

$$\partial B = -2(z^3 dz^1 \wedge dz^2 + z^2 dz^1 \wedge dz^3) \wedge e_1 \wedge e_2 = -J[\mu,\mu]. \tag{XVIII.6.26}$$

This is the Tian identity in our contraction and product conventions. A source prime notation with the opposite printed sign must be translated together with its product and inverse conventions. It cannot be substituted for J term by term.

Since a' is exact, write $a' = \partial\phi$, where ϕ is a smooth global $(1,1)$ form. For fixed x and symbolic $\kappa_{\mathrm{KS}} \neq 0$, define

$$I[\phi; x] \equiv \frac{S_{\mathrm{KS}}}{\kappa_{\mathrm{KS}}} = -\frac{1}{2}\int_X \partial\phi \wedge \bar\partial\phi + \frac{1}{6}\int_X J(\mu\mu) \wedge J\mu, \qquad \mu = x + a. \tag{XVIII.6.27}$$

The coefficients are fixed by the variation. The primitive ϕ is not a new physical field with a separately imposed gauge condition. Every smooth $\delta\phi$ is permitted when deriving the Euler equation.

We display both kinetic variations because their total-degree signs are load-bearing. Compactness removes boundary terms. Since ϕ and $\delta\phi$ have degree two,

$$\int_X \partial\delta\phi \wedge \bar\partial\phi = -\int_X \delta\phi \wedge \partial\bar\partial\phi = \int_X \delta\phi \wedge \bar\partial\partial\phi, \tag{XVIII.6.28}$$

$$\int_X \partial\phi \wedge \bar\partial\delta\phi = -\int_X \bar\partial\delta\phi \wedge \partial\phi = \int_X \delta\phi \wedge \bar\partial\partial\phi. \tag{XVIII.6.29}$$

In the second line exchanging the two degree-three forms supplies the first minus sign; integration by parts supplies the second. Both original integrals therefore equal $\int \delta\phi \wedge \bar\partial\partial\phi$, and

$$\delta I_2 = -\int_X \delta\phi \wedge \bar\partial a'. \tag{XVIII.6.30}$$

The trilinear pairing $T(\mu,\nu,\rho)=\int J(\mu\nu)\wedge J\rho$ is symmetric on these bosonic degree-one fields. In components it has one holomorphic and one antiholomorphic epsilon tensor; exchanging two slots reverses both tensors. Its three variations are thus equal, giving

$$\delta I_3=\frac{1}{2}\int_X B\wedge\partial\delta\phi=\frac{1}{2}\int_X\delta\phi\wedge\partial B. \tag{XVIII.6.31}$$

Combining the two terms with (XVIII.6.21) yields

$$\delta I=\int_X\delta\phi\wedge\left(-\bar\partial a'+\frac{1}{2}\partial B\right)=-\int_X\delta\phi\wedge JF_\mu. \tag{XVIII.6.32}$$

The harmonic background is $\bar\partial$-closed. Arbitrary $(1,1)$ variations pair nondegenerately with the $(2,2)$ form JF_μ, so stationarity gives precisely $F_\mu=0$. Restricting $\delta\phi$ by a propagator gauge before this step would change the variational problem.

There is no dependence on an arbitrary choice of primitive. If $\phi\mapsto\phi+\chi$ with $\partial\chi=0$, the cubic is unchanged and the kinetic change contains

$$\int_X\partial\phi\wedge\bar\partial\chi=-\int_X\phi\wedge\partial\bar\partial\chi=0. \tag{XVIII.6.33}$$

Also $\bar\partial a'=-\partial\bar\partial\phi$ is ∂-exact, so $h_\partial\bar\partial a'$ is a primitive of $\bar\partial a'$. It differs from $-\bar\partial\phi$ by a ∂-closed form. Pairing that difference with $a'=\partial\phi$ integrates to zero. We may therefore rewrite the same relative functional as

$$I[a;x]=\frac{1}{2}\int_X a'\wedge h_\partial\bar\partial a'+\frac{1}{6}\int_X J(\mu\mu)\wedge J\mu. \tag{XVIII.6.34}$$

This construction fixes its own classical signs. It does not identify every scalar term with every printed source-prime convention or fix an absolute physical coupling.

The constrained domain also determines which coordinate variations are allowed. For an Ω-preserving parameter, $\partial J\epsilon=0$, take $V=\mu_a$ and $W=\epsilon$ in the Cartan calculation. Multiplication by e_a gives the mixed identity and the induced field variation,

$$J[\mu,\epsilon]=-\partial J(\mu\epsilon),\qquad J\delta\mu=\bar\partial J\epsilon-\partial J(\mu\epsilon). \tag{XVIII.6.35}$$

The first term is $\bar\partial$-exact and ∂-closed. The compact Kähler $\partial\bar\partial$ lemma makes it ∂-exact; the second term already is. Hence $J\delta\mu\in\operatorname{im}\partial$ and the harmonic x stays fixed. An unrestricted parameter need not work. At $\mu=0$ the periodic parameter $\epsilon=e^{ix_1}v_1$ gives

$$\delta\mu=\frac{i}{2}e^{ix_1}e_1v_1,\qquad \partial_1\delta\mu_1{}^1=-\frac{1}{4}e^{ix_1}\neq0. \tag{XVIII.6.36}$$

It violates volume preservation. Equation covariance alone therefore does not establish a symmetry of this constrained action domain.

The Hodge inverse also organizes perturbative solutions. For a harmonic first order field x, the quadratic equation reads

$$\bar\partial a_2'=\frac{1}{2}\partial J(xx),\qquad a_2'=\frac{1}{2}\bar\partial^\dagger G_{\bar\partial}\partial J(xx). \tag{XVIII.6.37}$$

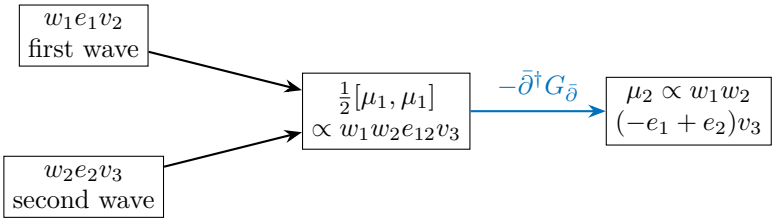


Figure XVIII.6.3: Two periodic nonharmonic waves generate a nonzero bracket source. The projected Green operator gives its coclosed second-order correction. Overall coefficients are derived in the text. This example tests nonlinear cancellation; it is not the recursion for the constant harmonic torus family.

The $\partial\bar\partial$ lemma makes the source $\bar\partial$-exact, so it has no harmonic component; the homotopy identity then verifies the solution. Jacobi organizes higher formal orders. General analytic convergence requires the imported complex-deformation theorem rather than this quadratic calculation.

A nonharmonic example makes the correction visible. Put $w_j = e^{ix_j}$ and

$$\mu_1 = \frac{iu}{2}w_1e_1v_2 + \frac{iv}{2}w_2e_2v_3 = \bar\partial(uw_1v_2 + vw_2v_3). \tag{XVIII.6.38}$$

Thus μ_1 is a pure-gauge linear direction, not a harmonic modulus. Its vector derivative produces a nonzero source,

$$\frac{1}{2}[\mu_1,\mu_1] = -\frac{iuv}{8}w_1w_2e_1\wedge e_2v_3. \tag{XVIII.6.39}$$

An ansatz proportional to $(-e_1+e_2)v_3$ gives

$$\mu_2 = \frac{uv}{8}w_1w_2(-e_1+e_2)v_3, \tag{XVIII.6.40}$$

$$\bar\partial\mu_2 = \frac{iuv}{8}w_1w_2e_1\wedge e_2v_3, \qquad \bar\partial\mu_2 + \tfrac{1}{2}[\mu_1,\mu_1] = 0. \tag{XVIII.6.41}$$

The coefficient is independent of z^3, so the divergence vanishes. Contracting the antiholomorphic symbol $(i/2, i/2, 0)$ with $(-1, 1, 0)$ shows flat $\bar\partial^\dagger$-coclosedness. Figure XVIII.6.3 shows this second-order calculation. It establishes neither a nonzero harmonic obstruction nor an all-order solution for this chosen ansatz.

XVIII.6.4 A nonzero cubic on an unobstructed torus family

A cubic action often makes a student expect a quadratic obstruction equation for every coordinate appearing in it. Here that inference would confuse the fixed background

with the dynamical field. Let

$$x = ue_1v_1 + ve_2v_2 + re_3v_3, \qquad a = 0 \tag{XVIII.6.42}$$

on the flat complex three-torus. All coefficients are constant, so

$$\bar\partial x = 0, \qquad [x,x] = 0, \qquad F_x = 0. \tag{XVIII.6.43}$$

For $|u|, |v|, |r| < 1$, the three coordinate transformations from the first section have nonzero real determinants. Their product is

$$\det_{\mathbb{R}} \frac{\partial \zeta}{\partial z} = (1-|u|^2)(1-|v|^2)(1-|r|^2) > 0. \tag{XVIII.6.44}$$

Here the notation denotes the full real-linear transformation, including its $\bar z$ dependence. The transformed lattice supplies a genuine nearby complex torus. Thus this is an actual small family, beyond a formal solution of MC.

To evaluate the action we must retain both wedge slots. Their signs combine to make the bosonic products commute. The square and its contraction are

$$xx = 2uv\, e_{12}v_{12} + 2ur\, e_{13}v_{13} + 2vr\, e_{23}v_{23}, \tag{XVIII.6.45}$$

$$J(xx) = 2uv\, dz^3 \wedge e_{12} - 2ur\, dz^2 \wedge e_{13} + 2vr\, dz^1 \wedge e_{23}. \tag{XVIII.6.46}$$

Meanwhile

$$Jx = u\, dz^{23} \wedge e_1 - v\, dz^{13} \wedge e_2 + r\, dz^{12} \wedge e_3. \tag{XVIII.6.47}$$

Only complementary index pairs survive in $J(xx) \wedge Jx$. Each of the three terms contributes $2uvr\,\Omega \wedge e_{123}$, giving

$$J(xx) \wedge Jx = 6uvr\,\Omega \wedge e_{123}, \qquad V = \int_X \Omega \wedge e_{123} = -8i(2\pi)^6. \tag{XVIII.6.48}$$

The factorial in the action removes precisely these six ordered contributions. The relative background response is therefore

$$\frac{S_{\mathrm{KS}}(0;x)}{\kappa_{\mathrm{KS}} V} = uvr, \qquad \frac{1}{\kappa_{\mathrm{KS}} V}\partial_u\partial_v\partial_r S_{\mathrm{KS}}(0;x) = 1. \tag{XVIII.6.49}$$

This calculation uses the chosen complex orientation and symbolic coupling. It does not supply an absolutely normalized physical Yukawa coupling.

Why does the nonzero cubic not obstruct this family? For every allowed exact variation the answer is already contained in the Euler formula,

$$\delta_a S_{\mathrm{KS}}|_{a=0} = -\kappa_{\mathrm{KS}} \int_X \delta\phi \wedge JF_x = 0. \tag{XVIII.6.50}$$

Changing a harmonic source asks a different question. Its derivatives are

$$\frac{1}{\kappa_{\mathrm{KS}} V}(\partial_u S, \partial_v S, \partial_r S) = (vr, ur, uv). \tag{XVIII.6.51}$$

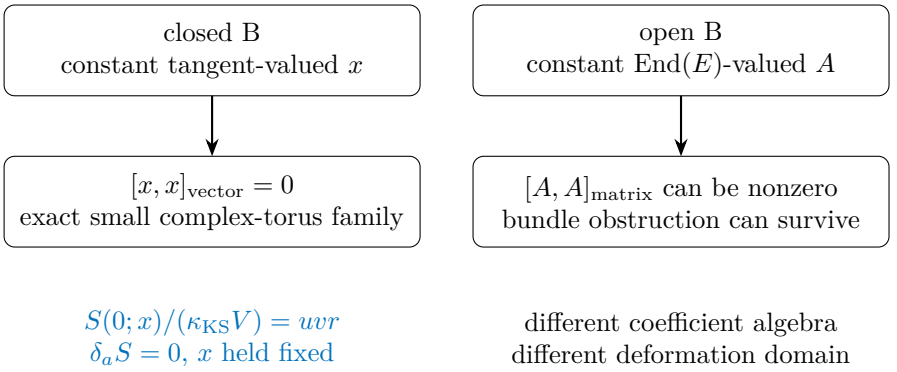


Figure XVIII.6.4: Constant fields in the closed and open B-model examples. The left panel separates the vector bracket, which vanishes, from the cubic pairing, which need not vanish. The right panel recalls why a constant matrix-valued field can still be obstructed. The panels compare deformation equations and do not assert an open/closed quantum equivalence.

Setting these derivatives to zero would incorrectly restrict the background to $vr = ur = uv = 0$. Nothing in our variational domain imposes such equations. Figure XVIII.6.4 makes this distinction alongside the open-B example.

In XVIII.5, constant fields take values in End(E) and their matrix commutators can remain nonzero. A quadratic obstruction can then exist already for constant coefficients. Here constant holomorphic vector fields commute, while the two epsilon tensors in the cubic pairing still give a nonzero number. The interaction pairing and the obstruction bracket perform different operations. Even a cubic bare action can induce higher effective vertices when nonharmonic fields are eliminated. No conclusion that all higher-point amplitudes vanish follows from its polynomial degree.

The example answers the classical cubic puzzle without constructing a four-dimensional superpotential. Such a construction must relate geometry to fluxes, branes and physical couplings. That is the separate task of XVIII.7; the torus calculation supplies none of those additional identifications.

XVIII.6.5 Long tubes, sewing and the one-loop determinant

The fixed-worldsheet large-volume limit localizes the B-model on constant maps. Why should a target-space field theory with propagators remain? The limit is not uniform near a degeneration of the worldsheet. A long thin tube can carry intermediate states for an arbitrarily long proper time. The tube length and the large-volume limit must therefore be considered together. The geometric nonzero modes which appeared in our Hodge construction encode a surviving channel in the sourced sewing argument.

In an ordinary spectral picture, integration over a tube length ℓ has the characteristic

behavior

$$\int_0^\infty d\ell\, e^{-\ell\lambda} = \lambda^{-1} \quad (\lambda > 0), \qquad \lambda = 0 \quad \text{requires a residual-state treatment.} \tag{XVIII.6.52}$$

This explains the inverse and its zero-mode qualification. The actual worldsheet propagator also includes antighost insertions and the BRST-compatible measure. Those are physical ingredients of sewing, not consequences of the finite integral. Figure XVIII.6.5 shows both channels.

The dictionary at this stage can be displayed without identifying the full quantum theories,

closed B-model object	geometric representative
marginal state	$H^{0,1}(X, T^{1,0}X)$
BRST differential	$\bar\partial$
volume-preserving constraint	$\partial J\mu = 0$
residual channel	P
nonharmonic homotopy	$\partial^\dagger G_\partial$
cubic pairing	$\int J(\mu\mu) \wedge J\mu$

(XVIII.6.53)

The state and operator entries are worldsheet inputs. Our calculation derives the relative classical functional and its Euler equation using them. The source tree comparison additionally chooses canonical coordinates and its own normalization. We recall what it compares using source-only notation. Let $A_0(x)$ be the source dynamical field solving the classical equation at fixed harmonic x, and let S_0 denote the source action evaluated on that solution. Its tree generating function obeys

$$W_0^{\mathrm{src}}(x) = \lambda_{\mathrm{src}}^2 S_0^{\mathrm{src}}(x, A_0(x)), \qquad \left.\frac{\delta S^{\mathrm{src}}}{\delta A}\right|_{A_0(x)} = 0. \tag{XVIII.6.54}$$

The stationary condition cancels implicit field-variation terms when taking background derivatives. Differentiating that condition also cancels the terms containing second background derivatives of A_0 in the third derivative of the on-shell action. The remaining cubic is the source pairing of three deformed marginal representatives $\mu_i + \partial_i A_0$. In the source's canonical coordinates it gives

$$\partial_i\partial_j\partial_k W_0^{\mathrm{src}}(x) = C_{ijk}^{\mathrm{src}}(x), \qquad W_0^{\mathrm{src}}\big|_{x^0,x^1,x^2} = 0. \tag{XVIII.6.55}$$

The matching third derivative and the absence of lower terms reconstruct the tree comparison locally in those coordinates. Further background derivatives insert further marginal states, so the four-point and five-point trees are organized by $\partial_l C_{ijk}^{\mathrm{src}}$ and $\partial_s\partial_l C_{ijk}^{\mathrm{src}}$. This is the sourced canonical-coordinate result, including its pairing and normalization conventions. Neither $\lambda_{\mathrm{src}}^2 S_0^{\mathrm{src}}$ nor its cubic is silently identified with our κ_{KS}-normalized functional. The explicit torus calculation establishes our relative cubic without completing that scalar-action translation.

At one loop the source comparison involves holomorphic analytic torsion. For a holomorphic bundle E, the convention we recall is

$$I(E) = \prod_q \left(\det{}' L_{(0,q)}(E)\right)^{(-1)^q q}, \qquad F_1 = \frac{1}{2}\sum_p (-1)^p p \log I(\wedge^p T^* X). \quad \text{(XVIII.6.56)}$$

The displayed one-loop comparison fixes the moduli-dependent part, up to moduli-independent terms or normalization in the source regulator. It is not an absolute equality fixing that normalization. The primes remove zero eigenvalues. Work on a patch where the residual dimensions stay fixed; a jump changes the omitted spectral space. The infinite products require a regulator, and their moduli dependence is accompanied by zero-mode metrics and contact terms in the physical comparison. These are conditions on the sourced large-volume result. A finite matrix example can teach the prime and degree weight; it cannot replace that spectral and measure analysis.

Consider the Hermitian complex

$$C^0 = \mathbb{C} \xrightarrow{d_0} C^1 = \mathbb{C}^3 \xrightarrow{d_1} C^2 = \mathbb{C}, \qquad d_0 = \begin{pmatrix} a \\ 0 \\ 0 \end{pmatrix}, \quad d_1 = \begin{pmatrix} 0 & b & 0 \end{pmatrix}, \quad a, b > 0. \tag{XVIII.6.57}$$

Its composition vanishes. The three Laplacians follow from adjacent maps,

$$L_0 = d_0^\dagger d_0 = a^2, \quad L_1 = d_0 d_0^\dagger + d_1^\dagger d_1 = \mathrm{diag}(a^2, b^2, 0), \quad L_2 = d_1 d_1^\dagger = b^2. \quad \text{(XVIII.6.58)}$$

The first two directions of C^1 pair with C^0 and C^2 respectively. The third is neither exact nor mapped out, so

$$H^0 = 0, \qquad H^1 = \mathbb{C}[(0,0,1)], \qquad H^2 = 0. \tag{XVIII.6.59}$$

The ordinary alternating primed product cancels, whereas the degree-weighted one retains the ratio of the two nonzero scales,

$$\prod_{q=0}^{2} (\det{}' L_q)^{(-1)^q} = \frac{a^2 b^2}{a^2 b^2} = 1, \tag{XVIII.6.60}$$

$$\prod_{q=0}^{2} (\det{}' L_q)^{(-1)^q q} = (a^2 b^2)^{-1} (b^2)^2 = \frac{b^2}{a^2}. \tag{XVIII.6.61}$$

Omitting the prime would insert a zero determinant. Omitting the degree weight would erase the ratio. The finite complex in the lower panel of Figure XVIII.6.5 is only this example; it is not the BV state space of the closed B-model.

There is a useful warning in the limit $a \to 0$. At $a = 0$, d_0 loses rank, H^0 becomes $\mathbb{C}$, and H^1 has two independent classes. Removing all zero eigenvalues at the new rank gives a weighted product b^2, rather than the divergent limit b^2/a^2. A primed determinant belongs to a specified residual space. A rank-changing limit cannot be evaluated by keeping the old residual space implicit.

The classical bosonic functional has not supplied a regulated quantum master equation, all descendants, an integration cycle or a nonperturbative completion. These

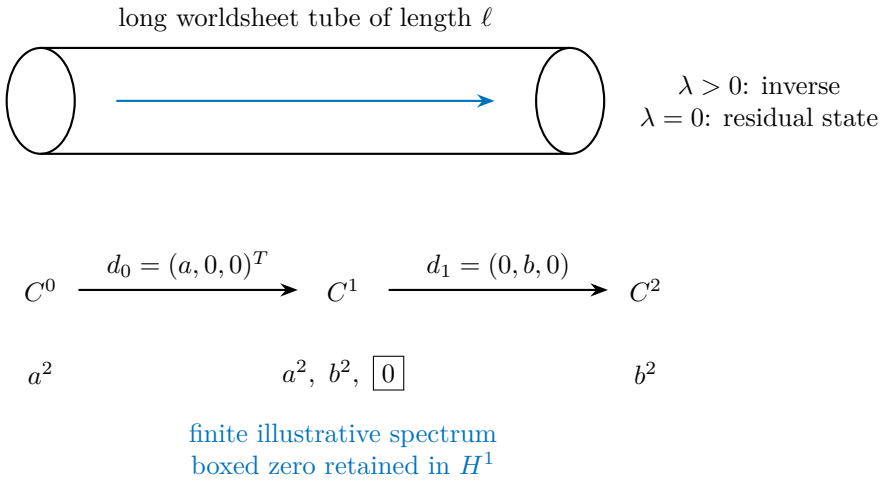


Figure XVIII.6.5: Upper panel, the long-tube sewing channel of a closed worldsheet. Positive eigenvalues produce inverse operators; zero states require separate treatment. Lower panel, the finite $1 \to 3 \to 1$ complex illustrates the prime and degree weight in a determinant. Its eigenvalues are not the actual CY spectral data or the BCOV BV complex.

require additional fields and quantum definitions. The one-loop source comparison is useful precisely at its stated scope, and leads to a second physical question: how can topological amplitudes retain antiholomorphic dependence?

XVIII.6.6 Nodal boundaries and the holomorphic anomaly

An insertion which is BRST-exact decouples only when the moduli-space integral has no surviving boundary contribution. Closed worldsheets have nodal boundaries. Moving an antiholomorphic variation through the BRST measure produces contributions from a pinched handle and from a surface splitting into two components. These are the two terms of the holomorphic anomaly. Their derivation uses protected marginal-state factorization, regulated sewing and the corresponding contact terms.

We recall the local Hodge geometry because it affects the differential equation. On a regular patch of complex-structure moduli space, t^i are local coordinates and $\mathcal{L}$ is the Hodge line with local holomorphic frame Ω. Its potential and moduli metric are

$$K = -\log\left(i\int_X \Omega\wedge\bar{\Omega}\right), \qquad G_{i\bar{j}} = \partial_i\partial_{\bar{j}}K, \qquad G^{i\bar{j}}G_{k\bar{j}} = \delta^i{}_k. \tag{XVIII.6.62}$$

The positive volume pairing uses the chosen complex orientation. The connection on

lower moduli indices and the Euler characteristic are

$$\Gamma^{k}{}_{ij} = G^{k\bar{l}}\partial_i G_{j\bar{l}}, \qquad \chi(X) = \sum_{k=0}^{6}(-1)^k b_k(X). \tag{XVIII.6.63}$$

Here $b_k(X)$ are the real-cohomology Betti numbers. The amplitudes carry the Hodge weight specified below, or equivalently the line power $\mathcal{L}^{2-2g}$ in this frame convention. Under a holomorphic rescaling,

$$\Omega \mapsto e^{h}\Omega, \quad K \mapsto K - h - \bar{h}, \quad F_g \mapsto e^{(2-2g)h}F_g. \tag{XVIII.6.64}$$

Thus F_g is a section of weight $w = 2 - 2g$. The chosen derivative and the raised conjugate cubic are

$$D_i F_g = (\partial_i + wK_i)F_g, \tag{XVIII.6.65}$$

$$D_i D_j F_g = (\partial_i + wK_i)D_j F_g - \Gamma^{k}{}_{ij} D_k F_g, \tag{XVIII.6.66}$$

$$\bar{C}_{\bar{i}}{}^{jk} = e^{2K}G^{j\bar{j}}G^{k\bar{k}}\bar{C}_{\bar{i}\bar{j}\bar{k}}. \tag{XVIII.6.67}$$

Even when $w = 0$, a second derivative has the Christoffel term because its first derivative carries a lower tensor index. The selected sign follows our existing Hodge frame; the source prints differing connection signs in separate passages, and no general equivalence of those operator conventions is assumed here.

For $g \geq 2$ the sourced anomaly equation is

$$\partial_{\bar{i}} F_g = \frac{1}{2}\bar{C}_{\bar{i}}{}^{jk}\left(D_j D_k F_{g-1} + \sum_{s=1}^{g-1} D_j F_s \, D_k F_{g-s}\right). \tag{XVIII.6.68}$$

The first term comes from pinching a handle. The resulting connected surface has genus $g-1$ and two marked insertions. The second comes from a separating node, with genera s and $g-s$ and one insertion on each component. The sum is ordered; the overall $1/2$ accounts for interchange of the two branches. The two genus-two channels are drawn in Figure XVIII.6.6.

For a single component, denote the supplied covariant jets by

$$C = \bar{C}_{\bar{t}}{}^{tt}, \qquad f_j = D_t F_j, \qquad h_j = D_t D_t F_j. \tag{XVIII.6.69}$$

They are values of compatible covariant source tensors, not a choice of globally constant amplitudes. At genus two there is one ordered separating term, while at genus three there are two,

$$\partial_{\bar{t}} F_2 = \frac{C}{2}(h_1 + f_1^2), \tag{XVIII.6.70}$$

$$\partial_{\bar{t}} F_3 = \frac{C}{2}(h_2 + f_1 f_2 + f_2 f_1) = \frac{C}{2}(h_2 + 2f_1 f_2). \tag{XVIII.6.71}$$

For $(C, f_1, h_1) = (2, 3, 5)$ the first source is 14. For $(C, f_1, f_2, h_2) = (2, 3, 5, 7)$ the second is 37. These short calculations exhibit the ordered multiplicity. They evaluate the right-hand side at specified jets; they do not solve for a function over moduli space.

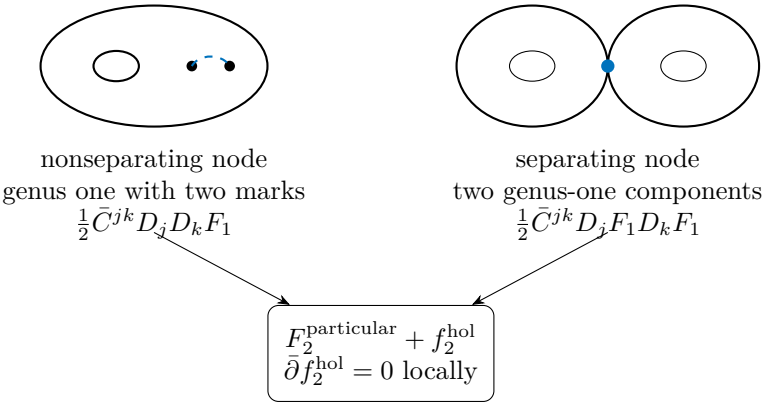


Figure XVIII.6.6: The two genus-two nodal channels, depicted schematically. A handle pinches to two marked points on one genus-one component, or a separating cycle gives two genus-one components meeting at a node. Interchange of the two branches supplies the factor $1/2$ in the ordered formula. Their source does not fix the holomorphic section shown in the lower box.

Genus one obeys a separate mixed trace equation. In the conventional compact CY marginal sector it takes the form

$$\partial_i \partial_{\bar{\jmath}} F_1 = \frac{1}{2}\,\mathrm{Tr}(C_i \bar{C}_{\bar{\jmath}}) - \frac{\chi(X)}{24} G_{i\bar{\jmath}}, \tag{XVIII.6.72}$$

where the trace is over the source chiral ground-state space, with its regulated index and contact-term content. Here C_i is chiral multiplication, so this trace is not defined to be just a contraction of three-index Yukawa tensors. Substituting $g = 1$ into (XVIII.6.68) does not produce this formula.

Finally suppose two compatible local sections solve the same higher-genus inhomogeneous equation. Their difference satisfies

$$\bar{\partial}(F_g - \widetilde{F}_g) = 0, \qquad F_g = F_g^{\text{particular}} + f_g^{\text{hol}}, \qquad f_g^{\text{hol}} \in \mathcal{O}(\mathcal{L}^{2-2g}) \text{ locally.} \tag{XVIII.6.73}$$

This describes the local kernel, conditional on the existence of the particular solution. Boundary conditions, singular behavior and global compatibility must determine the remaining holomorphic section. A full nonholomorphic amplitude and a chosen holomorphic limit are different objects. The anomaly equation by itself does not select every amplitude.

We have followed a closed-string state into a classical field equation, constructed a relative cubic action with that Euler equation, and exhibited an exact torus family on which the cubic survives without an obstruction. Worldsheet sewing adds the source-scoped tree, one-loop and nodal-boundary statements. The next chapter needs an additional geometry, flux and coupling map to reach a four-dimensional $\mathcal{N} = 1$ superpotential. Neither the classical cubic nor the finite determinant supplies that map.

Choosing the variable that is allowed to vary

There are three distinct uses of the word field in the relative Kodaira–Spencer construction. The harmonic component specifies the fixed background. The exact component is the variable entering the constrained functional. A primitive represents that exact component and permits a local integration-by-parts calculation. Keeping these roles visible is the shortest route through the action variation. In particular, a derivative with respect to a background parameter is a different operation from an allowed exact-field variation at that background.

To repeat the derivation of (XVIII.6.32), hold the harmonic component fixed and vary the global primitive. In the kinetic term, integrating the derivative from the varied first factor gives one term. Varying the second factor gives another. The latter requires exchanging two degree-three forms before integrating by parts. That exchange supplies a minus sign. Both contributions then have the same sign and cancel the factor one half. Treating the coefficients as commuting scalars throughout this operation would lose the form-degree sign that fixes the equation.

The cubic term requires a different count. Its trilinear pairing is symmetric in the stated bosonic component convention because exchanging two slots reverses both epsilon tensors. Thus its three variations are equal. The original factor one sixth leaves one half multiplying the differentiated quadratic product. The Tian identity converts that derivative into the bracket with the minus sign fixed earlier in this chapter. Only after these two calculations are combined does arbitrary primitive variation impose the integrability equation.

A propagator gauge has a later purpose. It selects an inverse for solving the exact-field equation perturbatively on the complement of the harmonic space. Applying that gauge as a restriction on the primitive variations before deriving the equation changes the variational problem. The quadratic recursion illustrates the correct order. First determine its source using the bracket; then use the $\partial\bar{\partial}$ statement to identify the source as exact; finally use the projected inverse. A general convergence claim would still require the imported deformation theorem.

The constant torus family makes the background distinction concrete. Its periodic differentials define the deformed complex structure, and the stated smallness conditions preserve the real coordinate Jacobians. Although the classical integrability equation is satisfied, the cubic functional evaluated at those backgrounds depends on their constant parameters. Differentiating that cubic varies the background. It does not test stationarity under the exact-field variations used in the preceding derivation. There is consequently no conflict between a nonzero cubic and an unobstructed family in this example.

In XVIII.7, derivatives of a planar free energy will also be taken while specified data are held fixed. There the fixed data include fillings and a normalization scheme. The lesson carried forward is to state the variable and the fixed data before interpreting a derivative as a physical coupling.

Exercises

E1. On a complex torus with $z = x + iy$ and real periods 2π, let $D = \partial_{\bar{z}} + u\partial_z$ for constant complex u. Find a locally annihilated linear coordinate, its real Jacobian, and a sufficient domain for a nearby transverse real complex structure. Explain periodic differentials and the transformed lattice.

E2. On the six-real-period torus derive both Fourier symbols for $e^{i(m\cdot x+n\cdot y)}$. Prove the exterior homotopy identity at every nonzero (m, n) and use averaging to rule out a global ∂ inverse on constant forms. Distinguish $L_{\bar{\partial}}$ from $\Delta = 2L_{\bar{\partial}}$.

E3. With $\mu = z^3 e_1 v_2 + z^2 e_2 v_3$ and $\Omega = dz^1 \wedge dz^2 \wedge dz^3$, compute the divergence, $[\mu, \mu]/2$, $J(\mu\mu)$ and $\partial J(\mu\mu)$. Fix the sign of the constrained Tian identity. Explain why this local polynomial example is not a periodic torus deformation.

E4. Let $w_j = e^{ix_j}$ and $\mu_1 = (iu/2)w_1 e_1 v_2 + (iv/2)w_2 e_2 v_3$. Solve the second-order MC equation with $\mu_2 = cw_1 w_2(-e_1 + e_2)v_3$. Check divergence and flat $\bar{\partial}^\dagger$-coclosedness. Explain why the first-order field is not a harmonic modulus and why this calculation gives neither a genuine obstruction nor an all-order solution.

E5. Derive the variation of (XVIII.6.27) with ordinary total-degree signs. For fixed $x = ue_1 v_1 + ve_2 v_2 + re_3 v_3$ and $a = 0$, compute $S/(\kappa_{\mathrm{KS}} V)$ and its mixed cubic derivative. Show that all allowed exact-field variations vanish and identify the spurious restrictions from imposing stationarity in x. Give the small real-complex-structure domain.

E6. For $C^0 = \mathbb{C}$, $C^1 = \mathbb{C}^3$, $C^2 = \mathbb{C}$, $d_0 = (a, 0, 0)^T$, $d_1 = (0, b, 0)$ and $a, b > 0$, calculate all three Laplacians, cohomology, ordinary alternating primed determinant and degree-weighted primed determinant. Describe the rank-changing limit $a = 0$ and the additional ingredients required for infinite-dimensional analytic torsion.

E7. Treat C, f_1, f_2, h_1, h_2 as supplied covariant source jets. Expand the genus-two and genus-three anomaly sources, keeping the ordered separating terms. Evaluate $(C, f_1, h_1) = (2, 3, 5)$ and $(C, f_1, f_2, h_2) = (2, 3, 5, 7)$. Explain the local holomorphic kernel, the separate genus-one equation and the difference between a polynomial source evaluation and a full B-model amplitude or a DV superpotential.

Sources and scope

§XVIII.6.1. The B-state/BRST/antighost dictionary [WS-T] assumes the ordinary B-twist and the worldsheet measure; Bershadsky et al. (1994), physical PDF pp. 18–20, 65–66, 73. Graph integrability, the infinitesimal quotient and the small transverse domain are [MATH], with the displayed local commutator and standard smooth complex-integrability input, source (5.1)–(5.2).
§XVIII.6.2. The all-mode Fourier homotopy and averaging obstruction are [MATH]. The calculation assumes compact Kähler Hodge and $\partial\bar{\partial}$ results. The torus has the real periods and complex orientation of XVIII.5. The literal comparison of BCOV PDF p. 67, $\Delta = 2\{\bar{\partial}, \bar{\partial}^\dagger\}$, with the inverse identity on PDF p. 73 exhibits a discrepancy if both equations use the same Δ. No source erratum is inferred.
§XVIII.6.3. The explicit negative Tian identity is [MATH]; the primitive-independent relative functional and unrestricted primitive variation at fixed x are [MATH]. The formal recursion is [MATH], conditional

on the imported Hodge/$\partial\bar{\partial}$ inputs; general analytic convergence is cited, not proved here. The nonharmonic second-order example is [MATH]. Bershadsky et al. (1994), (5.6)–(5.15), PDF pp. 66–75, supplies the constrained construction and Ω-preserving parameter restriction. Our J identity has the opposite explicit sign to the source's plus-sign priming shorthand. Full prime/product/trace/inverse scalar-action translation remains unidentified. The supplementary $\bar{\partial}^\dagger$ propagator gauge is not imposed on arbitrary primitive variations.

§XVIII.6.4. The small actual complex-torus family is [MATH]; its relative cubic and exact-field stationarity are [MATH], by the displayed contraction and Jacobian calculations. Bershadsky et al. (1994), PDF pp. 71, 76, discusses the related torus and cubic puzzle. No absolute Yukawa, physical coupling or four-dimensional superpotential follows.

§XVIII.6.5. Long-tube survival is [WS-T]; the source-specific canonical-coordinate tree comparison and regulated one-loop torsion comparison are [WS-T], Bershadsky et al. (1994), (5.21), (5.27), PDF pp. 64–65, 72–78, 83–85. Worldsheet measure, sewing, zero-mode metrics and contact terms are physical inputs. The finite complex and its weighted determinant are [MATH], not the CY spectrum or the full BV complex.

§XVIII.6.6. The nodal anomaly is [WS-T], Bershadsky et al. (1994), (3.6)–(3.10), PDF pp. 47–48; genus one is separate. The ordered source evaluations and local holomorphic kernel are [MATH]. The Hodge connection follows the convention of Volume V, Chapter 5. The differing signs at PDF pp. 35 and 48 leave general operator equivalence open. Finite source evaluations do not determine full amplitudes or global existence.

Full regulated quantum KS/BV equivalence, nonperturbative completion, an original proof of the general deformation theorem, absolute physical normalization and DV transfer remain outside this chapter.

References

Bershadsky, M. et al. (1994). "Kodaira-Spencer Theory of Gravity and Exact Results for Quantum String Amplitudes". In: *Commun. Math. Phys.* 165, pp. 311–428. DOI: 10.1007/BF02099774. arXiv: hep-th/9309140.

Chapter XVIII.7

Dijkgraaf–Vafa: matrix models and glueball superpotentials

A massive adjoint field can be integrated out of an $\mathcal{N} = 1$ gauge theory. The resulting holomorphic couplings remember its interactions even at energies where the adjoint no longer propagates. Which part of this low-energy information can a worldsheet construction calculate? The Dijkgraaf–Vafa construction answers this question through a matrix integral. Wrapped branes supply the gauge theory, the selected open B-model sector supplies the integral, and a proposed geometric transition turns its spectral periods into a flux superpotential. A separate four-dimensional calculation explains why planar matrix graphs encode the perturbative glueball coupling dependence.

The chapter develops this dictionary rather than assuming it from the resemblance of two curves. The recurring example is a massive adjoint with a quartic interaction. We will compute its first two interaction corrections both from a continuous eigenvalue density and from discrete Wick contractions. The Gaussian limit then tests the holomorphic mass threshold. These examples also expose the extra gauge-dynamics information needed to complete the answer.

Reader contract

Use the $\mathcal{N} = 1$ superfield language of Volume I, the periods and fixed-filling matrix integrals of Volume V, and the relative open and closed B-model actions of XVIII.5–6. The local derivations below recall their needed normalizations. Our target is a flat-space Wilsonian holomorphic F-term with abelian gaugino backgrounds set to zero. The Kähler potential, a mass-gap calculation and gravitational F-terms are separate questions.

XVIII.7.1 From wrapped curves to a protected coupling

Begin with N D5-branes filling spacetime and wrapping isolated resolved curves in a local type-IIB Calabi–Yau threefold. The local brane-engineering dictionary associates

their transverse position with an adjoint chiral field Φ of a $U(N)$ gauge theory. A polynomial deformation supplies its superpotential:

$$W_{\text{tree}} = \operatorname{Tr} V(\Phi), \qquad V(x) = \sum_k \frac{g_k}{k+1} x^{k+1}. \tag{XVIII.7.1}$$

The trace is the ordinary fundamental trace. Near a semisimple critical-point vacuum, eigenvalues sit at simple roots a_i of V'. The rank partition and adjoint masses are

$$V'(a_i) = 0, \qquad V''(a_i) \neq 0, \qquad N = \sum_i N_i, \qquad U(N) \longrightarrow \prod_i U(N_i). \tag{XVIII.7.2}$$

Branes on different curves give the different factors. Strings connecting different groups of branes account for massive off-diagonal fields. We use the sourced spectrum and potential as local physical input; the equation of a threefold by itself does not determine a brane spectrum.

At energies below these masses, retain the nonabelian glueball variables

$$S_i = -\frac{1}{32\pi^2} \operatorname{Tr}_i W_\alpha W^\alpha, \qquad w_{\alpha,i} = 0. \tag{XVIII.7.3}$$

Here $w_{\alpha,i}$ is the abelian trace component of the gaugino field; setting it to zero removes single-gaugino trace insertions. The spinor order in the definition of S_i fixes a sign used throughout. Dynamical pure-$SU(N_i)$ examples require $N_i \geq 2$. A local decoupling limit is assumed to remove string, Kaluza–Klein and gravity sectors while retaining the stated masses and couplings. Noncompactness alone does not establish this factorization. The polynomial interactions are holomorphic effective couplings at a fixed ultraviolet cutoff.

The selected B-brane theory has an auxiliary matrix description. Denote its size by $\widehat{N}$, keeping it distinct from the physical gauge rank. At fixed occupations the matrix variables are

$$Z = \int dM\, e^{-\operatorname{Tr} V(M)/\hbar_{\text{m}}}, \qquad t_i = \hbar_{\text{m}} \widehat{N}_i, \qquad t = \sum_i t_i. \tag{XVIII.7.4}$$

The quotient measure and holomorphic contour, or formal occupied Gaussian saddle, are part of the prescription. The planar limit sends $\hbar_{\text{m}}$ to zero with t_i fixed. It does not send the physical N_i to infinity. In the four-dimensional normalization,

$$[x] = [M] = [\Phi] = 1, \quad [V] = [\hbar_{\text{m}}] = [t_i] = [S_i] = 3, \qquad [m] = 1, \quad [g] = -1 \tag{XVIII.7.5}$$

for $V = mx^2/2 + gx^4/4$. Thus $\hbar_{\text{m}}$ is not literally the dimensionless physical string coupling.

The geometric proposal replaces the wrapped curves by deformed three-spheres carrying RR flux ranks N_i. In the calibrated protected dictionary the compact periods are identified with S_i. The matrix free energy is defined with a minus sign relative to the logarithmic convention of V.9:

$$F_0 = \big[-\hbar_{\text{m}}^2 \log Z \big]_{\text{planar}} = -F_0^{\log}, \qquad W_{\text{pert}} = \sum_i N_i \partial_{t_i} F_{0,\text{pert}} \Big|_{t_i = S_i}. \tag{XVIII.7.6}$$

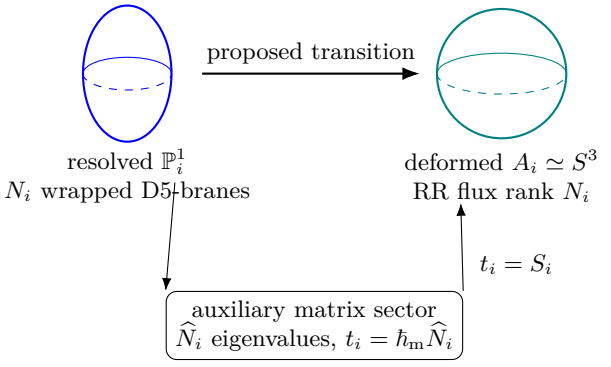


Figure XVIII.7.1: The local resolved curve and the deformed compact three-cycle. The arrows separate the chosen topological matrix reduction from the proposed physical transition. Physical flux ranks N_i and auxiliary occupations $\widehat{N}_i$ remain different data; only the protected periods are matched.

Sections XVIII.7.4 and XVIII.7.5 explain the separate field-theory premises and flux calibration in this formula. It determines perturbative coupling dependence. A coupling-independent function of S_i still requires pure-gauge or precisely fixed measure information.

For orientation, the one-cut quartic example will give

$$F_{0,\mathrm{int}} = \frac{gt^3}{2m^2} - \frac{9g^2t^4}{8m^4} + O(g^3), \qquad W_{\mathrm{int}} = \frac{3NgS^2}{2m^2} - \frac{9Ng^2S^3}{2m^4} + O(g^3). \quad \text{(XVIII.7.7)}$$

Here interactions mean the ratio Z/Z_{G}. For a displayed finite-rank example take $N \geq 4$, keeping these powers below the pure-$SU(N)$ degree-N relation. The general coupling series is formal before finite-rank quantum relations are imposed. XVIII.5 supplied the relative open action; the new physical embedding and gauge dictionary are what let it address this F-term.

XVIII.7.2 Why the open theory becomes a matrix

The geometric question is how a polynomial potential isolates curves. Cover the resolved $\mathbb{P}^1$ by coordinates z, z' and use a constant normal coordinate x. The deformed transition is

$$x' = x, \qquad z' = z^{-1}, \qquad z'\phi_1' = z\phi_1 + V'(x). \quad \text{(XVIII.7.8)}$$

This is also a way to see why critical points of V matter. Introduce functions on the contracted space by

$$\omega = z'\phi_1', \qquad u = 2\phi_1', \qquad v = 2\phi_1, \qquad y_g = i(2\omega - V'). \quad \text{(XVIII.7.9)}$$

The transition gives $\phi_1' = z\omega$ and $\phi_1 = (\omega - V')/z$. Consequently

$$uv = 4\omega(\omega - V'), \qquad y_g^2 = -(2\omega - V')^2, \qquad uv + y_g^2 + V'(x)^2 = 0. \quad \text{(XVIII.7.10)}$$

This calculation checks the chart-to-hypersurface map without invoking a gauge-theory claim. When V' has isolated simple zeros, it supplies the local geometry used in the brane construction.

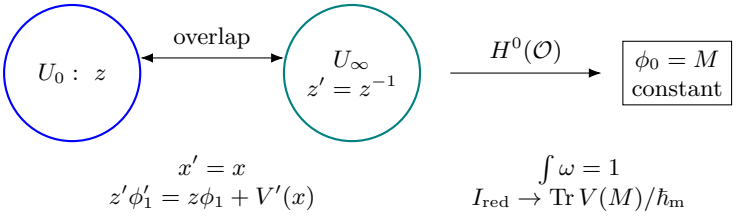


Figure XVIII.7.2: The two charts of $\mathbb{P}^1$ and the surviving normal scalar. The transition contains the potential deformation. In the stated trivial bundle sector a holomorphic scalar is constant; linear-field localization and its supplied measure turn that zero mode into the matrix variable.

In the topological sector the normal scalar is an adjoint field ϕ_0, and its partner ϕ_1 is a $(1,0)$ form on the curve. With a $(0,1)$ connection A, write $\bar\partial_A = \bar\partial + [A, \cdot\,]$ for the covariant Dolbeault operator on adjoint-valued forms. The sourced reduced action is

$$I_{\rm red} = \frac{1}{\hbar_{\rm m}} \int_{\mathbb{P}^1} \operatorname{Tr}\big(\phi_1 \wedge \bar\partial_A \phi_0 + V(\phi_0)\omega_{\mathbb{P}^1}\big), \qquad \int_{\mathbb{P}^1} \omega_{\mathbb{P}^1} = 1. \tag{XVIII.7.11}$$

Work with smooth fields, no punctures and a trivial holomorphic Chan–Paton bundle. Integrating the field appearing linearly imposes

$$\bar\partial_A \phi_0 = 0, \qquad H^0(\mathbb{P}^1, \mathcal{O}) = \mathbb{C} \quad \Longrightarrow \quad \phi_0 = M. \tag{XVIII.7.12}$$

In a holomorphic trivialization the scalar is therefore a constant matrix. Substitution into (XVIII.7.11) leaves $\operatorname{Tr} V(M)/\hbar_{\rm m}$. The step from this formal constraint to the matrix integral uses the supplied B-brane BRST, gauge-fixing and measure prescription. It is not a determinant-cancellation proof for all bundles or boundary conditions.

The exterior sign deserves a derivation, since the one-form precedes the Dolbeault derivative in the action. For a scalar variation on the compact curve, Stokes gives

$$0 = \int \bar\partial \operatorname{Tr}(\phi_1 \delta\phi_0) = \int \operatorname{Tr}\big((\bar\partial\phi_1)\delta\phi_0 - \phi_1 \wedge \bar\partial\delta\phi_0\big). \tag{XVIII.7.13}$$

Hence the scalar Euler equation, in the exterior convention used here, is

$$\bar\partial_A \phi_1 + V'(\phi_0)\omega_{\mathbb{P}^1} = 0. \tag{XVIII.7.14}$$

For $\phi_1 = f\,dz$ and $\omega = w\,dz \wedge d\bar z$ this becomes

$$\bar\partial\phi_1 = -(\partial_{\bar z} f)\, dz \wedge d\bar z, \qquad \partial_{\bar z} f = V'(\phi_0) w. \tag{XVIII.7.15}$$

A coefficient derivative with dz written first thus has the opposite displayed derivative sign from the exterior equation. Mixing the two notations would change the classical constraint.

Integrating (XVIII.7.14) with $\phi_0 = M$ gives $V'(M) = 0$. Why can this matrix be diagonalized? Its minimal polynomial divides V'. If V' is square-free, the minimal polynomial has distinct roots, so M is semisimple. The variation of A also imposes $[\phi_0, \phi_1] = 0$; after holomorphic trivialization $H^0(\mathbb{P}^1, K) = 0$, with $K = T^{*(1,0)}\mathbb{P}^1$ the canonical bundle, removes a surviving holomorphic one-form. Commutation alone would not establish diagonalizability. For example,

$$V'(x) = x^2, \qquad M = \begin{pmatrix} 0 & 1 \\ 0 & 0 \end{pmatrix}, \qquad M^2 = 0, \quad M \neq 0 \tag{XVIII.7.16}$$

is a repeated-root counterexample. The simple-root condition is doing physical work: it selects isolated massive adjoint vacua. The finite algebra and global sections explain the reduction of fields; the functional measure remains the topological input inherited at the stated scope from the open B-model construction.

XVIII.7.3 Cuts, Ward identities and glueballs

The matrix integral packages infinitely many moments into a resolvent. Before taking a planar limit, distinguish its random value and its mean:

$$\widehat{R}(z) = \hbar_{\mathrm{m}} \operatorname{Tr} G(z), \qquad G(z) = (z - M)^{-1}, \qquad R_{\mathrm{m}}(z) = \langle \widehat{R}(z) \rangle. \tag{XVIII.7.17}$$

Assume integration by parts has no boundary term on the specified contour or formal saddle. Under $\delta M = G$, the matrix derivative gives

$$\frac{\partial G_{ij}}{\partial M_{kl}} = G_{ik} G_{lj}, \qquad \sum_{ij} \frac{\partial G_{ij}}{\partial M_{ij}} = (\operatorname{Tr} G)^2. \tag{XVIII.7.18}$$

The Jacobian balances the potential variation. Multiplying the resulting identity by $\hbar_{\mathrm{m}}^2$ yields

$$\hbar_{\mathrm{m}}^2 \langle (\operatorname{Tr} G)^2 \rangle = \hbar_{\mathrm{m}} \langle \operatorname{Tr} V'(M) G \rangle. \tag{XVIII.7.19}$$

Subtract $V'(z)$ inside the right-hand side to obtain a polynomial:

$$\langle \widehat{R}(z)^2 \rangle - V'(z) R_{\mathrm{m}}(z) + P(z) = 0, \qquad P(z) = \hbar_{\mathrm{m}} \left\langle \operatorname{Tr} \frac{V'(z) - V'(M)}{z - M} \right\rangle. \tag{XVIII.7.20}$$

The degree of P is at most $\deg V' - 1$. In particular, this is an expectation of a square. It is not generally the square of an expectation.

For a scalar Gaussian, $\widehat{N} = 1$, moments already diagnose the distinction:

$$R_{\mathrm{m}}(z) = \frac{\hbar_{\mathrm{m}}}{z} + \frac{\hbar_{\mathrm{m}}^2}{m z^3} + \frac{3\hbar_{\mathrm{m}}^3}{m^2 z^5} + \cdots, \qquad R_{\mathrm{m}}^2 - m z R_{\mathrm{m}} + m\hbar_{\mathrm{m}} = -\frac{\hbar_{\mathrm{m}}^3}{m z^4} + \cdots. \tag{XVIII.7.21}$$

The false factorization fails at finite size. At fixed fillings the formal topological expansion instead has connected covariance $O(\hbar_{\mathrm{m}}^2)$, so its leading mean R_0 obeys

$$R_0^2 - V' R_0 + P = 0, \qquad R_0(z) \sim \frac{t}{z}. \tag{XVIII.7.22}$$

Here and below P in a planar formula means its leading value. There is also a distinct equation for one stationary eigenvalue configuration. Writing $r(z) = \hbar_{\mathrm{m}} \sum_a (z - \lambda_a)^{-1}$ and using $V'(\lambda_a) = 2\hbar_{\mathrm{m}} \sum_{b \neq a} (\lambda_a - \lambda_b)^{-1}$ gives

$$r^2 + \hbar_{\mathrm{m}} r' - V' r + P_{\mathrm{stat}} = 0. \tag{XVIII.7.23}$$

The derivative subtracts the diagonal pole sum of that stationary configuration. It does not replace the covariance in (XVIII.7.20).

Define the force variable and choose its sheet by its asymptotics:

$$Y = V' - 2R_0, \qquad Y^2 = V'^2 - 4P, \qquad Y \sim V' - \frac{2t}{z}. \tag{XVIII.7.24}$$

The square of Y alone leaves a sign ambiguity. The sheet and filling fix that sign. For a real cut, the Sokhotski jump of the resolvent gives the unit-normalized eigenvalue density. Here the bank values mean $R_\pm(x) = \lim_{\epsilon \downarrow 0} R_0(x \pm i\epsilon)$, and likewise for $Y_\pm$. With a full counterclockwise contour A_i around a cut on the physical sheet,

$$\rho(x) = \frac{R_-(x) - R_+(x)}{2\pi i t} = \frac{Y_+(x) - Y_-(x)}{4\pi i t}, \qquad t_i = \frac{1}{2\pi i} \oint_{A_i} R_0 \, dz = -\frac{1}{4\pi i} \oint_{A_i} Y \, dz. \tag{XVIII.7.25}$$

The minus sign follows because the upper edge of a counterclockwise contour runs from right to left. For the Gaussian cut $[-a, a]$, the upper value is $Y_+ = im\sqrt{a^2 - x^2}$. The jump gives the positive semicircle density and the full contour returns $t = ma^2/4$.

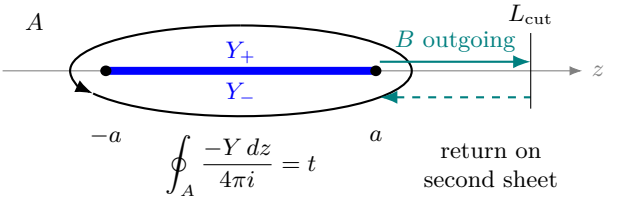


Figure XVIII.7.3: A full counterclockwise A contour around a one-cut curve and a doubled relative B path. The upper A edge runs right to left. The dashed return of B lies on the other sheet where Y changes sign, so its integral is twice the outgoing force integral, with the chosen orientation. For the quartic branch $a^2 = s$ and $Y_+ = i(gx^2 + b)\sqrt{s - x^2}$; as $g \to 0$, $s \to 4t/m$ and the curve becomes Gaussian.

The geometric coordinate of (XVIII.7.10) is $y_g = iY$. Consequently the deformed hypersurface and the matrix curve are related by

$$uv + y_g^2 + V'^2 - 4P = 0, \qquad f_{\mathrm{DV,matrix}} = 4P, \quad f_{\mathrm{DV,geometry}} = f_{\mathrm{CDSW}} = -4P. \tag{XVIII.7.26}$$

These are changes of variables in one curve. They acquire a gauge-theory meaning through separate physical input. Define the chiral resolvent

$$R_{4d}(z) = -\frac{1}{32\pi^2} \left\langle \mathrm{Tr} \, \frac{W_\alpha W^\alpha}{z - \Phi} \right\rangle. \tag{XVIII.7.27}$$

The generalized Konishi anomaly and chiral-ring relations, with their supplied normalization, give a quadratic equation of the form (XVIII.7.22). In a selected supersymmetric vacuum, chiral position independence and cluster decomposition factorize the gauge-theory correlators. This is a different reason for factorization from auxiliary matrix large $\widehat{N}$. Matching the equation, asymptotics and fillings identifies $R_{4d} = R_0$ at $t_i = S_i$. The matrix mathematics of V.9 is thereby applied to a protected gauge observable, with the anomaly and vacuum assumptions explicitly supplied.

XVIII.7.4 Why four dimensions select planar graphs

The spectral equation suggests a dictionary. The superspace calculation explains its planar derivative. Integrate out the massive adjoint in a fixed chiral gaugino background. For a connected orientable vacuum ribbon graph, let E, V, h count edges, vertices and color faces, let L count momentum loops, and let q be the genus. Then

$$L = E - V + 1, \qquad V - E + h = 2 - 2q, \qquad h = L + 1 - 2q. \tag{XVIII.7.28}$$

The superspace loop integrations require $2L$ insertions of W_α. In the pure glueball chiral sector, at most two can lie on each color face; single insertions vanish with the abelian backgrounds set to zero. Thus

$$2h \geq 2L \quad \Longrightarrow \quad 1 - 2q \geq 0 \quad \Longrightarrow \quad q = 0. \tag{XVIII.7.29}$$

A planar graph has $h = L + 1$. Exactly one face is left empty and the other L carry pairs. Choosing its position and tracing its identity matrix produces

$$h\, N\, S^{h-1} = N \frac{\partial}{\partial S} S^h. \tag{XVIII.7.30}$$

For several occupied cuts the empty face may have any color label i, giving $\sum_i N_i \partial_{S_i}$. This counting uses the supplied chiral relations; unrestricted products of gauginos would not justify the face bound.

Topology alone does not show that the momentum integrals leave a matrix amplitude. Their cancellation is the other essential step of the superspace derivation. Assign positive Schwinger parameters s_e and write edge momenta as $p_e = \sum_a L_{ea} p_a$. The quadratic form is

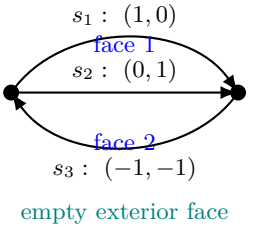
$$Q_{ab} = \sum_e s_e L_{ea} L_{eb}. \tag{XVIII.7.31}$$

The bosonic Gaussian in four dimensions contributes

$$B = (4\pi)^{-2L} (\det Q)^{-2}. \tag{XVIII.7.32}$$

The fermionic momentum integrals and allowed commutator insertions contribute, in the sourced spinor and glueball normalization,

$$F = N h S^{h-1} (4\pi)^{2L} (\det Q)^2, \qquad BF = N h S^{h-1}. \tag{XVIII.7.33}$$



$$L = 2,\ h = 3$$
$$B \propto D_s^{-2}$$
$$F \propto 3NS^2D_s^2$$
$$D_s = s_1s_2 + s_1s_3 + s_2s_3$$

Figure XVIII.7.4: A planar sunset ribbon embedding, shown by its center lines. The two bounded faces may carry gaugino pairs while the exterior face is empty; the factor three counts all choices of empty face. Edge labels give the rows of the loop matrix used in the determinant calculation.

Thus the Schwinger dependence cancels before the remaining ordinary massive propagators are integrated. The relative signs of the two ribbon edges in the adjoint commutator are needed for this result.

The sunset graph makes the determinant visible. For rows $(1,0),(0,1),(-1,-1)$ of the loop matrix,

$$Q = \begin{pmatrix} s_1+s_3 & s_3 \\ s_3 & s_2+s_3 \end{pmatrix}, \qquad D_s := \det Q = s_1s_2 + s_1s_3 + s_2s_3. \tag{XVIII.7.34}$$

One can isolate the Grassmann algebra from the physical functional-integral input. For a single spinor component expand $\exp(-\sum_{ab} W_a Q_{ab}\pi_b)$. Its coefficient of $W_1W_2\pi_1\pi_2$ is $-\det Q$. Taking the ordered product of the two spinor components gives

$$[W_{1+}W_{2+}\pi_{1+}\pi_{2+}W_{1-}W_{2-}\pi_{1-}\pi_{2-}]\exp\left(-\sum_{\sigma,a,b} W_{a\sigma}Q_{ab}\pi_{b\sigma}\right) = D_s^2. \tag{XVIII.7.35}$$

The bracket here extracts a coefficient. The two minus signs cancel. This explains the determinant power in (XVIII.7.33); the overall spinor/color normalization remains that of the superspace derivation. Changing only the first loop matrix in the fermionic exponent tests the mechanism. If its third row is $(-1,0)$ while the momentum matrix is unchanged, the fermionic determinant becomes $s_2(s_1+s_3)$. At $(s_1,s_2,s_3) = (1,2,4)$,

$$\frac{\det(Q_{\text{ferm}})^2}{\det(Q_{\text{bos}})^2} = \frac{100}{196} = \frac{25}{49}. \tag{XVIII.7.36}$$

The cancellation is then lost. A common change of loop basis would preserve both determinants and would not test this relative structure.

There is also a dimensional test. Continuing only the bosonic integral to D dimensions leaves the determinant residue

$$(\det Q)^{2-D/2}, \tag{XVIII.7.37}$$

with the corresponding $(4\pi)^{2L-DL/2}$ factor. It becomes parameter independent at $D = 4$. Setting momenta to zero in another dimension would miss this cancellation.

Under the stated superspace premises, each planar matrix graph therefore receives precisely the empty-face replacement in (XVIII.7.30). With $F_0 = -[\hbar_{\mathrm{m}}^2 \log Z]_{\mathrm{planar}}$ in the CDSW normalization, this yields (XVIII.7.6). It explains perturbative holomorphic couplings rather than a full equivalence of the gauge theory and a zero-dimensional integral.

XVIII.7.5 Gaussian periods, thresholds and gauge input

The simplest period calculation asks whether the construction reproduces the threshold of a massive adjoint. Take $m, t > 0$ and choose the physical sheet

$$Y = m\sqrt{z^2 - a^2}, \qquad a^2 = \frac{4t}{m}, \qquad \sqrt{z^2 - a^2} \sim z. \tag{XVIII.7.38}$$

Its A period has already fixed the filling. A noncompact period needs a cutoff $L_{\mathrm{cut}} > a$. The one-sheet force integral is elementary, but retaining its endpoint is essential:

$$I(t, L_{\mathrm{cut}}) = \int_a^{L_{\mathrm{cut}}} Y\, dz = \frac{m}{2}\left[L_{\mathrm{cut}}\sqrt{L_{\mathrm{cut}}^2 - a^2} - a^2 \log \frac{L_{\mathrm{cut}} + \sqrt{L_{\mathrm{cut}}^2 - a^2}}{a}\right]. \tag{XVIII.7.39}$$

At fixed m, L_{cut}, differentiating under the integral has no endpoint term because $Y(a) = 0$. It gives

$$\partial_t I = -2\int_a^{L_{\mathrm{cut}}} \frac{dz}{\sqrt{z^2 - a^2}} = -2\,\mathrm{arcosh}(L_{\mathrm{cut}}/a). \tag{XVIII.7.40}$$

For large cutoff the square root and logarithm give

$$I = \frac{mL_{\mathrm{cut}}^2}{2} - t - t\log\frac{mL_{\mathrm{cut}}^2}{t} + \frac{t^2}{mL_{\mathrm{cut}}^2} + \frac{t^3}{m^2 L_{\mathrm{cut}}^4} + O(L_{\mathrm{cut}}^{-6}). \tag{XVIII.7.41}$$

The first correction is already a reason to distinguish a finite geometric period from a continuum Gaussian matrix expression.

Normalize the reduced CY one-form by its full A contour:

$$\lambda_A = -\frac{Y\, dz}{4\pi i}, \qquad \oint_A \lambda_A = t, \qquad \Pi_B = -\frac{I}{2\pi i}. \tag{XVIII.7.42}$$

Here B is the doubled relative path: it goes from the branch point to the cutoff on one sheet and returns on the other, with orientation chosen as in Figure XVIII.7.3. A single outgoing interval would give half this result. Define the scaled, subtracted dual period

$$\widehat{B} = -I + \frac{mL_{\mathrm{cut}}^2}{2} = t\left[1 - \log\frac{t}{mL_{\mathrm{cut}}^2}\right] - \frac{t^2}{mL_{\mathrm{cut}}^2} - \frac{t^3}{m^2 L_{\mathrm{cut}}^4} + O(L_{\mathrm{cut}}^{-6}). \tag{XVIII.7.43}$$

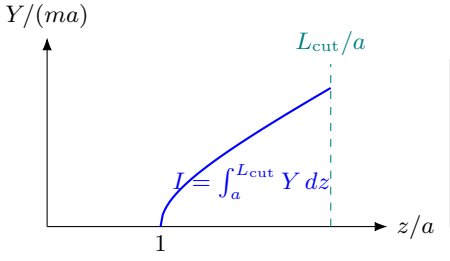
An antiderivative in t, up to a t-independent constant, is

$$F_{0,\mathrm{G}}^{\mathrm{finite}} = -\frac{t^2}{2}\log\frac{t}{mL_{\mathrm{cut}}^2} + \frac{3t^2}{4} - \frac{t^3}{3mL_{\mathrm{cut}}^2} - \frac{t^4}{4m^2 L_{\mathrm{cut}}^4} + O(L_{\mathrm{cut}}^{-6}). \tag{XVIII.7.44}$$

The notation $F_{0,\mathrm{G}}$ without the superscript will refer only to the leading large-cutoff Gaussian expression in the chosen cutoff scheme, namely the first two terms of this equation. It still contains a logarithmic cutoff dependence at fixed t, m; the running bare coupling will cancel that dependence in the superpotential below. For example, the continuum Gaussian determinant gives

$$\partial_m F_{0,\mathrm{G}} = \frac{t^2}{2m}. \tag{XVIII.7.45}$$

The inverse-cutoff terms in (XVIII.7.44) have further mass dependence and cannot be included in that exact continuum identity.



$$\widehat{B} \;=\; -I \,+\, mL_{\mathrm{cut}}^2/2$$
finite cutoff: $-t^2/(mL_{\mathrm{cut}}^2) + \cdots$
$L_{\mathrm{cut}} \;\to\; \infty$, strong scale fixed
$$W_{\mathrm{G}} \;=\; NS[1 - \log(S/\Lambda_{\mathrm{lo}}^3)]$$

Figure XVIII.7.5: The positive-sheet Gaussian force outside the cut and its cutoff integral. The right panel separates subtraction of the quadratic divergence from the renormalized limit. Flux/scale and pure-gauge input are needed to interpret the limiting expression as a glueball superpotential.

The physical transition proposal now supplies RR A-flux N and fixed noncompact flux or bare coupling. In our threshold-calibrated one-cut frame,

$$W_{\mathrm{flux}} = N\widehat{B} + 2\pi i \tau_{\mathrm{UV}} t. \tag{XVIII.7.46}$$

This convention defines τ by its source term and instanton factor. It does not calculate an absolute ten-dimensional DBI normalization. For the Gaussian mass deformation the higher-energy theory is $\mathcal{N} = 2$ and the low-energy nonabelian theory is pure $\mathcal{N} = 1$. Their holomorphic scale matching is

$$\Lambda_{\mathrm{hi}}^{2N} = L_{\mathrm{cut}}^{2N} e^{2\pi i \tau_{\mathrm{UV}}}, \qquad \Lambda_{\mathrm{lo}}^{3N} = m^N \Lambda_{\mathrm{hi}}^{2N}. \tag{XVIII.7.47}$$

The exponents $2N$ and $3N$ are the respective holomorphic beta-function coefficients. Identifying $t = S$ gives at finite cutoff

$$W_{\mathrm{G}}^{\mathrm{finite}} = NS\left[1 - \log\frac{S}{\Lambda_{\mathrm{lo}}^3}\right] - \frac{NS^2}{mL_{\mathrm{cut}}^2} + O(L_{\mathrm{cut}}^{-4}). \tag{XVIII.7.48}$$

Run τ_{UV} as $L_{\mathrm{cut}} \to \infty$ to keep the strong scale fixed. Only this renormalized limit gives the VY form in our spinor/free-energy frame:

$$W_{\mathrm{G}} = NS\left[1 - \log\frac{S}{\Lambda_{\mathrm{lo}}^3}\right]. \tag{XVIII.7.49}$$

The flux-to-rank interpretation and pure-gauge or measure/scale completion are physical inputs. The integral of a square root has checked their threshold dependence, not established the transition or confinement.

There is a direct way to see the remaining freedom. Potential-coupling derivatives determine F_0 only up to a function $H(t_i)$ independent of those couplings. In one cut,

$$F_0 \longmapsto F_0 + H(S), \qquad H(S) = cS^2 \quad \Longrightarrow \quad W \longmapsto W + 2NcS. \tag{XVIII.7.50}$$

All mass and interaction-coupling derivatives at fixed S are unchanged. Thus the anomaly/coupling equations alone cannot choose the complete superpotential. Once the Gaussian measure/volume has already supplied (XVIII.7.49), adding a second independent VY term would count the same completion twice.

Taking this pure-gauge completion as input, the exponentiated stationarity condition is

$$S^N = \Lambda_{\rm lo}^{3N}, \qquad S_k = \Lambda_{\rm lo}^3 e^{2\pi i k/N}, \quad k = 0, \dots, N-1. \tag{XVIII.7.51}$$

A single chosen logarithm sees one local solution. The full set requires the theta and logarithm lifts. For $N = 2$ these are the two opposite points $\pm\Lambda_{\rm lo}^3$. Their algebraic enumeration is not a mass-gap or confinement derivation. This is precisely where the period construction needs more physical information than the relative closed action of XVIII.6.

XVIII.7.6 A quartic interaction by two routes

We can test the perturbative dictionary without fixing H. Use the Gaussian ratio and take

$$V(x) = \frac{m}{2}x^2 + \frac{g}{4}x^4, \qquad m, t > 0, \quad g \geq 0. \tag{XVIII.7.52}$$

These inequalities define a convergent positive real one-cut branch. For other holomorphic couplings the following series is formal around the nondegenerate Gaussian saddle. Symmetry places the cut at $[-\sqrt{s}, \sqrt{s}]$. Write

$$Y = (gz^2 + b)\sqrt{z^2 - s}, \qquad \sqrt{z^2 - s} = z - \frac{s}{2z} - \frac{s^2}{8z^3} - \cdots. \tag{XVIII.7.53}$$

Matching $Y \sim V' - 2t/z$ fixes first the z coefficient and then the $1/z$ coefficient:

$$b = m + \frac{gs}{2}, \qquad \frac{ms}{2} + \frac{3gs^2}{8} = 2t, \qquad s = \frac{8t}{m + \sqrt{m^2 + 12gt}}. \tag{XVIII.7.54}$$

The rationalized root has a smooth Gaussian limit $s \to 4t/m$. The other root of the quadratic does not describe that branch. The jump formula gives

$$\rho(x) = \frac{gx^2 + b}{2\pi t}\sqrt{s - x^2}, \qquad |x| \leq \sqrt{s}, \qquad \int \rho\, dx = 1. \tag{XVIII.7.55}$$

Both the polynomial factor and square root are nonnegative in this domain.

To compute the coupling derivative, define the unnormalized moments $M_k = t\int \rho(x)x^k dx$. Rescale $x = \sqrt{s}\,u$; the needed integrals are

$$J_n = \int_{-\sqrt{s}}^{\sqrt{s}} x^{2n}\sqrt{s-x^2}\,dx = s^{n+1}B\left(n+\tfrac{1}{2},\tfrac{3}{2}\right), \tag{XVIII.7.56}$$

$$J_0 = \frac{\pi s}{2}, \quad J_1 = \frac{\pi s^2}{8}, \quad J_2 = \frac{\pi s^3}{16}, \quad J_3 = \frac{5\pi s^4}{128}. \tag{XVIII.7.57}$$

Normalization gives $M_0 = ms/4 + 3gs^2/16 = t$, reproducing the endpoint condition. The next moments are

$$M_2 = \frac{ms^2}{16} + \frac{gs^3}{16}, \qquad M_4 = \frac{ms^3}{32} + \frac{9gs^4}{256}. \tag{XVIII.7.58}$$

At $g = 0$ these give $M_2 = t^2/m$ and $M_4 = 2t^3/m^2$, as required by the Gaussian density. At small g the endpoint and fourth moment become

$$s = \frac{4t}{m} - \frac{12gt^2}{m^3} + \frac{72g^2t^3}{m^5} + \cdots, \qquad M_4 = \frac{2t^3}{m^2} - \frac{9gt^4}{m^4} + O(g^2). \tag{XVIII.7.59}$$

Differentiate the matrix integral at fixed filling with the ordinary trace:

$$\partial_g F_{0,\mathrm{int}} = \frac{1}{4}\lim_{\text{planar}} \hbar_{\mathrm{m}}\langle \mathrm{Tr}\, M^4\rangle = \frac{M_4}{4}. \tag{XVIII.7.60}$$

Integrating from $g = 0$ gives the first formula in (XVIII.7.7). The factor $\hbar_{\mathrm{m}}$ follows directly by differentiating $-\hbar_{\mathrm{m}}^2 \log Z$; omitting it would change both the large-size order and the normalization.

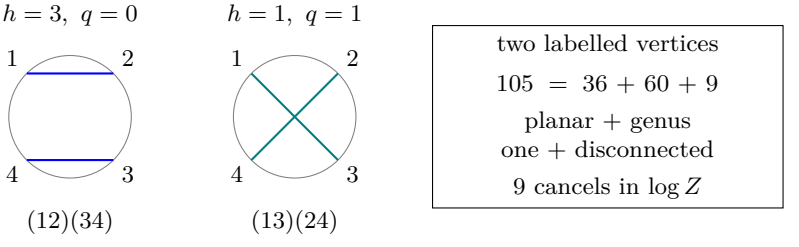


Figure XVIII.7.6: Pairing chords on a cyclic quartic vertex. The cyclic order determines the ribbon faces: adjacent pairings are planar, while the crossed pairing has genus one. The second planar one-vertex pairing is obtained by rotation. The right panel records the independent two-vertex classification.

An independent route uses Gaussian index contractions. For one labelled cyclic quartic vertex there are three pairings, two planar and one of genus one.

Two labelled vertices give $7!! = 105$ pairings. A pairing is an involution α of the half-edges; let σ be their cyclic order at each vertex. Faces are cycles of $\sigma\alpha$. Connectivity and Euler characteristic classify all of them:

For one vertex the pairings (12)(34) and (14)(23) have three faces; (13)(24) has one. For two vertices the nine disconnected pairings are the 3×3 independent one-vertex pairings. The remaining 96 are connected; counting cycles gives 36 with four faces and 60 with two. This is a finite enumeration of these two orders, not an all-order proof.

Vertices	Connected planar	Connected genus one	Disconnected
One	2	1	0
Two	36	60	9

Table XVIII.7.1: Wick pairings classified by connectivity and ribbon genus. The vertices are labelled and each has a fixed cyclic half-edge order.

Each propagator is

$$\langle M_{ab} M_{cd} \rangle_{\mathrm{G}} = \frac{\hbar_{\mathrm{m}}}{m} \delta_{ad} \delta_{bc}. \tag{XVIII.7.61}$$

The expansion factors are $-g/(4\hbar_{\mathrm{m}})$ at one vertex and $g^2/(2 \cdot 16\hbar_{\mathrm{m}}^2)$ at two. The two connected planar contributions to the logarithm are therefore

$$\log \frac{Z}{Z_{\mathrm{G}}}\bigg|_{\mathrm{planar}} = -\frac{g}{4\hbar_{\mathrm{m}}}\, 2 \left(\frac{\hbar_{\mathrm{m}}}{m}\right)^2 \widehat{N}^3 + \frac{g^2}{32\hbar_{\mathrm{m}}^2}\, 36 \left(\frac{\hbar_{\mathrm{m}}}{m}\right)^4 \widehat{N}^4 + O(g^3). \tag{XVIII.7.62}$$

Multiplication by $-\hbar_{\mathrm{m}}^2$ and substitution $t = \hbar_{\mathrm{m}} \widehat{N}$ gives

$$F_{0,\mathrm{int}} = \frac{g t^3}{2m^2} - \frac{9 g^2 t^4}{8 m^4} + O(g^3). \tag{XVIII.7.63}$$

The nine disconnected contractions cancel against one half the square of the one-vertex term in $\log Z$. The sixty connected genus-one terms remain in the full logarithm, but carry the different topological order. The insertion count of Section XVIII.7.4 excludes them from the flat pure-glueball superpotential considered here.

Finally use $N\partial_t$ while keeping physical N independent:

$$W_{\mathrm{int}}(S) = \frac{3NgS^2}{2m^2} - \frac{9Ng^2S^3}{2m^4} + O(g^3), \qquad \epsilon = \frac{gS}{m^2}. \tag{XVIII.7.64}$$

The expansion parameter is dimensionless, $[F_0] = 6$ and $[W] = 3$. The spectral and Wick routes agree at g and g^2 through different calculations. Turning this finite check into the general protected formula uses the four-dimensional premises already stated, rather than the agreement alone. This worked example applies the matrix techniques of V.9 to the gauge-theory observable selected by the B-model construction.

XVIII.7.7 What the dictionary determines

The physical chain starts from a local brane theory with an adjoint potential. Its chosen topological sector reduces to a matrix integral. The proposed brane-to-flux transition relates compact and relative periods to a protected superpotential, while the

superspace and chiral-anomaly routes explain its perturbative coupling dependence in four dimensions. These statements have different premises. Figure XVIII.7.7 separates the calculable steps from the physical identifications.

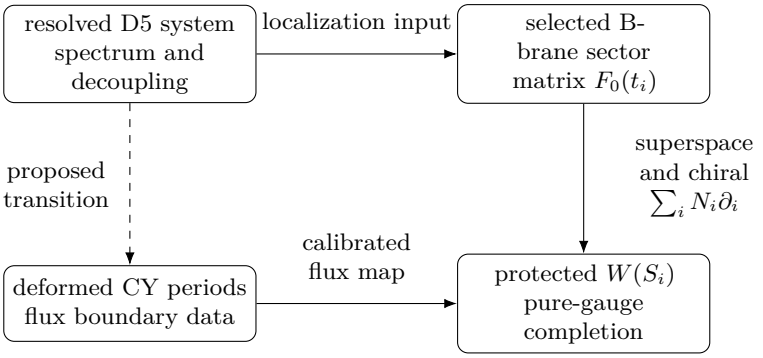


Figure XVIII.7.7: The physical dictionary and its premises. Solid arrows state scoped sourced reductions or protected maps; the dashed arrow marks the proposed geometric transition. Period algebra and matrix combinatorics test the construction, while $H(S_i)$ still requires the completion indicated at the lower right.

For the quartic example the usable low-energy expression, after a chosen Gaussian and pure-gauge completion, is

$$W(S) = NS\left[1 - \log\frac{S}{\Lambda_{\mathrm{lo}}^3}\right] + \frac{3NgS^2}{2m^2} - \frac{9Ng^2S^3}{2m^4} + O(g^3). \tag{XVIII.7.65}$$

The VY term uses the renormalized limit and separate gauge input; the displayed interaction terms use a fixed-cutoff holomorphic EFT and the protected perturbative formula. For a finite-rank illustration use $N \geq 4$. The expression is a Wilsonian F-term, not a prediction of an elementary glueball kinetic term or physical mass spectrum. The freedom $H(S)$ explains why knowing every potential-coupling derivative would still leave a completion choice.

XVIII.5 constructed a relative classical open action. XVIII.6 described the relative closed B-model deformation theory. Neither result fixes an absolute ten-dimensional normalization or identifies its relative coupling with $\hbar_{\mathrm{m}}$. The threshold-calibrated form (XVIII.7.42), flux boundary data and gauge-theory normalization supply additional information here. Equating the two polynomial curves merely translates variables within that dictionary; it is not another independent physical test. Superspace and chiral anomaly arguments provide distinct explanations but share supersymmetry and chiral premises, so their agreement does not automatically create two independent construction routes.

There is a different question in XVIII.8: a double-scaling limit near a matrix critical point can retain nonplanar contributions and describe minimal-string physics. The fixed-filling expansion used here selects the planar data of a protected four-dimensional coupling. It neither classifies general holomorphic contours nor proves an all-genus

BCOV equality. The two matrix applications share techniques while retaining different physical targets.

The practical calculation can now be repeated for another massive polynomial saddle: specify occupations and a sheet, solve the asymptotic moment problem, integrate coupling derivatives at fixed fillings, and apply the physical empty-face derivative. A complete answer must also state its noncompact flux/coupling data and pure-gauge prescription. The Gaussian threshold and the two-order quartic agreement are concrete tests of this procedure at its stated scope.

Repeating the quartic calculation at fixed filling

The quartic example is a useful calculation to repeat because the density, free energy and proposed glueball coupling each use a different operation. Start on the positive real branch specified in the text. The cut endpoint is not an independent coupling. It is determined by the large-z normalization of the resolvent at fixed filling. Expanding the square root in the ansatz first fixes its polynomial coefficient, then its inverse-z coefficient fixes the endpoint equation. Choosing the Gaussian-connected root is necessary before taking any small-coupling expansion.

The endpoint moves when the quartic coupling changes. Consequently the fourth moment changes through both the polynomial factor of the density and the integration interval. Using the beta integrals automatically accounts for the moving interval through the powers of the endpoint. Substituting its series into (XVIII.7.58) gives the fourth-moment series displayed in the text. Holding the Gaussian endpoint fixed during this substitution would retain only part of the linear correction to that moment and would give the wrong second-order free energy.

The next operation is a coupling derivative at fixed filling. The ordinary trace in the exponent contributes one factor of the inverse matrix coupling when differentiated. The definition of F_0 supplies two factors of that coupling with the opposite logarithmic sign. The surviving single factor is the one in (XVIII.7.60). The limiting moment is therefore divided by four, which originates in the normalization of the quartic term in the potential. Integrating in the quartic coupling gives another order-dependent denominator. These two divisions have different origins and should both remain visible.

The Gaussian ratio chooses the interaction integration constant. It does not by itself determine every filling-dependent term in the complete free energy. Equation (XVIII.7.50) displays this freedom without changing a single potential-coupling derivative. The Gaussian period and pure-gauge completion deal with that remaining information under their own stated physical and normalization assumptions. This is why the interaction calculation can be checked independently of the full superpotential, while a second added VY term would duplicate an already included completion.

Only after the planar function is determined do we apply the protected identification and take the filling derivative that enters the proposed four-dimensional coupling. The physical gauge rank multiplying this derivative is not the auxiliary matrix size used to organize the planar limit. The two Wick orders give an independent calculation of the interaction coefficients. Their agreement with the moment calculation tests the finite perturbative result; the geometric transition and chiral physical interpretation retain

the separate premises stated in the chapter.

This distinction prepares XVIII.8. Its matrix size also organizes surfaces, but the boundary observable there is not a glueball. Reusing the expansion method is useful. Reusing the physical identification without a new boundary dictionary would change the problem.

Exercises

Use the ordinary trace, $F_0 = -[\hbar_{\mathrm{m}}^2 \log Z]_{\mathrm{planar}}$ and the physical-sheet conventions of the chapter. Interaction free energies use Z/Z_{G}. Written derivations and explanations are part of each answer.

1. Derive (XVIII.7.10) from the chart transition (XVIII.7.8). Explain why a square-free V' makes a constant matrix solution of $V'(M) = 0$ semisimple, and give a repeated-root counterexample. Vary (XVIII.7.11) using exterior Dolbeault differentiation, showing the Stokes sign and its translation to $\phi_1 = f\,dz$. State the separate localization and measure input.

2. Derive the finite expectation Ward identity for $\widehat{R} = \hbar_{\mathrm{m}} \operatorname{Tr}(z - M)^{-1}$ by the boundary-free matrix variation $\delta M = (z - M)^{-1}$. Define its mean separately. Derive the polynomial P and state the assumption needed for the planar equation. For a scalar Gaussian compute the first nonzero falsely factorized residual. Contrast this with the stationary-eigenvalue equation. Derive the jump-density and full counterclockwise A-period factors. Why does gauge chiral factorization not require physical $N \to \infty$?

3. For the sunset matrix with rows

$$(1, 0), \quad (0, 1), \quad (-1, -1),$$

compute $Q = L^T \operatorname{diag}(s_1, s_2, s_3) L$ and its determinant. Independently obtain the two-spinor Grassmann top coefficient of

$$\exp\left[-\sum_{\sigma ab} W_{a\sigma} Q_{ab} \pi_{b\sigma}\right]$$

in the order

$$(W_{1+}, W_{2+}, \pi_{1+}, \pi_{2+}, W_{1-}, W_{2-}, \pi_{1-}, \pi_{2-}).$$

Combine it with the bosonic determinant in general D, stating the supplied normalization needed for the (4π) factors. Change only the first loop matrix in the fermionic exponent to have third row $(-1, 0)$ and evaluate the residual ratio at $(s_1, s_2, s_3) = (1, 2, 4)$. Derive the genus restriction and empty-face derivative from the ribbon Euler and insertion counts.

4. Evaluate the Gaussian force integral at finite $L_{\mathrm{cut}} > a$ and its t derivative. Expand through L_{cut}^{-4}, integrate $\widehat{B}$ in t, and distinguish its finite primitive from

continuum $F_{0,\mathrm{G}}$. Use the doubled relative B path, $W_{\mathrm{flux}} = N\widehat{B} + 2\pi i \tau_{\mathrm{UV}} t$ and (XVIII.7.47) to derive the renormalized mass threshold. State the transition and pure-gauge/measure input required for VY, and explain its N logarithm branches for pure $SU(N)$, $N \geq 2$. What does this establish about confinement?

5. Starting from $Y = (gz^2 + b)\sqrt{z^2 - s}$ for $m, t > 0, g \geq 0$, derive the Gaussian-connected endpoint, the positive normalized density and M_4 using beta integrals. Integrate $\partial_g F_{0,\mathrm{int}} = M_4/4$ at fixed t through order g^2 and obtain W_{int} with physical N held fixed. Check dimensions and the small parameter; explain the $N \geq 4$ restriction for the displayed finite-rank example.

6. Independently enumerate the one- and two-vertex cyclic quartic Wick pairings with covariance $\hbar_{\mathrm{m}} \delta_{ad} \delta_{bc}/m$. An explicit classified count or a short independently written enumeration is acceptable. Separate connectivity and genus, insert the vertex expansion factors, and recover the first two planar coefficients of $-\hbar_{\mathrm{m}}^2 \log(Z/Z_{\mathrm{G}})$. Show the disconnected cancellation and explain why genus one does not enter the stated flat glueball term. State the finite order covered by this calculation.

7. Add $H(S) = cS^2$, with c independent of the mass and potential couplings. Identify unchanged coupling/anomaly tests and the shift in W. Explain the need for a pure-gauge/measure prescription and the error in adding VY twice. Why do identifying $\widehat{N} = N$, omitting noncompact flux and cutoff data, or using the relative KS cubic of XVIII.6 to fix an absolute DV coupling fail to complete the dictionary? Distinguish the physical spectrum/decoupling, topological localization, chiral/superspace input and proposed transition.

Sources and scope

§XVIII.7.1. The wrapped-D5 spectrum, adjoint potential and critical-point ranks are [GEO-E], under the local resolved embedding of Dijkgraaf and Vafa 2002, §2.1, pp. 4–6 and Cachazo, Intriligator, et al. 2001, §3. The removal and factorization of gravity, string and Kaluza–Klein sectors at fixed gauge data is a [DEC] premise. The brane-to-flux transition is [CONJ+], with the Gaussian threshold and protected perturbative checks specified below; it is not a full-QFT duality.

§XVIII.7.2. The trivial-bundle reduced B-brane action and its formal localization are [WS-T], with BRST, gauge-fixing, measure and occupied-saddle assumptions; Dijkgraaf and Vafa 2002, §2.2, (2.8)–(2.9), §2.4. The chart identity, exterior Euler sign and square-free semisimplicity argument are [MATH] under the displayed hypotheses. Repeated roots admit the nilpotent counterexample. The printed plus-sign display can be represented in K-first coefficient notation. The source does not specify its exterior convention; we do not attribute an unstated convention to it. The exterior Euler sign used here is derived explicitly, and no source erratum for that sign is asserted.

§XVIII.7.3. The finite random-resolvent Ward identity, formal planar equation, sheet, jump and full-A normalization are [MATH]; Cachazo, Douglas, et al. 2002, §4.2, (4.24)–(4.31) and the explicit derivations. The chiral-resolvent identification is [BPS:1/8|holo],

conditional on the anomaly coefficient, chiral-ring relations and selected-vacuum factorization; Cachazo, Douglas, et al. 2002, §3, (3.14)–(3.15), §4.1–4.2. The supersymmetry fraction counts four of type-IIB's 32 supercharges, not a particle BPS fraction. No finite-rank quantum-ring completion follows.

§XVIII.7.4. Euler/insertion counting and the encoded bosonic/fermionic determinant calculation are [MATH], conditional on the sourced superspace integrand and pure-glueball chiral restrictions. The perturbative $\sum_i N_i \partial_i F_0$ coupling formula is [BPS:1/8|holo]; Dijkgraaf, Grisaru, et al. 2003, §3–4, (4.5)–(4.10) and Cachazo, Douglas, et al. 2002, §4.1–4.2. The Grassmann calculation tests that integrand rather than deriving its functional measure. The source with $W^\alpha W_\alpha$ uses the opposite index order from our definition of S; its bare VY sign sentence is not combined with the CDSW frame.

§XVIII.7.5. The exact finite-cutoff periods, their inverse-cutoff expansion and the $H(S)$ counterexample are [MATH]. The limiting VY expression and branch algebra are conditional [MATH] consequences of the separate flux, scale and pure-gauge/measure inputs; comparison Cachazo, Intriligator, et al. 2001, §2, pp. 6–7 and Cachazo, Douglas, et al. 2002, (1.5)–(1.10), (4.22), (4.34). The full-contour reduced form and doubled relative path used here are threshold-calibrated; they are not literal raw-Ω or one-interval source normalizations. No confinement or absolute ten-dimensional coupling has been derived.

§XVIII.7.6–XVIII.7.7. The positive one-cut solution, beta moments and independently enumerated Wick coefficients at g, g^2 are [MATH]. The displayed W_{int} is a conditional [MATH] consequence of the protected derivative formula, with $N \geq 4$ in the finite-rank example and formal coupling expansion otherwise. This check covers two interaction orders, not all genera or general contours. The comparison with IV.9 reuses its matrix mathematics; XVIII.5–6 retain their relative-action scope. No full-QFT, Kähler, mass-gap, finite-rank-ring or all-genus BCOV completion is asserted.

Conventions and source qualifications. The conventions use ordinary traces, $F_0 = -\hbar_{\text{m}}^2 \log Z$, physical N_i versus auxiliary $\widehat{N}_i$, the stated spinor order and exterior Dolbeault signs, a full counterclockwise A contour and a doubled relative B path. Three printed formulas differ from these conventions. Dijkgraaf and Vafa 2002, (3.9), p. 14, text below (3.10), p. 15 prints density and filling-change factors inconsistent with the normalized definitions used here. In addition, Cachazo, Douglas, et al. 2002, (4.33), p. 41 omits $\hbar_{\text{m}}$ under a literal same ordinary-trace reading of its (4.23). We use the jump formula (XVIII.7.25), $\Delta t = \hbar_{\text{m}} \Delta \widehat{N}$ and the differentiated $-\hbar_{\text{m}}^2 \log Z$ formula. These are explicit local corrections, not claimed published errata. Page numbers refer to the cited arXiv versions.

References

Cachazo, F., K. Intriligator, and C. Vafa (2001). "A Large N Duality via a Geometric Transition". In: *Nucl. Phys. B* 603, pp. 3–41. DOI: 10.1016/S0550-3213(01)00228-0. arXiv: hep-th/0103067.

Cachazo, F., M. R. Douglas, et al. (2002). "Chiral Rings and Anomalies in Supersymmetric Gauge Theory". In: *JHEP* 12, p. 071. DOI: 10.1088/1126-6708/2002/12/071. arXiv: hep-th/0211170.

Dijkgraaf, R., M. T. Grisaru, et al. (2003). "Perturbative Computation of Glueball Superpotentials". In: *Phys. Lett. B* 573, pp. 138–146. DOI: 10.1016/j.physletb.2003.08.060. arXiv: hep-th/0211017.

Dijkgraaf, R. and C. Vafa (2002). "Matrix Models, Topological Strings, and Supersymmetric Gauge Theories". In: *Nucl. Phys. B* 644, pp. 3–20. DOI: 10.1016/S0550-3213(02)00766-6. arXiv: hep-th/0206255.

Chapter XVIII.8

Minimal strings, Kontsevich and JT gravity

XVIII.8.1 What the boundary remembers

A matrix integral can organize a sum over surfaces. Its size counts topology, while its eigenvalues can encode a boundary observable. These two roles raise a physical question: how much of a gravitational theory is determined by its disk amplitude? A disk gives a spectral density, but a connected surface with two boundaries also tells us what kind of spectral quantity is being averaged. This chapter follows that question through minimal strings, intersection theory and Jackiw–Teitelboim (JT) gravity.

The matrix size in this chapter is an auxiliary parameter, denoted by $\widehat{N}$. In Chapter XVIII.7 an auxiliary matrix model organized particular gauge-theory F-terms. Here the quantities of interest are random-surface and thermal-boundary observables. We will derive a critical planar density, a coefficient of the Kontsevich free energy and three JT amplitudes. These calculations share useful mathematics without identifying their entire physical theories.

For a minimal-string boundary, the source is a boundary cosmological constant μ_B. For a Hermitian matrix it is the loop variable z. For a thermal boundary it is the inverse temperature β. Their elementary observables are

$$\partial_{\mu_B} Z_{\text{disk}}, \qquad W_Q(z) = \frac{1}{\widehat{N}} \left\langle \operatorname{Tr} \frac{1}{z - M} \right\rangle, \qquad Z_H(\beta) = \operatorname{Tr} e^{-\beta H}. \tag{XVIII.8.1}$$

The first varies a worldsheet boundary condition; the second probes the matrix spectrum; the third weights energy levels. A dictionary must specify both an observable and the operation relating it to the others. In particular, a continuum disk curve already involves rescalings and subtractions. It is not a literal finite-size resolvent.

The route has four steps. We first construct a minimal worldsheet and its boundary curve. We then tune a formal matrix model until its endpoint changes order. Intersection theory gives a precise all-orders statement in a different matrix integral. Finally, cutting JT surfaces turns geometric integration into connected spectral amplitudes. The disk,

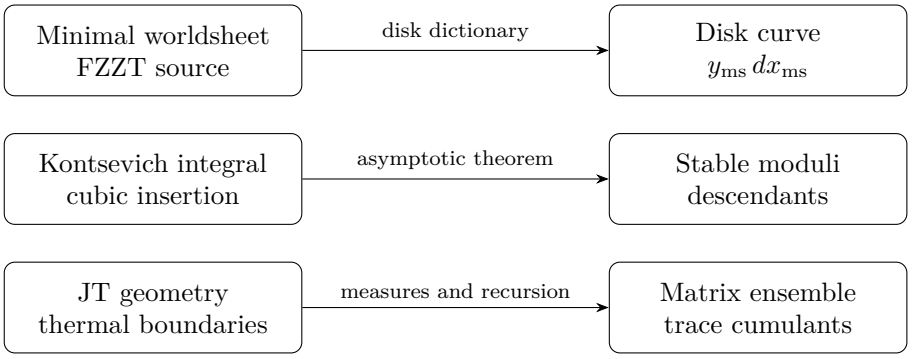


Figure XVIII.8.1: Three typed relations used in the chapter. Each arrow names the operation or supplied ingredients needed for that comparison. The separate rows do not assert a full minimal-string/Kontsevich/JT equivalence. The formal quartic example diagnoses critical matrix surfaces within this broader use of matrix expansions.

cylinder and handle will let us separate spectral edge control from control of the topology expansion.

XVIII.8.2 Building a minimal worldsheet

The fluctuating conformal factor of a two-dimensional metric becomes a Liouville field. Coupling it to a minimal matter model gives a concrete worldsheet system with matter, Liouville and reparametrization ghosts. For coprime integers $2 \le p < q$, define

$$b_L^2 = \frac{p}{q}, \qquad Q_L = b_L + b_L^{-1} = \frac{p+q}{\sqrt{pq}}, \qquad c_m = 1 - \frac{6(p-q)^2}{pq}. \tag{XVIII.8.2}$$

The Liouville background charge contributes $c_L = 1 + 6Q_L^2$, and the ghosts contribute $c_{bc} = -26$. Their sum cancels because

$$c_m + c_L + c_{bc} = -24 + \frac{6\big[(p+q)^2 - (p-q)^2\big]}{pq} = 0. \tag{XVIII.8.3}$$

This is the local central-charge consistency condition. It does not establish a no-ghost theorem or unitarity. The matter central charge is zero for $(2,3)$, $1/2$ for the Ising model $(3,4)$ and $-22/5$ for $(2,5)$. Thus the family includes nonunitary matter models even though the cancellation works throughout it.

A matter primary must also acquire a Liouville dressing so that it can be inserted on a fluctuating surface. The Kac labels satisfy $1 \le r \le p-1$, $1 \le s \le q-1$, with $(r,s) \sim (p-r, q-s)$. Write $d = |qr - ps|$. The matter weight and the source lower Liouville root are

$$h_{r,s} = \frac{d^2 - (p-q)^2}{4pq}, \qquad \alpha_{r,s} = \frac{p+q-d}{2\sqrt{pq}}. \tag{XVIII.8.4}$$

The Liouville exponential $e^{2\alpha\phi}$ has weight $\alpha(Q_L-\alpha)$. Substitution gives

$$\alpha_{r,s}(Q_L-\alpha_{r,s})=\frac{(p+q)^2-d^2}{4pq}, \tag{XVIII.8.5}$$

$$h_{r,s}+\alpha_{r,s}(Q_L-\alpha_{r,s})=\frac{(p+q)^2-(p-q)^2}{4pq}=1. \tag{XVIII.8.6}$$

The ghost c has weight -1, so the unintegrated dressed vertex $c\bar{c}\,\mathcal{O}_{r,s}e^{2\alpha_{r,s}\phi}$ has weights $(0,0)$. This verifies the dressing condition given the worldsheet field content and conformal weights. Reflection $\alpha\mapsto Q_L-\alpha$ preserves the weight, but the chosen source convention uses the lower root.

For the $(2,3)$ identity, $d=1$, $h=0$ and $\alpha=\sqrt{2/3}$. In the Ising example, the spin field $(r,s)=(1,2)$ has $d=2$, hence $h=1/16$ and $\alpha=5/(4\sqrt{3})$. The Liouville part supplies $15/16$, rather than one. For $(2,5)$ the same labels give $h=-1/5$ and a Liouville weight $6/5$. The calculation shows what dressing does: it compensates the particular matter scaling dimension, including a negative one.

A boundary supplies a more geometric probe. With positive real bulk cosmological constant μ, the FZZT boundary parameter σ determines rescaled variables

$$x_{\mathrm{ms}}=\frac{\mu_B}{\sqrt{\mu}}=\cosh(\pi b_L\sigma),\qquad y_{\mathrm{ms}}=\frac{\partial_{\mu_B}Z_{\mathrm{disk}}}{\sqrt{\widetilde{\mu}}}=\cosh(\pi\sigma/b_L),\qquad \widetilde{\mu}=\mu^{q/p}. \tag{XVIII.8.7}$$

The normalization and the positive real-σ branch are supplied by the worldsheet disk calculation. Setting $\mu=1$ for the example and introducing $u=\cosh(\pi\sigma/\sqrt{pq})$ gives a polynomial uniformization in terms of Chebyshev polynomials:

$$x_{\mathrm{ms}}=T_p(u),\qquad y_{\mathrm{ms}}=T_q(u),\qquad T_q(x_{\mathrm{ms}})-T_p(y_{\mathrm{ms}})=0. \tag{XVIII.8.8}$$

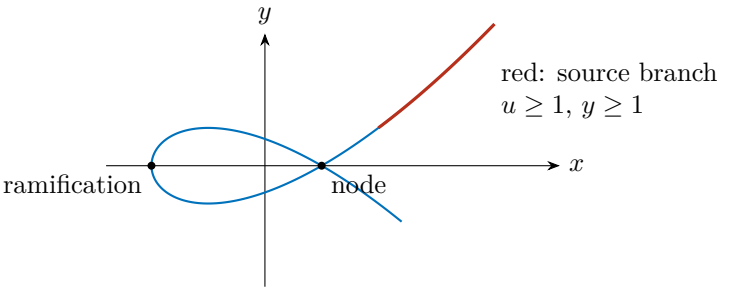
The last equation follows by composing T_p and T_q. The disk amplitude is recovered by integrating its derivative, with a basepoint-dependent additive constant. The derivative is the local observable that the curve records.

For $(p,q)=(2,3)$, suppress the subscript on x,y temporarily. Then

$$x=2u^2-1,\qquad y=4u^3-3u=u(2x-1),\qquad y^2=\frac{(x+1)(2x-1)^2}{2}. \tag{XVIII.8.9}$$

This squared relation has a node at $(x,y)=(1/2,0)$, with two preimages $u=\pm\sqrt{3}/2$. The map to x ramifies at $u=0$, where $(x,y)=(-1,0)$. These are different local phenomena. Near the node, the two tangent slopes are $dy/dx=\pm\sqrt{3}$; near $u=0$, $x+1=2u^2$ and $y=-3u+O(u^3)$. The node identifies two distinct points on the uniformizing line, whereas the ramification point is one point where the projection has zero derivative.

For real σ, $u\geq 1$; neither distinguished point is on that locus. Moreover $y\geq 1$ there. Replacing y by $-y$ preserves (XVIII.8.9), but changes the disk derivative in (XVIII.8.7). This is why the source branch must be chosen before a curve is compared with a matrix resolvent. The polynomial alone loses physical boundary data. Question 1 practices dressing; Question 2 practices precisely this distinction between a curve and its projection.



Blue: real slice of the analytic continuation.

Figure XVIII.8.2: The parameterized $(2, 3)$ curve. The node and the ramification point belong to the analytic continuation, outside the real-σ source locus. The red segment is part of the physical source branch and fixes the sign of y. The blue slice depicts its algebraic continuation, not another real-σ boundary condition.

XVIII.8.3 Why matrix size must scale with criticality

A matrix Feynman graph has two lines on each propagator. Closing an index loop produces a factor $\widehat{N}$. With an action $\widehat{N} \operatorname{Tr} V(M)$, a vertex contributes $\widehat{N}$ and a propagator contributes $\widehat{N}^{-1}$. A connected vacuum ribbon graph with V vertices, E edges and F faces therefore carries

$$\widehat{N}^{V-E+F} = \widehat{N}^{\chi} = \widehat{N}^{2-2g}. \tag{XVIII.8.10}$$

Thickening the graph produces an orientable surface. Thus matrix size controls the topology expansion, while the coupling weights the number of vertices. At a critical coupling, large graphs proliferate. A continuum scaling must balance this growth with the suppression of handles.

A useful explicit witness is the quartic potential

$$V(x) = \frac{x^2}{2} - \frac{g_Q x^4}{4}, \qquad Z_Q = \int dM\, e^{-\widehat{N} \operatorname{Tr} V(M)}, \qquad F_Q = \log Z_Q. \tag{XVIII.8.11}$$

For $g_Q > 0$, this real-Hermitian integral diverges: along an eigenvalue going to infinity the exponent grows as $+\widehat{N} g_Q x^4/4$. Here Z_Q denotes its formal ribbon expansion around the Gaussian point. A formal series and its planar one-cut solution can diagnose a critical scaling without supplying a positive finite-size measure or a nonperturbative completion.

In the planar limit, introduce a normalized density on $[-a, a]$ and write

$$W_Q(z) = \int_{-a}^{a} \frac{\rho(x)\, dx}{z - x}, \qquad \int_{-a}^{a} \rho(x)\, dx = 1, \qquad W_Q(z) \sim \frac{1}{z}. \tag{XVIII.8.12}$$

The saddle equation fixes the sum of the two boundary values of W_Q to $V'(x)$. For an even one-cut solution this suggests

$$W_Q(z) = \frac{1}{2}\left[z - g_Q z^3 - (-g_Q z^2 + c)\sqrt{z^2 - a^2}\right]. \tag{XVIII.8.13}$$

The square root is the exterior sheet, with $\sqrt{z^2 - a^2} = z\sqrt{1 - a^2/z^2}$ and $\sqrt{z^2 - a^2} \sim z$ at infinity. In particular it is negative on the negative real exterior axis. Taking the principal root of the composed expression $z^2 - a^2$ there would select the wrong sheet and violate (XVIII.8.12).

Expand at large exterior z:

$$\sqrt{z^2 - a^2} = z - \frac{a^2}{2z} - \frac{a^4}{8z^3} + O(z^{-5}). \tag{XVIII.8.14}$$

The coefficient of z must cancel and the coefficient of $1/z$ must be one. These two requirements give

$$c = 1 - \frac{g_Q a^2}{2}, \qquad \frac{a^2}{4} - \frac{3g_Q a^4}{16} = 1, \qquad a^2 = \frac{2(1 - \sqrt{1 - 12g_Q})}{3g_Q}. \tag{XVIII.8.15}$$

The last expression chooses the branch tending to $a^2 = 4$ at $g_Q = 0$. Across the cut, the jump of the root yields

$$\rho(x) = \frac{1 - g_Q a^2/2 - g_Q x^2}{2\pi}\sqrt{a^2 - x^2}, \qquad |x| \le a. \tag{XVIII.8.16}$$

For example, integrating with $\int_{-a}^{a}\sqrt{a^2 - x^2}\,dx = \pi a^2/2$ and $\int_{-a}^{a} x^2\sqrt{a^2 - x^2}\,dx = \pi a^4/8$ recovers the normalization condition in (XVIII.8.15). This ties the asymptotic resolvent condition to eigenvalue counting.

For $0 \le g_Q \le 1/12$, the density is nonnegative on the selected interval. At the critical point the prefactor vanishes at the endpoint:

$$g_c = \frac{1}{12}, \qquad a_c^2 = 8, \qquad \rho_c(x) = \frac{(8 - x^2)^{3/2}}{24\pi}. \tag{XVIII.8.17}$$

The edge now vanishes as a power $3/2$, instead of the Gaussian power $1/2$. The difference changes the scale at which individual eigenvalues become visible. If $s = a_c - x$, then

$$\widehat{N}\int_{a_c - \epsilon}^{a_c}\rho_c(x)\,dx \;\propto\; \widehat{N}\int_0^{\epsilon} s^{3/2}ds \;\propto\; \widehat{N}\epsilon^{5/2}. \tag{XVIII.8.18}$$

Resolving order-one eigenvalues consequently requires

$$\delta x \sim \widehat{N}^{-2/5}, \qquad a_c^2 - a^2 \sim \sqrt{g_c - g_Q}, \qquad g_c - g_Q \sim \widehat{N}^{-4/5}. \tag{XVIII.8.19}$$

Equivalently, the local balance keeps $\widehat{N}(g_c - g_Q)^{5/4}$ fixed. This is the critical-scaling diagnosis. It motivates double scaling, rather than deriving a complete all-genus continuum measure from endpoint counting alone.

The Gaussian edge gives a discriminating comparison. Its integrated edge population is proportional to $\widehat{N}\epsilon^{3/2}$ and its microscopic scale is $\widehat{N}^{-2/3}$. The exponent $2/5$ therefore diagnoses the tuned critical endpoint; it is not a universal consequence of matrix size. Question 3 asks the reader to reconstruct both exponents directly from eigenvalue counting.

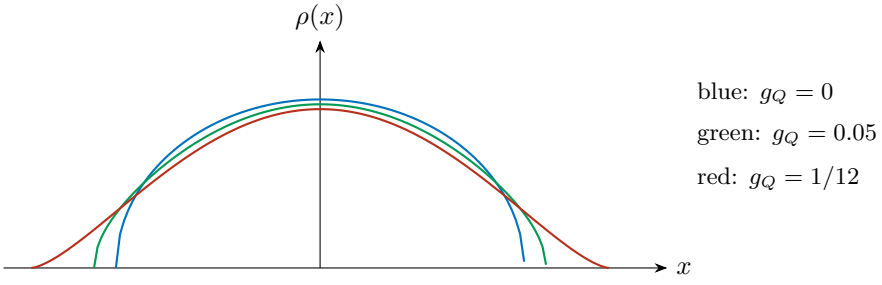


Figure XVIII.8.3: Normalized planar densities on their actual supports for the formal quartic solution. The critical red density has a wider support and a flatter vanishing endpoint. The plots describe the planar solution of the formal model; the real positive-g_Q quartic integral is divergent.

XVIII.8.4 What the Kontsevich integral proves

The relation between matrix graphs and surfaces can be made into a precise statement about moduli spaces. Let $\overline{\mathcal{M}}_{g,n}$ be the compactified moduli orbifold of stable marked curves, with $2g-2+n>0$. A marked point has a cotangent line bundle, whose first Chern class is ψ_i. Its powers define

$$\left\langle \prod_{i=1}^{n} \tau_{d_i} \right\rangle_g = \int_{\overline{\mathcal{M}}_{g,n}} \prod_{i=1}^{n} \psi_i^{d_i}, \qquad \sum_i d_i = 3g-3+n. \tag{XVIII.8.20}$$

The dimension constraint makes the integrand top degree. These are geometric intersection numbers, rather than arbitrary graph weights. The descendant free energy packages them into

$$F_{\mathrm{desc}}(t) = \sum_{\substack{g,n\geq 0 \\ 2g-2+n>0}} \frac{1}{n!} \sum_{d_1,\dots,d_n\geq 0} \left\langle \prod_i \tau_{d_i} \right\rangle_g \prod_i t_{d_i}. \tag{XVIII.8.21}$$

The $n!$ accounts for indistinguishable insertions in the generating function. The logarithm of a matrix partition function likewise organizes connected graphs. This is the natural place to compare the two constructions.

Take a positive Hermitian matrix Λ and a Hermitian integration variable X. The normalized Gaussian measure and the cubic insertion define

$$d\mu_\Lambda(X) = \frac{e^{-\operatorname{Tr}(\Lambda X^2)/2}\, dX}{\int e^{-\operatorname{Tr}(\Lambda X^2)/2}\, dX}, \qquad Z_K(\Lambda) = \left\langle e^{i \operatorname{Tr} X^3/6} \right\rangle_\Lambda, \qquad F_K = \log Z_K. \tag{XVIII.8.22}$$

The source-native Miwa times have a minus sign:

$$t_d = -(2d-1)!!\, \operatorname{Tr} \Lambda^{-2d-1}, \qquad (-1)!! = 1. \tag{XVIII.8.23}$$

Before stating the all-orders result, we can test a coefficient which sees two topologies. At matrix size one, $\Lambda = \lambda > 0$, and a Gaussian variable has $\langle X^2 \rangle = 1/\lambda$. Its sixth moment is the sum over fifteen pairings. The odd cubic term vanishes, so

$$\langle X^6 \rangle_G = 15\lambda^{-3}, \tag{XVIII.8.24}$$

$$Z_K(\lambda) = 1 + \frac{1}{2!}\left(\frac{i}{6}\right)^2 15\lambda^{-3} + O(\lambda^{-6}) = 1 - \frac{5}{24\lambda^3} + O(\lambda^{-6}), \tag{XVIII.8.25}$$

$$F_K(\lambda) = -\frac{5}{24\lambda^3} + O(\lambda^{-6}). \tag{XVIII.8.26}$$

Taking the logarithm does not change this first correction because the product of two corrections starts at λ^{-6}.

The intersection values $\langle \tau_0^3 \rangle_0 = 1$ and $\langle \tau_1 \rangle_1 = 1/24$ contribute

$$\frac{t_0^3}{6} + \frac{t_1}{24} = -\frac{1}{6\lambda^3} - \frac{1}{24\lambda^3} = -\frac{5}{24\lambda^3}. \tag{XVIII.8.27}$$

The first term comes from a sphere with three markings; the second comes from a torus with one marking. They collapse to the same power of λ in this one-variable specialization. Thus the test checks their sum and cannot separately determine every independent Miwa coefficient. Changing i to 1 in (XVIII.8.22) flips the Wick coefficient while keeping (XVIII.8.23) fixed, and fails this comparison.

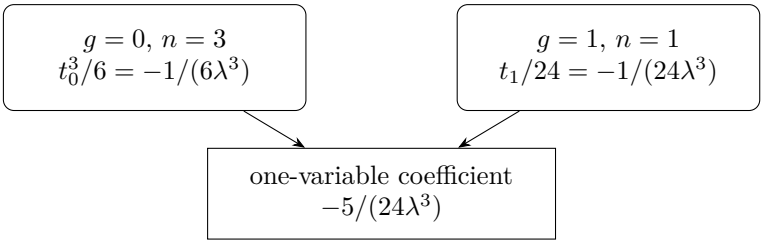


Figure XVIII.8.4: The coefficient decomposition in the matrix-size-one Kontsevich test. Two intersection contributions specialize to the same inverse-λ power. This is a decomposition by moduli-space topology, not a picture of one graph exhausting all graph symmetry factors.

Kontsevich's theorem identifies the formal asymptotic expansion of F_K with F_{desc} under (XVIII.8.23), for the stable compactified-moduli intersection numbers. The accompanying theorem gives the KdV structure of the descendant generating function. These are cited all-orders mathematical results. The calculation above fixes conventions and illustrates their content; it is not a new proof from one coefficient.

It is useful to separate convergence of an integral from convergence of an expansion. For positive Λ, $\mathrm{Tr}(\Lambda X^2)$ is a positive quadratic form on Hermitian matrices. Also $\mathrm{Tr}\, X^3$ is real, so

$$\left| e^{-\mathrm{Tr}(\Lambda X^2)/2} e^{i\,\mathrm{Tr}\, X^3/6} \right| = e^{-\mathrm{Tr}(\Lambda X^2)/2}. \tag{XVIII.8.28}$$

The finite-dimensional integral is absolutely integrable. Its cubic factor is oscillatory, so it is not a positive cubic probability weight. Expanding that factor generates increasingly high Gaussian moments; integrability does not make the resulting inverse-Λ series convergent. The theorem concerns its formal asymptotic expansion. This differs both from the divergent real quartic integral and from an undamped Airy Fourier integral. Question 4 asks which of these distinctions is visible in the first coefficient.

XVIII.8.5 From JT geometry to a density

JT gravity gives a particularly sharp use of boundary observables. Work with orientable Euclidean surfaces and AdS radius one. The action is

$$I = -S_0\chi - \frac{1}{2}\int_\Sigma \sqrt{g}\,\phi(R+2) - \int_{\partial\Sigma}\sqrt{h}\,\phi(K-1), \qquad \chi = 2-2g-n. \tag{XVIII.8.29}$$

The asymptotic boundary has proper length β/ϵ and dilaton $\phi = \gamma/\epsilon$, with $\gamma = 1/2$ in our energy units. The dilaton contour is chosen along an imaginary direction to impose $R = -2$. Reduction to the boundary Schwarzian theory and its functional measure are physical inputs. They supply the disk density

$$\rho_0(E) = \frac{\sinh(2\pi\sqrt{E})}{4\pi^2}, \qquad E \geq 0. \tag{XVIII.8.30}$$

Neither ρ_0 nor the amplitudes $Z_{g,n}$ below include their topological factor $e^{(2-2g-n)S_0}$. The density is an input from the path integral; its Laplace transform can now be derived independently.

To evaluate a disk thermal boundary, set $E = u^2$ and introduce a Gaussian parameter integral for real a and $\beta > 0$:

$$G(a) = \int_0^\infty e^{-\beta u^2}\cosh(au)\,du = \frac{\sqrt{\pi}}{2\sqrt{\beta}}\exp\left(\frac{a^2}{4\beta}\right). \tag{XVIII.8.31}$$

The formula follows by completing the square on the full line and using the evenness of the integrand. Differentiating with respect to a gives

$$G'(a) = \int_0^\infty u e^{-\beta u^2}\sinh(au)\,du = \frac{a\sqrt{\pi}}{4\beta^{3/2}}e^{a^2/(4\beta)}. \tag{XVIII.8.32}$$

Gaussian domination justifies this derivative on every finite interval in a. The Jacobian $dE = 2u\,du$ therefore yields

$$Z_{0,1}(\beta) = \int_0^\infty \rho_0(E)e^{-\beta E}\,dE = \frac{1}{2\pi^2}G'(2\pi) \tag{XVIII.8.33}$$

$$= \frac{e^{\pi^2/\beta}}{4\sqrt{\pi}\,\beta^{3/2}}. \tag{XVIII.8.34}$$

The physical disk contribution is $e^{S_0}Z_{0,1}$. The transform establishes the normalization relation between the supplied density and the disk partition function. It does not derive the Schwarzian measure that supplied the density.

Near the threshold, expanding the hyperbolic sine gives

$$\rho_0(E) = \frac{\sqrt{E}}{2\pi}\left[1 + \frac{2\pi^2}{3}E + O(E^2)\right]. \tag{XVIII.8.35}$$

Thus $\rho_{\text{edge}}(E) = \sqrt{E}/(2\pi)$ is the leading low-energy disk approximation. It is normalized here to match (XVIII.8.30); the often used Airy density $\sqrt{E}/\pi$ differs by a factor of two. Its transform is

$$Z_{\text{edge}}(\beta) = \frac{\Gamma(3/2)}{2\pi\beta^{3/2}} = \frac{1}{4\sqrt{\pi}\,\beta^{3/2}}, \qquad \frac{Z_{0,1}}{Z_{\text{edge}}} = e^{\pi^2/\beta} = 1 + \frac{\pi^2}{\beta} + O(\beta^{-2}). \tag{XVIII.8.36}$$

Large β suppresses high energies in the Laplace integral and makes the relative correction small. At $\beta = \pi^2$ the ratio is already e, so a local threshold expansion cannot give an all-temperature disk answer.

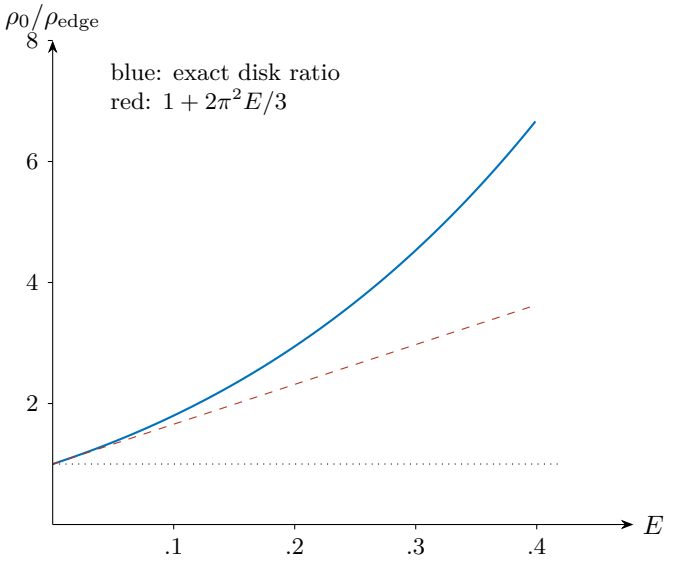


Figure XVIII.8.5: The dimensionless JT disk-density ratio, continuously extended to one at $E = 0$, and its first correction. The local approximation improves toward the threshold. In a thermal transform this is the large-β regime; the plot contains no assertion about higher topology.

A spectral curve is a useful way to organize the sourced JT recursion. In its own coordinates it is

$$x_{\text{JT}} = z_{\text{JT}}^2 = -E, \qquad y_{\text{JT}} = \frac{\sin(2\pi z_{\text{JT}})}{4\pi}. \tag{XVIII.8.37}$$

These coordinates and their analytic continuation are distinct from $x_{\text{ms}}, y_{\text{ms}}$. Their local leading edge is Airy-like, but a local edge does not determine the full sine curve or a unique exact spectral completion. To learn what the boundary observable means beyond a disk, we must keep track of connected surfaces.

XVIII.8.6 Cutting surfaces and knowing what is averaged

A hyperbolic surface can be cut along a geodesic. An asymptotic boundary of renormalized length β connected to a geodesic of length $b_{\rm geo}$ gives a trumpet. In the conventions above the supplied trumpet amplitude is

$$T(\beta, b_{\rm geo}) = \frac{e^{-b_{\rm geo}^2/(4\beta)}}{2\sqrt{\pi\beta}}. \tag{XVIII.8.38}$$

The variable $b_{\rm geo}$ is a geometric length and is unrelated to b_L. Gluing requires integration over length and twist. A twist has period $b_{\rm geo}$, so the length/twist measure reduces to $b_{\rm geo}\, db_{\rm geo}$. This factor changes the thermal dependence and cannot be replaced by $db_{\rm geo}$.

Gluing two trumpets gives a connected cylinder, called the double trumpet. With $A = (\beta_1 + \beta_2)/(4\beta_1\beta_2) > 0$, its amplitude is

$$Z_{0,2}(\beta_1, \beta_2) = \int_0^\infty b_{\rm geo}\, db_{\rm geo}\, T(\beta_1, b_{\rm geo}) T(\beta_2, b_{\rm geo}) \tag{XVIII.8.39}$$

$$= \frac{1}{4\pi\sqrt{\beta_1\beta_2}} \int_0^\infty b_{\rm geo} e^{-A b_{\rm geo}^2}\, db_{\rm geo} = \frac{\sqrt{\beta_1\beta_2}}{2\pi(\beta_1+\beta_2)}. \tag{XVIII.8.40}$$

The elementary integral is $1/(2A)$. At equal positive temperatures the answer is $1/(4\pi) > 0$. Its Euler characteristic is zero, so it has no factor of e^{S_0}. In particular the connected cylinder is a distinct topology, rather than the product of two disconnected disks.

For one asymptotic boundary and one handle, glue a trumpet to a compact one-holed torus. With Weil–Petersson normalization $\alpha_{\rm WP} = 1$, the supplied orbifold volume is

$$V_{1,1}(b_{\rm geo}) = \frac{b_{\rm geo}^2 + 4\pi^2}{48}. \tag{XVIII.8.41}$$

The denominator includes the $\mathbb{Z}_2$ automorphism factor of this moduli orbifold. It is already part of the volume, not a further divisor to apply at the end. The two moments needed for gluing follow from $t = b_{\rm geo}^2/(4\beta)$:

$$\int_0^\infty b_{\rm geo} e^{-b_{\rm geo}^2/(4\beta)} db_{\rm geo} = 2\beta, \qquad \int_0^\infty b_{\rm geo}^3 e^{-b_{\rm geo}^2/(4\beta)} db_{\rm geo} = 8\beta^2. \tag{XVIII.8.42}$$

Substitution gives a nontrivial topology correction,

$$Z_{1,1}(\beta) = \int_0^\infty b_{\rm geo}\, db_{\rm geo}\, T(\beta, b_{\rm geo}) V_{1,1}(b_{\rm geo}) \tag{XVIII.8.43}$$

$$= \frac{8\beta^2 + 8\pi^2\beta}{96\sqrt{\pi\beta}} = \frac{\sqrt{\beta}(\beta+\pi^2)}{12\sqrt{\pi}}. \tag{XVIII.8.44}$$

Omitting the automorphism divisor doubles this answer. Its Euler characteristic is -1, so the contribution is $e^{-S_0} Z_{1,1}$. The disk and handle thus enter the connected one-boundary expansion as

$$\mathcal{Z}_1(\beta) \sim e^{S_0} Z_{0,1}(\beta) + e^{-S_0} Z_{1,1}(\beta) + \cdots . \tag{XVIII.8.45}$$

The expansion is formal and asymptotic in topology. The sourced correspondence between Weil–Petersson recursion and matrix loop/topological recursion extends this matching to all genus under the stated geometric and path-integral premises. Deriving the two Gaussian integrals above does not establish that recursion correspondence by itself.

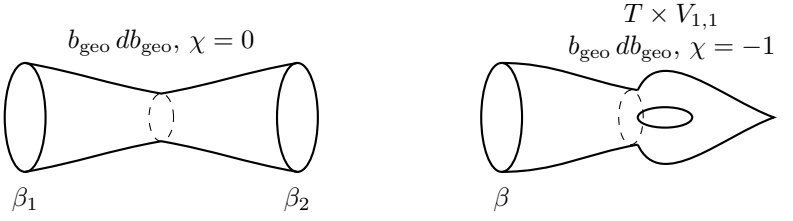


Figure XVIII.8.6: Schematic cuts of the double trumpet (left) and a trumpet glued to a one-holed torus (right). Dashed seams label the integrated geodesic length; its twist produces the measure $b_{\mathrm{geo}}\, db_{\mathrm{geo}}$. The corresponding weights are one and e^{-S_0}. Boundary labels β_i denote renormalized asymptotic lengths, not geodesic lengths.

The first handle also distinguishes two approximations that can pull in opposite directions. Using (XVIII.8.34) and (XVIII.8.44),

$$\frac{e^{-S_0} Z_{1,1}}{e^{S_0} Z_{0,1}} = e^{-2S_0} \frac{\beta^2(\beta + \pi^2)}{3} e^{-\pi^2/\beta}. \tag{XVIII.8.46}$$

At large β this grows as $e^{-2S_0}\beta^3/3$, even while the disk edge approximation improves. For large S_0 a parametric window satisfying both requirements, at the level of this first correction, is

$$\pi^2 \ll \beta \ll e^{2S_0/3}. \tag{XVIII.8.47}$$

One handle provides a first-correction diagnostic; it does not bound every higher-genus term. Question 5 asks the reader to compare the two controls, and Question 6 checks the geometric normalization of the handle.

What spectral observable does the connected cylinder compute? For one fixed deterministic Hamiltonian, the thermal traces are numbers. Their connected product without an averaging operation vanishes:

$$Z_H(\beta_1) Z_H(\beta_2) - Z_H(\beta_1) Z_H(\beta_2) = 0. \tag{XVIII.8.48}$$

An ensemble of Hamiltonians has an additional operation, denoted by brackets, and its covariance can instead be nonzero:

$$\langle Z_H(\beta_1) Z_H(\beta_2) \rangle_c = \langle Z_H(\beta_1) Z_H(\beta_2) \rangle - \langle Z_H(\beta_1) \rangle \langle Z_H(\beta_2) \rangle . \tag{XVIII.8.49}$$

In the JT/matrix interpretation, the formal sum of connected two-boundary geometries computes this connected ensemble observable; the double trumpet is its genus-zero contribution. The comparison at equal temperature diagnoses why it cannot be equated to the connected product of deterministic traces in a single fixed system. It does not rule out every individual-theory interpretation supplied with further data. Nor does a formal topology series choose a unique nonperturbative matrix completion. Question 7 asks the reader to state the averaging operation explicitly rather than infer it from the word "partition function."

XVIII.8.7 Exit dictionary

A boundary curve encodes a derivative of a disk amplitude, a matrix resolvent encodes a spectral density, and a thermal trace is its Laplace-weighted observable. Following each operation is more informative than identifying curves by appearance. In the minimal string, the disk source chooses a positive branch before one eliminates the uniformizing parameter. In the formal quartic model, the changed endpoint order determines a critical local scale. In the Kontsevich model, the intersection theorem fixes the all-orders asymptotic series in specified Miwa times. In JT gravity, geodesic gluing exposes connected ensemble amplitudes and their topology weights.

These are different levels of information. The elementary worldsheet charge and dressing identities do not prove unitarity. An edge exponent does not select a continuum completion. An intersection theorem is not a proof of the JT functional measure. The three computed JT topologies test the physical ensemble interpretation under that measure and the sourced recursion correspondence. The stronger targets, a fixed Hamiltonian, nonperturbative uniqueness and full minimal-string/JT equivalence, require additional input. The following chapters return to worldsheets with spacetime field-theory observables; Chapter XVIII.12 studies the reverse direction in which a gauge expansion generates string surfaces.

Which limit controls a thermal boundary?

The disk, cylinder and handle calculations answer different questions about the same boundary prescription. To compare them, first retain the Euler weight separately from the amplitude with that weight removed. A change in inverse temperature affects the latter. A change in S_0 affects the relative weight of topologies. Confusing these two changes would turn a large-temperature-scale approximation into an unsupported statement about which surfaces dominate.

The disk density demonstrates the first distinction directly. Near its edge the hyperbolic sine has a leading square-root term. Laplace transformation of that term gives the edge disk amplitude in the text. The exact disk contains the additional exponential dependence on inverse temperature. Its ratio to the edge result tends to one in the stated large-β limit, so this limit measures how well the edge controls the disk. It does not eliminate the handle contribution with its own β dependence. Comparing

the weighted handle and disk is a separate calculation, and it is the comparison needed before asserting disk dominance.

The cylinder diagnoses a second issue. Multiplying two thermal traces for one fixed Hamiltonian and subtracting that same product gives no connected fluctuation. The nonzero double-trumpet result instead belongs to the connected ensemble observable specified in the chapter. Its gluing integral includes the shared geodesic length and its twist measure. Removing that measure would change the computed observable. Thus even a correct one-boundary spectral density does not settle the interpretation of a connected two-boundary answer.

The minimal-string curve and the Kontsevich expansion should be read with the same care. A branch and a rescaling are needed before a disk curve is compared with a loop observable. An all-orders asymptotic intersection statement specifies formal coefficients but does not choose a unique nonperturbative integral. These are productive limits of the construction, because they identify exactly which further data would be needed for a stronger conclusion. The following self-dual and twistor chapters change the target observable to classical fields and scattering amplitudes.

XVIII.8.8 Written exercises

1. For the Ising spin primary $(p, q; r, s) = (3, 4; 1, 2)$, use (XVIII.8.4) to compute h and the lower α, and verify (XVIII.8.6). Test the replacement $\alpha = b_L$. Explain why central-charge cancellation does not prove general minimal-model unitarity.

2. Eliminate u from $x = 2u^2 - 1$, $y = 4u^3 - 3u$. Locate the node and its two preimages, and distinguish it from ramification of $u \mapsto x$. Which lie on $u = \cosh(\pi\sigma/\sqrt{6})$ for real σ? Explain the sign information lost on squaring y.

3. For $\rho_G = \sqrt{4 - x^2}/(2\pi)$ and $\rho_c = (8 - x^2)^{3/2}/(24\pi)$ on their respective supports, count eigenvalues within ϵ of a right endpoint and derive the scales resolving order-one eigenvalues. Explain the divergence of the real positive-g_Q quartic integral and the usefulness of its formal planar solution.

4. At matrix size one, derive the first nonzero term of $\log\langle e^{iX^3/6}\rangle_G$ for variance $1/\lambda$. Compare with $t_0^3/6 + t_1/24$ using the two supplied intersections and (XVIII.8.23). Test replacing i by 1. Distinguish absolute integrability, asymptotic expansion and identification of independent Miwa coefficients.

5. Derive (XVIII.8.34) from (XVIII.8.30) and the Gaussian integral. Compute the exact disk-to-edge ratio and its leading large-β correction. Then compare the weighted handle and disk terms. Does large β alone establish disk dominance at fixed S_0?

6. Integrate the trumpet against $V_{1,1}$ with measure $b_{\mathrm{geo}}\, db_{\mathrm{geo}}$. Display both Gaussian moments, explain the twist measure and the included $\mathbb{Z}_2$ divisor, and identify the Euler weight. What happens if the automorphism divisor is omitted?

7. Integrate two trumpets for positive β_1, β_2 and specialize to equal temperature. Compare with deterministic thermal traces of one fixed Hamiltonian. State precisely the connected ensemble observable represented by the topology expansion, and explain why this does not select a unique nonperturbative completion or full minimal-string/JT identification.

Sources and scope

§2: minimal worldsheet and boundary. The supplied bosonic matter/Liouville/ghost construction and BRST dressing are [WS]; cancellation is necessary local consistency, with general coprime $2 \le p < q$ and the lower root, not a no-ghost theorem. Conditional charge/weight algebra and the $(2,3), (3,4), (2,5)$ examples are [MATH]. Seiberg and Shih (2004), §2.1, printed pp. 7–9, Eqs. (2.1), (2.5), (2.6), (2.12), (2.13). The supplied conformal-background FZZT disk dictionary and positive real-σ branch are [WS], with positive real μ and the stated rescalings. It is not a finite-matrix literal resolvent identity. Same source, printed pp. 21–23, Eqs. (4.4), (4.8)–(4.10), (4.13). The $(2,3)$ polynomial, node and ramification calculation is [MATH], on the algebraic analytic continuation; these points are outside real σ.

§3: formal critical matrix surfaces. Ribbon counting, the conditional quartic one-cut solution on its Gaussian-connected branch, critical density and local scaling diagnosis are [MATH]. The density illustration has $0 \le g_Q \le 1/12$ and the resolvent uses the exterior sheet. The positive-g_Q real quartic integral diverges; no completion or all-genus construction follows from the local balance. The derivation is given here; matrix-surface context is in Seiberg and Shih (2004), §9, printed pp. 54–56.

§4: intersection theorem. Equality of the formal inverse-Λ asymptotic free energy with stable compactified-moduli descendants under negative Miwa times, and the KdV theorem, are cited [MATH], not proved here. Kontsevich (1992), printed pp. 2–3, Theorems 1.1–1.2, and §3.2, §4.1–4.2. The size-one Gaussian sixth-moment coefficient and its combined sphere/torus comparison are [MATH]; one Miwa specialization does not identify all independent times. The finite Gaussian-damped integral is absolutely integrable, whereas the expansion is asymptotic.

§5–6: JT boundary amplitudes. The positive-β Laplace transform of the supplied disk density is [MATH]; the Schwarzian measure is an input. Saad et al. (2019), printed pp. 4–5, Eqs. (4), (7), with $\gamma = 1/2$. Supplied trumpet and $b_{\mathrm{geo}}\, db_{\mathrm{geo}}$ gluing give the cylinder [MATH]; its observable is an ensemble connected amplitude. Same source, §3.4, Eqs. (127), (130), (134)–(135). The orbifold $V_{1,1}$ gives the handle [MATH], with $\alpha_{\mathrm{WP}} = 1$ and its included $\mathbb{Z}_2$; printed p. 17, Eq. (59), footnote 18, and §3.4. This divisor is not a universal instruction to divide every topology by two. The disk edge series, exact transform ratio and separate first-handle control diagnostic are [MATH], with low energy/large β for the edge, not an exact Airy completion; Eqs. (48), (53) fix the source comparison. The physical JT/matrix-ensemble interpretation is [CONJ+], conditional on the imaginary dilaton contour, boundary conditions, Schwarzian and Weil–Petersson measures and the sourced all-genus recursion correspondence. The checks developed

here span disk, cylinder and one handle, with separate edge and topology diagnostics. The recursion identity is a sourced mathematical ingredient; it is not the entirety of this physical interpretation. Same source, §3.4–3.5, Eqs. (127)–(145), and printed pp. 5–6 for nonunique completions. No fixed Hamiltonian, nonperturbative uniqueness or full minimal-string/JT/QFT equivalence is inferred.

References

Kontsevich, M. (1992). "Intersection Theory on the Moduli Space of Curves and the Matrix Airy Function". In: *Commun. Math. Phys.* 147, pp. 1–23. DOI: 10.1007/BF02099526.

Saad, P., S. H. Shenker, and D. Stanford (2019). "JT Gravity as a Matrix Integral". In: arXiv: 1903.11115 [hep-th].

Seiberg, N. and D. Shih (2004). "Branes, Rings and Matrix Models in Minimal (Super)string Theory". In: *JHEP* 02, p. 021. DOI: 10.1088/1126-6708/2004/02/021. arXiv: hep-th/0312170.

Chapter XVIII.9

$N = 2$ strings and self-dual fields

A gauge connection and a metric have several components. How can a string whose physical spectrum contains a single scalar state describe either of them? The answer is that the scalar supplies a potential for a constrained field. Differentiating the potential reconstructs the connection or metric; a nonlinear equation then selects its self-dual sector. The absence of a massive tower makes this dictionary unusually direct, but does not remove the interaction.

We develop this construction in a flat critical worldsheet theory with two complex matter coordinates, in split signature or its complexification. We use the conventional zero worldsheet $U(1)$-instanton frame and the same complex structure in the two closed chiral sectors. No instanton sum or alternative closed-sector choice is asserted. The open and closed theories will be treated as separate pure sectors. The central examples are a nonzero three-point amplitude, a connection with nonzero curvature and a curved metric with constant determinant. Together they explain how a small spectrum can encode nonlinear target-space physics. Basic BRST terminology, complex coordinates, differential forms and matrix Lie algebras are assumed. Chapter XVIII.10 will use the component definition of self-duality developed here when it introduces twistor descriptions.

XVIII.9.1 What the worldsheet constraints remove

The familiar string spectrum arises by imposing the worldsheet constraints on matter oscillators. Increasing the local worldsheet symmetry changes both the constraints and the ghosts required to impose them. In the $N = 2$ NSR string, the gauged currents are a stress tensor T, two supercurrents $G^{\pm}$ and a $U(1)$ current J. The supersymmetry here acts on the worldsheet and is a gauge symmetry. Its name does not assign a spacetime supersymmetry multiplet to the surviving state.

The central-charge balance gives a first quantitative consequence. A first-order

anticommuting pair of conformal weights $(\lambda, 1-\lambda)$ contributes

$$c_{\rm F}(\lambda) = -2(6\lambda^2 - 6\lambda + 1), \qquad c_{\rm B}(\lambda) = +2(6\lambda^2 - 6\lambda + 1) \tag{XVIII.9.1}$$

for the opposite, commuting statistics. The stress tensor requires the fermionic (b, c) pair with $\lambda = 2$. Each supercurrent requires a commuting (β, γ) pair with $\lambda = 3/2$. The $U(1)$ current requires a fermionic $(\widetilde{b}, \widetilde{c})$ pair with $\lambda = 1$. Substitution gives

$$c_{bc} = -26, \qquad c_{\beta\gamma} = 11, \qquad c_{\widetilde{bc}} = -2, \qquad c_{\rm gh} = -26 + 2(11) - 2 = -6. \tag{XVIII.9.2}$$

Each complex matter coordinate contributes two real bosons and their complex fermion, hence $c = 2 + 1 = 3$. For d complex matter multiplets the balance is

$$c_{\rm matter} + c_{\rm gh} = 3d - 6 = 0, \qquad d = 2, \qquad \dim_{\mathbb{R}} X = 4. \tag{XVIII.9.3}$$

This arithmetic fixes the critical matter content. It does not solve the BRST cohomology. In particular, cancellation of central charge is not a count of individual physical oscillator states.

For the spectrum we use the relative chiral BRST result at nonzero momentum. In the canonical $(-1, -1)$ picture the massless representative can be written

$$V_{-1,-1} = c\, e^{-\varphi_+ - \varphi_-} e^{ik\cdot Z}, \qquad k^2 = 0, \qquad k \neq 0. \tag{XVIII.9.4}$$

Here $\varphi_\pm$ bosonize the superghosts and Z denotes the matter coordinates. The relative space imposes the appropriate zero-mode conditions,

$$L_0 = J_0 = b_0 = \widetilde{b}_0 = 0. \tag{XVIII.9.5}$$

For the conventional flat critical complex, the nonzero-momentum relative cohomology has one scalar state and no massive tower in this picture. Its picture comparison also has a nonzero-momentum hypothesis. Zero momentum, absolute ghost copies and the closed matching prescription require separate analysis. In the closed theory we impose the usual matching and semi-relative conditions rather than interpreting two chiral copies as two unrelated particles.

A useful distinction concerns the vertex itself. The exponential used in matter superspace amplitudes is not the full ghost-dressed representative in (XVIII.9.4). Integrating its fermionic coordinates produces a descendant containing derivatives and matter fermions. On a disk the boundary identifies the left and right fields. Two bottom insertions and a descendant then produce the cubic momentum factor. The ghost fixing, picture prescription and integration measure are physical ingredients of this calculation. They cannot be recovered from the central-charge polynomial.

The scalar label therefore says how many independent states propagate at generic nonzero momentum. It does not say that the field is an ordinary free scalar. To determine its role we must examine how three such states interact. This is the next step from spectrum to target-space dynamics.

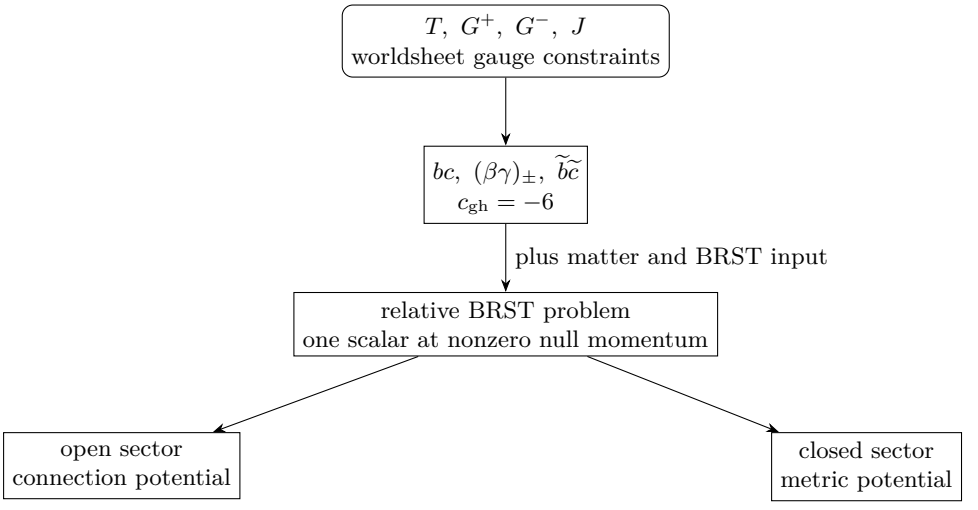


Figure XVIII.9.1: The constraint and potential dictionary. The arrow to the relative state includes a sourced cohomology calculation; the ghost central-charge sum alone does not establish that arrow. The two lower arrows refer to separate pure sectors.

XVIII.9.2 One state with a nonzero cubic interaction

The momentum geometry matters before any amplitude is evaluated. Adopt coordinates and metric

$$x = (y, z, \bar{y}, \bar{z}), \qquad ds^2 = 2(dy\, d\bar{y} - dz\, d\bar{z}), \qquad \eta_{a\bar{b}} = \mathrm{diag}(1, -1). \tag{XVIII.9.6}$$

Bars initially label independent coordinates. One real slice takes all four coordinates real. Another takes barred coordinates to be complex conjugates, giving $\mathbb{C}^{1,1}$. Both describe real split signature $(2, 2)$. We can also complexify the four momentum components while retaining this algebra. Two complex matter coordinates must not be confused with four complex matter coordinates.

The amplitude formulas use a particular source momentum label $k = (k_y, k_z, k_{\bar{y}}, k_{\bar{z}})$. Define

$$k_{ij} = k_{iy}k_{j\bar{y}} - k_{iz}k_{j\bar{z}}, \qquad s_{ij} = k_{ij} + k_{ji}, \qquad c_{ij} = k_{ij} - k_{ji}, \qquad k_i^2 = 2k_{ii}. \tag{XVIII.9.7}$$

The plane-wave phase and the actual coordinate covector p are

$$\Theta = k_y\bar{y} - k_z\bar{z} + k_{\bar{y}}y - k_{\bar{z}}z, \qquad p = (k_{\bar{y}}, -k_{\bar{z}}, k_y, -k_z). \tag{XVIII.9.8}$$

Thus $c_{ij}(p) = -c_{ij}(k)$ if the same component formula is applied to p, while the norm is unchanged. We use k in every amplitude below. This prevents an unnoticed sign change when moving between plane-wave derivatives and source labels.

The antisymmetric factor c_{12} comes from the derivative contractions in the descendant vertex. A closed insertion has two chiral sectors and hence two such factors. The open scalar is Lie-algebra-valued, with one oscillator species per color; matrix components do not add spacetime polarizations. In source-normalized vertices the three-point formulas are

$$A_3^{\mathrm{ord}} = g_o c_{12}, \qquad A_3^{abc} = -i g_o c_{12} f_{\mathrm{src}}^{abc}, \qquad A_3^{\mathrm{cl}} = \kappa_c c_{12}^2. \tag{XVIII.9.9}$$

The color tensor f_{src}^{abc} is the one in the source amplitude. Identifying it with a separately normalized Hermitian-generator convention would require an explicit conversion. Likewise g_o and κ_c are independent source-local couplings. The statement that survives after dividing them out is a kinematic square,

$$\frac{A_3^{\mathrm{cl}}}{\kappa_c} = \left(\frac{A_3^{\mathrm{ord}}}{g_o}\right)^2. \tag{XVIII.9.10}$$

A concrete null triad shows that these interactions are nonzero. Set

$$k_1 = (1,1,1,1), \qquad k_2 = (i,-i,-i,i), \qquad k_3 = (-1-i,-1+i,-1+i,-1-i). \tag{XVIII.9.11}$$

The last vector enforces conservation. The first two ordered cross products are $k_{12} = -2i$ and $k_{21} = 2i$. Their symmetric sum vanishes while their difference does not. Direct substitution for all legs gives

$$k_i^2 = 0, \qquad s_{12} = s_{23} = s_{31} = 0, \qquad c_{12} = c_{23} = c_{31} = -4i. \tag{XVIII.9.12}$$

Consequently the reduced amplitudes are

$$A_3^{\mathrm{ord}} = -4i g_o, \qquad A_3^{\mathrm{cl}} = -16\kappa_c. \tag{XVIII.9.13}$$

Interchanging two external labels reverses c_{12}, so the ordered open factor changes sign and the closed factor does not. These are amplitudes in the specified split/complex source convention, not positive probabilities.

For real Lorentzian momenta in signature $(3,1)$, the familiar three-null collinearity argument removes generic real three-point kinematics. Its reality assumptions are absent here. The complex-conjugate pairs in this example belong to $\mathbb{C}^{1,1}$ and retain split signature. Applying Lorentzian collinearity would erase a valid interaction by changing the problem. The fixed complex structure makes $U(1,1)$ manifest; it does not make an arbitrary change of all split momentum components a symmetry of c_{ij}.

XVIII.9.3 Why generic four-point scattering vanishes

The cubic interaction survives, yet the conventional pure four-point tree amplitudes vanish on generic on-shell kinematics. The mechanism is an algebraic cancellation special to the null momenta in this target dimension. It can be derived without dividing by a momentum channel, which also exposes the limits of the amplitude statement.

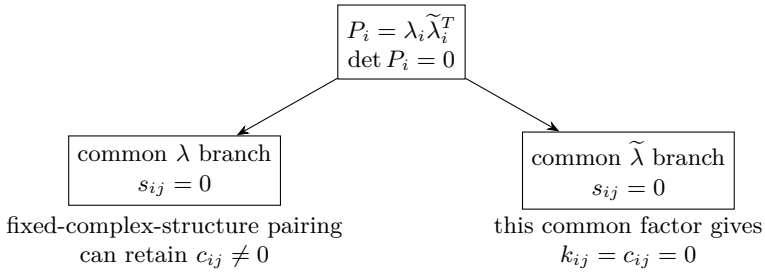


Figure XVIII.9.2: Momentum geometry of null rank-one matrices. Orthogonal conserved triads lie on null-plane branches. The amplitude uses the antisymmetric pairing in a fixed complex structure, so the equation $s_{ij} = 0$ must be distinguished from $c_{ij} = 0$. The explicit triad in the text resolves the distinction without a reality extrapolation. The matrix P and its spinors are defined in (XVIII.9.14).

Represent a momentum label by

$$P_i = \begin{pmatrix} k_{iy} & k_{iz} \\ k_{i\bar{z}} & k_{i\bar{y}} \end{pmatrix}, \qquad \det P_i = k_{ii} = 0. \tag{XVIII.9.14}$$

A nonzero null P_i is rank one, so it has a spinor factorization $P_i = \lambda_i \widetilde{\lambda}_i^T$. Independently of choosing such a chart, the ordered-pairing matrix of three momenta factorizes through two components,

$$M_{ij} = k_{ij} = \begin{pmatrix} k_{iy} & k_{iz} \end{pmatrix} \begin{pmatrix} k_{j\bar{y}} \\ -k_{j\bar{z}} \end{pmatrix}, \qquad \operatorname{rank} M \leq 2. \tag{XVIII.9.15}$$

For three null legs the diagonal of M is zero. Expanding its determinant therefore gives

$$\det M = k_{12}k_{23}k_{31} + k_{21}k_{32}k_{13} = 0. \tag{XVIII.9.16}$$

This step uses rank and nullness; no generic spinor-basis invariance of the antisymmetric c was assumed.

Let $k_4 = -k_1 - k_2 - k_3$ also be null and define

$$S = s_{12}, \qquad T = s_{23}, \qquad U = s_{13}, \qquad S + T + U = 0. \tag{XVIII.9.17}$$

These variables are symmetric pairings. A particle convention with $-(k_i + k_j)^2$ instead gives $-2s_{ij}$ and must be converted before use. Introduce the six ordered products

$$a = k_{12},\ b = k_{21},\ c = k_{13},\ d = k_{31},\ e = k_{23},\ f = k_{32}, \qquad L = a+b+c+d+e+f = 0. \tag{XVIII.9.18}$$

Conservation gives $c_{34} = c+e-d-f$ and $c_{41} = a+c-b-d$. Expanding the numerator relevant for four-point scattering yields

$$N = STU - Tc_{12}c_{34} - Sc_{23}c_{41}, \tag{XVIII.9.19}$$

$$= 4(aed + cbf) + (a-b)(f-e)L = 0. \tag{XVIII.9.20}$$

The first term vanishes by (XVIII.9.16); the second vanishes by the fourth null condition. Thus the polynomial identity holds even when a channel degenerates.

In the source disk and sphere calculations the rational factors are respectively F and F^2, with

$$F = 1 - \frac{c_{12}c_{34}}{SU} - \frac{c_{23}c_{41}}{TU} = \frac{N}{STU} = 0, \qquad STU \neq 0. \tag{XVIII.9.21}$$

The remaining beta or Gamma-function factors come from the insertion-position integral. Inferring a zero amplitude also requires being away from their poles. Equation (XVIII.9.20) is division-free; equation (XVIII.9.21) is a rational presentation with a smaller domain. Neither equation prescribes a distribution supported at a singular channel. In particular one must not multiply an undefined pole by zero and declare the result established.

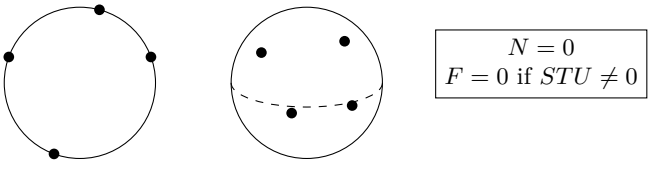


Figure XVIII.9.3: The position integrals supply the source beta/Gamma factors, while null kinematics supplies the common rational cancellation. The diagram concerns pure tree disk and sphere amplitudes. It makes no statement about higher genus.

For a numerical example with no vanishing channel take

$$k_1 = (-10, -13, 0, 0), \qquad k_2 = (0, 0, -18, -14), \tag{XVIII.9.22}$$

$$k_3 = (2, 3, 3, 2), \qquad k_4 = (8, 10, 15, 12). \tag{XVIII.9.23}$$

All four are null and conserved. Evaluation gives

$$(S, T, U) = (-2, 6, -4), \qquad (c_{12}, c_{34}, c_{23}, c_{41}) = (-2, -10, -6, -6), \tag{XVIII.9.24}$$

so $F = 1 - 20/8 - 36/(-24) = 0$. A common rescaling preserves the rational cancellation and can move the dimensionless source-scaled momenta away from the discrete accompanying Gamma poles. No universal α' normalization is being assigned by this operation.

This four-point zero coexists with the nonzero cubic amplitude of the previous section. It is therefore a cancellation of scattering contributions, not a diagnosis of a free theory. To understand what interacts, we now reconstruct the target connection.

XVIII.9.4 Reconstructing a self-dual connection

A scalar prepotential can encode a connection because the curvature constraints first remove redundant components. We work locally with a complex matrix gauge group and impose

$$F_{yz} = F_{\bar{y}\bar{z}} = 0, \qquad F_{y\bar{y}} - F_{z\bar{z}} = 0, \qquad F = dA + A \wedge A. \tag{XVIII.9.25}$$

Flatness in the barred directions allows a local frame with $A_{\bar{y}} = A_{\bar{z}} = 0$. Flatness in the unbarred directions then permits

$$A_a = J^{-1}\partial_a J, \qquad A_{\bar{a}} = 0, \qquad a = y, z. \tag{XVIII.9.26}$$

This is a local reconstruction. Patching and residual semi-local frame freedom remain; no compact reality condition on J follows from the notation.

To verify the first flatness equation differentiate the inverse,

$$\partial_a J^{-1} = -J^{-1}(\partial_a J)J^{-1}, \qquad \partial_a A_b - \partial_b A_a = -[A_a, A_b]. \tag{XVIII.9.27}$$

The commutator in F_{ab} cancels the last expression. The mixed curvature is instead

$$F_{a\bar{b}} = -\bar{\partial}_b(J^{-1}\partial_a J). \tag{XVIII.9.28}$$

The remaining component condition becomes the Yang equation,

$$E_Y = \bar{\partial}_y(J^{-1}\partial_y J) - \bar{\partial}_z(J^{-1}\partial_z J) = 0. \tag{XVIII.9.29}$$

Here $\bar{\partial}_y$ means $\partial/\partial\bar{y}$. An arbitrary J guarantees the two flatness equations but need not obey (XVIII.9.29). The nonlinear dynamics is precisely this remaining restriction.

Why call the sector self-dual? On the all-real split slice choose orientation $dy \wedge dz \wedge d\bar{y} \wedge d\bar{z}$. With indices $0, 1, 2, 3$ in this order, the metric has $G_{02} = 1$, $G_{13} = -1$ and their symmetric partners. A two-form obeying (XVIII.9.25) has independent entries

$$F_{02} = F_{13} = A, \qquad F_{03} = B, \qquad F_{12} = C, \qquad F_{01} = F_{23} = 0. \tag{XVIII.9.30}$$

Inserting these entries into the Hodge formula gives

$$(*F)_{ij} = \frac{1}{2}\epsilon_{ijkl}G^{km}G^{ln}F_{mn}, \qquad *F = F, \qquad \epsilon_{0123} = 1. \tag{XVIII.9.31}$$

Reversing orientation changes $*$ to $-*$ and swaps the self-dual/anti-self-dual label. The component equations (XVIII.9.25) remain the definition used here and in the next chapter. On a conjugate complex slice the corresponding real orientation must be stated before importing a Hodge name.

To see the scalar interactions set $J = e^{\Psi}$. Differentiating the exponential through an integral gives

$$J^{-1}dJ = \int_0^1 e^{-t\,\mathrm{ad}_\Psi}(d\Psi)\,dt = d\Psi - \frac{1}{2}[\Psi, d\Psi] + \frac{1}{6}[\Psi, [\Psi, d\Psi]] + O(\Psi^4). \tag{XVIII.9.32}$$

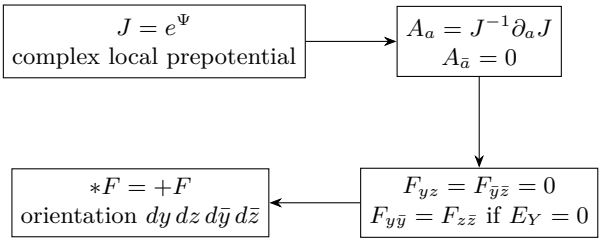


Figure XVIII.9.4: Local reconstruction of the constrained connection. The first two curvature constraints follow from the chosen frame and Maurer form. The primitive mixed constraint requires the Yang equation. The Hodge sign belongs to the displayed real split orientation.

The sign of the quadratic term follows from conjugation by $e^{-t\Psi}$, and integrating $t^2/2$ gives $1/6$. Define $D = \partial_y\bar{\partial}_y - \partial_z\bar{\partial}_z$. Substitution in the Yang equation gives

$$E_Y = D\Psi - \frac{1}{2}\{\bar{\partial}_y[\Psi, \partial_y\Psi] - \bar{\partial}_z[\Psi, \partial_z\Psi]\} \tag{XVIII.9.33}$$

$$+ \frac{1}{6}\{\bar{\partial}_y[\Psi, [\Psi, \partial_y\Psi]] - \bar{\partial}_z[\Psi, [\Psi, \partial_z\Psi]]\} + O(\Psi^4). \tag{XVIII.9.34}$$

The one-state field has nonlinear matrix interactions. An action expressed in another prepotential can have different polynomial vertices, so a cubic action in a different gauge cannot be substituted into this infinite Yang-coordinate expansion without a field map. In the source exponential $\Psi = i\varphi_{\text{rescaled}}$, with $\varphi_{\text{rescaled}} = 2g_o\varphi_{\text{canonical}}$.

An exact example makes both the curvature and the nonlinear constraint visible. Let E_{12}, E_{21} be elementary 2×2 matrices and set

$$J = (I + uE_{12})(I + vE_{21}) = \begin{pmatrix} 1+uv & u \\ v & 1 \end{pmatrix}, \qquad u = y + z, \quad v = \bar{y} + \bar{z}, \quad \det J = 1. \tag{XVIII.9.35}$$

The two nilpotent factors do not commute. Multiplying $J^{-1}\partial J$ gives

$$A_y = A_z = \begin{pmatrix} v & 1 \\ -v^2 & -v \end{pmatrix}, \qquad F_{y\bar{y}} = \begin{pmatrix} -1 & 0 \\ 2v & 1 \end{pmatrix} \neq 0. \tag{XVIII.9.36}$$

Because $\bar{\partial}_y v = \bar{\partial}_z v = 1$, the two terms in E_Y cancel. This is a curved connection in the required sector. Replacing u by y and v by $\bar{y}$ keeps the local reconstruction but gives $A_z = 0$ and

$$E_Y = \begin{pmatrix} 1 & 0 \\ -2\bar{y} & -1 \end{pmatrix} \neq 0. \tag{XVIII.9.37}$$

The nearby failure explains why the scalar field still obeys a dynamical equation. The source identification of the open string scalar with this prepotential uses the low-point amplitudes and the classical target dictionary; our local reconstruction then exhibits what that dictionary means.

XVIII.9.5 Reconstructing self-dual geometry

In the closed sector the scalar perturbs a Kähler potential. The metric is obtained after two derivatives, so calling the physical state a scalar does not imply a scalar matter field coupled to a separate graviton. In the local complex or pseudo-Kähler chart use

$$K = y\bar{y} - z\bar{z} + \Phi, \qquad g_{a\bar{b}} = \partial_a \bar{\partial}_{\bar{b}} K = \eta_{a\bar{b}} + H_{a\bar{b}}, \qquad H = \partial\bar{\partial}\Phi. \tag{XVIII.9.38}$$

The sourced vacuum closed-string equation is the constant-determinant condition $\det g = -1$. Its nonlinear sign follows by expanding the actual matrix rather than guessing it from a Euclidean metric.

Write $H = \left(\begin{smallmatrix} A & B \\ C & D_0 \end{smallmatrix}\right)$. Then

$$\det(\eta + H) = (1 + A)(-1 + D_0) - BC = -1 + D_0 - A + AD_0 - BC. \tag{XVIII.9.39}$$

Thus the Plebański equation in this convention is

$$D\Phi - \det(\partial\bar{\partial}\Phi) = 0, \qquad D\Phi = \Phi_{y\bar{y}} - \Phi_{z\bar{z}}. \tag{XVIII.9.40}$$

The linearized equation is $D\Phi = 0$. The quadratic Hessian determinant supplies the nonlinear correction. In the source normalization the geometric field and canonical closed scalar are related by

$$\Phi = 4\kappa_c \phi_{\text{canonical}}. \tag{XVIII.9.41}$$

This rescaling is essential when comparing the metric potential with the normalized cubic amplitude. It does not identify κ_c with an absolute ten-dimensional gravity coupling.

A constant nonzero determinant implies Ricci flatness in this local Kähler setting because

$$R_{a\bar{b}} = -\partial_a \bar{\partial}_{\bar{b}} \log|\det g| = 0. \tag{XVIII.9.42}$$

In a complex chart one uses a local branch of $\log\det g$; its derivatives are the same. The identification with the self-dual vacuum curvature sector is the accompanying four-dimensional Kähler geometry input. Ricci flatness alone in an arbitrary dimension or arbitrary metric class would not establish that identification.

Consider the quartic family

$$u = y + z, \qquad v = \bar{y} + \bar{z}, \qquad \Phi = \epsilon u^2 v^2, \qquad h = 4\epsilon uv. \tag{XVIII.9.43}$$

Every mixed Hessian entry equals h, so

$$H = h\begin{pmatrix} 1 & 1 \\ 1 & 1 \end{pmatrix}, \qquad g = \begin{pmatrix} 1+h & h \\ h & -1+h \end{pmatrix}, \qquad \det g = (1+h)(-1+h) - h^2 = -1. \tag{XVIII.9.44}$$

The equality is exact for all ϵ in this local chart. The inverse exists everywhere in the algebraic family. On the conjugate slice with real ϵ the Hermitian matrix has one positive and one negative eigenvalue, since its determinant is negative. On the all-real chart the corresponding symmetric metric likewise retains split signature.

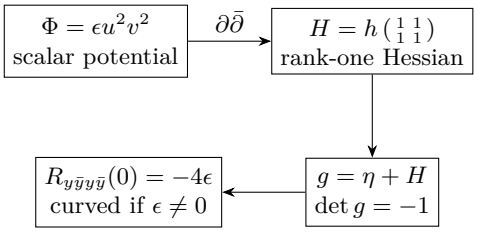


Figure XVIII.9.5: From the scalar to a curved metric. The rank-one Hessian has zero determinant, while its addition to the split background preserves the nonzero metric determinant. Constant volume density and nonzero Riemann curvature coexist.

Constant determinant does not mean that every component is constant. To compute a local curvature component take the explicit convention

$$R_{a\bar{b}c\bar{d}} = -\partial_a \bar{\partial}_b g_{c\bar{d}} + g^{e\bar{f}} (\partial_a g_{c\bar{f}})(\bar{\partial}_b g_{e\bar{d}}). \tag{XVIII.9.45}$$

At the origin h and its first derivatives vanish, but $\partial_y \bar{\partial}_y h = 4\epsilon$. Consequently

$$R_{y\bar{y}y\bar{y}}(0) = -4\epsilon. \tag{XVIII.9.46}$$

The metric is curved whenever $\epsilon \neq 0$, even though its Ricci tensor vanishes. In the limit $\epsilon \to 0$ it returns to the flat background. This gives a concrete geometric meaning to the closed scalar interaction.

The choice of null combinations u, v was doing work. For comparison take $\Phi = \epsilon y^2 \bar{y}^2$. Then $H_{y\bar{y}} = 4\epsilon y\bar{y}$ is the only nonzero Hessian component, and

$$D\Phi - \det H = 4\epsilon y\bar{y}, \qquad \det g = -1 - 4\epsilon y\bar{y}. \tag{XVIII.9.47}$$

A generic quartic potential therefore fails the heavenly equation. Nor can the successful rank-one family determine the sign of a general nonlinear term by itself, since $\det H = 0$ there. The matrix expansion preceding (XVIII.9.40) fixes that sign for arbitrary mixed Hessian.

XVIII.9.6 What the dictionary establishes

We can now answer the opening question. In the pure open theory a single relative state supplies a matrix prepotential whose derivatives reconstruct a constrained connection. In the pure closed theory it supplies a Kähler-potential perturbation whose Hessian reconstructs a vacuum metric. The spectrum, vertices and target equations perform different jobs in this reasoning. Their correspondence is a classical, source-controlled dictionary in the specified split/complex sector.

The cubic square gives the relation (XVIII.9.10) between momentum factors. Multiplying one vertex normalization by a constant changes its coupling but leaves that

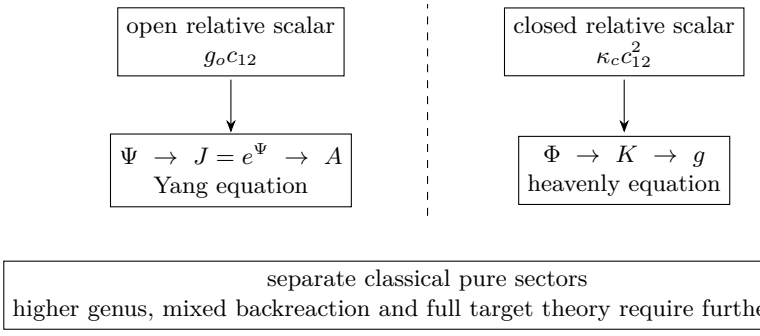


Figure XVIII.9.6: The bounded state-to-field dictionary. The dashed separation means that the pure open and pure closed reconstructions were performed separately. The bottom boundary lists extensions for which the low-point calculation supplies no completion.

relation after division intact. Thus the square cannot fix an absolute gravitational or gauge coupling. The field maps contain further information,

$$\Psi = i\varphi_{\text{rescaled}}, \qquad \varphi_{\text{rescaled}} = 2g_o\varphi_{\text{canonical}}, \qquad \Phi = 4\kappa_c\phi_{\text{canonical}}. \tag{XVIII.9.48}$$

They specify which variable is being differentiated; they do not promote a source convention into a universal coupling identity.

Similarly, the four-point cancellation constrains on-shell scattering but does not uniquely determine an arbitrary off-shell action. A local invertible change of field coordinates can alter the displayed vertices while preserving the on-shell amplitudes. One must specify the prepotential, gauge and admissible boundary conditions before comparing off-shell formulations. The geometric reconstructions in the previous sections supply exactly such local variables. The nonzero examples,

$$F_{y\bar{y}} = \begin{pmatrix} -1 & 0 \\ 2v & 1 \end{pmatrix}, \qquad R_{y\bar{y}y\bar{y}}(0) = -4\epsilon, \tag{XVIII.9.49}$$

show directly why vanishing generic four-point scattering is compatible with nonlinear curvature.

There are two further boundaries a reader must keep separate. First, the target equations describe the self-dual sector, not all polarization sectors of Yang–Mills or Einstein theory. To reconstruct a larger target theory one would need its additional states and their interactions. The component equations (XVIII.9.25) are the useful input for twistor methods in the next chapter. They are not an assertion that a full target QFT has already been constructed.

Second, tree disk and sphere data do not compute higher-point amplitudes or loop measures. A claim about five or more external legs needs the corresponding correlator or a general factorization argument with its contact terms. An all-genus claim needs the genus-dependent ghost, picture and $U(1)$-instanton measure and its degenerations. The nonzero-momentum cohomology theorem also leaves its zero-momentum extension

separate. Each stronger assertion asks for information absent from the low-point null identity.

Finally, adding open fields to the closed geometry changes the vacuum equation through gauge-field sources. The determinant condition (XVIII.9.40) was derived here for the pure closed sector. A mixed calculation must determine the backreaction and its coefficients before using that equation in a coupled theory. This distinction is physical: the local Ricci-flat metric family solved a vacuum equation, while the local Yang example was built on a fixed flat background.

Checking a zero without erasing the interaction

The four-point example separates two stages that are often compressed into a single cancellation. First use nullness and momentum conservation to prove the polynomial identity (XVIII.9.20). The determinant of the ordered-pairing matrix vanishes because that matrix factors through two components. The null fourth momentum supplies the other polynomial relation. Neither step divides by a channel. The result therefore remains a valid polynomial statement at degenerate momenta.

The source amplitude is expressed differently. Its rational factor is the same polynomial divided by the product of three channel invariants. Using it requires those invariants to be nonzero. The accompanying position-integral factors also have their own singularities. A valid substitution in the polynomial identity need not be a valid substitution in the entire amplitude. To reproduce the numerical example, compute the ordered pairings first, form their symmetric and antisymmetric combinations, and only then substitute into the two rational terms. This keeps the channel convention and the relative signs visible.

The earlier cubic amplitude prevents an incorrect physical interpretation of the zero. The split or complex triad has nonzero antisymmetric pairings even though the relevant symmetric null pairings vanish. It supplies a nonzero interaction in the stated source convention. Real Lorentzian three-point collinearity uses a different reality condition and cannot remove that example. A four-point cancellation in an interacting self-dual sector is compatible with this cubic; it is not a proof that the target field is free.

The connection reconstruction then explains what the field describes. The two flatness conditions admit a local matrix representation, while the remaining mixed-curvature equation imposes nonlinear dynamics. The chosen orientation fixes the self-dual name. Chapter XVIII.10 uses related twistor geometry but brings in a current correlator, odd moduli and a separate amplitude prescription. Those ingredients are needed to obtain the larger gluon-amplitude family, rather than inferred from the four-point zero here.

Exercises

1. Starting from $c_{\mathrm{F}} = -2(6\lambda^2 - 6\lambda + 1)$ and the opposite sign for commuting ghosts, evaluate the contributions of one fermionic pair of weight 2, two bosonic pairs of weight 3/2 and one fermionic pair of weight 1. Each complex matter multiplet has

central charge 3. Determine the critical matter dimension and explain why the count alone determines neither BRST cohomology nor spacetime supersymmetry.

2. For $k_1 = (1,1,1,1)$, $k_2 = (i,-i,-i,i)$ and $k_3 = -k_1 - k_2$, verify conservation, nullness and the three cyclic c_{ij}. Compute the reduced open and closed cubic amplitudes and their response to swapping two labels. Explain why real Lorentzian collinearity does not apply.

3. Factor the ordered-pairing matrix $M_{ij} = k_{ij}$ through two components and derive its determinant identity for three null momenta. For a fourth conserved null leg, use $a = k_{12}$, $b = k_{21}$, $c = k_{13}$, $d = k_{31}$, $e = k_{23}$, $f = k_{32}$ and $L = a+b+c+d+e+f$ to expand $N = STU - Tc_{12}c_{34} - Sc_{23}c_{41}$. Evaluate F on the four momenta in §XVIII.9.3. Explain both the channel and Gamma-pole restrictions in the four-point amplitude conclusion.

4. Derive the Yang equation from $A_{\bar{a}} = 0$, $A_a = J^{-1}\partial_a J$ and the curvature conditions (XVIII.9.25). Derive $J^{-1}dJ$ through cubic order in Ψ for $J = e^{\Psi}$. For $J = (I + uE_{12})(I + vE_{21})$, first take $u = y + z$, $v = \bar{y} + \bar{z}$ and compute $A_y, A_z, F_{y\bar{y}}$ and E_Y. Then take $u = y, v = \bar{y}$ and determine whether it still solves the equation.

5. Expand $\det(\eta + \partial\bar{\partial}\Phi)$ and derive the heavenly equation. For $\Phi = \epsilon(y+z)^2(\bar{y}+\bar{z})^2$, compute g, its determinant, its Ricci tensor and $R_{y\bar{y}y\bar{y}}(0)$ in the stated curvature convention. Compare $\Phi = \epsilon y^2\bar{y}^2$. Why does fixed determinant not imply flatness?

6. Explain which information the cubic kinematic square and generic four-point zeros determine. Do they establish absolute coupling equality, a unique off-shell action, the full Yang–Mills/Einstein theories, higher-point vanishing or all-genus equivalence? Give concrete further calculations needed for those assertions. Distinguish separate pure sectors from mixed backreaction.

7. In the real split chart with $G_{02} = G_{20} = 1$, $G_{13} = G_{31} = -1$ and $\epsilon_{0123} = 1$, compute all six independent components of $*F$ for $F_{02} = F_{13} = A$, $F_{03} = B$, $F_{12} = C$, $F_{01} = F_{23} = 0$. Reverse the orientation. Which component equations persist, and which duality label changes?

Sources and scope

§1. The first-order central charge is computed here [MATH]. The nonzero-momentum relative BRST result is a separate worldsheet input [WS]. The ghost/current setup is in Lechtenfeld 1995, physical PDF p. 1; relative conditions, representative and massive-state result are in Jünemann and Lechtenfeld 1997, physical PDF pp. 4,6,9, eqs. (1)–(3), (11)–(13), (25), with picture scope in section 3. Closed matching, zero momentum and absolute copies remain separate.
§2. The matter vertices, descendants and source-normalized cubics [WS] are in the conventional zero $U(1)$-instanton frame from Marcus 1992, physical PDF pp. 3–5, eqs. (1)–(12). The null triad is an explicit calculation [MATH]. The formulas follow

Marcus's normalization, including his stated relative π difference. The chapter uses no absolute α' or ten-dimensional coupling conversion.
§3. The rank/determinant identity [MATH] is for the complexification of four real target components, not four complex matter coordinates. The pure disk/sphere amplitude factors [WS] come from Marcus 1992, physical PDF pp. 4,6, eqs. (6)–(7),(13). Its zero conclusion requires $STU \neq 0$ and absence of accompanying Gamma poles. The kinematic comparison and singular-channel caution are in Parkes 1992, physical PDF pp. 4,8–9, eqs. (2.4)–(2.7). No distributional or higher-genus assertion follows.
§4. The local reconstruction, orientation-specific Hodge sign, Maurer expansion and exact nonabelian example are explicit calculations [MATH]. The classical open-string/prepotential identification [WS] follows Marcus 1992, physical PDF p. 15, eqs. (48)–(49), and Parkes 1992, physical PDF pp. 9–10, eqs. (3.1)–(3.4). The component equations fix the sector independently of naming conventions. No global compact reality or unrestricted Lorentzian completion is supplied.
§5. The determinant equivalence, curved family and Kähler Ricci calculation are explicit [MATH]. The pure closed dictionary [WS] uses the same left/right complex structure, in the zero $U(1)$-instanton frame of Marcus 1992, physical PDF pp. 14–15, eqs. (44)–(46) and the following geometric interpretation. The source rescaling is retained. The self-dual curvature interpretation uses four-dimensional Kähler geometry, separately from the scalar determinant expansion.
§6. The preceding statements use the stated source conventions and the pure open or pure closed sector. Mixed equations in Marcus 1992, physical PDF p. 15, eqs. (51)–(52), establish the need for a separate backreaction treatment; their coefficients are outside this chapter.

References

Jünemann, K. and O. Lechtenfeld (1997). "Chiral BRST Cohomology of N=2 Strings at Arbitrary Ghost and Picture Number". In: arXiv: hep-th/9712182.

Lechtenfeld, O. (1995). "On the BRST Cohomology of N=2 Strings". In: arXiv: hep-th/9508100.

Marcus, N. (1992). "The N=2 open string". In: *Nucl. Phys. B* 387, pp. 263–279. DOI: 10.1016/0550-3213(92)90161-4. arXiv: hep-th/9207024.

Parkes, A. (1992). "On N=2 strings and classical scattering solutions of self-dual Yang-Mills in (2,2) space-time". In: *Nucl. Phys. B* 376, pp. 279–296. DOI: 10.1016/0550-3213(92)90126-V. arXiv: hep-th/9110075.

Chapter XVIII.10

Twistor lines and gluon amplitudes

XVIII.10.1 Why a line can know an amplitude

A color-ordered gluon tree amplitude usually emerges from a sum of Feynman diagrams. Individual diagrams depend on gauge choices and contain poles that cancel in the sum. For two negative-helicity gluons the answer is much simpler than this calculation suggests. The question of this chapter is whether a string construction can make that simplicity visible before the diagram sum.

The relevant string picture places the external states on a projective line in supertwistor space. A cyclic contraction of currents supplies one denominator for each pair of neighboring insertions. Eight fermionic moduli supply the numerator. These two operations organize different information: the current cycle remembers color order, while the fermionic integral remembers the helicities. We will evaluate them separately and then combine them.

We assume familiarity with the open B-model and holomorphic Chern–Simons theory of XVIII.5, elementary complex analysis and massless four-dimensional gauge fields. The necessary spinor variables are introduced here. XVIII.9 supplies a nearby example of a chiral gauge sector, but the orientation-dependent self-duality names of that chapter will not be identified with the present spinor conventions. Our objective is a relative tree amplitude and a diagnosis of the original twistor-string model's additional sector.

A complex null momentum is a rank-one matrix. Write its two factors as column spinors and define both brackets by determinants:

$$p_i = \lambda_i \widetilde{\lambda}_i^{\mathsf{T}}, \qquad \langle ij \rangle = \lambda_{i1}\lambda_{j2} - \lambda_{i2}\lambda_{j1}, \qquad [ij] = \widetilde{\lambda}_{i1}\widetilde{\lambda}_{j2} - \widetilde{\lambda}_{i2}\widetilde{\lambda}_{j1}. \tag{XVIII.10.1}$$

All momenta are outgoing. Throughout the chapter the invariant is the determinant convention

$$s_{ij} = \det(p_i + p_j) = \langle ij \rangle [ij]. \tag{XVIII.10.2}$$

For example, $p = \mathrm{diag}(1, 0)$ and $q = \mathrm{diag}(0, 1)$ have $s_{pq} = 1$. This fixes the propagators used below without an implicit conversion to a different sigma-matrix normalization.

Let a_n denote a color-ordered Yang–Mills amplitude with its color trace, momentum delta function, conventional overall i, and coupling g^{n-2} stripped off. The four-gluon function that will guide us is

$$a_4(1^-, 2^-, 3^+, 4^+) = \frac{\langle 12\rangle^4}{\langle 12\rangle\langle 23\rangle\langle 34\rangle\langle 41\rangle}. \tag{XVIII.10.3}$$

An MHV amplitude has exactly two negative-helicity gluons, with the other gluons positive. The neighboring brackets in (XVIII.10.3) suggest a cyclic object, not a sum over spacetime interaction vertices. Figure XVIII.10.1 shows the construction we will test. The independent Yang–Mills recursion is essential: evaluating a proposed string integral is different from establishing its physical identification.

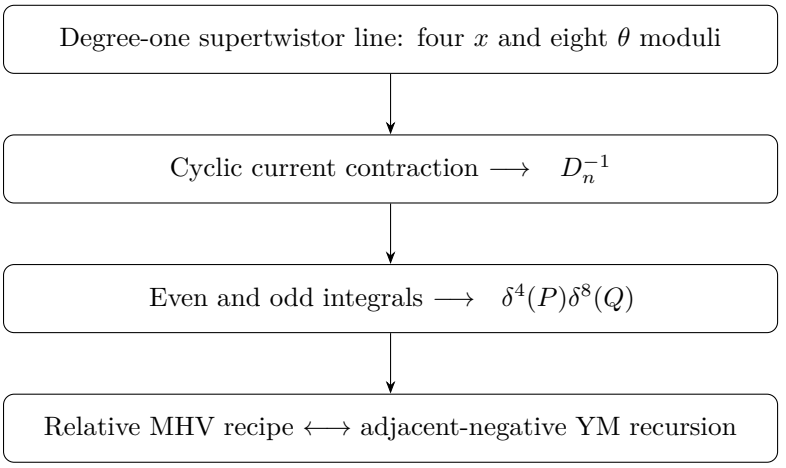


Figure XVIII.10.1: The construction's objects and operations. The downward arrows evaluate a supplied line prescription. The bottom comparison uses an independent ordinary-Yang–Mills tree calculation, with its own factorization and large-z inputs. This map is not a full-theory duality assertion.

XVIII.10.2 Spacetime points become twistor lines

The denominator suggests a projective line. To understand why its moduli should include four spacetime coordinates, start with the incidence relation. A twistor has homogeneous coordinates $Z = (\lambda_a, \mu_{\dot a})$. On the open twistor space $\mathbb{PT}' = \mathbb{CP}^3 \setminus \{\lambda = 0\}$, associate to a complex spacetime matrix x the set

$$L_x : \quad \mu = -x^{\mathsf{T}}\lambda, \qquad (\lambda, \mu) \sim (t\lambda, t\mu), \qquad \lambda \neq 0. \tag{XVIII.10.4}$$

The free projective spinor makes $L_x \simeq \mathbb{CP}^1$. Thus a spacetime point is a line of twistors. The reverse correspondence sends a fixed twistor to a family of spacetime points satisfying two linear equations.

Two such lines share a twistor precisely when a nonzero spinor satisfies

$$(x-y)^{\mathsf{T}}\lambda = 0 \quad \Longleftrightarrow \quad \det(x-y) = 0. \tag{XVIII.10.5}$$

If $x - y = \mathrm{diag}(1, 0)$, the kernel is generated by $(0, 1)$ and the distinct spacetime points are null separated. If $x - y$ is the identity, the kernel is zero and the lines do not meet. Figure XVIII.10.2 illustrates these incidence statements in complex projective geometry. The drawn curves are schematic; they are not real spatial trajectories.



$\det(x - y) = 0$
shared twistor

$\det(x - y) \neq 0$
no intersection

Figure XVIII.10.2: Schematic incidence in complex twistor space. A spacetime point gives an entire projective line; null separation corresponds to a shared projective spinor in the kernel of $(x - y)^{\mathsf{T}}$. The drawn lines and ellipses represent complex projective lines, not trajectories in real spacetime.

Incidence does more than encode null separation. It turns homogeneous functions on twistor space into solutions of wave equations. For a weight -2 Čech cocycle f, consider the local contour transform

$$\phi(x) = \frac{1}{2\pi i} \oint_C \langle \lambda \, d\lambda \rangle \, f(\lambda, -x^{\mathsf{T}}\lambda). \tag{XVIII.10.6}$$

The measure has weight two, so the integrand is projectively invariant. The contour lies in a patch overlap and separates its singularities. We restrict x to a region where it deforms without crossing poles. A cocycle shifted by functions holomorphic on the two patches has the same integral: each extra term has a contour that contracts in its own patch. This explains why cohomology, rather than an arbitrary pointwise twistor function, is the natural input.

The wave equation follows locally from the chain rule. Differentiating through incidence gives

$$\frac{\partial}{\partial x_{a\dot{a}}} f(\lambda, -x^{\mathsf{T}}\lambda) = -\lambda_a \frac{\partial f}{\partial \mu_{\dot{a}}}, \qquad (\partial_{11}\partial_{22} - \partial_{12}\partial_{21})\,\phi = 0. \tag{XVIII.10.7}$$

In the second relation the two terms have the same factor $\lambda_1\lambda_2\partial_{\mu_1}\partial_{\mu_2} f$ and cancel. No equation of motion for f had to be imposed beyond its holomorphic patch description.

A residue makes this map concrete. Restrict to $\mu \neq 0$, cover by the patches $\mu_1 \neq 0$ and $\mu_2 \neq 0$, and choose $f = 1/(\mu_1\mu_2)$. On $\lambda = (1, z)$ we obtain

$$\phi(x) = \frac{1}{2\pi i}\oint_C \frac{dz}{(x_{11} + x_{21}z)(x_{12} + x_{22}z)} = \frac{1}{x_{21}x_{12} - x_{22}x_{11}} = -\frac{1}{\det x}. \quad \text{(XVIII.10.8)}$$

Here $x_{21}x_{22} \neq 0$, $\det x \neq 0$, and the positively oriented contour encloses $z = -x_{11}/x_{21}$ alone. The residue denominator is $x_{21}(x_{12} - x_{22}x_{11}/x_{21})$. These conditions keep the poles finite and distinct. A different local coordinate can cover cases with a pole at infinity.

The answer is singular on a null cone and solves (XVIII.10.7) away from it. It does not specify a Lorentzian causal prescription or a distributional delta-source normalization. This local calculation is the forward scalar Penrose transform; a global correspondence requires additional analytic-region hypotheses. In particular, the relevant local field space cannot be replaced by global $H^1(\mathbb{CP}^3, \mathcal{O}(-2))$. Question 2 asks for a direct derivative check of the example, making the contour conditions part of the calculation.

XVIII.10.3 The chiral content of the open B-model

The line must also carry helicity information. The original proposal enlarges twistor space by four odd homogeneous coordinates ψ^A, $A = 1, \ldots, 4$, with the super-incidence relation

$$\psi^A = -\theta^{aA}\lambda_a. \quad \text{(XVIII.10.9)}$$

A line now has four even moduli x and eight odd moduli θ. Before using them in an amplitude, we need to explain why four odd coordinates and how the fields are encoded.

Under a common scaling of homogeneous coordinates, an ordinary differential scales as $dZ \mapsto t\,dZ$, whereas a Berezin differential scales as $d\psi \mapsto t^{-1}d\psi$. The homogeneous measure therefore has weight

$$\mathrm{wt}\left(d^4Z\, d^N\psi\right) = 4 - N. \quad \text{(XVIII.10.10)}$$

After the projective quotient, this is the Berezinian weight of $\mathbb{CP}^{3|N}$. It vanishes at $N = 4$. Ordinary $\mathbb{CP}^3$ has canonical bundle $\mathcal{O}(-4)$; the four odd directions compensate this weight. This geometric cancellation permits the formal B-model setup but is not a proof of a quantum integration measure.

Expand a weight-zero $(0, 1)$ superconnection in the odd variables:

$$\mathcal{A} = A + \psi^A\chi_A + \frac{1}{2}\psi^A\psi^B\phi_{AB} + \frac{1}{3!}\psi^A\psi^B\psi^C\widetilde{\chi}_{ABC} + \frac{1}{4!}\psi^A\psi^B\psi^C\psi^D G_{ABCD}. \quad \text{(XVIII.10.11)}$$

Since every ψ has weight one, the degree-k component has weight $-k$. The local Penrose field dictionary assigns weight $2h - 2$ to helicity h. Solving for h gives

$$-k = 2h - 2, \qquad h = 1 - \frac{k}{2}, \qquad k = 0, 1, 2, 3, 4. \quad \text{(XVIII.10.12)}$$

Figure XVIII.10.3 displays the resulting gluons, fermions and scalars. The positive and negative gluons occupy opposite ends of the same superfield. This is a field

correspondence on admissible open regions, not the dual external-state pairing used in a scattering integral.

odd degree k	component	weight	helicity	
0	A	0	1	
1	χ	-1	$1/2$	
2	ϕ	-2	0	$h = 1 - k/2$
3	$\widetilde{\chi}$	-3	$-1/2$	
4	G	-4	-1	

Figure XVIII.10.3: The five degrees of a weight-zero superconnection on $\mathbb{CP}^{3|4}$. Degree k contributes $\binom{4}{k}$ components. The weight-to-helicity arrow uses the local field Penrose dictionary $\mathcal{O}(2h-2)$, rather than an external-state dual pairing.

The open B-model action recalled from XVIII.5 is formally holomorphic Chern–Simons theory:

$$S_{\mathrm{hCS}} = \int \Omega^{3|4} \ \mathrm{Tr}\left(\frac{1}{2}\mathcal{A}\bar{\partial}\mathcal{A} + \frac{1}{3}\mathcal{A}^3\right). \tag{XVIII.10.13}$$

Keep only the bosonic A, G fields and saturate the four odd coordinates. Up to the overall action convention, the result is

$$S_{A,G} = \int \Omega' \ \mathrm{Tr}\, G\left(\bar{\partial}A + A \wedge A\right), \qquad \delta_G S_{A,G} = 0 \implies F^{0,2} = 0. \tag{XVIII.10.14}$$

Thus G is a multiplier enforcing holomorphic bundle data. The sourced Ward correspondence turns bundles trivial on every spacetime line into a chiral Yang–Mills sector. Its analytic region must have connected, simply connected intersections with the relevant alpha-planes; line triviality is a separate condition, not a consequence of writing (XVIII.10.14). We use this theorem as input rather than proving a global existence statement.

The equation explains the limitation of the perturbative open sector. It imposes a chiral gauge equation, while full Yang–Mills scattering contains interactions outside that sector. Witten calls this sector anti-self-dual in his conventions. The explicit equation and incidence map carry our meaning; the adjective does not supply a map to XVIII.9's Hodge convention. To obtain the MHV function in the original proposal, one adds D1 curves and their current system. Question 3 separates this physical addition from the geometric Berezinian calculation.

XVIII.10.4 A current cycle and eight odd moduli

A degree-one D1 curve is precisely a supertwistor line. Its D1–D5 fields α, β couple to the open connection through a chiral action of the form

$$S_{\alpha\beta} = \int_C \beta(\bar{\partial} + \mathcal{A})\alpha, \qquad J_i = \beta T_i \alpha. \tag{XVIII.10.15}$$

Here T_i is the color generator of the ith insertion. The physical interpretation supplies fermionic statistics, the degree -1 line bundle for the chiral fields, their determinant normalization, the integration contour and the moduli measure. We evaluate the prescription conditional on those inputs. None follows merely from the projective weight in (XVIII.10.10).

The propagator on the line connects an α to a β. Choosing a Wick contraction that visits every insertion once produces a color cycle. In an affine coordinate it has the structure

$$\langle J_1 \cdots J_n \rangle_{\text{cycle}} = C_n \frac{dz_1 \cdots dz_n}{(z_2 - z_1)(z_3 - z_2) \cdots (z_1 - z_n)} \operatorname{Tr}(T_1 \cdots T_n). \qquad \text{(XVIII.10.16)}$$

A contraction that closes before visiting every insertion produces more than one trace. Figure XVIII.10.4 separates these two possibilities. The relative kinematic denominator of the single cycle, after restoring homogeneous coordinates and pairing external states, is

$$D_n = \prod_{i=1}^{n} \langle i, i+1 \rangle, \qquad n+1 \equiv 1. \qquad \text{(XVIII.10.17)}$$

The external wavefunctions cancel the remaining insertion weights. We use this forward bracket order consistently; an overall current normalization or orientation sign is absorbed into a coefficient that remains undetermined.



one trace
D_4^{-1}

two traces
$\langle 12 \rangle^{-2} \langle 34 \rangle^{-2}$

Figure XVIII.10.4: Wick cycles of the supplied chiral current system. An arrow represents a propagator linking color indices. One cycle produces a single trace; two closed cycles produce the (12)(34) color structure. Overall orientation signs and current normalizations are not fixed by this drawing.

The even moduli explain momentum conservation. Plane-wave states restricted to a line produce a factor whose x dependence is $\exp(ix \cdot \sum_i p_i)$. On a split-real Fourier contour the integral is

$$\int d^4x \, e^{ix \cdot P} = (2\pi)^4 \delta^4(P), \qquad P = \sum_i p_i. \qquad \text{(XVIII.10.18)}$$

The displayed contour is part of the prescription. It does not manufacture a preferred real integration cycle on the full complex moduli space.

The odd moduli impose supermomentum conservation. Introduce external odd variables η_i^A and define

$$Q_a^A = \sum_i \lambda_{ia}\eta_i^A, \qquad Q_1^A Q_2^A = \sum_{i<j}\langle ij\rangle \eta_i^A \eta_j^A, \qquad \delta^8(Q) = \prod_{A=1}^{4} Q_1^A Q_2^A. \quad \text{(XVIII.10.19)}$$

For a fixed species, the $i = j$ terms vanish. Combining the i, j and j, i terms antisymmetrizes the spinor factors, giving exactly the bracket in (XVIII.10.19). Integrating the eight θ variables with a fixed Berezin orientation extracts this product. The prescribed relative superamplitude is consequently

$$\mathcal{A}_n^{\text{line}} = N_n \frac{\delta^4(P)\delta^8(Q)}{D_n}. \qquad \text{(XVIII.10.20)}$$

The unknown N_n includes Fourier conventions, external-state normalization and the physical current/moduli measure. We leave it unfixed at each multiplicity. The equality is an evaluation of a formal integral with supplied input, not a claim of protected full scattering.

To extract two negative gluons at legs $r < s$, take one $\eta_r^A \eta_s^A$ from each species. Rearranging species order into leg order crosses $3 + 2 + 1 = 6$ odd pairs, so

$$[\eta_r^1\eta_r^2\eta_r^3\eta_r^4\eta_s^1\eta_s^2\eta_s^3\eta_s^4]\,\delta^8(Q) = (-1)^6\langle rs\rangle^4 = \langle rs\rangle^4. \qquad \text{(XVIII.10.21)}$$

The rational gluon function is $\langle rs\rangle^4/D_n$. An all-plus or single-minus gluon state has insufficient odd degree to saturate eight integrations and gives zero in this formula.

The same operation handles mixed states. For the ordered monomial

$$M = \eta_1^1\eta_1^2\eta_2^3\eta_2^4\eta_3^1\eta_3^2\eta_4^3\eta_4^4, \qquad \text{(XVIII.10.22)}$$

the selected pairs are (13) for species 1,2 and (24) for species 3,4. Their species-ordered leg sequence is $(1, 3, 1, 3, 2, 4, 2, 4)$. It has six inversions, so the coefficient is $+\langle 13\rangle^2\langle 24\rangle^2$. Question 4 performs this independent component extraction. It tests the full odd polynomial rather than a single helicity projection.

XVIII.10.5 An independent Yang–Mills recursion

The string recipe produces the desired rational function, but agreement at one multiplicity could conceal a wrong physical prescription. We now derive the adjacent-negative family directly from ordinary Yang–Mills trees. The independent inputs are tree rationality, physical factorization, vanishing all-plus and single-minus amplitudes for $n \geq 4$, and the large-complex-momentum estimate for a good shift. No current correlator or D1 measure enters.

Complex three-point momenta are crucial. Momentum conservation implies that all angle brackets or all square brackets vanish, giving two distinct branches. The nonzero seeds are

$$a_3(1^-, 2^-, 3^+) = \frac{\langle 12\rangle^3}{\langle 23\rangle\langle 31\rangle}, \qquad a_3(1^-, 2^+, 3^+) = \frac{[23]^3}{[31][12]}. \qquad \text{(XVIII.10.23)}$$

The first is evaluated on the square-zero branch and the second on the angle-zero branch. With real Lorentzian momenta the spinors are related by conjugation; both types of bracket then vanish together at three points. Such real kinematics cannot replace the complex seeds in a residue calculation.

For negative leg 1 and positive leg n, deform

$$\widetilde{\lambda}_1(z) = \widetilde{\lambda}_1 - z\widetilde{\lambda}_n, \qquad \lambda_n(z) = \lambda_n + z\lambda_1. \tag{XVIII.10.24}$$

The two changes in momentum cancel, and each shifted momentum remains rank one. With generic fixed reference spinors, the two shifted polarization vectors together scale as z^{-2}. Along the hard path of a tree graph, r propagators contribute z^{-r}, and at most $r+1$ cubic derivative vertices contribute z^{r+1}. Quartic vertices do not worsen this bound. Thus the ordinary Yang–Mills Feynman argument gives

$$a_n(z) = O(z^{-1}), \qquad 0 = \oint_\infty \frac{dz}{z} a_n(z), \qquad a_n(0) = \sum_{\text{channels},h} a_L(z_*) \frac{1}{\det P} a_R(z_*). \tag{XVIII.10.25}$$

The last equality follows by the residue theorem at the poles where the shifted internal momentum becomes null. Its propagator is evaluated at the unshifted channel invariant. This large-z step is a field-theory theorem input; little-group covariance alone would not provide it.

For $(1^-, 2^-, 3^+, \dots, n^+)$, helicity selection leaves the anti-MHV three-point corner containing $a = n-1$ and n. If both subamplitudes have at least four legs, the side without the two external negative helicities has at most one negative helicity and vanishes. The left three-point end containing legs 1 and 2 needs a separate check. Under the shift,

$$[\widehat{1}, 2] = [12] - z[n2], \qquad z_{12} = \frac{[12]}{[n2]}, \qquad \langle \widehat{1}, 2\rangle = \langle 12\rangle \neq 0. \tag{XVIII.10.26}$$

It lies on the square-zero MHV branch and its $(--+)$ seed can be nonzero. For $n > 4$, the opposite subamplitude has one negative helicity and at least four legs, so that factor vanishes. At $n = 4$, this partition is the surviving $(12)|(34)$ channel itself: its left MHV and right anti-MHV three-point seeds are both allowed. The surviving term is shown in Figure XVIII.10.5. At its pole,

$$z_* = -\frac{\langle an\rangle}{\langle a1\rangle}, \qquad \lambda_n(z_*) = c\lambda_a, \qquad c = \frac{\langle 1n\rangle}{\langle 1a\rangle}, \qquad P = \lambda_a(\widetilde{\lambda}_a + c\widetilde{\lambda}_n). \tag{XVIII.10.27}$$

Use $\lambda_{-P} = -\lambda_a$, $\widetilde{\lambda}_{-P} = \widetilde{\lambda}_a + c\widetilde{\lambda}_n$. The three square brackets at the right corner are

$$[na] = -[an], \qquad [n, -P] = -[an], \qquad [-P, a] = -c[an], \qquad a_R = \frac{[an]}{c}. \tag{XVIII.10.28}$$

Inserting the propagator removes the square bracket:

$$\frac{a_R}{s_{an}} = \frac{1}{c\langle an\rangle} = \frac{\langle a1\rangle}{\langle an\rangle\langle n1\rangle}. \tag{XVIII.10.29}$$

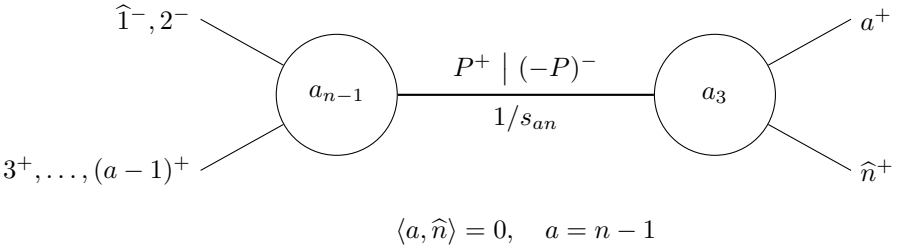


Figure XVIII.10.5: The surviving adjacent-negative BCFW channel. Internal momenta are outgoing from each subamplitude, hence opposite. The right anti-MHV seed is evaluated on the angle-zero branch, while the left amplitude contains the two negative external gluons.

The lower-point MHV denominator ends with $\langle a1\rangle$. Equation (XVIII.10.29) cancels this closing link and replaces it by the two links through leg n. Starting from the first seed in (XVIII.10.23), induction yields

$$a_n(1^-, 2^-, 3^+, \ldots, n^+) = \frac{\langle 12\rangle^4}{D_n}. \tag{XVIII.10.30}$$

This proof is restricted to adjacent negative helicities. The general nonadjacent-negative Parke–Taylor formula is a separately sourced result. Algebraically, arbitrary r, s follow from (XVIII.10.20); their physical identification there remains conditional on the D1 prescription.

A four-point example shows the internal helicity and signs in elementary variables. Take

$$\begin{aligned} &\lambda_1 = (1,0), \quad \lambda_2 = (0,1), \quad \lambda_3 = (a,b), \quad \lambda_4 = (c,d), \\ &\widetilde{\lambda}_3 = (u,v), \quad \widetilde{\lambda}_4 = (w,t), \quad \widetilde{\lambda}_1 = -a\widetilde{\lambda}_3 - c\widetilde{\lambda}_4, \quad \widetilde{\lambda}_2 = -b\widetilde{\lambda}_3 - d\widetilde{\lambda}_4. \end{aligned} \tag{XVIII.10.31}$$

These spinors satisfy momentum conservation identically. Put $\Delta = ad - bc$ and $U = ut - vw$, with all required denominators nonzero. Then

$$z_* = \frac{\Delta}{b}, \qquad c_{\text{pole}} = \frac{d}{b}, \qquad a_L = \frac{1}{ab}, \qquad a_R = \frac{bU}{d}, \qquad s_{34} = \Delta U. \tag{XVIII.10.32}$$

For the cyclic order $(1, 2, P)$, the brackets are $\langle 2P\rangle = -a$ and $\langle P1\rangle = -b$. Both minus signs enter the lower-point seed, so

$$a_L = \frac{1}{ab}, \qquad \frac{a_L a_R}{s_{34}} = \frac{1}{ad\Delta} = \frac{\langle 12\rangle^4}{\langle 12\rangle\langle 23\rangle\langle 34\rangle\langle 41\rangle}. \tag{XVIII.10.33}$$

The explicit brackets resolve the sign. The square-spinor parameters disappear after division by the propagator, as required by the holomorphic MHV function. This example also exposes why a four-point check that simply substitutes the proposed n-point answer at both ends would test nothing.

XVIII.10.6 What the answer says in singular limits

An amplitude formula must transform as the external particles do. The factorization $p_i = \lambda_i \widetilde{\lambda}_i^{\mathsf{T}}$ is unchanged under

$$(\lambda_i, \widetilde{\lambda}_i) \mapsto (t_i \lambda_i, t_i^{-1} \widetilde{\lambda}_i), \qquad a_n \mapsto t_i^{-2h_i} a_n. \tag{XVIII.10.34}$$

Every leg occurs twice in D_n. Thus D_n^{-1} has weight t_i^{-2} at every leg; the numerator adds four powers at each negative leg. The MHV function consequently has weight $+2$ for the negative gluons and -2 for the positive ones. Since each bracket has mass dimension one,

$$[a_n] = 4 - n. \tag{XVIII.10.35}$$

At four points the result is dimensionless. These are necessary checks on the spin and coupling conventions, but they do not fix residues.

To resolve the physical content of the neighboring denominator, make a positive leg s soft between hard legs a, b. Use the holomorphic scaling $\lambda_s = \epsilon \lambda_{s0}$ with $\widetilde{\lambda}_s$ fixed. In the ratio of the n- and $(n-1)$-point MHV functions, every numerator and every unaffected denominator cancels:

$$\frac{a_n}{a_{n-1}} = \frac{\langle ab \rangle}{\langle as \rangle \langle sb \rangle} = \epsilon^{-2} \frac{\langle ab \rangle}{\langle as_0 \rangle \langle s_0 b \rangle}. \tag{XVIII.10.36}$$

A momentum-conserving family can recoil the hard momenta by $O(\epsilon)$. At generic hard kinematics this does not alter the leading pole. The exponent is tied to this holomorphic scaling; it is not the exponent for scaling both spinors by $\sqrt{\epsilon}$ along a real soft family.

Next take adjacent positive legs a, b toward the holomorphic collinear branch. With a nonzero fraction z different from one, write

$$\lambda_a \to \sqrt{z} \lambda_P, \qquad \lambda_b \to \sqrt{1-z} \lambda_P, \qquad \widetilde{\lambda}_P = \sqrt{z} \widetilde{\lambda}_a + \sqrt{1-z} \widetilde{\lambda}_b. \tag{XVIII.10.37}$$

Then $p_a + p_b \to p_P$. If l and r are the neighbors outside the pair, the three denominator links reduce to

$$\langle la \rangle \langle ab \rangle \langle br \rangle \to \sqrt{z(1-z)} \langle lP \rangle \langle ab \rangle \langle Pr \rangle. \tag{XVIII.10.38}$$

The negative legs have not been merged, so their numerator is unchanged. We obtain

$$a_n \longrightarrow \frac{a_{n-1}(\ldots, P^+, \ldots)}{\sqrt{z(1-z)} \langle ab \rangle}. \tag{XVIII.10.39}$$

Figure XVIII.10.6 shows which links survive. Generic other brackets and a single collinear limit are assumed; simultaneous singularities and the other helicity channels require their own analysis.

Why not stop at weights and a few successful limits? Multiplying the function by any little-group-invariant scalar preserves its helicity weights. For example, at sufficiently many legs one can form a dimensionless ratio of invariants and deform

$$a_n \mapsto a_n \left(1 + \gamma \frac{s_{12} s_{34}}{s_{13} s_{24}} \right), \tag{XVIII.10.40}$$

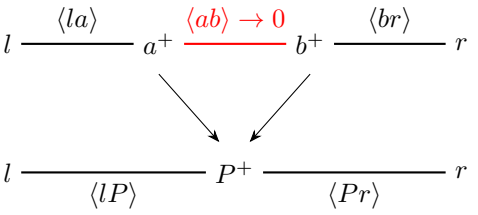


Figure XVIII.10.6: Denominator links in an adjacent positive-positive collinear limit. The outer links yield $\sqrt{z(1-z)}$ and the inner link supplies the singular bracket. The negative legs remain outside the pair, so the MHV numerator is unchanged.

where the denominators are nonzero at the comparison point and γ is dimensionless. This preserves dimension and little-group weights while changing physical residues or introducing nonadjacent poles. Local color-ordered factorization and the good-shift large-z behavior exclude such arbitrary modifications. The independent recursion therefore supplies information that projective covariance does not. Question 6 asks the reader to design a deformation and locate its failure rather than merely verify another successful limit.

XVIII.10.7 Double traces reveal the extra sector

The very contraction that generates the MHV denominator also produces terms with more than one color trace. They are a diagnostic, not a nuisance to erase. At four points, close the first current cycle after insertions 1,2 and the second after 3,4. With a nonzero symbolic current normalization K, the (12)(34) contraction has the rational structure

$$K\ \mathrm{Tr}(T_1T_2)\,\mathrm{Tr}(T_3T_4)\frac{1}{\langle 12\rangle^2\langle 34\rangle^2}. \tag{XVIII.10.41}$$

The signs from reversing the brackets within the two cycles and the physical overall normalization are included in K. Saturating the odd moduli for $1^+, 2^+, 3^-, 4^-$ gives

$$F^{++--}_{(12)(34)} = K\frac{\langle 34\rangle^4}{\langle 12\rangle^2\langle 34\rangle^2} = K\frac{\langle 34\rangle^2}{\langle 12\rangle^2} = K\frac{[12]^2\langle 34\rangle^2}{s_{12}^2}. \tag{XVIII.10.42}$$

The last step uses exactly (XVIII.10.2). It introduces no extra factor of two and no change in Fourier normalization. The amplitude has a double pole in s_{12}. An ordinary second-order scalar propagator contributes $1/s$, whereas a fourth-order kinetic operator can contribute $1/s^2$. Thus this is compatible with fourth-order exchange; it is not a fourth-order pole in s.

The color structure is consistent with a color singlet coupling to each pair of gluons. The helicity numerators further constrain the couplings. A useful schematic model is

$$\phi_+\,\mathrm{Tr}(F_+)^2 + \phi_-\,\mathrm{Tr}(F_-)^2, \qquad \langle\phi_+\phi_-\rangle \propto \frac{1}{s^2}, \qquad \langle\phi_+\phi_+\rangle = \langle\phi_-\phi_-\rangle = 0. \tag{XVIII.10.43}$$

The labels here specify the on-shell helicities of the gluon pairs. The first coupling supplies $[12]^2$ for two positive gluons and the second $\langle 34\rangle^2$ for two negative gluons. Their off-diagonal propagator gives (XVIII.10.42). Figure XVIII.10.7 displays this mechanism. A single real scalar coupled to both helicity bilinears would also propagate between two equal-helicity vertices, producing unwanted all-plus and all-minus structures. The pair makes clear which propagator must vanish.

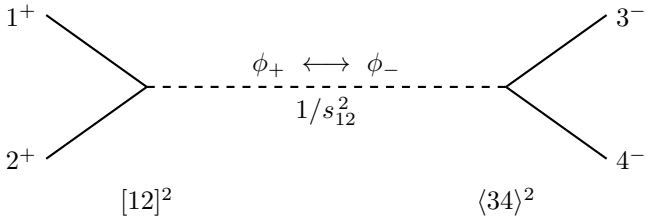


Figure XVIII.10.7: A possible fourth-order color-singlet exchange with the double-trace helicity numerator. The dashed line is an off-diagonal propagator between two scalar labels. Its double pole in s is compatible with a fourth-order kinetic operator; this one diagram alone does not identify the full conformal-supergravity spectrum.

This rational pole is not by itself a determination of the full exchanged spectrum. The identification of conformal-supergravity modes uses the source's spectrum and coupling analysis in addition to the amplitude diagnostic. For the original B-model, those modes have the same coupling and contribute to gluon loops. Selecting a single color trace at tree level isolates the tree Yang–Mills result but does not remove the extra sector from loop amplitudes. It therefore cannot establish a pure-Yang–Mills loop construction.

This limitation is specific to the worked original model and its supplied physical prescription. It is not a no-go theorem for every later twistor-string or ambitwistor model. Nor does a formal B-model calculation turn unprotected scattering into a protected quantity. The payoff is more focused: the line's geometry explains momentum and supermomentum conservation, the current cycle explains cyclic poles, and the double cycle reveals why the same construction contains more than the desired gluon sector. The following chapter turns to a different use of holomorphic gauge theory, where integrability rather than a four-dimensional scattering prescription is the principal output.

Extracting a component before comparing amplitudes

The odd-moduli calculation can be repeated without guessing a gluon numerator. For each of the four species, select two external legs from (XVIII.10.19). Anticommuting the external variables combines the two orders of that pair into an angle bracket. Multiply the four selected brackets in species order, then reorder the eight external variables into the declared component order. This last permutation fixes the sign. A comparison

of component formulas that skips the permutation can retain the correct powers of brackets while giving the wrong mixed-state answer.

For two negative gluons, every species chooses the same pair of legs. The six odd crossings in (XVIII.10.21) make the sign positive. The mixed example tests more information. Two species choose one pair and two choose another, so the resulting polynomial has two different bracket factors. The inversion count of the resulting species-ordered sequence still supplies its sign. Degree counting also explains the zeros for the all-plus and single-minus gluon components within this formula. Those components cannot saturate all eight odd integrations.

The denominator has a separate origin in the cyclic current expression. It must be carried with the extracted numerator before comparison with ordinary Yang–Mills theory. The recursion in the earlier Section XVIII.10.5 supplies that independent comparison for the stated adjacent-negative family. Its complex three-point seeds, factorization and large-momentum behavior are physical inputs of the field-theory derivation. Odd-degree counting in the string expression does not replace those inputs.

Agreement of the rational functions leaves the multiplicity-dependent normalization N_n unfixed. It also does not remove double-trace terms from the original prescription. The singular-limit and double-trace calculations therefore remain necessary parts of interpreting the result. This chapter obtains a relative amplitude recipe with stated inputs. The next chapter obtains a spectral crossing from line observables. The rational functions in both stories arise from different physical objects, and their comparison must retain those objects and their normalization.

Written exercises

Use complex outgoing momenta and the determinant convention of this chapter. In Questions 4 and 7 use the stated species-first definition of $\delta^8(Q)$ and increasing leg/species component order. Overall physical normalizations remain symbolic.

1. Derive the intersection condition for L_x, L_y from $\mu = -x^{\mathsf{T}}\lambda$. Give a rank-one and an invertible example for $x - y$. Explain which object represents a spacetime point and what a fixed twistor represents.

2. Evaluate the scalar contour transform for $f = 1/(\mu_1\mu_2)$ with $\lambda = (1, z)$, enclosing only the zero of $x_{11} + x_{21}z$. State the domain and contour assumptions. Check $(\partial_{11}\partial_{22} - \partial_{12}\partial_{21})\phi = 0$ directly. Explain why this does not fix a Lorentzian causal propagator.

3. Derive the homogeneous Berezinian weight of $\mathbb{CP}^{3|N}$ and determine N for which it vanishes. Derive the five component weights and helicities of the weight-zero superconnection using $\mathcal{O}(2h-2)$. Vary the formal bosonic hCS truncation with respect to G. State the analytic-region and line-triviality assumptions in the Ward input, and the physical ingredient needed beyond the perturbative open sector for MHV scattering.

4. Derive the two-negative-gluon coefficient of $\delta^8(Q)$, including its reordering sign. Also compute the coefficient of the mixed monomial (XVIII.10.22). Given the

chiral propagator proportional to $1/\langle ij\rangle$ and current $J = \beta T\alpha$, derive the cyclic trace denominator. Identify which statistics, normalization, contour and moduli-measure facts are supplied physical inputs.

5. For the spinors (XVIII.10.31), use the shift of legs 1 and 4 to find z_* and factor $P_{34}(z_*)$. Assume all needed denominators are nonzero. Evaluate the two complex seeds $a_3(1^-, 2^-, P^+)$ and $a_3((-P)^-, 3^+, 4^+)$ with $\lambda_{-P} = -\lambda_P$, $\widetilde{\lambda}_{-P} = \widetilde{\lambda}_P$. Divide their product by s_{34} and compare with (XVIII.10.3). Explain the two complex three-point branches and why real Lorentzian seeds cannot replace them.

6. Derive the positive holomorphic-soft and adjacent positive-positive collinear factors of $\langle rs\rangle^4/D_n$, leaving both negative legs unmerged. State the scaling and genericity assumptions and verify helicity weights and mass dimension. Construct a dimensionless weight-zero deformation which changes a residue or introduces a spurious pole. Explain which additional ordinary-Yang–Mills inputs exclude it.

7. Derive the $++--$ component of the double-current structure $1/(\langle 12\rangle^2\langle 34\rangle^2)$ and rewrite it using s_{12}. Explain the fourth-order exchange interpretation and its limits. Compare the off-diagonal scalar pair in (XVIII.10.43) with a single real scalar coupled to both helicity bilinears. Why does tree single-trace selection not prove pure-Yang–Mills loops for the original B-model?

Sources and scope

§1–2. Incidence/null intersection is determinant algebra [MATH]. The local forward scalar Penrose transform and wave equation are established under the contour hypotheses stated above [MATH]. The residue example is $-1/\det x$ on the stated open domain [MATH]. Source: Witten (2004), hep-th/0312171v2, Appendix A, (A.2), printed p. 83 and (A.19), printed p. 89. No global real-causal Green function is asserted.
§3. The homogeneous Berezinian weight is $4 - N$ [MATH]. The component weights/helicities use the local Penrose field theorem on admissible regions [MATH]. Formal hCS variation gives $F^{0,2} = 0$ [MATH]. The Ward correspondence is an imported theorem with analytic-region and line-triviality hypotheses [MATH]. Source: Witten, §4.1, (4.16), (4.19)–(4.21), printed pp. 57–59; Appendix A, printed pp. 87–89. These statements establish neither the physical D1 measure nor full Yang–Mills from the perturbative open sector. The chirality labels are not identified with XVIII.9.
§4. A supplied chiral current system gives the cyclic rational denominator [MATH]. Evaluation of the supplied even/odd degree-one integral and its component coefficients is algebraic [MATH]. Identifying this prescribed relative single-trace result with the physical MHV amplitude is [CONJ+], conditional on the D1–D5 statistics, measure, contour and external normalization, with unfixed N_n. Source: Witten, (4.42)–(4.55), printed pp. 71–75. Checks span current cycles, odd-component extraction including a mixed-state determinant, weights, singular limits and the independent adjacent-negative field-theory route; a finite four-point component comparison is not a general physical measure theorem.

§5–6. Adjacent-negative all-n recursion follows under ordinary Yang–Mills tree factorization, rationality, helicity zeros and the good-shift large-z result [MATH]. Source: Britto et al. (2005), hep-th/0501052v2, §2, (2.1)–(2.7), and §3.1, printed p. 7. Little-group weights and dimension are algebraic [MATH]. The stated positive holomorphic-soft and adjacent positive-positive collinear limits are algebraic [MATH]. The general MHV formula is separately sourced to Witten (2.14), printed p. 9; a new nonadjacent-negative all-n proof is not claimed.
§7. The nonzero double-trace prescription gives a double pole in s with the stated helicity numerator [MATH]. Its interpretation as a diagnostic of the original model's conformal-supergravity sector is [CONJ+], using the source's spectrum/coupling analysis as an additional premise. Sources: Witten (5.1)–(5.5), printed pp. 77–78; Berkovits and Witten (2004), hep-th/0406051v2, §1, printed pp. 1–2 and footnote 2. The original B-model's same-coupling loop statement is retained. The alternative open model's current-level discussion is not converted into a blanket decoupling impossibility.

Three literal discrepancies in Witten's printed formulas remain visible. Equation (4.48) reverses each bracket relative to the forward ordering used in (4.51), giving $(-1)^n$; we choose the latter orientation and do not calibrate the absolute sign. Equation (5.1) contains $(2\pi)^4$, while (5.2) prints $4(2\pi)^2$; a kinematic rewrite cannot change a Fourier delta normalization, so only the stripped rational function is used here. Finally, the determinant definition (2.3) conflicts with the factor two implied by (2.7) and the line preceding (5.2): the diagonal rank-one example below (XVIII.10.2) gives one, not two. This is an internal literal discrepancy, not a consistently different metric convention. No published erratum is asserted.

The calculations leave open questions of absolute D1/Yang–Mills coupling, global Penrose/Ward existence, all-degree and all-genus extensions, pure-Yang–Mills loop and full-QFT equivalence, and general no-go results.

References

Berkovits, N. and E. Witten (2004). "Conformal Supergravity in Twistor-String Theory". In: *JHEP* 08, p. 009. DOI: 10.1088/1126-6708/2004/08/009. arXiv: hep-th/0406051.

Britto, R. et al. (2005). "Direct Proof of Tree-Level Recursion Relation in Yang-Mills Theory". In: *Phys. Rev. Lett.* 94, p. 181602. DOI: 10.1103/PhysRevLett.94.181602. arXiv: hep-th/0501052.

Witten, E. (2004). "Perturbative Gauge Theory as a String Theory in Twistor Space". In: *Commun. Math. Phys.* 252, pp. 189–258. DOI: 10.1007/s00220-004-1187-3. arXiv: hep-th/0312171.

Chapter XVIII.11

4d Chern–Simons, twisted M-theory and integrability

XVIII.11.1 A position that becomes a spectral parameter

An integrable lattice model assigns a linear operator to the crossing of two lines. Each line carries a state space and a spectral parameter. The Yang–Baxter equation says that two sequences of three crossings define the same operator. Why should this algebraic consistency relation follow from a field theory? A useful answer makes the lines into gauge-theory defects. Their crossings can then be rearranged in a topological plane, while their spectral parameters become positions in an additional complex direction.

The extra direction has a specific job. In ordinary three-dimensional Chern–Simons theory a line can move in all three directions, subject to framing. Here only two directions are topological. A line stays at a fixed complex coordinate z, and its interactions depend on the differences of these coordinates. The complex direction separates lines whose projections cross. It also supplies a continuous label without spoiling topological invariance of their planar arrangement. The rational example will give

$$R_{V,W}(z_1 - z_2) = 1 + \hbar \frac{C_{V,W}}{z_1 - z_2} + O(\hbar^2), \qquad z_1 \neq z_2, \tag{XVIII.11.1}$$

where $C_{V,W}$ is the trace-dual quadratic invariant acting on the two line state spaces. We shall derive its coefficient by integrating an actual gauge propagator. The result will teach us both why the answer is holomorphic and why colliding spectral parameters are singular.

This is a holomorphic-topological theory of a partial connection, not ordinary four-dimensional Yang–Mills theory. Its relation to the string constructions of this volume is a frontier interface. A distinct five-dimensional theory, with a Moyal product in two complex directions, has a proposed protected origin in twisted M-theory. We shall calculate its associative algebra explicitly and state which part of that origin is

a supergravity construction and which part remains a conditional identification. The four-dimensional crossing calculation stands on its own; it does not establish that origin.

The prerequisites are exterior calculus with matrix-valued forms, an invariant Lie-algebra pairing, tensor products, and formal perturbation theory. Our principal physical object is the line defect. Follow first how its allowed motion fixes the field content, then how exchanging a gauge field produces its crossing operator. The classical Yang–Baxter equation will emerge from color invariance and an elementary identity among spectral differences. An exact fundamental GL_N example will then distinguish a classical consistency check from a full quantum relation.

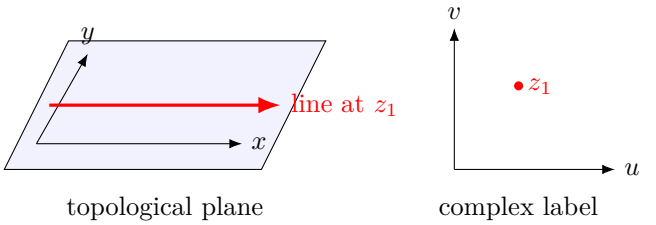


Figure XVIII.11.1: A line moves in the topological (x, y) plane while its complex position stays fixed. The second plane records the holomorphic label, rather than an additional direction of ordinary parallel transport. The missing $A_z\,dz$ component is part of the definition of the theory.

A repeated distinction will matter. A formal loop parameter is not an integer Chern–Simons level, and a complex gauge field does not by itself specify an integration contour. We work with source-local perturbative Feynman rules. The familiar topological and holomorphic vocabulary describes dependence on coordinates within that formal theory. It is not a statement that the full physical target theory loses all local degrees of freedom under an unrestricted limit.

XVIII.11.2 Partial flatness and the role of the boundary

Take $\mathbb{R}^2_{x,y} \times \mathbb{C}_z$, write $z = u + iv$, and orient it by $dx \wedge dy \wedge du \wedge dv$. Let $\mathfrak{g}$ be a finite-dimensional complex Lie algebra with a nondegenerate invariant symmetric pairing κ. For the matrix examples we use $\kappa(X, Y) = \mathrm{Tr}_{\mathrm{fund}}(XY)$. This choice fixes the dual basis; it does not introduce the factor $1/2$ of an orthonormal Hermitian-generator convention. Define

$$D = dx\,\partial_x + dy\,\partial_y + d\bar{z}\,\partial_{\bar{z}}, \qquad A = A_x\,dx + A_y\,dy + A_{\bar{z}}\,d\bar{z}, \qquad F = DA + A^2. \tag{XVIII.11.2}$$

All three coefficient fields may depend on all four real coordinates. There is no reality condition and no A_z. The missing component is what permits topological line transport in the plane and holomorphic dependence in z to coexist. It would be incorrect to

obtain this theory by silently setting one component of an arbitrary full Yang–Mills connection to zero.

A holomorphic one-form ω completes the three-form Chern–Simons density to a top form. On the rational patch $\omega = dz$ the convention is

$$S_4 = \frac{1}{2\pi} \int \omega \wedge \operatorname{Tr}\left(A\, DA + \frac{2}{3} A^3 \right), \qquad \exp(iS_4/\hbar). \tag{XVIII.11.3}$$

The exponent is formal. Under a common rescaling $z \mapsto \lambda z$, $\hbar \mapsto \lambda \hbar$, it is unchanged. Thus the spectral coordinate and $\hbar$ have the same scaling weight. No integer quantization of $\hbar^{-1}$, large-gauge invariance, or oscillatory integration contour is assumed here.

Let $B = \delta A$. The sign in the boundary term is worth deriving because the exterior factor ω reverses a familiar intermediate sign. Graded cyclicity gives

$$\delta \operatorname{Tr}(A\, DA) = \operatorname{Tr}(B\, DA + A\, DB) = 2 \operatorname{Tr}(B\, DA) - D \operatorname{Tr}(AB), \tag{XVIII.11.4}$$

$$\delta \operatorname{Tr}(\tfrac{2}{3} A^3) = 2 \operatorname{Tr}(BA^2), \tag{XVIII.11.5}$$

$$\delta \operatorname{CS}(A) = 2 \operatorname{Tr}(BF) - D \operatorname{Tr}(AB). \tag{XVIII.11.6}$$

On a smooth patch with $d\omega = 0$, holomorphic derivatives disappear after wedging with ω. Since $d(\omega \wedge \beta) = -\omega \wedge d\beta$, the variation of the action is

$$\delta S_4 = \frac{1}{\pi} \int \omega \wedge \operatorname{Tr}(BF) + \frac{1}{2\pi} \int_{\partial M} \omega \wedge \operatorname{Tr}(AB). \tag{XVIII.11.7}$$

Compactly supported variations, or sufficient falloff and compatible boundary conditions, remove the last term. Varying the three independent components then yields

$$F_{xy} = F_{x\bar{z}} = F_{y\bar{z}} = 0. \tag{XVIII.11.8}$$

These equations describe flat transport in the topological plane varying holomorphically in the transverse coordinate. They say nothing about $F_{z\bar{z}}$ of a full connection, because such a curvature component is not part of the defined field content.

For clarity, the curvature components in (XVIII.11.8) are

$$F_{xy} = \partial_x A_y - \partial_y A_x + [A_x, A_y], \tag{XVIII.11.9}$$

$$F_{x\bar{z}} = \partial_x A_{\bar{z}} - \partial_{\bar{z}} A_x + [A_x, A_{\bar{z}}], \tag{XVIII.11.10}$$

$$F_{y\bar{z}} = \partial_y A_{\bar{z}} - \partial_{\bar{z}} A_y + [A_y, A_{\bar{z}}]. \tag{XVIII.11.11}$$

The equation $F_{xy} = 0$ says that infinitesimal transport around a planar rectangle is trivial. The other two equations compare this transport at nearby antiholomorphic positions. In a local gauge where $A_{\bar{z}} = 0$, they reduce to $\partial_{\bar{z}} A_x = \partial_{\bar{z}} A_y = 0$. Thus the phrase "varying holomorphically" has a concrete local meaning. It uses a local gauge choice; it does not remove possible bundle information on a compact spectral curve.

A small Abelian example checks the boundary sign independently of noncommuting matrices. On the unit box in (x, y, u, v) take $A = x\, dy$ and $B = u\, d\bar{z}$, with $\omega = dz$. Directly, $\delta \operatorname{CS} = B\, dA + A\, dB$. After wedging dz, its coefficient in the real volume form integrates to $-i$ before the overall factor $1/(2\pi)$. The bulk expression $2dz \wedge B\, dA$

integrates to $-2i$. The boundary integral $dz \wedge AB$ contributes $+i$, so bulk plus boundary reproduces the direct answer. The fields deliberately do not vanish at the boundary. Suppressing that contribution would change the variational problem, even in this elementary Abelian case.

The infinitesimal gauge transformation is $B = D_A\epsilon = D\epsilon + [A, \epsilon]$. Associativity and the graded Leibniz rule give the Bianchi identity $D_A F = 0$. Substituting into the variation produces

$$\delta_\epsilon \operatorname{CS}(A) = D\left[2\operatorname{Tr}(\epsilon F) - \operatorname{Tr}(AD_A\epsilon)\right]. \tag{XVIII.11.12}$$

Consequently gauge invariance uses the same closure of ω and boundary assumptions as the variational problem. Gauge transformations are $A^g = g^{-1}Ag + g^{-1}Dg$; their behavior at a pole or an outer boundary is physical information, not a harmless gauge-fixing choice.

For example, the rational coordinate on the sphere has a double pole at infinity. The prescription used here requires $A = 0$ and $g = 1$ at a double pole. Simple poles need additional boundary information and cannot automatically use this prescription. A meromorphic one-form is closed away from its poles, but its distributional derivative can contribute at them. Omitting those contributions because a pole has measure zero loses exactly the term that an integration-by-parts argument must retain. Boundary conditions therefore enter before one concludes that the action is gauge invariant or that its only equations are the bulk partial-flatness equations.

XVIII.11.3 The spectral curve selects possible families

Why is the rational kernel only one member of a larger collection? Replace the complex plane by a compact smooth curve C and retain a nonzero meromorphic one-form ω with no zeros in the setup under consideration. The divisor of a meromorphic one-form has degree $2g - 2$, so

$$\deg \operatorname{div}(\omega) = \sum_p \operatorname{ord}_p(\omega) = 2g - 2. \tag{XVIII.11.13}$$

With no zeros, every nontrivial term on the left is a negative pole order. It follows that $g \leq 1$. On a sphere the total pole order is two. There may be one double pole or two simple poles. On a torus the degree is zero, so a zero-free one-form has no poles. This is a geometric restriction on the admissible action, rather than a classification of every integrable model.

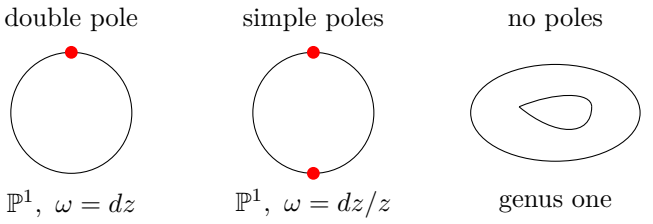


Figure XVIII.11.2: Zero-free meromorphic one-forms on compact curves give three basic geometric possibilities. The sphere carries one double pole for dz or two simple poles for dz/z; a torus carries a nowhere-zero holomorphic one-form. Boundary and bundle choices are still needed before an R-matrix is determined.

Curve	One-form and poles	Orientation toward an integrable family
$\mathbb{P}^1$	dz, double pole at infinity	Rational dependence on a local difference, with the double-pole prescription
$\mathbb{P}^1$	dz/z, simple poles at $0, \infty$	Trigonometric behavior after the additional pole conditions
Genus one	Holomorphic one-form	Elliptic behavior with the required bundle information

There is a simple way to read the trigonometric coordinate without asserting a complete model. On $\mathbb{C}^\times$, a local logarithm $w = \log z$ gives $dw = dz/z$. The one-form is locally constant in w, while w has a periodic identification. This explains why replacing an additive spectral coordinate by a multiplicative one changes the natural functional dependence. It does not determine the treatment of the two removed endpoints. Likewise a holomorphic one-form on a torus is locally dw, but its periods and the gauge bundle are global information. Local constancy of the differential therefore does not make these theories copies of the rational plane.

The local coordinate at the double pole makes its order transparent. Setting $w = 1/z$ gives $dz = -dw/w^2$. For dz/z the same change gives $-dw/w$, so both 0 and infinity are simple poles. The distinction is not just the number of marked points. The admissible boundary conditions change, and the field theory can consequently have different defect algebras. The genus alone does not choose a unique quantum R-matrix.

There is also a reason to state the no-zero assumption explicitly. Where ω vanishes, the coefficient of the kinetic operator degenerates. The propagator and perturbative argument used below do not extend by simply dividing by that zero. Studying such points would require additional local information. We now restrict to the rational patch with $\omega = dz$, keeping its boundary prescription implicit only after having stated it.

XVIII.11.4 A nonholomorphic propagator produces a holomorphic crossing

To calculate one exchange between two lines, introduce the flat auxiliary metric $ds^2 = dx^2 + dy^2 + dz\,d\bar{z}$ and impose

$$\partial_x A_x + \partial_y A_y + 4\partial_z A_{\bar{z}} = 0. \tag{XVIII.11.14}$$

The metric is a gauge-fixing aid. It does not turn the planar directions into metric-dependent observables. Strip off the inverse pairing in color space and the factor $\hbar$ of a contraction. With $\rho^2 = x^2 + y^2 + z\bar{z}$, the remaining two-form propagator is

$$P = \frac{x\,dy \wedge d\bar{z} + y\,d\bar{z} \wedge dx + 2\bar{z}\,dx \wedge dy}{2\pi\rho^4}. \tag{XVIII.11.15}$$

A useful way to reconstruct its numerator and denominator is

$$P = -\frac{1}{4\pi}\,(dy \wedge d\bar{z}\,\partial_x + d\bar{z} \wedge dx\,\partial_y + 4dx \wedge dy\,\partial_z)\,\frac{1}{\rho^2}. \tag{XVIII.11.16}$$

In particular, $\partial_z \rho^{-2} = -\bar{z}\rho^{-4}$. This both fixes the bar on z and identifies the fourth power in the denominator. The middle component equality in the source's equation (4.4) appears to omit a square; its derivative expression and two-form equation (4.5) give the consistent expression above. This is a local reading diagnosis, not a published erratum.

The off-origin closure can also be seen in real coordinates. Set $Q = \rho^{-4}$ and let N denote the numerator without $1/(2\pi)$. The three terms in dN all contribute to the same top form after wedging dz, giving

$$dz \wedge dN = 4\,dx \wedge dy \wedge dz \wedge d\bar{z}.$$

Differentiating Q supplies the opposite contribution. In $dz \wedge dQ \wedge N$, only derivatives along $x, y, \bar{z}$ survive, and their numerator is proportional to $x^2 + y^2 + z\bar{z} = \rho^2$. Consequently

$$dz \wedge dQ \wedge N = -4\rho^{-4} dx \wedge dy \wedge dz \wedge d\bar{z},$$

which cancels $Q\,dz \wedge dN$ whenever $\rho \neq 0$. The cancellation shows why the radial denominator and complex numerator belong together. A merely holomorphic guess for P would miss this kinetic inverse.

Away from the origin, differentiating the displayed two-form gives $dz \wedge dP = 0$. The gauge contraction also vanishes,

$$(\partial_x \iota_x + \partial_y \iota_y + 4\partial_z \iota_{\bar{z}})P = 0, \qquad \iota_{\bar{z}} = \tfrac{1}{2}(\iota_u + i\iota_v). \tag{XVIII.11.17}$$

These tests constrain the shape of the propagator but do not fix a multiplicative constant. The kinetic inverse must also have the correct contact term at the origin. A singular kernel can have zero derivative at every other point and still have a nonzero distributional derivative.

To determine that contact term, restrict to the unit sphere and replace the singular kernel inside the unit ball by the smooth extension

$$P_{\mathrm{ext}} = \frac{1}{2\pi}(x\,dy \wedge d\bar{z} + y\,d\bar{z} \wedge dx + 2\bar{z}\,dx \wedge dy). \tag{XVIII.11.18}$$

It agrees with P on the sphere. Direct differentiation yields

$$dz \wedge dP_{\mathrm{ext}} = \frac{4}{2\pi} dx \wedge dy \wedge dz \wedge d\bar{z} = \frac{-8i}{2\pi} dx \wedge dy \wedge du \wedge dv. \tag{XVIII.11.19}$$

The real volume of the unit four-ball is $\pi^2/2$. Stokes' theorem and the equality on its boundary therefore give

$$\frac{i}{2\pi}\int_{B^4} dz \wedge dP = \frac{i}{2\pi}\frac{-8i}{2\pi}\frac{\pi^2}{2} = 1, \qquad \frac{i}{2\pi} dz \wedge dP = \delta_0. \tag{XVIII.11.20}$$

The last equality is distributional. The smooth extension evaluates its flux, not a fictitious smooth derivative of the singular expression at the origin. Replacing $\bar{z}$ by z spoils the derivative structure; rescaling P preserves off-origin closure but spoils the unit contact term. Both parts of the calculation are necessary.

Now place an x-directed line at z_1 and a y-directed line at z_2. Let $d = z_1 - z_2 \neq 0$. In the crossing orientation used here their pullback contraction is

$$I_1 = \hbar C_{V,W} \int_{\mathbb{R}^2} \frac{\bar{d}\,dx\,dy}{\pi(x^2 + y^2 + |d|^2)^2}. \tag{XVIII.11.21}$$

The factor of $\bar{d}$ looks nonholomorphic. Integration over the two topological directions will remove this dependence. Put $a_0^2 = |d|^2 > 0$ to separate a positive real radial scale from the complex spectral difference. In polar coordinates,

$$\int_{\mathbb{R}^2} \frac{dx\,dy}{(x^2 + y^2 + a_0^2)^2} = 2\pi \int_0^\infty \frac{r\,dr}{(r^2 + a_0^2)^2} \tag{XVIII.11.22}$$

$$= \pi \int_{a_0^2}^\infty \frac{ds}{s^2} = \frac{\pi}{a_0^2}. \tag{XVIII.11.23}$$

Thus $I_1 = \hbar C_{V,W}\,\bar{d}/|d|^2 = \hbar C_{V,W}/d$.

A second integration route makes the convergence assumption visible without rotational coordinates. For $b_0^2 = x^2 + a_0^2$, set $y = b_0 \tan\theta$. Then

$$\int_{-\infty}^\infty \frac{dy}{(y^2 + b_0^2)^2} = \frac{1}{b_0^3}\int_{-\pi/2}^{\pi/2} \cos^2\theta\,d\theta = \frac{\pi}{2b_0^3}, \tag{XVIII.11.24}$$

$$\int_{-\infty}^\infty \frac{dx}{(x^2 + a_0^2)^{3/2}} = \left[\frac{x}{a_0^2\sqrt{x^2 + a_0^2}}\right]_{-\infty}^{\infty} = \frac{2}{a_0^2}. \tag{XVIII.11.25}$$

The product again gives π/a_0^2. Absolute convergence holds because $a_0 > 0$ and the denominator falls as the fourth power of distance. At $d = 0$, the integral develops

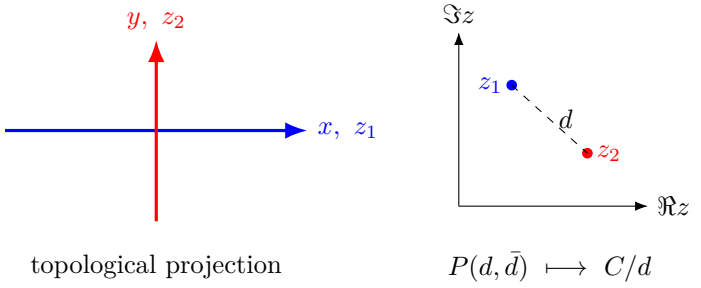


Figure XVIII.11.3: Two oriented lines cross in their topological projection and sit at distinct complex positions. The kernel before integration depends on d and $\bar{d}$; the integrated correction is $\hbar C/d$. Reversing the stated crossing orientation changes the associated sign convention. The coincident label $d = 0$ is excluded.

a short-distance singularity and these operations no longer define a finite crossing operator.

The propagator is therefore allowed to depend on the auxiliary metric and on $\bar{z}$, while the integrated observable has the required holomorphic spectral dependence. The local crossing is extracted with framing fixed in the stretched-topological-metric limit. Orthogonal lines suffice for this first calculation. For $|d| \gg |\hbar|$ the correction is small, whereas the perturbative expansion is nonuniform near $d = 0$. The pole is a feature of the operator product, not an invitation to replace $R(0)$ by a finite matrix.

XVIII.11.5 Color invariance gives the classical Yang–Baxter equation

The color factor is defined by the pairing, not merely by the name of a gauge algebra. If t_a, t^a are dual bases, let $C = \sum_a t_a \otimes t^a$. In the fundamental representation of $\mathfrak{gl}_N$, matrix units satisfy $\mathrm{Tr}(E_{ij}E_{kl}) = \delta_{jk}\delta_{il}$. Hence

$$C_{\mathfrak{gl}_N} = \sum_{i,j} E_{ij} \otimes E_{ji} = P, \qquad P(v \otimes w) = w \otimes v. \tag{XVIII.11.26}$$

For example, acting on $e_k \otimes e_l$, only $j = k$ and $i = l$ survive, giving $e_l \otimes e_k$. This proves the identity for every N, rather than inferring it from a few small matrices.

The identity matrix has squared norm $\mathrm{Tr}\, I^2 = N$. Splitting off this orthogonal central direction gives

$$C_{\mathfrak{sl}_N} = P - \frac{1}{N} I \otimes I. \tag{XVIII.11.27}$$

On $\mathbb{C}^2 \otimes \mathbb{C}^2$, the GL_2 tensor exchanges $e_1 \otimes e_2$ and $e_2 \otimes e_1$ and fixes $e_i \otimes e_i$. The SL_2 tensor also subtracts half of each original vector. The central term disappears inside commutators, but it changes the crossing operator itself. This distinction will become decisive in the exact quantum example.

Consider three line labels and set

$$a = z_1 - z_2, \qquad b = z_2 - z_3, \qquad z_1 - z_3 = a + b, \qquad ab(a+b) \neq 0. \quad \text{(XVIII.11.28)}$$

The spectral classical Yang–Baxter equation is

$$[r_{12}(a), r_{13}(a+b)] + [r_{12}(a), r_{23}(b)] + [r_{13}(a+b), r_{23}(b)] = 0. \qquad \text{(XVIII.11.29)}$$

Its general proof separates color from geometry. Invariance of κ, equivalently $\kappa([X,Y],Z) = \kappa(X,[Y,Z])$, implies that the diagonal action on the two factors annihilates C. Applying that identity within three tensor factors gives

$$[C_{12}, C_{13} + C_{23}] = 0, \qquad [C_{12} + C_{13}, C_{23}] = 0. \qquad \text{(XVIII.11.30)}$$

To see what is used, expand the first commutator as sums of $[t_a, t_b] \otimes t^a \otimes t^b$ and $t_a \otimes [t^a, t_b] \otimes t^b$. Pair the first two slots with arbitrary X, Y. Their coefficients cancel by the displayed invariance of κ and antisymmetry of the bracket. Nondegeneracy then gives the tensor identity. The argument applies to any finite-dimensional quadratic Lie algebra; semisimplicity is unnecessary.

Let $X_0 = [C_{12}, C_{13}]$. The two identities imply $[C_{12}, C_{23}] = -X_0$ and $[C_{13}, C_{23}] = X_0$. Substitution of $r(d) = C/d$ reduces the whole equation to

$$X_0 \left[\frac{1}{a(a+b)} - \frac{1}{ab} + \frac{1}{(a+b)b} \right] = X_0 \frac{b - (a+b) + a}{ab(a+b)} = 0. \qquad \text{(XVIII.11.31)}$$

The additive relation among the three spectral differences is doing real work. Three arbitrary independent denominators would not cancel. Nor would replacing $1/d$ by $1/d^2$ preserve this identity. The result is a spectral equation, not a statement that a constant invariant tensor solves the nonspectral classical equation.

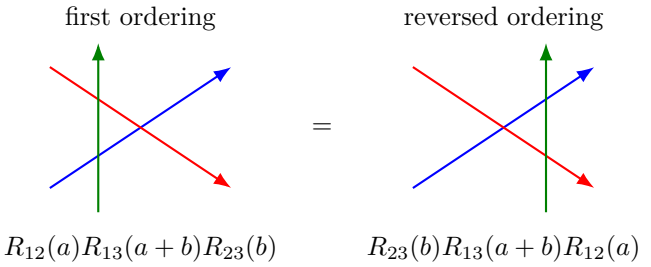


Figure XVIII.11.4: The two triple-crossing orderings use the same three pairs. Their labels are a, b, and $a+b$, not three independent numbers. The classical cancellation combines invariant color tensors with this additive relation. Quantum use of the picture also requires compatible line and framing prescriptions.

One can check the color relation without naming a particular representation. Write $[t_a, t_b] = f_{ab}{}^c t_c$ and lower an index with κ. Invariance makes the resulting three-index tensor antisymmetric under exchanging any two adjacent arguments. The same trilinear

tensor appears in all three commutators of (XVIII.11.30), with signs fixed by which tensor slot contains the bracket. The cancellation is therefore an identity in the universal enveloping algebra tensored three times. Applying representations V_1, V_2, V_3 preserves it. What may fail quantum mechanically is the existence of the corresponding line after renormalization, not this classical tensor identity.

It is useful to separate two limits. For fixed distinct labels, the formal expansion organizes the quantum correction by powers of $\hbar$. For fixed $\hbar$ and a shrinking spectral difference, the rational term grows without bound. The latter does not test a higher-order coefficient at an ordinary point; it probes a singular operator product. These limits cannot be exchanged by treating $\hbar/d$ as small uniformly on the whole spectral curve. The excluded divisors $a = 0$, $b = 0$ and $a + b = 0$ in the classical equation express the same fact for three lines.

To connect this calculation to quantum consistency, write $R_{ij} = 1 + \hbar r_{ij} + \hbar^2 s_{ij} + \cdots$ in

$$R_{12}(a)R_{13}(a+b)R_{23}(b) = R_{23}(b)R_{13}(a+b)R_{12}(a). \tag{XVIII.11.32}$$

The order-$\hbar$ sums coincide. At order $\hbar^2$, each s_{ij} appears once on both sides and cancels. The remaining pairwise products differ precisely by the three commutators in (XVIII.11.29). Thus the one-gluon crossing passes the first nontrivial quantum consistency condition. This deduction neither supplies the higher coefficients nor proves that an arbitrary classical representation defines an anomaly-free quantum line.

XVIII.11.6 An exact fundamental matrix and the framing qualification

For fundamental GL_N state spaces there is a complete algebraic example,

$$R_0(a) = I + \frac{\hbar P}{a}. \tag{XVIII.11.33}$$

Substituting into (XVIII.11.32) gives a cubic polynomial in $\hbar$. Its constant and linear terms agree, and its quadratic terms vanish by the classical calculation. The cubic terms agree because

$$P_{12}P_{13}P_{23} = P_{23}P_{13}P_{12}. \tag{XVIII.11.34}$$

Both sides send $v_1 \otimes v_2 \otimes v_3$ to $v_3 \otimes v_2 \otimes v_1$. This proves the exact relation for every N. It is an algebraic result about the fundamental permutation operator; it is not a summation of all gauge-theory loop diagrams.

For a concrete two-state example, choose the ordered basis $e_1 \otimes e_1$, $e_1 \otimes e_2$, $e_2 \otimes e_1$, $e_2 \otimes e_2$. Then

$$R_0(a) = \begin{pmatrix} 1+\hbar/a & 0 & 0 & 0 \\ 0 & 1 & \hbar/a & 0 \\ 0 & \hbar/a & 1 & 0 \\ 0 & 0 & 0 & 1+\hbar/a \end{pmatrix}. \tag{XVIII.11.35}$$

The crossing mixes the two middle states by exchanging their colors. Their sum and difference diagonalize this block. The same exchange mechanism works in higher rank,

where the symmetric and antisymmetric subspaces replace these two combinations. Thus diagonalizing P, rather than a large matrix entry by entry, is the natural way to understand the spectrum.

On symmetric tensors $P = +1$, and on antisymmetric tensors $P = -1$. The two eigenvalues of R_0 are therefore $1 + \hbar/a$ and $1 - \hbar/a$. Since $P^2 = I$,

$$R_0(a)R_{0,21}(-a) = \left(1 - \frac{\hbar^2}{a^2}\right) I. \tag{XVIII.11.36}$$

Multiplying an R-matrix by any scalar function preserves QYBE, because the same three scalar factors occur on each side. One useful normalization is

$$\widehat{R}(a) = \frac{aI + \hbar P}{a + \hbar}, \qquad \lambda_{\mathrm{sym}} = 1, \quad \lambda_{\mathrm{anti}} = \frac{a - \hbar}{a + \hbar}. \tag{XVIII.11.37}$$

Where both factors are defined, $\widehat{R}(a)\widehat{R}_{21}(-a) = I$. The normalization changes the leading coefficient to $(P - I)/a$. It must therefore be declared before comparison with the gauge-normalized C/a. Strict algebraic unitarity in this example fixes a scalar convention; it does not prove a physical Hilbert-space unitarity statement for the complex gauge theory.

Now try the apparently natural truncation $R_{\mathrm{sl}}(a) = I + \hbar(P - I/N)/a$. The central shift leaves CYBE unchanged, but QYBE at cubic order contains products rather than commutators. To exhibit the difference explicitly, put $Q_{ij} = P_{ij} - cI$ with $c = 1/N$. Expanding gives

$$Q_{12}Q_{13}Q_{23} - Q_{23}Q_{13}Q_{12} = -c\big([P_{12}, P_{13}] + [P_{12}, P_{23}] + [P_{13}, P_{23}]\big) \tag{XVIII.11.38}$$

$$= -c[P_{12}, P_{13}], \tag{XVIII.11.39}$$

where the cubic permutation terms cancel and the same invariant-tensor relations reduce the three commutators. For $N = 2$ the last operator is nonzero. For instance, on $e_1 \otimes e_1 \otimes e_2$, the commutator gives $e_1 \otimes e_2 \otimes e_1 - e_2 \otimes e_1 \otimes e_1$. At $a = 2$, $b = 3$, $\hbar = 1$ the QYBE residual is therefore $-1/60$ times that vector. This excludes the displayed truncation as an exact solution. It does not exclude scalar and higher-order completed SL_N quantum matrices.

The planar picture also acquires a quantum geometric qualification. In the clockwise angle convention for a bent line, the source's framing result keeps

$$z - \frac{\hbar h^\vee}{2\pi}\varphi \quad \text{constant along the line}, \qquad h^\vee = N \text{ for } \mathfrak{sl}_N \tag{XVIII.11.40}$$

with the trace convention used here. Thus fixed z is the classical straight-line picture. After a full planar turn the tangent angle changes, so a simple closed planar fixed-z line is obstructed within this prescription. The standard same-function QYBE uses the compatible framing and nearly parallel crossing limit. One should not import ordinary knot invariance into this setting.

There are source-local normalization hazards worth retaining. The opening of the source's section 6 writes π where its section 3.6, equation (6.4), and later derivation give 2π; its printed (6.5) sign conflicts with the stated cancellation. A local sign

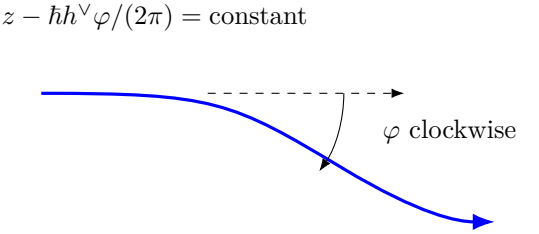


Figure XVIII.11.5: A clockwise bend changes the tangent angle φ. The quoted quantum line prescription preserves the shifted combination $z - \hbar h^\vee \varphi/(2\pi)$ rather than fixed z alone. The curve illustrates the local prescription, not an unrestricted knot observable.

check is possible without recomputing the loop diagram. Write $\kappa_0 = \hbar h^\vee/(2\pi)$ and $z(x) = z_0 - \kappa_0 y'(x)$. Integration of a total derivative with vanishing endpoints gives

$$\int dx\, \partial_x \epsilon(x, z(x))\big|_{z \text{ fixed}} = -\int dx\, z'(x) \partial_z \epsilon = \kappa_0 \int dx\, y''(x) \partial_z \epsilon. \tag{XVIII.11.41}$$

With $\varphi \simeq -y'$, this agrees with (XVIII.11.40) and the stated anomaly cancellation. We quote the loop result, retaining these local reading qualifications; no published erratum or new independent loop calculation is asserted.

XVIII.11.7 A distinct five-dimensional noncommutative theory

The next theory shares the partial-connection mechanism but changes the geometry and the coefficient algebra. On $\mathbb{R}_t \times \mathbb{C}^2_{Z,W}$ define

$$D_5 = dt\, \partial_t + d\bar{Z}\, \partial_{\bar{Z}} + d\bar{W}\, \partial_{\bar{W}}, \quad A = A_t dt + A_{\bar{Z}} d\bar{Z} + A_{\bar{W}} d\bar{W}, \quad \Omega_2 = dZ \wedge dW. \tag{XVIII.11.42}$$

There is one topological direction and two holomorphic directions. The coefficients take values in the full associative matrix algebra $\mathfrak{gl}_N$, now with a Moyal product,

$$f \star g = m \exp\left[\frac{\epsilon}{2}(\partial_Z \otimes \partial_W - \partial_W \otimes \partial_Z)\right](f \otimes g). \tag{XVIII.11.43}$$

Here m multiplies the two factors after differentiation. This is a formal series, terminating on polynomials. The parameter ϵ measures noncommutativity. It is distinct from $\hbar$ of the four-dimensional theory.

The simplest calculation gives $Z \star W = ZW + \epsilon/2$ and $W \star Z = ZW - \epsilon/2$, so $[Z, W]_\star = \epsilon$. Quadratic polynomials already see the second-order term,

$$Z^2 \star W^2 = Z^2 W^2 + 2\epsilon ZW + \frac{\epsilon^2}{2}, \tag{XVIII.11.44}$$

$$W^2 \star Z^2 = Z^2 W^2 - 2\epsilon ZW + \frac{\epsilon^2}{2}, \tag{XVIII.11.45}$$

$$[Z^2, W^2]_\star = 4\epsilon ZW. \tag{XVIII.11.46}$$

The even-order contribution cancels in this commutator, but it remains necessary for associativity of the full product. It cannot be discarded just because these two brackets look first-order.

To prove associativity, label three tensor factors and let B_{ij} be the constant bidifferential operator between factors i, j. All coordinate derivatives commute, so B_{12}, B_{13}, B_{23} commute. Leibniz' rule lets the outer product act on each factor of the inner product, giving in either order

$$(f \star g) \star h = f \star (g \star h) = m_3 \exp\left[\frac{\epsilon}{2}(B_{12} + B_{13} + B_{23})\right](f \otimes g \otimes h). \quad \text{(XVIII.11.47)}$$

This is an all-order formal proof for the constant bivector, not an extrapolation from the displayed quadratic example. By contrast, $f \star_1 g = fg + (\epsilon/2)\{f, g\}$ is generally only a first-order approximation. Taking $f = Z^2$, $g = W$, $h = W$ gives

$$(Z^2 \star_1 W) \star_1 W - Z^2 \star_1 (W \star_1 W) = \frac{\epsilon^2}{2}. \quad \text{(XVIII.11.48)}$$

The missing second-order term is precisely what the exponential product supplies.

Matrix multiplication and the Moyal product are used together. Ordinary traceless matrices do not close under the resulting gauge bracket. With $T = \mathrm{diag}(1, -1)$,

$$[ZT, WT]_\star = \epsilon T^2 = \epsilon I. \quad \text{(XVIII.11.49)}$$

The result has a central component, so an ordinary $\mathfrak{sl}_2$ restriction is inconsistent with these gauge parameters. This is a different reason for retaining $\mathfrak{gl}_N$ from the scalar issue in the four-dimensional exact R example.

With compact support or sufficient falloff to justify integration by parts, the action is

$$S_5 = \frac{1}{\delta}\int \Omega_2 \wedge \mathrm{Tr}\left(\frac{1}{2}AD_5A + \frac{1}{3}A \star A \star A\right). \quad \text{(XVIII.11.50)}$$

The loop parameter is δ, distinct from both ϵ and $\hbar$. The integral of a star product is cyclic under the same support assumptions, because derivative terms can be integrated by parts. Since D_5 is a derivation,

$$\delta S_5 = \frac{1}{\delta}\int \Omega_2 \wedge \mathrm{Tr}\left(\delta A \star (D_5A + A \star A)\right) + \text{boundary terms}. \quad \text{(XVIII.11.51)}$$

Gauge transformations use the star commutator. Even at rank one the equation is nonlinear because the scalar coefficient functions need not star commute. The common Chern–Simons form has thus survived a change of associative algebra; the physical dimensions and deformation parameters have changed with it.

XVIII.11.8 What the twisted M-theory origin supplies

A proposed string or M-theory origin should identify the background, the protected operation, and the resulting field theory. In the source considered here these steps have

different logical strength. First there is a complex supergravity construction. Given a G_2-holonomy seven-manifold with a circle isometry preserving its G_2 structure and a hyperkähler four-manifold, the source constructs an Ω background whose generalized Killing spinor squares to ϵV. Its three-form includes $V^\flat \wedge \omega^{(0,2)}$. This is a supergravity result used as an input here; we do not reproduce its eleven-dimensional field-equation calculation.

The protected identification on $TN_k \times \mathbb{R}^3 \times \mathbb{C}^2$ is a further proposed step. In the source's convention it leads to the $\mathfrak{gl}_{k+1}$ version of (XVIII.11.50). The reasoning changes the Taub–NUT radius by a Q-exact deformation within a specified background family, including the normalization of the supercharge and C field. At small radius it uses a type IIA description with D6-branes, a conjectural twisted type IIA supergravity input, the noncommutativity induced by a B field, and Ω localization from seven to five dimensions. Each of these operations has a role in the proposed physical dictionary. The source also records that an explicit map of the classical solutions was not obtained. Thus the protected identification is a frontier proposal with concrete supporting arguments, rather than a definition of full M-theory.

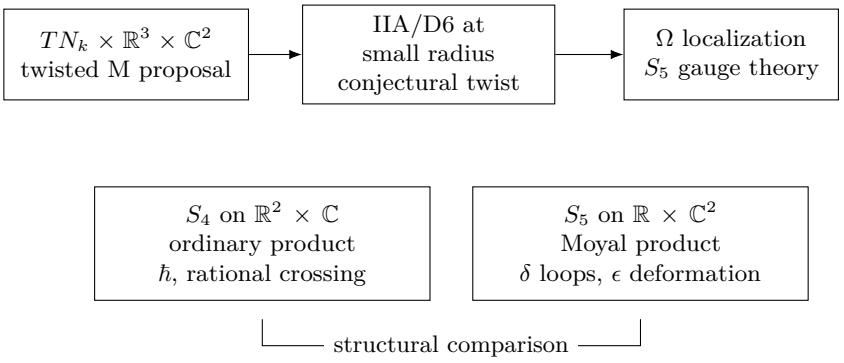


Figure XVIII.11.6: The upper path reports the source-conditioned twisted-M proposal, including its conjectural twisted IIA input. The lower comparison lists structural features of the two partial-connection theories. It is a comparison, with no derived arrow from the five-dimensional action to the four-dimensional crossing theory. The parameters δ, ϵ, and $\hbar$ remain distinct.

One supporting result is an obstruction and deformation calculation for quantizing the five-dimensional gauge theory. The precise statement concerns $\mathbb{C}^2$, uniformly in matrix rank. It requires $\mathbb{C}^\times$ compatibility, $\mathfrak{sl}_2$ invariance, and holomorphic translation invariance. Antiholomorphic translations are BRST or homotopically trivial, and scaling transforms the deformation parameters as well as the coordinates. Coefficients may contain $\epsilon^{-r}\delta^n$ only for $r \leq n$. The two deformation types are over $\mathbb{C}[N]$ in the uniform-rank treatment, with rank dependence allowed, and are absorbed into redefinitions of ϵ and δ. This is not a statement that every fixed-rank quantization has exactly two rank-independent numerical choices.

For example, a term proportional to $\delta\epsilon^{-1}$ is allowed by $r \leq n$, whereas $\delta\epsilon^{-2}$ at the

same loop order is outside the stated coefficient class. At order δ^2, the term $\delta^2\epsilon^{-2}$ is allowed. This hierarchy belongs to the formal coefficient ring, not to an estimate that bounds a convergent sum. It gives a concrete meaning to the restriction before any physical limit is considered. Rank dependence is also part of the assertion: a polynomial in N may multiply a permitted deformation. Forgetting that coefficient space would change the quoted theorem.

The two supporting directions answer different questions. The obstruction calculation asks whether a local formal gauge theory can be consistently quantized under specified symmetries. The defect comparison asks whether two constructions produce the same protected algebra in a stable tree-level regime. Neither calculation by itself reconstructs all spacetime observables. Together they make the protected proposal calculable in two ways, while leaving its stronger finite-rank and quantum identifications open.

The coefficient restriction explains an important limit. A formal expansion in δ can involve negative powers of ϵ, so putting $\epsilon = 0$ at fixed nonzero δ is not an allowed specialization of the theorem. A heuristic hierarchy $|\delta| \ll |\epsilon| \ll 1$ does not prove analytic convergence. The proof also leaves the modified infinity boundary condition on $S^1 \times \mathbb{P}^1 \times \mathbb{C}$ outside its scope. It cannot establish the nonzero-δ holographic conjecture that uses that boundary problem. We quote this quantization theorem with its hypotheses; we do not reproduce its BV cohomology calculation.

A second quantitative comparison concerns protected M5-defect algebras at $\delta = 0$. One side is the stable $GL(N+M|M)$-invariant free-field algebra as $M \to \infty$ at fixed super-rank N. The other is a tree-level boundary algebra. In the source both give the algebra denoted $W_{k+1+\infty}$ with central parameter N. This comparison checks a protected algebra in a stable, tree-level regime. It does not identify the finite-N, nonzero-δ theories. The proposed nonzero-δ Yangian identification remains conjectural. Nor do the quantization calculation and the defect comparison count as two independent constructions of full M-theory; they test different controlled consequences of the proposed sector.

The relation to the first half of this chapter is therefore a precise structural comparison. Both theories use three partial-connection components, a holomorphic volume form that completes the Chern–Simons density, and an associative algebra governing operations on defects. The four-dimensional theory has two topological directions and one complex direction; the five-dimensional theory has one topological direction and two complex directions with a Moyal product. To assert an actual reduction between them would require a specified geometry, boundary conditions, parameter map, surviving field content, and a derivation of the reduced action and defect observables. Those ingredients have not been supplied by the comparison. The explicit rational crossing remains a useful calculation without that extra arrow.

The chapter's output is a method for turning position into a spectral parameter and for testing the resulting algebra. Normalize the contact term before integrating the crossing, separate color identities from spectral identities, and distinguish exact fundamental examples from general quantum representation claims. The twisted-M proposal then shows how a related partial-connection theory can enter a protected string-theoretic construction, while leaving its genuinely stronger claims visible as future physical questions.

What an exact permutation matrix tests

The fundamental matrix example lets us distinguish three assertions without solving a general quantization problem. The propagator gives a first-order crossing with the gauge-normalized invariant tensor. Color invariance then yields the classical Yang–Baxter equation. In the specified GL_N fundamental representation, the permutation operator gives an exact algebraic solution. The third assertion has more algebraic information than the first two, but it still does not evaluate every gauge-theory loop.

To check the exact example, expand the two products in powers of $\hbar$. The linear terms only sum the three pairwise exchanges. The quadratic terms are controlled by the classical commutator identity with the stated spectral denominators. The cubic terms test an ordered product of three permutations. Acting on a pure three-tensor makes their equality explicit, as in (XVIII.11.34). This last step is not just another commutator test, which explains why a central modification can preserve the classical equation yet spoil the proposed exact truncation.

The two-state block also explains the scalar normalization. Its sum and difference eigenvectors are symmetric and antisymmetric tensors. Dividing by the declared scalar makes the symmetric eigenvalue one and changes the antisymmetric eigenvalue to the displayed rational ratio. Multiplying a solution by a scalar preserves the Yang–Baxter relation, but changes its first-order identity component. A comparison with the propagator must therefore specify which scalar has been chosen. Algebraic inversion of these matrices is a different question from positivity or unitarity of a physical Hilbert space.

The twisted-M discussion supplies a separate proposal for the origin of the theory. It is not obtained by reading the exact permutation matrix backwards. Likewise, the distinct five-dimensional theory is not an unwritten derivation of the four-dimensional model. Keeping these routes separate makes the chapter's integrability result usable without importing a stronger spacetime claim. The final chapter reverses the direction more explicitly, starting with a defined field theory and organizing its partition function as a surface expansion.

Written exercises

The separate question sheet contains seven problems on variation and poles, propagator normalization, two crossing integrals, invariant tensors, quantum matrices, the Moyal product, and the twisted-M premises. Work the mathematical problems before consulting the separate worked solutions. The questions use the orientations, traces and formal parameters of this chapter. In particular, keep ϵ, δ and $\hbar$ distinct.

Sources and scope

The rational partial-connection action, boundary variation, normalized gauge kernel, two crossing integrations, invariant-tensor CYBE, exact fundamental GL_N matrix, scalar normalization and explicit SL_N truncation obstruction are bounded mathematical

statements conditional on the specified formal gauge theory [MATH]. The constant-bivector Moyal product and its gauge-action variation are mathematical statements with the stated support conditions [MATH]. The complex Ω background is an imported supergravity result [SUGRA]; the protected twisted-M identification remains source-bound [CONJ+]. The quantization theorem and stable/tree-level algebra comparison are quoted in their stated domains [MATH].

The four-dimensional source is Costello et al. (2018), arXiv version 2. The action and pole geometry are in section 3.1–3.2, printed pages 11–16; the propagator and crossing are in (4.4)–(4.14), printed pages 31–32. Scalar ambiguity and framing are in sections 3.5–3.6 and 6, with line anomalies in section 8. The local denominator, factor-of-two and cancellation-sign hazards discussed above are reading diagnoses, not published errata. The five-dimensional source is Costello (2016), version 1. Its theorem 1.0.1 gives the complex background; proposition 1.2.1 reports the protected origin; theorem 9.0.3, printed page 41 and appendix, states the quantization result. Propositions 15.3.1 and 17.3.1, printed pages 74 and 89, supply the stable free-field and tree-level boundary comparisons. Section 18, printed pages 95–96, identifies the modified-boundary limitation.

The four-dimensional calculation uses Euclidean coordinates, the fundamental trace and the partial connection specified above. The ordinary three-dimensional integer level plays no role. The all-rank identities follow from the displayed algebra. The four- and five-dimensional constructions use separate physical inputs, and no reduction from one to the other is derived here.

References

Costello, K. (2016). *M-theory in the Omega-background and 5-dimensional non-commutative gauge theory*. arXiv: 1610.04144 [hep-th].

Costello, K., E. Witten, and M. Yamazaki (2018). "Gauge Theory and Integrability, I". In: *ICCM Notices* 6.1, pp. 46–119. DOI: 10.4310/ICCM.2018.v6.n1.a6. arXiv: 1709.09993 [hep-th].

Chapter XVIII.12

Two-dimensional Yang–Mills and the Gross–Taylor expansion

A gauge theory can produce a string expansion even when the gauge theory was defined first. Two-dimensional Yang–Mills gives a particularly concrete example. Gauss' law removes local gluon oscillators, but a spatial circle retains its holonomy and a spectrum of electric fluxes. The exact partition function is a sum over representations. At large rank, the same representation data can be reorganized into permutations of sheets, branch points and powers of the Euler characteristic of a covering surface.

The useful question is how much geometry this reorganization determines. We shall derive an exact identity at fixed polynomial degree, then read its ordinary-cover terms geometrically. Degree two already exposes the branch sign, the covering symmetry factor and the subtraction of disconnected surfaces. It also shows why twist insertions cannot be discarded. Two further examples locate the limits of a naive extrapolation: an inverse twist element becomes singular at forbidden rank, and opposite orientations in $SU(N)$ fail to factorize. The sphere density bound finally separates this coefficientwise dictionary from a statement about the entire large-N theory.

Reader contract and direction of construction

We use elementary compact-group representation theory and canonical gauge quantization. Covering monodromy and the required symmetric-group algebra are developed here. The QFT is the independently defined heat-kernel theory on a closed connected oriented surface M_G of genus G and area $A > 0$, with normalized Haar measure and zero theta angle. Unlike the direction in Chapter XVIII.1, this chapter starts from QFT data and constructs a string counting dictionary. The fixed-degree polynomial $U(N)$ sector is a selected part of the full theory.

XVIII.12.1 Electric flux and sewing

The surviving coordinate on a spatial circle of circumference L is its holonomy U. A gauge transformation changes U by conjugation, so physical wave functions are class functions. With Haar measure of total mass one, irreducible characters form an orthonormal basis,

$$\langle \chi_R, \chi_S \rangle = \int dU\, \overline{\chi_R(U)} \chi_S(U) = \delta_{RS}. \tag{XVIII.12.1}$$

The representation R labels an electric state rather than a local particle. This makes the spectral calculation possible without a tower of gluon modes.

We first fix the normalization, since a factor of two here would change every branch coefficient. For Hermitian generators with $\mathrm{Tr}_f(T^a T^b) = \delta^{ab}/2$, the book and Gross–Taylor actions are

$$S_E = \frac{1}{4g_{\mathrm{YM}}^2} \int F^a_{\mu\nu} F^a_{\mu\nu} = \frac{1}{2g_{\mathrm{YM}}^2} \int \mathrm{Tr}_f\, F_{\mu\nu} F_{\mu\nu}, \tag{XVIII.12.2}$$

$$S_{\mathrm{GT}} = \frac{1}{4g_{\mathrm{GT}}^2} \int \mathrm{Tr}_f\, F_{\mu\nu} F_{\mu\nu}. \tag{XVIII.12.3}$$

Here the two formulas use the same matrix-valued curvature. Equating their coefficients gives

$$g_{\mathrm{YM}}^2 = 2g_{\mathrm{GT}}^2, \qquad C_{\mathrm{GT}}(R) = 2C_{\mathrm{book}}(R), \qquad a = g_{\mathrm{GT}}^2 NA = \frac{g_{\mathrm{YM}}^2 NA}{2}. \tag{XVIII.12.4}$$

The squared couplings have mass dimension two, and a is dimensionless. For $U(N)$ we include $T^0 = I/\sqrt{2N}$ with this same kinetic coefficient. An independent abelian coupling would define a different problem.

To recover the energy, use temporal gauge and the constant spatial mode. Its Lorentzian electric kinetic term is $L\dot{A}^a_1 \dot{A}^a_1/(2g_{\mathrm{YM}}^2)$. Momentum differentiation with respect to the holonomy gives the invariant group Laplacian, whose eigenvalue is $C_{\mathrm{book}}(R)$. Consequently

$$H_R = \frac{g_{\mathrm{YM}}^2 L}{2} C_{\mathrm{book}}(R), \qquad e^{-\beta H_R} = e^{-g_{\mathrm{YM}}^2 A C_{\mathrm{book}}(R)/2} = e^{-aC_{\mathrm{GT}}(R)/(2N)}, \quad A = L\beta. \tag{XVIII.12.5}$$

The group heat kernel with identity initial holonomy therefore has character expansion

$$K_a(U) = \sum_R D_R \chi_R(U) e^{-aC_{\mathrm{GT}}(R)/(2N)}, \qquad D_R = \dim R. \tag{XVIII.12.6}$$

At zero area this is the group delta function in the distributional sense. We use positive area for the partition functions below.

Sewing turns this spectral answer into the answer on an arbitrary target. The relevant identity is

$$\int dU\, \chi_R(XU) \chi_S(U^{-1}Y) = \frac{\delta_{RS}}{D_R} \chi_R(XY). \tag{XVIII.12.7}$$

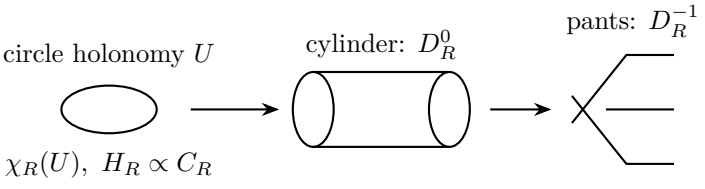


Figure XVIII.12.1: Electric-state and sewing dictionary. The circle, cylinder and schematic three-boundary piece depict holonomy data and character coefficients, derived from (XVIII.12.7). The lines on the right mark boundaries schematically; this is not a covering worldsheet or a local gluon diagram.

Integration identifies the electric labels on the two sides and removes one dimension factor. A disk has coefficient D_R, a cylinder has coefficient one, and a pair of pants has coefficient D_R^{-1}. More generally an oriented piece with b boundaries has coefficient D_R^{2-2G-b} multiplying its boundary characters and its area exponential. Gluing adds areas and Euler characteristics; the boundary Haar integrals identify labels. Closing every boundary gives

$$Z_G(a) = \sum_{R\in\widehat{\mathcal{G}}} D_R^{2-2G} e^{-aC_{\mathrm{GT}}(R)/(2N)}. \tag{XVIII.12.8}$$

The vacuum has zero energy and we add no Euler or area counterterm. Those choices fix otherwise possible overall factors. The heat-kernel quantization is the QFT input; finite representation calculations do not derive its continuum identification.

The group choice matters before any large-N expansion. Full $U(N)$ has integral highest weights $m_1 \geq \cdots \geq m_N$, including negative values. A polynomial representation has nonnegative row lengths. For $U(1)$, $C_{\mathrm{GT}}(m) = m^2$ and

$$Z_{U(1)}(a) = \sum_{m\in\mathbb{Z}} e^{-am^2/2} = 1 + 2\sum_{m=1}^{\infty} e^{-am^2/2}, \qquad Z^+_{U(1)}(a) = 1 + \sum_{m=1}^{\infty} e^{-am^2/2}. \tag{XVIII.12.9}$$

Keeping only Young diagrams loses one copy of every nonzero signed charge already at rank one. We now deliberately select that polynomial sector to construct the fixed-degree dictionary.

XVIII.12.2 A Young diagram separates area from branching

Let $r = (r_1, r_2, \ldots)$ be a polynomial $U(N)$ diagram with $n = \sum_i r_i$ boxes and at most N rows. The box number will become the number of covering sheets. Define the content

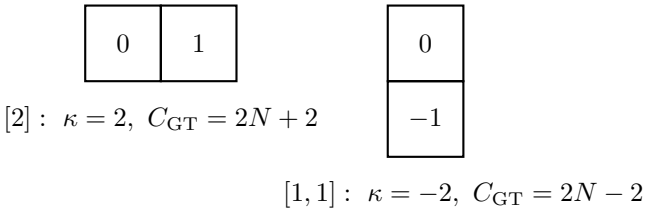


Figure XVIII.12.2: Contents of the two-box diagrams. The labels inside the boxes are $j-i$; twice their sum supplies the correction to Nn. This original diagram illustrates (XVIII.12.11); its boxes label electric representations rather than spatial cells. The column requires $N \geq 2$.

sum

$$\kappa_r = \sum_i r_i(r_i - 2i + 1) = 2 \sum_{(i,j)\in r} (j - i). \tag{XVIII.12.10}$$

The quadratic Casimir and dimension are

$$C_{\mathrm{GT},U}(r) = Nn + \kappa_r, \qquad D_r(N) = \prod_{(i,j)\in r} \frac{N + j - i}{h_r(i,j)}, \qquad d_r = \frac{n!}{\prod_{(i,j)\in r} h_r(i,j)}. \tag{XVIII.12.11}$$

Here $h_r(i,j)$ counts the box itself and the boxes to its right and below; d_r is the dimension of the corresponding S_n representation. The highest-weight Casimir splits into the uniform term $N\sum r_i$ and its content correction. The hook formula is the polynomial form of Weyl's dimension formula. For two boxes the hooks are $2, 1$, while the contents are $0, 1$ for a row and $0, -1$ for a column. Thus

r	D_r	κ_r	$C_{\mathrm{GT},U}$
$[1]$	N	0	N
$[2]$	$N(N+1)/2$	2	$2N+2$
$[1,1]$	$N(N-1)/2$	-2	$2N-2$

(XVIII.12.12)

The energy of a symmetric pair is higher than that of an antisymmetric pair. Transposing any diagram changes the sign of κ_r; it exchanges these two corrections while preserving n.

The same diagram restricted to $SU(N)$ loses its central electric energy. Its $U(1)$ generator acts with charge $n/\sqrt{2N}$, so

$$C_{\mathrm{book},SU} = C_{\mathrm{book},U} - \frac{n^2}{2N}, \qquad C_{\mathrm{GT},SU} = Nn + \kappa_r - \frac{n^2}{N}. \tag{XVIII.12.13}$$

For example the fundamental gives $C_{\mathrm{GT},SU} = N - 1/N$ and $C_{\mathrm{book},SU} = (N^2-1)/(2N)$. The central subtraction grows as n^2, not as n: the two-box charge is twice the one-box charge, so its squared charge is four times as large. For $SU(N)$ determinant columns are equivalent. A stable chiral degree convention uses a chosen lift with $N > n$; it does not count arbitrary determinant-shifted diagrams as distinct irreducibles.

Finally split the Boltzmann factor:

$$e^{-aC_{\mathrm{GT},U}/(2N)} = e^{-na/2} e^{-a\kappa_r/(2N)}. \tag{XVIII.12.14}$$

The first term assigns area nA to n sheets, with tension $g_{\mathrm{GT}}^2 N/2$ in our conventions. The second will create branch insertions. This tension is a parameter of the counting dictionary; no relation to a critical-string α' is being made.

XVIII.12.3 From electric representations to sheet permutations

A covering can be studied by cutting the target along loops and recording how its sheets are permuted when the cuts are crossed. We first derive why those permutations appear in the QFT answer. Fix n and $N \geq n$. This stable-rank condition includes every partition of n and makes the twist element below invertible.

Schur–Weyl duality decomposes the tensor space into commuting $U(N)$ and S_n actions,

$$(\mathbb{C}^N)^{\otimes n} = \bigoplus_{r \vdash n} V_r^{U(N)} \otimes V_r^{S_n}. \tag{XVIII.12.15}$$

The trace of a permutation σ on the tensor space is N^{K_σ}: each of its K_σ cycles forces equal tensor indices and leaves one independent index sum. Taking its trace in the decomposition, then using character orthogonality, gives

$$N^{K_\sigma} = \sum_{r \vdash n} D_r(N) \chi_r(\sigma), \qquad D_r(N) = \frac{1}{n!} \sum_{\sigma \in S_n} \chi_r(\sigma) N^{K_\sigma}. \tag{XVIII.12.16}$$

Thus the dimension in the electric sum already counts cycles of sheet permutations.

Let the linear functional δ extract the identity coefficient in the group algebra, and compose pq by acting with q first. Introduce three central elements,

$$\Omega_n = \sum_{\sigma \in S_n} N^{K_\sigma - n} \sigma, \qquad T_n = \sum_{i<j} (ij), \qquad H_n = \sum_{s,t \in S_n} s t s^{-1} t^{-1}. \tag{XVIII.12.17}$$

Centrality follows by relabeling every permutation in the sums. On r their scalar eigenvalues are

$$\omega_r = \frac{n! D_r}{N^n d_r}, \qquad t_r = \frac{\kappa_r}{2}, \qquad h_r = \left(\frac{n!}{d_r}\right)^2. \tag{XVIII.12.18}$$

The first follows by tracing Ω_n and using (XVIII.12.16). For the second, the sum of the Jucys–Murphy operators $\sum_j \sum_{i<j} (ij)$ acts by the sum of all box contents, $\kappa_r/2$. The factor one-half is essential for the branch weight.

For completeness the handle eigenvalue follows directly from matrix orthogonality. For a fixed t, averaging $\rho_r(s)\rho_r(t)\rho_r(s)^{-1}$ over s gives $(n!/d_r)\chi_r(t) I$. Multiplication by $\rho_r(t)^{-1}$ and summation over t uses

$$\sum_t \chi_r(t) \rho_r(t^{-1}) = \frac{n!}{d_r} I, \tag{XVIII.12.19}$$

so $\rho_r(H_n) = (n!/d_r)^2 I$. The regular representation gives one more useful identity: for any central X with eigenvalues x_r,

$$n!\,\delta(X) = \mathrm{Tr}_{\mathrm{reg}}\, X = \sum_{r\vdash n} d_r^2 x_r. \tag{XVIII.12.20}$$

These are finite-dimensional algebra statements, before any geometric interpretation.

Set $\chi = 2 - 2G$. The fixed-degree polynomial contribution therefore equals

$$\begin{aligned} Z^+_{G,n}(a) &= \sum_{r\vdash n} D_r(N)^\chi e^{-a(Nn+\kappa_r)/(2N)} \\ &= \frac{e^{-na/2}N^{n\chi}}{n!}\delta\left[\Omega_n^\chi e^{-aT_n/N} H_n^G\right]. \end{aligned} \tag{XVIII.12.21}$$

To check every normalization, substitute the eigenvalues in the second line. The coefficient multiplying $e^{-a\kappa_r/(2N)}$ is

$$\frac{N^{n\chi}d_r^2}{(n!)^2}\left(\frac{n!D_r}{N^n d_r}\right)^\chi \left(\frac{n!}{d_r}\right)^{2G} = D_r^\chi (n!)^{\chi+2G-2} d_r^{2-\chi-2G} = D_r^\chi. \tag{XVIII.12.22}$$

Both residual powers vanish because $\chi + 2G = 2$. This proves the identity for all $G \geq 0$ at fixed n, $N \geq n$. The exponential can be treated as a finite-dimensional matrix exponential or expanded in a. A negative power of Ω is rational in N and has a formal expansion near $1/N = 0$. This proof makes no exchange of an infinite degree sum and a large-N limit.

The exponential gives the elementary branch insertion:

$$e^{-aT_n/N} = \sum_{i=0}^{\infty} \frac{(-a)^i}{i!N^i} \sum_{\tau_1,\dots,\tau_i\ \text{transpositions}} \tau_1 \cdots \tau_i. \tag{XVIII.12.23}$$

A transposition interchanges two sheets around a simple ramification point, locally $w = z^2$. The negative sign follows from the positive electric energy in Euclidean evolution. These are signed coefficients, not probabilities. The $i!$ accounts for indistinguishable area-integrated branch positions, whereas the separate $n!$ in (XVIII.12.21) removes sheet labels.

The identity coefficient in (XVIII.12.21) enforces the target's monodromy relation: branch permutations, fixed twist permutations and the G handle commutators multiply to the identity. Simultaneous conjugation relabels sheets. A relabeling orbit has $n!/|\,\mathrm{Aut}\,|$ elements, so division by $n!$ produces $1/|\,\mathrm{Aut}\,|$. For ordinary covers with i simple branch points, Riemann–Hurwitz gives

$$\chi(\Sigma) = n(2 - 2G) - i. \tag{XVIII.12.24}$$

A resolved twist σ contributes a further deficit $n - K_\sigma$. Its factor in Ω_n reduces the power of N by exactly that amount. The algebra has therefore supplied area, branching, symmetry and Euler weights separately.

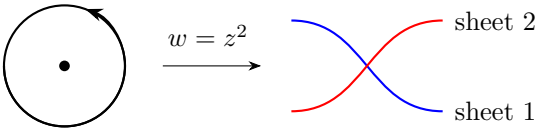


Figure XVIII.12.3: Local simple-branch monodromy. Lifting one circuit about $w = 0$ exchanges the two sheets; the colored lines record that exchange rather than embedded physical strings. The local map gives a ramification deficit of one, and the algebraic weight $-a/N$ follows from (XVIII.12.23).

XVIII.12.4 Connected surfaces at degree two

The representation sum includes disconnected coverings. To separate them, remove the elementary area factor and write $z_n = e^{na/2} Z^+_{G,n}$ and

$$\mathcal{Z}(Q) = 1 + Qz_1 + Q^2 z_2 + \cdots, \qquad [Q^2] \log \mathcal{Z} = z_2 - \frac{1}{2} z_1^2. \tag{XVIII.12.25}$$

For multiplicative ordinary-cover weights, a disconnected surface is an unordered collection of connected components. Expanding the exponential of their weighted sum counts those collections with their permutation symmetries. This exponential formula makes the formal logarithm select connected surfaces. The area dependence is restored by replacing Q with $Qe^{-a/2}$ after extracting coefficients.

On the sphere, $\chi = 2$. The two diagrams in (XVIII.12.12) give

$$z_1 = N^2, \tag{XVIII.12.26}$$

$$\begin{aligned} z_2 &= \frac{N^2(N+1)^2}{4} e^{-a/N} + \frac{N^2(N-1)^2}{4} e^{a/N} \\ &= \frac{N^2(N^2+1)}{2} \cosh(a/N) - N^3 \sinh(a/N). \end{aligned} \tag{XVIII.12.27}$$

The disconnected contribution $N^4/2$ is precisely the leading zero-branch term. Expanding at fixed degree after its removal yields

$$[Q^2] \log \mathcal{Z} = N^2 \left(\frac{1}{2} - a + \frac{a^2}{4} \right) + O(N^0). \tag{XVIII.12.28}$$

The linear term detects the branch sign; the constant and linear terms will detect the fixed twist points. This polynomial is the leading large-N coefficient at degree two, not the entire sphere planar free energy.

The torus has $\chi = 0$, so no dimension or Ω factors remain. Hence

$$z_1 = 1, \qquad z_2 = e^{-a/N} + e^{a/N} = 2\cosh(a/N), \qquad [Q^2] \log \mathcal{Z} = 2\cosh(a/N) - \frac{1}{2}. \tag{XVIII.12.29}$$

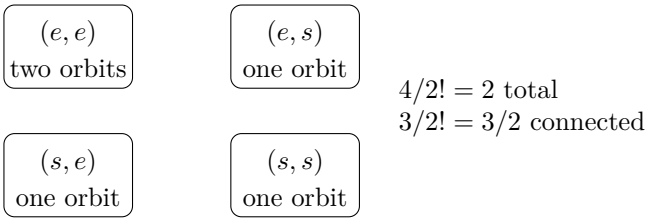


Figure XVIII.12.4: The four degree-two unbranched torus monodromies. Each box represents a pair of commuting permutations assigned to the two target cycles. Orbit count determines ordinary-cover connectedness: only (e, e) is disconnected. The weights are an explicit enumeration, not four distinct embedded surface shapes.

We can now recover its connected coefficient without the representation formula. Put $S_2 = \{e, s\}$ with $s = (12)$. Every pair (u, v) commutes; the four pairs are $(e, e), (e, s), (s, e), (s, s)$. At zero branch order the total weight is $4/2! = 2$. Only (e, e) fails to act transitively on the two sheets. The other three give connected weight $3/2$, in agreement with $2 - 1/2$ from the logarithm.

With two simple branches, the only possible ordered transposition tuple is (s, s). Its product is the identity, and each of the four handle pairs satisfies the relation. The branches themselves act transitively, so all these covers are connected. Including both factorials gives

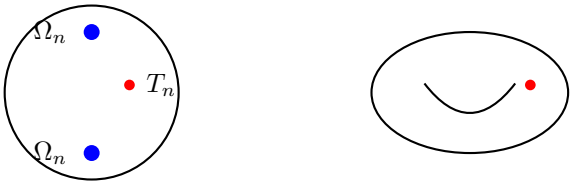
$$\frac{4}{2!}\frac{a^2}{2!N^2} = \frac{a^2}{N^2}. \tag{XVIII.12.30}$$

Riemann–Hurwitz gives $\chi(\Sigma) = 2 \cdot 0 - 2 = -2$ and covering genus $h = 2$. At zero branch order the connected degree-two covers instead have $h = 1$. The same target thus receives covering surfaces of different genera as branching is added.

Degree three tests the method beyond S_2. There are $6 \times 3 = 18$ commuting pairs in S_3: summing centralizer sizes over elements gives $6 + 3 \cdot 2 + 2 \cdot 3 = 18$. Division by $3!$ gives total unbranched weight three. Exactly eight pairs act transitively. They are the pairs in the cyclic subgroup $A_3 = \{e, c, c^2\}$ except (e, e): any nonidentity three-cycle generates a transitive subgroup, whereas a commuting pair involving a transposition preserves its fixed sheet. Their connected weight is $8/6 = 4/3$. From the representation side $z_n(0) = p(n)$ on a torus, where $p(n)$ is the number of integer partitions of n. Thus

$$[Q^3] \log \mathcal{Z} = 3 - (1)(2) + \frac{1^3}{3} = \frac{4}{3}. \tag{XVIII.12.31}$$

The commuting-pair count and the logarithm compute the same ordinary-cover quantity by different routes.



sphere: two fixed twists torus: no Ω points

Figure XVIII.12.5: Target surfaces and their insertions. Blue points are fixed twists from the Euler-characteristic factor, while red points stand for area-integrated simple branches. The torus drawing is schematic. These target-space pictures explain the factors Ω_n^2 and Ω_n^0 in the exact algebraic identity; they do not specify all covering maps.

XVIII.12.5 Fixed twist points and the information in an inverse

Why did the sphere have terms absent from the branch-only torus calculation? Its Ω_n^2 supplies two fixed twist insertions. These points are distinguished on the target and have no area integration. Each sums over arbitrary sheet permutations with their cycle deficits. They are different from the area-integrated simple branch points generated by T_n.

For two sheets the entire distinction is visible in a two-dimensional algebra. Since $s^2 = e$,

$$\Omega_2 = e + \frac{s}{N}, \qquad T_2 = s, \qquad H_2 = 4e, \qquad e^{-as/N} = e\cosh(a/N) - s\sinh(a/N). \tag{XVIII.12.32}$$

Squaring Ω_2 gives $(1 + N^{-2})e + 2s/N$. Therefore

$$z_2^{\text{sphere}} = \frac{N^4}{2}\delta\left[\left((1 + N^{-2})e + \frac{2s}{N}\right)(e\cosh(a/N) - s\sinh(a/N))\right] \tag{XVIII.12.33}$$

$$= \frac{N^4}{2}\left[(1 + N^{-2})\cosh(a/N) - \frac{2}{N}\sinh(a/N)\right]. \tag{XVIII.12.34}$$

This independently recovers (XVIII.12.27). At zero branch order, the two nontrivial fixed twists can multiply to e and give the extra $N^2/2$. With one branch, either fixed point can contribute s, giving the $-aN^2$ term. With two branches, trivial fixed twists give $a^2N^2/4$ at leading order. Replacing Ω_2 by e erases the first two of these three connected contributions.

For $G > 1$, the power $2 - 2G$ is negative. At two sheets inversion gives

$$\Omega_2^{-1} = \frac{e - s/N}{1 - N^{-2}} = e - \frac{s}{N} + \frac{e}{N^2} - \frac{s}{N^3} + O(N^{-4}). \tag{XVIII.12.35}$$

Its eigenvalues before inversion are $1 + 1/N$ and $1 - 1/N$. At $N = 1$ the antisymmetric eigenvalue vanishes, matching $D_{[1,1]}(1) = 0$. The unrestricted S_2 inverse cannot be

evaluated there. Positive-area $U(1)$ theory in (XVIII.12.9) is finite: it never contained the forbidden two-row representation. Projecting a finite-rank representation sum and inverting the unrestricted algebra element are different operations.

An inverse also changes the geometric information that must be retained. In the formal expansion

$$\Omega_n^{-1} = \sum_{k=0}^{\infty} (-1)^k (\Omega_n - e)^k, \tag{XVIII.12.36}$$

each factor retains an internal nonidentity permutation. Two internal twists (s, s) have net product e, yet together connect the two sheets and carry total deficit two. Replacing this internal pair by its net identity would declare two orbits and zero deficit if no other monodromy were present. Thus neither connectedness nor genus can be inferred from the compressed net permutation of an inverse point.

For higher genus, (XVIII.12.21) remains an exact fixed-degree algebraic identity with signed formal generalized twist weights. The formal logarithm remains algebraically defined. A geometric connected-cover interpretation there requires the expanded singularity information; this chapter supplies no generalized high-genus connectivity algorithm. Our explicit connected enumeration used the ordinary torus, where this inverse-point complication is absent.

XVIII.12.6 Opposite orientations interact in $SU(N)$

The central subtraction in (XVIII.12.13) changes the fixed-lift chiral answer by

$$\exp\left(\frac{an^2}{2N^2}\right) = \exp\left(\frac{an}{2N^2} + \frac{an(n-1)}{2N^2}\right). \tag{XVIII.12.37}$$

The two pieces have the Gross–Taylor interpretation of a collapsed handle and an orientation-preserving tube. Their pointlike nature matters: they are generalized singularities, beyond smooth ordinary covers with simple branch points. The algebraic correction follows from removing the central energy; the full singularity interpretation uses additional geometric input.

A second issue arises when both orientations are included. For finite diagrams R, S of sizes n, m, sufficiently large N admits a composite $R\bar{S}$. The sourced highest-weight formula is

$$C_{\mathrm{GT},SU}(R\bar{S}) = C_{\mathrm{GT},SU}(R) + C_{\mathrm{GT},SU}(S) + \frac{2nm}{N}. \tag{XVIII.12.38}$$

It produces the extra factor e^{-anm/N^2}, so independent multiplication of the two chiral Boltzmann factors misses a coupling. We use this general formula as an imported representation result and independently reconstruct its smallest example.

Take $R = S = [1]$. The tensor product of a fundamental and antifundamental consists of a singlet and the adjoint, so $D_{\mathrm{adj}} = N^2 - 1$. The adjoint action on traceless

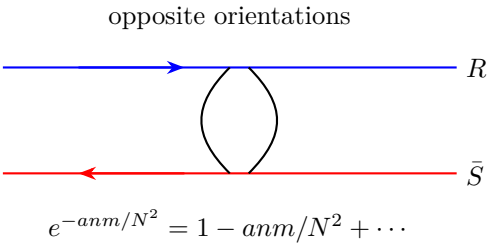


Figure XVIII.12.6: Pointlike coupling of opposite orientations. The joining neck is a schematic singular tube, with leading signed coupling $-anm/N^2$ from (XVIII.12.38); it is not a smooth simple-branch covering. For the adjoint witness the additional dimension ratio is $(1 - N^{-2})^\chi$. This illustration does not construct the general coupled-Ω theory.

matrices is $X \mapsto [T^a, X]$. Generator completeness gives

$$\sum_a T^a X T^a = \frac{1}{2}\left(\operatorname{Tr} X\, I - \frac{X}{N}\right), \qquad \sum_a [T^a, [T^a, X]] = 2\frac{N^2-1}{2N}X + \frac{X}{N} = NX. \tag{XVIII.12.39}$$

Thus $C_{\text{book,adj}} = N$ and $C_{\text{GT,adj}} = 2N$. The fundamental and antifundamental each have $C_{\text{GT},f} = N - 1/N$. Their difference is

$$C_{\text{GT,adj}} - 2C_{\text{GT},f} = \frac{2}{N}. \tag{XVIII.12.40}$$

The actual adjoint contribution and the product of separate contributions are consequently

$$W_{\text{adj}} = (N^2-1)^\chi e^{-a}, \tag{XVIII.12.41}$$

$$W_f W_{\bar{f}} = N^{2\chi} e^{-a(1-N^{-2})}, \tag{XVIII.12.42}$$

$$\frac{W_{\text{adj}}}{W_f W_{\bar{f}}} = (1-N^{-2})^\chi e^{-a/N^2}. \tag{XVIII.12.43}$$

On a torus the dimension ratio is one but the Casimir ratio remains e^{-a/N^2}. On a sphere the dimension ratio is $(1 - N^{-2})^2$ as well. This separates the energy coupling from the multiplicity coupling; a torus test alone would miss the latter. It is a representation-by-representation witness, rather than an assertion that the entire tensor product is only the adjoint.

Neither the chiral $SU(N)$ factor nor the adjoint witness completes the full theory by itself. The simply connected global form of $SU(N)$ has determinant-column identifications, and its two orientations interact. The full $U(N)$ theory also contains nonpolynomial highest weights. These facts prevent identifying a pair of independent polynomial sums with the unrestricted compact-group answer.

XVIII.12.7 The density cap and the direction of the dictionary

The fixed-degree identity is exact on its stated finite-rank domain. Summing every degree before taking large N asks a different question. The full $U(N)$ theory on a sphere gives a controlled way to see why the distinction matters. We use the Douglas–Kazakov variational description as input and examine the admissibility of its weak saddle.

Ordered integral weights imply a density cap. For example define shifted weights $h_i = (m_i + N - i)/N$, up to an irrelevant uniform translation of their center. Then

$$h_i - h_{i+1} = \frac{m_i - m_{i+1} + 1}{N} \geq \frac{1}{N}. \tag{XVIII.12.44}$$

A small interval dh can contain at most $N\,dh$ weights. The normalized continuum density therefore obeys

$$0 \leq \rho(h) \leq 1, \qquad \int \rho(h)\,dh = 1. \tag{XVIII.12.45}$$

The upper bound is a remnant of integral representation data, not a restriction invented for the continuum approximation.

Ignoring the cap in the Gaussian variational problem gives the centered semicircle

$$\rho_{\text{weak}}(h) = \frac{a}{2\pi}\sqrt{\frac{4}{a} - h^2}, \qquad |h| \leq \frac{2}{\sqrt{a}}. \tag{XVIII.12.46}$$

To normalize it, set $R = 2/\sqrt{a}$. The integral of $\sqrt{R^2 - h^2}$ from $-R$ to R is the area of a half-disk, $\pi R^2/2$. Hence

$$\int \rho_{\text{weak}}\,dh = \frac{a}{2\pi}\,\frac{\pi}{2}\,\frac{4}{a} = 1, \qquad \rho_{\text{weak}}(0) = \frac{\sqrt{a}}{\pi}. \tag{XVIII.12.47}$$

Its maximum first reaches one at $a = \pi^2$. At $a = 4\pi^2$ the same unconstrained expression has peak two and cannot describe allowed weights. This calculation derives the admissibility boundary of the weak saddle. The saturated solution and its free-energy comparison are additional work; the third-order Douglas–Kazakov transition at $a = \pi^2$ is a sourced result, not a consequence of the peak calculation alone.

The same distinction organizes the entire chapter. At fixed n the electric sum and the finite group-algebra expression are equal. Expanding at fixed degree and branch order gives powers of $1/N$ with geometric meanings where the resolved monodromy data suffice. The unrestricted degree sum, a uniform all-area large-N limit and a nonperturbative string definition each require further control. The forbidden-rank inverse and the inadmissible semicircle defeat particular naive extrapolations; they do not exclude every possible resummation or completion.

Returning to Chapter XVIII.1, the direction of explanation has changed. There a controlled worldsheet sector supplied target fields and interactions. Here electric energies and representation multiplicities supplied sheets, branch points and symmetry weights. The result is an explicit reverse dictionary for selected QFT data. It teaches which structures a string description must reproduce, while keeping the independent definition of the QFT visible.

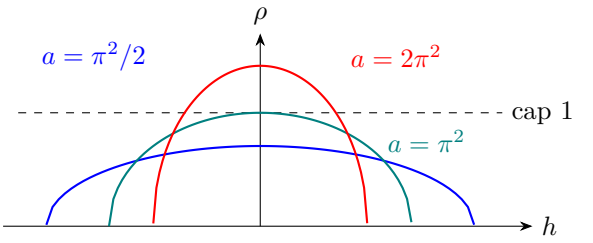


Figure XVIII.12.7: The unsaturated semicircle and the integer-weight cap. Horizontal coordinates are in units $2/\pi$, so the critical support ends at $h = \pm 2/\pi$ in physical units. Curves are (XVIII.12.46) at the three indicated areas; the red continuation violates the cap and is not the strong-phase density. No saturated saddle is drawn.

Following connectedness through the reverse dictionary

The degree-two torus calculation is a small example in which every weight has an identifiable origin. Choose the two monodromies around the target cycles. Their commutator must be trivial for an unbranched cover. In S_2 all four ordered pairs satisfy this condition. Division by the sheet-label permutation factorial gives the total weight in the text. To ask for a connected cover, inspect the orbits of the generated action on the sheets. The identity pair has two orbits; each remaining pair has one. Removing the former therefore gives the stated connected weight.

The formal logarithm performs the same removal on the representation answer. The quadratic term subtracts an unordered pair of degree-one components. This is why the subtraction includes one half. It is not an adjustment chosen to fit the permutation count. On the sphere the same operation removes the leading disconnected zero-branch term before the large-N expansion. The remaining area polynomial can then distinguish the branch sign and the fixed twist-point contributions. Taking a logarithm, selecting a degree and expanding at large N are all specified operations; none can be omitted from the comparison.

Adding two simple branches gives another physical change. Their transpositions can generate a transitive action even when the handle monodromies alone do not. The branch-position expansion brings its own factorial, separate from the sheet-label factorial. Riemann–Hurwitz then changes the genus of the covering surface while leaving the target torus fixed. Counting the genus of the target instead of that of the cover would misidentify the power of N associated with this contribution.

This concrete enumeration explains the direction of the chapter. The heat-kernel field theory was defined first. Its fixed-degree expansion is then reorganized using permutations, branching and connected surfaces. The independently defined gauge-theory answer supplies the quantity that is being rewritten. The construction therefore differs from the earlier chapters in which worldsheet states and sewing supplied the target field variables or selected observables. The distinction preserves a useful string

interpretation without making the reverse expansion a new worldsheet definition of every sector of two-dimensional Yang–Mills.

Written exercises

The separate worked solutions use the same trace convention and global groups. In Questions 3–4, Q records degree after extracting $e^{-na/2}$.

1. Derive the cylinder energy at circumference L from the electric kinetic term and compare the two actions to obtain the coupling conversion. For $U(1)$, identify the terms lost by retaining only nonnegative highest weights.

2. Compute D, C_{book} and C_{GT} for the fundamental, Sym^2 and $\wedge^2$ of $U(N)$ and their $SU(N)$ restrictions. Evaluate $N = 3$, explain the central charge subtraction, and give the minimum rank of existence, including determinant representations.

3. In $\mathbb{Q}(N)[S_2]$ form Ω_2, T_2, H_2. Derive the degree-two sphere and torus expressions by extracting the identity coefficient, tracking both factorials and the branch sign. Find the first sphere error if Ω_2 is replaced by e.

4. Enumerate the commuting S_2 pairs and their transitive subset. Recover the zero-branch total and connected weights. Add two simple branch points, include the branch factorial, and determine the connected covering genus.

5. Invert Ω_2 through order N^{-3}. Explain its positive-rank singularity using the absent $U(1)$ wedge representation. Why does the full positive-area $U(1)$ heat kernel remain finite? Show with two equal transpositions what a net inverse-point permutation can forget.

6. In simply connected $SU(N)$ compare the actual adjoint term with the product of fundamental and antifundamental terms, on torus and sphere. Reconstruct the adjoint dimension and Casimir. Separate the missing energy and dimension factors, and state what remains beyond this witness.

7. Normalize (XVIII.12.46), determine its maximum and cap threshold, and derive the cap from ordered integral weights. Explain why the fixed-degree identity survives an inadmissible global saddle. Does this calculation determine the order of the transition?

Sources and scope

§XVIII.12.1. The compact-group heat-kernel formula, action conversion and signed-weight distinction are mathematical statements under heat-kernel quantization, normalized Haar measure, zero theta angle and the stated counterterms. Gross and Taylor (1993b), equations (1.1)–(1.2), supplies the selected QFT input; sewing and the action comparison are displayed above. Full $U(N)$ integral weights appear in Douglas and

Kazakov (1993), equations (4)–(8). These are not physical-worldsheet derivations. [MATH]

§XVIII.12.2–XVIII.12.3. Dimension, Casimir and central-algebra identities hold on the specified polynomial and stable-rank domains. Sources are Gross and Taylor (1993b), equations (2.1)–(2.3) and appendix, and Gross and Taylor (1993a), equations (2.1)–(2.4), (2.13)–(2.24). The eigenvalue calculation proves the fixed-degree identity with the $U(N)$ Casimir; the full infinite representation sum is a distinct object. Orbit–stabilizer and Riemann–Hurwitz establish the weights of resolved ordinary covers, with the counting interpretation in the first paper, section 3, and the second, equations (2.25)–(2.27). [MATH]

§XVIII.12.4–XVIII.12.5. The sphere and torus examples are direct two-diagram and group-algebra calculations. Connectedness is derived for multiplicative ordinary-cover weights and explicitly enumerated on the torus. Formal inverse-Ω points require internal twist and singularity data; see Gross and Taylor (1993a), equations (2.18)–(2.28). The fixed-degree higher-genus identity does not supply a generalized connected-cover algorithm. [MATH]

§XVIII.12.6. The central $SU(N)$ correction is derived at a fixed Young lift with $N > n$. The collapsed-handle/tube reading uses Gross and Taylor (1993a), equations (2.11), (2.24), (2.27). The general composite Casimir is imported from Gross and Taylor (1993b), equations (2.6)–(2.10); the adjoint obstruction is separately reconstructed. General coupled-Ω calculus, discussed in the second paper, section 3, is not derived here. [MATH]

§XVIII.12.7. The full $U(N)$ sphere variational framework and weak saddle are imported from Douglas and Kazakov (1993), equations (7)–(25). The normalization, density cap and admissibility threshold are derived above. The third-order transition uses that paper's saturated-phase analysis, equations (38)–(40), and is source-bound rather than independently computed. [MATH]

The finite examples compare Weyl and hook dimensions, normalized-generator tensor Casimirs, representation and permutation coefficients, and torus transitivity. Aggregate coefficients alone leave the topology of individual monodromy words undetermined. A physical-string action, all-rank or all-area equivalence and a nonperturbative completion require additional arguments.

References

Douglas, M. R. and V. A. Kazakov (1993). "Large N Phase Transition in Continuum QCD_2". In: *Phys. Lett. B* 319, pp. 219–230. DOI: 10.1016/0370-2693(93)90806-S. arXiv: hep-th/9305047 [hep-th].

Gross, D. J. and W. Taylor (1993a). "Twists and Wilson Loops in the String Theory of Two Dimensional QCD". In: *Nucl. Phys. B* 403. DOI: 10.1016/0550-3213(93)90042-N. arXiv: hep-th/9303046 [hep-th].

Gross, D. J. and W. Taylor (1993b). "Two Dimensional QCD is a String Theory". In: *Nucl. Phys. B* 400. DOI: 10.1016/0550-3213(93)90403-C. arXiv: hep-th/9301068 [hep-th].